

LONDON
SCHOOL of
HYGIENE
& TROPICAL
MEDICINE



LSHTM Research Online

Ssewanyana, I; (2021) P. falciparum Transmission Intensity and the Quality of Antimalarial Antibodies. PhD thesis, London School of Hygiene & Tropical Medicine. DOI: <https://doi.org/10.17037/PUBS.04660682>

Downloaded from: <https://researchonline.lshtm.ac.uk/id/eprint/4660682/>

DOI: <https://doi.org/10.17037/PUBS.04660682>

Usage Guidelines:

Please refer to usage guidelines at <https://researchonline.lshtm.ac.uk/policies.html> or alternatively contact researchonline@lshtm.ac.uk.

Available under license. To note, 3rd party material is not necessarily covered under this license: <http://creativecommons.org/licenses/by-nc-nd/3.0/>

<https://researchonline.lshtm.ac.uk>

LONDON
SCHOOL of
HYGIENE
& TROPICAL
MEDICINE



LSHTM Research Online

Ssewanyana, I; (2021) *P. falciparum* Transmission Intensity and the Quality of Anti-malarial Antibodies. PhD thesis, London School of Hygiene & Tropical Medicine.
<https://researchonline.lshtm.ac.uk/id/eprint/4660682>

Downloaded from: <https://researchonline.lshtm.ac.uk/id/eprint/4660682/>

DOI:

Usage Guidelines:

Please refer to usage guidelines at <https://researchonline.lshtm.ac.uk/policies.html> or alternatively contact researchonline@lshtm.ac.uk.

Available under license: <http://creativecommons.org/licenses/by-nc-nd/2.5/>

<https://researchonline.lshtm.ac.uk>

LONDON
SCHOOL of
HYGIENE
& TROPICAL
MEDICINE



P. falciparum Transmission Intensity and the Quality of Antimalarial Antibodies

Isaac Ssewanyana

This thesis was submitted in accordance with the requirements for the degree of Doctor of Philosophy. University of London
April 2019

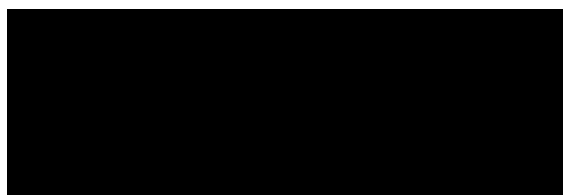
Department of Immunology and Infection
Faculty of Infectious and Tropical Diseases
London School of Hygiene & Tropical Medicine

Funded by: National Institutes of Health as part of the East African International Centers of Excellence in Malaria Research (ICMER) program (U19AI089674). Training in malaria research in Uganda (D43TW7375)

Research group affiliation(s): Infectious Diseases Research Collaboration, Uganda

Declaration

I, Isaac Ssewanyana, confirm that the work presented in this thesis is my own. Where information has been derived from other sources, I confirm that this has been indicated in the thesis.



Abstract

Immunity to malaria, where antibodies play a critical role, is acquired slowly, rarely sterile, and poorly maintained. The quality than just the quantity of antibodies may provide more insight into the slow acquisition and poor maintenance of immunity to malaria.

I hypothesized that frequent *P. falciparum* infections interrupt avidity maturation and IgG subclass composition, which affects the acquisition and maintenance of immunity to malaria.

In the first aim, the avidity index to AMA-1 and MSP1-19 was compared across three cross-sectional malaria transmission intensity sites. In the second and third aims, avidity index, total IgG, and IgG1 – 4 against 18 *P. falciparum* blood-stage antigens were measured in a longitudinal cohort at 4-time-points; 2 before and 2 after interruption of malaria transmission by IRS.

Results showed that avidity to both AMA-1 and MSP1-19 was significantly lower at the site of highest *P. falciparum* transmission in children above 5 years and adults.

In all 18 malaria blood-stage antigens, the avidity index was positively associated with days since the last infection independent of age and heterogeneous across antigens.

There was heterogeneity in antibody half-life estimation across antigens and IgG subclasses. IgG3 had the shortest half-life of the IgG subclasses. The predominance of IgG subclass in the absence of infection shifted from IgG1 to IgG3 with age. IgG3 improved the specificity of antigens as a marker of recent infection compared to total IgG.

Results provide supporting evidence to our hypothesis by demonstrating (i) preferential expansion of non-avid antibody pool that rapidly wane in the absence of infection (ii) slow acquisition of the avid antibody pool that persists in the absence of infection. (iii) slow acquisition of IgG3 memory.

The thesis provides the rationale for further investigation of malaria-specific MBC phenotypes, class switching, somatic hypermutation, the avidity of antibodies, and the antibody in vitro function. These further studies will provide more knowledge in the acquisition and maintenance of effective antibody memory.

Acknowledgments

First and foremost, I extend my heartfelt gratitude to my primary supervisor Kevin Tetteh for the support and guidance throughout this Ph.D. training. Thank you, Kevin, for teaching me the Luminex assay technique and guiding me through the antigen coupling, avidity, and IgG subclass assay development and optimization. Thank you for the mentorship. I have learned so much from you, and your vast knowledge and skills always remind me of how much more I yet to learn. My Ph.D. tenure has not been smooth due to many competing interests that many times derailed me. I sincerely thank you for being patient with me the many times I have been derailed, and I am very grateful for all the times you have brought me back in line. Thank you for always fast trucking shipment of my reagents from London, a process that was not obvious throughout the period and, thanks to you for fast-tracking review of my drafts during the writing.

I extend my deepest gratitude to Chris Drakeley and Bryan Greenhouse for guiding me through the development of the research questions, advising, mentoring, and supporting me through this training. Thank you for providing financial support for my research and travels to London, UCSF, and meetings that were not supported by FIC and PRISM projects. I am grateful to you for working with your groups in London and UCSF and the exposure you have given me in malaria immunology various networks.

Thank you, Harriet Mayanja-Kizza, for the guidance and continually asking me to scientifically or logically justify my approaches, methodology, and critique of my results and interpretations. I learned the valuable skill of looking at the alternatives.

Thank you very much, Isabel Rodriguez and Bryan Greenhouse, for coaching me through the data analysis, especially the multivariate analysis models, interpretation of statistical outcome, summarizing, and presenting large information in simplified Figures. I am grateful for the undivided dedication you accorded me during the three months I spent in San Fransisco. Thank you, too, for standing by my bedside and supporting me emotionally when I was admitted to intensive care. I did not feel the absence of my family, and I will always remember your kindness.

Lindsey Wu, thank you for supporting me with the normalization of the Luminex data. I treasure the valuable time you spared for me amid your Ph.D. submission deadline.

Philip Rosenthal, Grant Dorsey, and Moses Kamya, I am grateful for the funding opportunities you gave me to build my scientific career through the FIC and PRISM projects. Thank you for allowing me to leverage n the PRISM findings to accomplish most of my research requirements and travels that were not funded by the FIC.

To the PRISM teams in Nagongera, Walukuba, Kihhihi, and Kampala, thank you for the elegant work which provided me access to well-characterized populations and clean datasets that enhanced the quality of my work. To the PRISM study volunteers, your participation is

invaluable to my thesis, PRISM study findings, and the entire malaria research; thank you very much.

I extend my sincere gratitude to my wife Ritah Happy Namirembe Ssewanyana, to stand by me, encourage me, and support our entire family and me emotionally and financially through this training. You abandoned a paid position, risked your career to dedicate time to our home income generation projects to raise enough funds to support our family. Several times, these projects have been draining and stressful, but you have endured. Their overwhelming challenges have often distracted me from the Ph.D. activities, but you always shouldered the burdens and protected my time and emotions. Thank you for taking good care of our children whenever I traveled for long periods or whenever I needed time to focus on my work. I am proud that we have built a sound financial system that requires less of my time to support our family and guarantees my indulgence in research without compromising our quality of life. I thank our children, Jonathan Kuteesa Ssewanyana, Isaiah Cole Kawalya, Clare Mirembe Nakimera, Kaylee Rebecca Ggibwa, and Benon Kyome Mpagi, for being accommodative during my absence and for inspiring me to complete this training.

I dedicate this work to the memory of the late John Kyome Mponye. He gave me an opportunity and many others to access the best education in Uganda that my parent could not afford. He believed education was the solution to African challenges, and by educating his clan, he was eradicating poverty and diseases. His philosophy inspired me into science and has driven my desire to help others access opportunities to pursue their careers.

Contents

Declaration	1
Abstract	2
Acknowledgments.....	4
Acronyms	14
List of Figures	17
List of Tables.....	19
Chapter 1.....	21
1.1 Introduction to Malaria.....	21
1.2 Malaria parasite and life cycle.....	21
1.2.1 Asexual liver-stage.....	22
1.2.2 Asexual blood-stage	22
1.2.3 Sexual mosquito stage.....	23
1.3 Global Malaria Trends.....	24
1.4 Malaria status in Uganda.....	26
1.5 Malaria control strategies	27
1.6 Malaria elimination campaigns; the past, the present, and the future	30
1.7 Malaria Pathogenesis, Diagnosis, and Treatment.....	32
1.7.1 Malaria pathogenesis	32
1.7.2 Malaria diagnosis and treatment	34
1.8 Acquired immune responses to malaria	35
1.8.1 Immunity to severe disease	35
1.8.2 Anti-disease Immunity	37
1.8.3 Anti-parasite immunity	38
1.8.4 Sterile immunity	39
1.8.5 Evidence for the role of antibody responses in immunity to malaria.....	40
1.9 Malaria vaccine	41

1.9.1 Vaccines targeting liver Stage: RTS, S/AS01 as an example of a subunit vaccine	42
1.9.2 Whole sporozoite vaccines.....	43
1.9.3 Vaccines targeting blood-stage	44
1.9.4 Transmission-blocking Vaccine targeting the sexual Stages	45
1.10 IgG structural features that determine the function	47
1.11 Differences in IgG subclasses structures that affect half-life and function.	48
1.12 Antibody affinity and avidity	50
1.13 B-cell reaction pathways; the source of affinity and class switching.....	53
1.13.1 T-independent extra-follicular response of B-cell.....	54
1.13.2 T-dependent extra-follicular B cell response	54
1.13.3 Germinal center reaction	56
Chapter 2.....	59
2.1 Background and rationale	59
2.2 Hypothesis and aim	61
2.3 Study aim.....	62
Chapter 3.....	63
3.1 Methods	63
3.1.0 Study Population	63
3.1.1 Program for Resistance, Immunology, Surveillance, and Modeling of Malaria in Uganda....	63
3.1.2 Cross-Sectional Surveys.....	64
3.1.3 Description of the three epidemiological settings	65
3.1.4 Description of the Longitudinal Cohort at Nagongera	67
3.1.5 Interruption of transmission by IRS and Enhanced surveillance in Nagongera	69
3.1.6 IRS schedule and sampling time-points	69
3.1.7 Malaria status within the study population	72
3.1.8 Informed consent	74
3.2 Laboratory methods.....	75

3.2.1 <i>P. falciparum</i> Recombinant Antigens	75
3.2.2 Elution of antibodies from DBS	77
3.2.3 Avidity ELISA assay	77
3.2.4 Preparation of Luminex assay reagents	78
3.2.5 Luminex Bead counting	79
3.2.6 Determination of optimal antigen coupling concentration	80
3.2.7 Covalent coupling of antigens to magnetic microsphere Bead	83
3.2.8 Plasma dilution	84
3.2.9 Construction of hyperimmune control - PRISM pool 4	85
3.2.10 Luminex MagPex multiplex bead array assay to measure total IgG	86
3.2.11 Luminex Multiplex bead array assay to measure total IgG avidity responses	88
3.2.12 Luminex Multiplex bead array assay to measure IgG1 – 4s	90
3.3 Data Normalization to adjust for plate-to-plate variations.....	91
3.4 Statistical Analysis.	92
Chapter 4.....	94
Avidity of Antimalarial Antibodies Inversely Related to Transmission Intensity at Three Sites in Uganda	94
4.1 Introduction	94
4.1.1 Slow acquisition of Immunity to malaria.....	94
4.1.2 Role of antibodies in acquired immunity to malaria	95
4.1.3 Antibody affinity, avidity and the role in Antibody function.....	97
4.1.4 Evidence of acquisition of avidity during infection and role in immunity	98
4.1.5 Evidence of acquisition of avidity maturation during Malaria infection.....	99
4.1.6 What influences avidity maturation during Malaria infection?	100
4.2 Study aim.....	100
4.3 Methods.....	101
4.3.1 Study sites and cross-sectional surveys	101
4.3.2 Study population	102

4.3.3 Modified ELISA to Measure the Avidity index.....	103
4.3.4 Data Analysis	104
4.4 Results	104
4.4.1 Change in age with transmission site at OD 0.5 cut off	104
4.4.2 Relationship between age and antibody avidity	105
4.4.3 Relationship between malaria transmission and antibody avidity	107
4.4 Discussion	109
4.4.1 Summary of Results.....	109
4.4.2 Chronic infection may impair germinal center.....	110
4.2.3 Status of infection may influence Avidity index.....	112
4.3.4 Relationship between avidity index and immunity.....	112
4.3.4 Limitations.....	113
4.4 Conclusion	114
Chapter 5.....	115
<i>P. falciparum</i> infection is associated with a predominantly non-avid IgG antibody response that rapidly decays following IRS	115
5.1 Introduction.....	115
5.2 Hypothesis and Aim.....	118
5.3 Methods.....	119
5.3.1 Study population and time-points	119
5.3.2 Ethical consideration	120
5.3.3 Multiplex bead array assay to measure total and avid IgG.....	120
5.3.4 Statistical analysis.....	121
5.4 Results	122
5.4.1 Validation of an antibody avidity assay MagPix multiplex platform.....	122
5.4.2 Assay reproducibility to inform use if single well.....	122
5.4.3 Effect of GuHCl on the properties of magnetic beads	124
5.4.3 Effect of GuHCl on the antigens coupled to beads	125

5.4.4 Optimal GuHCl concentration and dissociation time	127
5.4.5 Heterogeneity in Avidity Index.....	130
12	131
5.4.6 Decreased total antibody levels and Increased avidity index between 6 months before and 12 after IRS	133
5.4.7 Increased avidity index was due to differential net loss in the total pool versus avid antibody at 6 months PRE and 12 post-IRS	137
5.4.8 Avidity index was positively associated with prior malaria infection	139
5.4.9 Total and avid antibody levels inversely associated with prior malaria infection	142
5.50 Changes in avidity index with Age.....	145
5.6 Discussion	148
5.6.1 Results summary	148
5.6.2 Rapid decay of non-avid antibody pool is due to rapid contraction of SLPC in the absence of infection	149
5.6.3 <i>P. falciparum</i> infection promotes the expansion of predominantly SLPC that result in short-lived responses	152
5.6.4 Intrinsic antigen properties may affect affinity maturation and antigen suitability for use in vaccine designs.....	153
5.6.5 Limitations.....	154
5.66 Conclusion	156
Chapter 6.....	157
Differences in the half-life of <i>P. falciparum</i> antigen-specific IgG subclasses are associated with age following interruption of exposure by IRS.	157
6.1 Introduction	157
6.1.1 Malaria challenges in the pre-elimination era	157
6.1.2 Role of anti-malarial IgG antibodies in immunity to malaria	158
6.1.3 IgG subclasses can influence the outcome of immunity to infections.....	159
6.14 IgG subclasses, placental transfer, glycosylation and longevity in circulation.....	161
6.1.5 Evidence IgG subclasses in the immunity to malaria	161

6.1.6 Evidence of differential malaria-specific IgG subclass switching	162
6.2 Rationale and aim.....	163
6.3 Methods.....	164
6.3.1 Study population and description of PRISM cohort at Nagongera	164
6.3.2 Ethical consideration	165
6.3.3 Luminex Multiplex bead array assay to measure Total IgG	165
6.3.4 Luminex Multiplex bead array assay to measure IgG1 - 4	165
6.3.5 Statistical analysis.....	166
6.4 Results	168
6.4.1 Relative responses of total and IgG subclasses.....	168
6.4.2 Association of total IgG and IgG subclasses responses with days since the last infection. .	173
6.4.3 Association of total IgG and IgG subclasses with age in the absence of infection.....	176
6.4.4 Differences in antibody half-life among IgG subclasses in the absence of infection.....	179
6.4.5 IgG subclass stratify into distinct clusters	182
6.4.6 IgG3 showed improved specificity of antigens to predict recent infection compared to total and IgG1	185
6.5 Discussion	188
6.5.1 Summary of results.....	188
6.5.2 Determinants of antibody decay Half-life	190
6.5.3 <i>P. falciparum</i> antigens may induce differential expansion of SLLC, LLPC, and MBC phenotypes.....	193
6.5.4 FcRn may influence half-lives of IgG3 compared to IgG1	194
6.5.5 Slowed acquisition of IgG3 memory	196
6.5.6 Prospects on using IgG3 as a marker of recent infection.....	197
6.5.7 Drivers of distinctive antibody clusters.....	198
6.5.8 Limitations.....	198
6.6 Conclusions	199
Chapter 7.....	200

7.1 Discussion	200
7.1.1 Summary of results.....	200
7.1.2 Does <i>P. falciparum</i> infection interfere with affinity maturation?.....	203
7.1.3 What is the implication of low antibody avidity (predominantly non-avid antibodies)?	205
7.1.4 Does malaria induce short-lived memory compared to other infections?	207
7.1.5 IgG subclass phenotypes and implication in immunity to malaria	209
7.1.6 Prospects of IgG3 as a diagnostic tool for malaria in the elimination era	209
7.2 Significance	210
7.3 Conclusions.....	211
7.4 Future Direction	213
Publications.....	215
Reference.....	217

Acronyms

ABRD	Antibody-dependent respiratory burst
ACT	Artemisinin based combination therapies
ADCC	Antibody dependent cytotoxicity
ADCI	Antibody-dependent cellular inhibition
AID	Activation-induced cytidine deaminase
AMA-1	Apical membrane antigen
AUC	Area under curve
BCR	B-cell receptor
CAM-1	Intercellular adhesion molecule 1
CHMI	Controlled human malaria infection
CM	Cerebral malaria
Coef	beta correlation coefficient
CSP	Circumsporozoite protein
DBC	Dried blood spots
EDC	Carbodiimide hydrochloride
EIR	Entomologic inoculation rate
FcR	Fc receptors
FcRn	Neonatal Fc receptor
FDC	Follicular dendritic cells
GAP	Genetically attenuated parasite
GEE	Generalized estimation equation

GIA	Growth inhibition assays
GST	Glutathione S-transferase
GuHCl	Guanidine hydrochloride
HRP	Horseradish peroxidase enzyme
HRP2	Histidine-rich protein-2
Hype2	Plasmodium exported protein
IFN- γ	Interferon-gamma
IL	Interleukin
IRS	Indoor insecticide residual spraying
ITN	Insecticide treated nets
LAMP	Loop-mediated isothermal amplification
LLPC	Long lived plasma cells
MBC	Memory B cell
MFI	Median fluorescent intensities
MHCII	Major Histocompatibility complex class II
MSP	Merozoites surface protein antigens
NK	Natural killer cells
OD	Optical densities
OPD	o-phenylenediamine
PBS	Phosphate buffered saline
PfEMP1	<i>P. falciparum</i> erythrocyte membrane protein 1
PfRH5	<i>P. falciparum</i> reticulocyte-binding protein homolog 5

PfSPZ	Irradiated attenuated sporozoites
PP4	Hyper immune control pooled form PRISM samples
PRISM	Program for Resistance, Immunology, Surveillance, and Modeling of Malaria
qPCR	Quantitative PCR
RBC	Red blood cells
RDT	Rapid diagnostic tests
ROC	Receiver operating characteristic curve
SLPC	Short lived plasma cells
TI	T-independent antigens
TLR	Toll like receptors
TNF- α	Tumor necrosis factor alpha
TT	Tetanus toxoid protein

List of Figures

Figure 1.1 Life Cycle of Malaria describing the three stages

Figure 1.2 Reduction in malaria incidence (a) and mortality (b) by WHO regions between 2010 and 2015.

Figure 1.4 Reduction in *P. falciparum* malaria burden and effect of interventions in endemic African countries between 2000 and 2015.

Figure 1.6 Schematic layout of IgG features and subclasses a) Basic structure of IgG composed of two heavy chains and two light chains linked together by disulfide bonds.

Figure 1.9 Illustration of affinity and avidity.

Figure 1.8 Schematic representation of the germinal center

Figure 3.1 Map of Uganda showing the three study

Figure 3.3 Summary of cohort malaria incidence, parasite rate, ITN, and IRS schedules in the upper panel.

Figure 3.6 Representative Graphs showing the titration of Stock coupling concentration in Bead.

Figure 3.8 Representative PP4 standard curves of 18 *P. falciparum* antigens and Tetanus toxoid PP4 was able to result in a saturation curve for all the antigens on the panel

Figure 4.31b Summary of the samples selected from the PRISM cross-sectional survey based on the OD 0.5 cut off for both AMA-1 and MSP1-19

Figure 4.33. Avidity index to MSP1-19 and AMA-1 across age groups.

Figure 4.33. Avidity index to MSP1-19 and AMA-1 across transmission sites.

Figure 5.50a Graph showing MFI of representative antigens tested in duplicate on one plate. A total of 40 sampled at a dilution of 1/1000 were included.

Figure 5.50b Graph showing MFI of representative antigens plate 1 PP4 curve plotted against the 7 plates.

Figure 5.51a Graph showing MFI readout for samples tested using GuHCl-treated and untreated antigen coupled MagPix microsphere beads.

Figure 5.51b Scatterplot showing the correlation between GuHCl-treated and untreated antigen-coupled MagPix Microsphere beads

Figure 5.52 Dot plots of avidity index at three GuHCl concentrations.

Figure 5.53 Representative graphs to show the change in the avidity index over incubation time.

Figure 5.54a Scatter plot of Log10 MFI by antigens.

Figure 5.54b Scatter plot of avidity index by antigens. AI is the percentage of the avid antibody of the total measured by MagPix luminal in a multiplex assay.

Figure 5.54c Avidity index representative antigen for representative participants across time-points.

Figure 5.55a Comparison of median MFI between T2 and T4.

Figure 5.55b Comparison of median avidity index between T2 and T4.

Figure 5.56 Plot of $\Delta \log_{10} \text{MFI}$ values shows the net MFI changes of the total (red circles) and avid antibody (blue squares) responses between T2 and T4.

Figure 5.57a Association of avidity index with days since parasitemia adjusted for age.

Figure 5.57b Association of avidity index with the proportion of months free of infection in the last 12 months, adjusted for age.

Figure 5.58a Association of Log10MFI with Days since parasitemia. Coef and 95% CI of the total (red), and avid antibody (blue).

Figure 5.58b Association log10MFI with the proportion of months free of infection in the last 12 months.

Figure 5.59a Association of avidity index with age in a GEE model adjusted for days since the last infection. Age category 1-4 years was the reference

Figure 5.59b-d Association of the total and avid antibody with age

Figure 5.510 Summary of the B cell reaction demonstrating the potential cause of low avidity index during chronic infection and high avidity index in the absence of infection.

Figure 6.51a - c Dot Plot of log10MFI for by malaria blood-stage antigens categories

Figure 6.52 GAM plots of estimated best fit Log10MFI responses against days since the last infection.

Figure 6.53a, b, c Association of Log10 MFI with days since the last infection

Figure 6.54a – c Log10 MFI IgG1 and IgG3 by age categories.

Figure 6.510 Examples of ROC curves for antigens ETRAMP5Ag1 Ag2Ag1, HSP40 AG1 Ag1, MSP1-19 for total IgG, IGg1 and IgG3

Figure 6.511 illustration the antibody source and destruction during acute infection and no infection.

List of Tables

Table 1.7 Summarize the properties of IgG subclasses (40)

Table 1.5 Summary of the malaria vaccine in Human trials

Table 3.2.Characteristics of study Districts

Table 3.4 Summary of the study population and malaria matrix by time-points

Table 3.5 Summary of the *P. falciparum* Blood-stage antigens

Table 3.7 Summary of the antigens concentrations required for large batch coupling

Table 3.8 Characteristics for the cross-sectional surveys

Table 6.55 Summary of population-based estimates of half-life

Table 6.511 Summary of AUC for defining infection status at 90 days

Chapter 1

1.1 Introduction to Malaria

Malaria is a mosquito-borne disease caused by obligate parasites of *Apicomplexa* phylum (1). There are 5 species known to cause malaria in humans, including *Plasmodium falciparum*, *Plasmodium vivax*, *Plasmodium ovale*, *Plasmodium malariae*, and most recently, zoonotic *Plasmodium knowlesi*, whose natural hosts are Macaques (2–4). Most deaths are caused by *P. falciparum* in endemic sub-Saharan Africa, and *P. vivax* contributes significantly to the disease burden outside of sub-Saharan Africa (4).

This section describes the malaria life cycle and global malaria trends (with a focus on Uganda). Also, the section describes malaria elimination efforts, interventions, and new global elimination targets and obstacles.

This thesis will focus on *P. falciparum* unless mentioned otherwise.

1.2 Malaria parasite and life cycle

Malaria infection is transmitted from one person to another by the bite from an infected female *Anopheles* mosquito, primarily *Anopheles gambiae* in Africa (5,6). The life cycle can be divided into three phases; (i) asexual liver-stage, (ii) asexual blood-stage, and (iii) sexual mosquito stage.

1.2.1 Asexual liver-stage

The asexual liver stage is initiated when an infective female *Anopheles* mosquito injects *P. falciparum* parasites in the form of sporozoites under the skin (7,8). It is estimated that mosquitoes generally transmit fewer than 100 sporozoites per bite (9) (Figure 1.1, stage 1).

The sporozoites pass quickly into the bloodstream, migrate through Kupffer cells, and translocate into several hepatocytes before infecting the final hepatocyte. This process happens in about nine minutes after injection into the skin to establish the liver stage infection. The speed at which it happens poses a challenge to immune interventions (10,11). The liver infection stage is asymptomatic, and sporozoites undergo cycles of asexual amplification called schizogony that lasts 5 to 10 days. Schizogony results in developing the exoerythrocytic schizont containing as many as 30,000 blood-stage merozoites (12) (Figure 1.1, stage 2-4).

1.2.2 Asexual blood-stage

The asexual blood-stage starts when membrane-bound merozoites, carrying clusters of 1000 - 2000 merozoites, are released into the bloodstream, where they rupture to release the merozoites (13). The merozoites quickly invade red blood cells (RBC) through elaborate interaction and processing of parasite antigens, resulting in attachment on RBC receptors, reorientation, irreversible junction formation between the parasite and RBC membranes, and eventually complete invasion (14,15). The RBC invasion starts the inflammatory asexual blood-stage responsible for the clinical symptoms (16) (Figure 1.1 stage 5). Merozoites inside the RBC

transform into ring stage trophozoites and then to schizonts containing 6 – 36 merozoites (17). After approximately 48 hours, the schizonts rupture in a synchronized manner, releasing merozoites into the bloodstream that quickly infect new RBC to repeat the blood-stage cycle(18). Some parasites infecting RBC differentiate into male or female gametocytes that circulate independently in the peripheral blood. *P. falciparum* gametocytes appear in peripheral circulation after about 7 to 15 days after the initial invasion of erythrocytes (19) (Figure 1.1, stage 6) and are not associated with clinical symptoms.

1.2.3 Sexual mosquito stage

Anopheles mosquito feeding on infected human blood ingests gametocytes to initiate the sexual mosquito stage (Figure 1.1, stage 7-8). The mosquitos are attracted to infected humans by volatile compounds that are either secreted by the parasite or skin bacteria, and this co-evolutionary adaptation increases parasite transmission success (20,21). A decrease in temperature triggers male gametes to flagellate within minutes of ingestion by mosquitos and fuse with the female gamete to form a diploid zygote where meiosis occurs to form haploid zygotes (22) (Figure 1.1, stage 9). The haploid zygote differentiates into an invasive ookinete that penetrates the gut wall and attaches to the mosquito gut's outer aspect (23) (Figure 1.1, stage 10-11). The ookinete differentiates into oocyst that matures and ruptures to release sporozoites (Figure 1.1, stage 12). The sporozoites penetrate the salivary glands and rest in the channels bearing saliva, awaiting access to the next human bite for the cycle to start again (24) (Figure 1.1, stage 13).

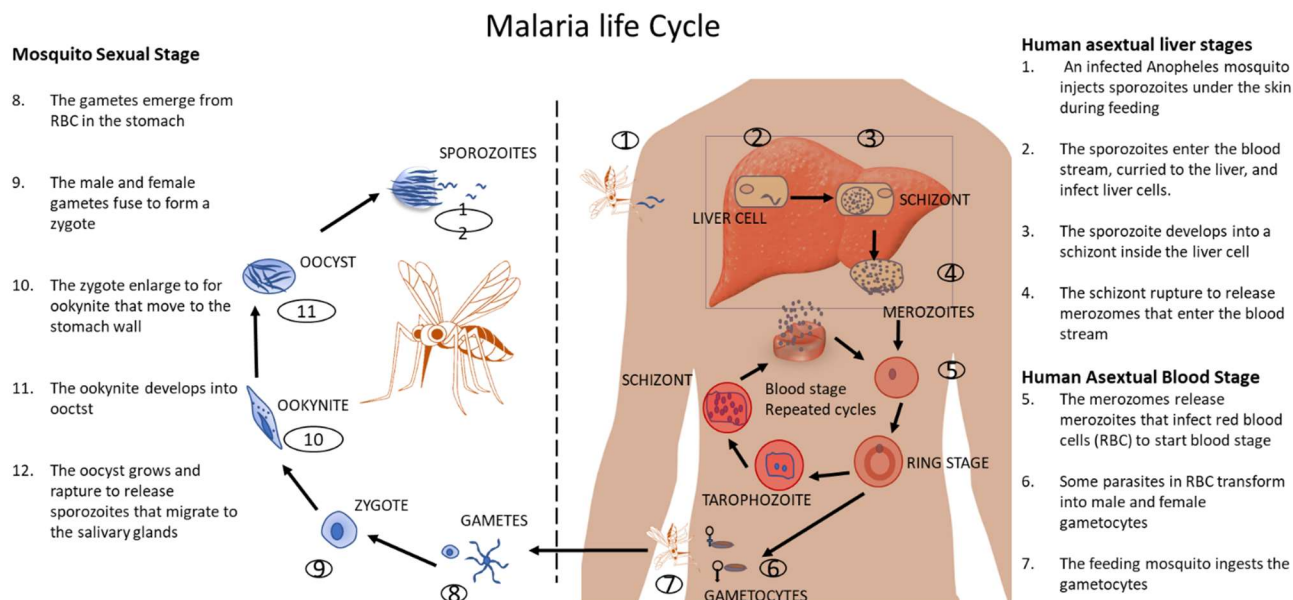


Figure 1.1 Life Cycle of Malaria describing the three stages

The asexual liver and blood-stage s complete in humans, and the sexual stage in mosquitos. The blood-stage is responsible for the pathology of the infection (25)

1.3 Global Malaria Trends

The global malaria burden has progressively declined over the last decade and a half, with the most remarkable progress seen between 2010 and 2015. An estimated 1.3 billion fewer malaria cases and 6.8 million fewer deaths occurred globally during this period(4). Malaria incidence declined by 21% and deaths by 29% globally (Figure 1.2 a&b). In the same period, up to 13 countries were declared malaria-free after reporting no indigenous case for at least three consecutive years.

Much of the progress we can attribute to the increased investment resulted in improved health care systems and scale-up of preventive, vector control, and case management interventions, especially in endemic countries (26).

Despite the previous progress, malaria remains a significant burden were 3.4 billion people in 91 countries are still at risk. WHO malaria report of 2017 indicated a setback in previous gains where more malaria cases were estimated at 216 million in 2016 compared to 211 million in 2015 and hardly any reduction in reported deaths; 445,000 in 2016 compared to 446 000 in 2015 (27).

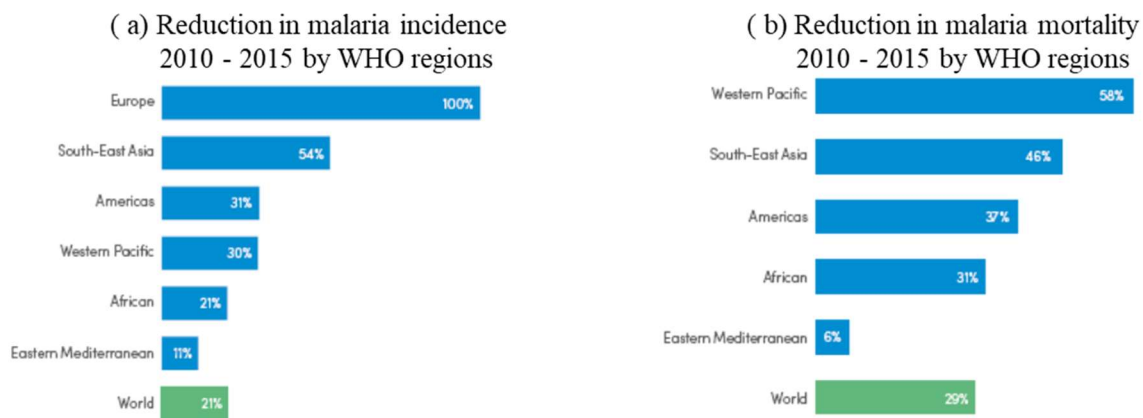


Figure 1.2 Reduction in malaria incidence (a) and mortality (b) by WHO regions between 2010 and 2015. African east Mediterranean areas with *P. falciparum* registered the least reductions in both incidence and mortality. (4) The figure was reproduced under a Creative Commons license.

1.4 Malaria status in Uganda

In the eastern part of Africa, Uganda is the 9th of the 15 countries, contributing 80% of the *P. falciparum* infections in 2016 (27). Uganda has an estimated population of 41 million by 2018, all at risk of malaria. In 2016 alone, 7.7 million malaria cases accounted for 4% of the world malaria cases and 12,060 deaths, mainly in children under five years (27). The annual numbers implied 16 malaria cases per minute, and one malaria-related death occurred every 35 minutes in 2016 alone. Hospital records suggest that malaria is responsible for 30 to 50% percent of outpatient visits, 15 to 20% of admissions, and 9 to 14% of inpatient deaths.

Uganda was among the countries that registered a 40% reduction in incidence between 2010 and 2015. In the same period, there was procurement and distribution of over 30 million free bed nets, which increased net ownership by up to 62%. Uganda is among the countries that threatened to lose the gains due to increased malaria cases by over 50,000 in 2015 – 2016.

Malaria transmission in Uganda is majorly by the vectors *A. gambiae* and *A. funestus*. Malaria is highly endemic in almost all parts of the country. Transmission occurs throughout the year, with seasonal variation peaks occurring at the end of the two rainy seasons (September to November and March to May)(28). Very high entomological inoculation rates (EIR) , a measure of the infective mosquito bites per person per year, have been recorded in Uganda. EIR rates as high as 1,586 were recorded in Apac in 2006 (29), and 306 in Tororo District in 2012 (30).

1.5 Malaria control strategies

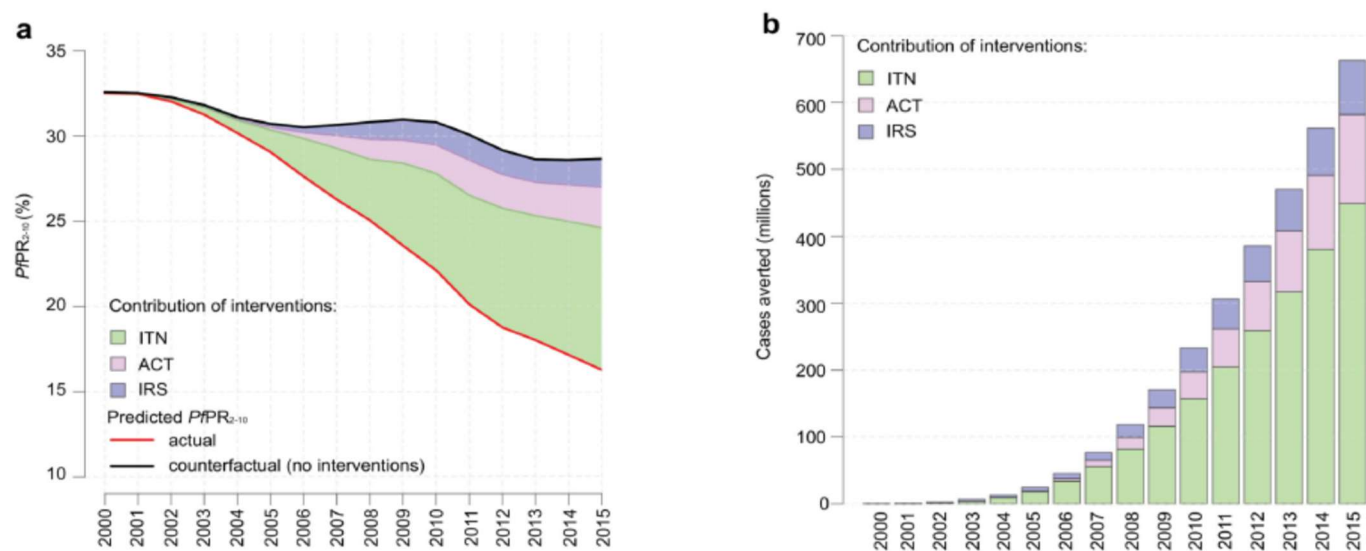
Substantial progress has been made over the past few years to reduce the global malaria burden through vector control and case management. The most widely used vector control measures include insecticide-treated nets (ITN), indoor insecticide residual spraying (IRS). Malaria cases are managed using artemisinin-based combination therapies (ACT) and intermittent preventive therapy for pregnant women using sulphadoxine-pyrimethamine.

The Roll Back Malaria initiative began in 1998 (31), followed by the Global Fund to Fight AIDS, Tuberculosis, and Malaria (GF). The later stimulated funding targeted towards meeting the United Nations millennium development goal C6, which aimed to halt by 2015 and begin to reverse the incidence of malaria and other major diseases (32). These initiatives resulted in a gradual scale-up of mainly insecticide-treated bed nets (ITN) and limited insecticide indoor residual spraying (IRS) in all malaria-endemic countries in the last decade. ITN use increased from below 3% to 53% between 2011 and 2015. IRS use rose from 5% to 11% covering 153 million people at risk, and approximately 50% of these living in high burden countries of sub-Saharan Africa. In the same period, over 56% of the population in sub Saharan Africa at risk of malaria slept under a mosquito net in 2015 mainly through mass distribution campaigns (27). It is estimated that 70% of the malaria cases averted between 2001 and 2015 were due to the implementation of malaria control interventions (Figure1.4). ITN, ACT, and IRS contributed 78%, 19%, and 13% respectively to the malaria cases averted due to the interventions ACT and

IRS interventions had larger proportional contributions where their coverage was high (Figure 1.4) (26)

Not all the reductions in malaria are attributed to preventative interventions. There is evidence to suggest that increased urbanization and overall economic development, which led to improved housing and nutrition, contributed to the decline in malaria prevalence (33–35).

The current interventions do not directly target asymptomatic and sub-patent infections, which promote a sizeable human reservoir. This reservoir fuels new infections when interventions are relaxed, and this is a big obstacle for countries to progress from malaria control to the malaria elimination phase. Other interventions like mass drug administration and intermittent preventive treatment provide high prospects. However, they pose prohibitive cost barriers and risks of drug resistance. Vaccinations against the liver stage infection and gametocytes are other prospects, although they face suboptimal efficacy and short-lived immunity challenges.



1Figure 1.4 Reduction in *P. falciparum* malaria burden and contribution of interventions in endemic African countries between 2000 and 2015. 1.4a show predicted parasite rate among children 2 – 10 years. The black line shows the expected rate if no interventions (counterfactual), and the red shows the actual rates with interventions. The different colors show the contribution of each of the three interventions. The parasite rate is estimated to have reduced by 50%, from 32% in 2000 to 16% by 2015. 1.4b shows the cumulative number of malaria cases averted in same endemic Africa due to the three interventions and their relative contribution by the different colors. Over 650 million malaria cases were prevented by 2015 (26) *The figure was reproduced under a Creative Commons license.*

1.6 Malaria elimination campaigns; the past, the present, and the future

WHO initiated Malaria eradication campaigns in the late 1940s to set the foundation for the global eradication of malaria. This campaign succeeded in eliminating malaria from Europe, North America, the Caribbean, and Asia and South-Central America (36,37). The campaign registered little success in Africa due to technical and political limitations, including high illiteracy levels, poor health infrastructure, and civil wars (38). Increased malaria burden in the 1980s and 1990s renewed the call to control malaria. It led to initiatives like Roll Back Malaria, Global Fund to fight HIV, malaria, tuberculosis, and the Presidential Malaria Initiative. These global frameworks set targets and strategies, increased advocacy, and funding that promoted increased investments towards malaria control and elimination. The approach and investments guided by the millennium goal C6 led to a scale-up of malaria control interventions and reduced malaria observed between 2000 and 2015.

The new UN Sustainable Development Goal 3C calls for reducing malaria mortality and morbidity by at least 90%, eliminating malaria in 35 countries, and preventing reestablishment in those with confirmed elimination by 2030 (39). WHO further outlined the strategy in the WHO Global Technical Development Goals for Malaria 2016-2030. The strategy included three pillars: (i) ensuring universal access to malaria prevention, diagnosis, and treatment, (ii)

accelerating efforts towards elimination and attainment of malaria-free status, (iii) and transforming malaria surveillance into a core intervention (40).

However, the new goals face challenges, especially in high malaria transmission intensity areas where recent WHO findings reported stalled progress or tendency towards increased malaria incidence and deaths in the 2017 malaria report. Such challenges include (i) stalled investment, (ii) political/civil unrest, uneven elimination progress by counties or within a country, (iii) risk of drug resistance against ACT and slow discovery pipeline of new cost-effective drugs (41), (iv) lack of drugs that effectively target gametocytes (42,43), (v) lack of cost-effective rapid diagnostic and surveillance tools (vi) insecticide resistance (44–46).

Overcoming the challenges calls for advocacy to promote funding, additional new and highly rigorous interventions, and surveillance tools. There is a need to identify asymptomatic and sub-patent infections known to fuel transmission and are not detected by the current conventional methods (47,48). Secondly, uneven progress towards elimination poses a high risk of epidemic outbreaks of severe malaria in non-immune populations. Therefore, it is critical to understand how immunity to malaria is acquired, maintained, evaded, or interrupted by the parasite, to accelerate efforts towards developing effective vaccines and other immunotherapies.

1.7 Malaria Pathogenesis, Diagnosis, and Treatment

Malaria is one of the leading causes of death globally. The interaction of the host immune reaction and the asexual blood-stage is the primary cause of malaria pathology. The disease diagnosis and treatment strategies target its highly inflammatory asexual blood-stage.

This section will describe malaria pathogenesis, diagnosis, and treatment.

1.7.1 Malaria pathogenesis

Symptoms in malaria develop when the asexual blood-stage cycle emerges. Malaria is characterized by general symptoms such as fever, headache, fatigue, muscle pain, and diarrhea, mainly due to the parasite's inflammatory immune response and toxins (49,50). The onset of fever is associated with a parasite load above a threshold referred to as pyrogenic threshold. In high malaria-endemic regions, the pyrogenic parasite threshold increase with age and exposure (51,52). Malaria can present as severe or uncomplicated based on the life-threatening pathology. The risk of occurrence of severe forms of malaria such as cerebral malaria (CM), lactic acidosis, respiratory distress and failure, severe anemia, among others, reduce with age (51,53,54) and with the number of pregnancies in the case of placental malaria (55). Severe malaria in *P. falciparum* infection is mainly due to; (i) sequestration of infected red blood cells in the microvasculature, mediated by cyto-adhesion molecules (ii) anemia direct destruction of erythrocytes, dyserythropoietic, and autoimmunity.

Parasite sequestration occurs inside small and medium-sized blood vessels and in tissues like the brain and placenta. Variants of *P. falciparum* erythrocyte membrane protein 1 (PfEMP1) mediate the sequestration (56) and host adhesion molecules such as CD36, ICAM-1, VCAM (57,58). PfEMP1 is a clonally variant set of proteins exported on infected erythrocytes' surfaces and encoded by the var gene family (59–61). The sequestration results in high parasite load due to parasite avoidance of clearance in the spleen (62), leading to detrimental local inflammation, host endothelial cell injury, and microvascular obstructions (63). The clinical effect of parasite sequestration depends on the organ involved and different PfEMP1 variants associated with a particular complication. In the brain, parasite sequestration is associated with cerebral malaria characterized by coma, and in the lungs, it results in respiratory distress or failure (64). In pregnancy, the PfEMP1 variant VARCSA causes cytoadherence to chondroitin sulfate A in the placenta to cause placental malaria (65,66). Placental malaria is characterized by an increased risk of abortion and stillbirth, preterm labor, and low birth weight (55,67).

Chronic anemia is a common feature of *P. falciparum* infection pathology. It results from direct destruction of erythrocytes, increased hemolysis of uninfected RBC, and bone marrow suppression resulting in dyserythropoiesis (68,69). On the other hand, Anaemia is linked to the host protective mechanism against the parasite, dependent on a high iron requirement for liver and blood-stage growth (70).

1.7.2 Malaria diagnosis and treatment

Malaria diagnosis is usually made using thin or thick blood smear and light microscopy, which is regarded as the standard gold method. The shortfall to microscopy requires a 1000x magnification, a highly trained microscopist, and failure to detect sub patent infection below 50-100parasites/ μ l (71).

Rapid diagnostic tests (RDT) that test for parasitic proteins such as histidine-rich protein-2 (HRP2) and lactate dehydrogenase aldolase in blood samples are more widely used have improved access to malaria diagnosis. The limitation to the HRP2 RDT is the protein deletion, especially in Southeast Asia (72,73). Some studies in several African countries, including Kenya, Rwanda, and Eretria, reported HRP2 deletions (74–76). Its distribution and prevalence in sub-Saharan Africa are not fully known, and increased use of HRP2 for diagnosis poses a potential risk for selecting HRP2 deletions (77). The second limitation is the persistence of the protein after parasite clearance, especially in ACT-based treatment, resulting in the accumulation of previously infected cells and can lead to false-positive readings (78).

For malaria control interventions that require active identification of malaria cases for treatment, microscopy, and parasite protein RDT are adequate. However, in the new era of malaria elimination, identifying any infections form is essential and renders the two methods inadequate. Current molecular techniques such as loop-mediated isothermal amplification (LAMP) and quantitative polymerase chain reaction (qPCR) can detect down to 0.01parasites/ μ l (79,80). These molecular methods are expensive, labor-intensive, and not suitable for massive public

health diagnosis. In the wake of malaria elimination, simple, cheaper, and rapid tests with the capacity to diagnose sub patent infections are required.

1.8 Acquired immune responses to malaria

In a typical malaria-endemic area, severe malaria occurs mainly in children, and as they grow older, they continue to suffer but from uncomplicated forms of malaria. By middle school, these children endure a high parasite burden without fevers. Eventually, in adulthood, the prevalence of chronic infection and parasite density reduces, and rarely do adults suffer from clinical malaria. In a typical household in endemic areas, the children will suffer from many malaria episodes but hardly any among their parents despite having the same risk of exposure. Despite these epidemiological indications of the gradual acquisition of immunity to malaria, correlates and mechanisms that mediate immunity are not fully understood.

This section describes the malaria immunity manifesting in distinct and overlapping forms, the role and evidence of humoral immunity, and efforts towards developing malaria vaccines and serological tools for diagnosis and surveillance.

1.8.1 Immunity to severe disease

In endemic areas, infants are highly susceptible to life-threatening malaria once they are infected. They rapidly overcome the severity of the disease but continue to suffer from milder forms. The reduction in risk of severe disease is termed as severe malaria immunity. The relationship between age and severe malaria immunity is dependent on the transmission setting. Immunity to

severe forms of malaria is acquired very early in life in the high transmission area and delayed with age in the low and unstable transmission areas. Severe malaria manifests, most commonly as cerebral malaria, severe anemia, and respiratory distress. Immunity to non-cerebral forms of severe malaria is acquired earlier after one to two infections, but immunity to cerebral malaria is acquired much later (81). Maternal transfer of immunity may explain early immunity's rare occurrence to the non-cerebral severe malaria forms among infants from high endemicity regions (54). These children emerge from maternal protection with the significant acquisition of their severe malaria protection associated with acquiring antibodies against PfEMP1 (81,82).

Cerebral malaria is associated with the sequestration of the parasite in the brain, mediated by parasite PfEMP1 and intercellular adhesion molecule 1 (ICAM-1) receptor, among others that lead to inflammatory pathology (83,84). A discrete set of PfEMP1 antigenic types that are not only common but also induce strain-specific immunity are thought to cause Cerebral malaria (85). Severe malaria occurs in a small proportion of the population, and this may be due to host immunological and genetic factors (86,87). Haemoglobin S has long been known to play an essential role in severe malaria. Polymorphisms in other genes like the tumor necrosis factor- α , major histocompatibility complex, interleukin receptors, toll-like receptor-4, among others, have been associated with severe malaria (86,88–91).

1.8.2 Anti-disease Immunity

As the children grow older in endemic areas, they increasingly become tolerant to high parasite load without developing a fever. The ability to tolerate high parasite load upon infection without developing clinical symptoms or having a high pyrogenic threshold is anti-disease immunity (92). This phenomenon is more pronounced among children to adolescents in high endemic areas where the pyrogenic parasite threshold can exceed 60,000 parasites/ μ l (51,52,92). Malaria symptoms result from the inflammatory response against parasite antigens and toxins. Therefore, immune tolerance or regulatory mechanisms, among others, are thought to mediate anti-disease immunity. Several studies show that chronic asymptomatic infection is associated with lower levels of pro-inflammatory cytokines, including tumor necrosis factor-alpha (TNF- α), interferon-gamma (IFN- γ), interleukin (IL)-1 β , IL-2, IL-6, IL-8, and IL-12 (93–95).

On the other hand, asymptomatic infections characterized by high parasite density are associated with increased anti-inflammatory cytokines, including IL-4, IL-7, IL-10, and IL-13 (96–98). Furthermore, loss of innate-like $\gamma\delta$ T-cells and alteration of their pro-inflammatory cytokine secretion profiles is associated with reduced clinical disease risk (99). anti-disease immunity is thought to be short-lived and may require continuous exposure to maintain. A study in Papua New Guinea showed that the odds of children presenting with malaria increased by 4 times after 8 years of malaria control, implying loss of anti-disease immunity. However, this study did not indicate whether the children's pyrogenic threshold was lowered (100). (100)(100)While adults are less likely to develop symptomatic malaria when infected in endemic areas, when they do,

the parasite density associated with fever is lower than in children (101). This observation may imply loss of anti-disease immunity at the cost of anti-parasite immunity in adults. It is important to note that no vaccine or therapeutic intervention currently in the development pipeline targets anti-disease immunity. Such a vaccine can play an essential role in preventing severe disease burden in case of reemergence in areas that have eliminated or are near elimination.

1.8.3 Anti-parasite immunity

In a typical endemic area, the prevalence of parasite and geometric mean parasite density decrease with age. Some adults will harbor parasites below the microscopic level but detectable by molecular methods(sub-patent). The ability to control parasite density to very low levels, up to sub-patent level, is anti-parasite immunity. This form of immunity is observed mainly in adults living in endemic areas, and there is a tendency of early acquisition in areas of high compared to low transmission (102). Anti-parasite immunity is acquired cumulatively as a function of age and exposure (92). In Papua New Guinea, the age at which *P. falciparum* density peaked shifted from 10 to 15 years after 4 years of sustained malaria control, implying a delayed acquisition of anti-parasite immunity when exposure is lowered (100). Anti-parasite immunity is targeted mainly against the blood-stage and mediated by innate and adaptive effector mechanisms where antibodies play a significant role (24,103,104).

Furthermore, immune tolerance thought to mediate anti-disease immunity can contribute to anti-parasite immunity by preventing activation of endothelial cells resulting in down-regulation of

adhesion molecules hence preventing *P. falciparum* cyto-adhesion. Failure of infected red blood cells to sequester in the microenvironments increases their clearance in the spleen, resulting in a reduction in parasite density. Anti-parasite immunity is not efficient at parasite elimination and does not seem to protect from new infection. Superinfection or complexity of infections are commonly observed in individuals who maintain low parasite densities, and the same conditions can last up to 180 days (105,106). One possible explanation is the inefficient acquisition of immunity to the asexual liver-stage, which allows for superinfections to occur. Lack of immunity to asexual-stage is supported by observing the clearance of chronic parasitemia in some individuals when the transmission is interrupted (107). It is also likely that the tolerance mechanisms that drive anti-disease immunity result in inefficient parasite clearance (108,109).

Failure to develop sterile immunity bears the consequence of maintaining parasite reservoirs that fuel new infections and, therefore, a significant obstacle to malaria elimination. The anti-disease immunity and anti-parasite immunity are both acquired in parallel as a function of age and exposure (92). While immune tolerance may potentially hamper effector mechanisms that mediate parasite clearance, there is no information about how the acquisition of anti-disease immunity affects the acquisition and maintenance of anti-parasite immunity.

1.8.4 Sterile immunity

The ability to abort or extinguish infection is defined as sterile immunity. It is rare and difficult to demonstrate in a natural setting. Sterile immunity has been shown in controlled human malaria

infection (CHMI) after vaccination with irradiated sporozoites (110,111) and in live non-attenuated sporozoites under chloroquine or mefloquine chemotherapy (112). The duration and efficacy of sterile immunity against natural exposure to many variant strains are poorly understood. This form of immunity is mediated by mechanisms that target the liver stage and prevent the emergence of blood-stage infection or arrest the early blood-stage emergence. Immune compartments such as CD4 T cells, CD8 T cells, $\gamma\delta$ T cells, and antibodies are involved in mechanisms that mediate sterile immunity (112–114). Sterile immunity is rare and difficult to demonstrate in natural infections due to lack of a direct measure of exposure and lack of protection correlations. However, there is still a proportion of individuals in high transmission areas, mostly adults, who are free from infection even by sensitive molecular tests and for an extended period even when they share households with chronically infected children. Both genetic and immunological mechanisms likely contribute to sterile immunity, but their independent effects are not known. Vaccination and CHMI studies indicate that sterile immunity protection is likely short-lived and may be strain-specific (115,116).

1.8.5 Evidence for the role of antibody responses in immunity to malaria

Antibody-mediated immune responses contribute significantly to the acquired immunity phenotypes against *P. falciparum* (described above; 1.81- 1.84). The importance of the antibody response is demonstrated by (i) the passive transfer of immunoglobulin that reduces parasitemia (anti-disease and anti-parasite immunity) (117,118), (ii) the role of maternal transferred IgG in protecting newborns from severe disease (anti-disease) (119–121) (iii) epidemiological studies

that show a positive association between parasite-specific antibodies with protection from symptomatic or severe malaria (61,122–128). (iv) in-vitro antibody-mediated function assays show parasite growth inhibition and destruction of infected red blood cells by complement-fixing, phagocytosis, and antibody-dependent cytotoxicity (ADCC) (129–134).

Overwhelming evidence for antibodies' role in natural immunity has led to a quest for vaccine strategies targeting antibody response across different life cycle stages.

1.9 Malaria vaccine

Vaccination is the holy grail of immunology, but the development of a malaria vaccine has eluded immunologists for more than 50 years since the proof of concept with irradiated sporozoites in mice (135). While antimalarial chemotherapies suffer from repeated medication, drug resistance, and drug tolerance, toxicities, and poor adherence, vaccination has been superior in containing infection when it is available. Near eradication of polio and smallpox diseases has been due to successful and effective vaccination campaigns (136,137). The rationale for a malaria vaccine is based on the epidemiological observation of the naturally acquired immunity previously described. Furthermore, the rationale is supported by the acquisition of immunity following the transfer of purified immunoglobulin from immune individuals to malaria-ridden children that drastically reduced parasite density and improved clinical prognosis (117,118,138).

This section provides updates on the different malaria vaccine approaches targeting various malaria life cycle stages and the current vaccine development status.

1.9.1 Vaccines targeting liver Stage: RTS, S/AS01 as an example of a subunit vaccine

The malaria vaccine concept was first demonstrated in mice using Irradiated sporozoite, followed by a challenge with *P.berghei* parasites. The vaccination challenge arrested the appearance of blood-stage merozoites responsible for the clinical disease (135). Similar challenges with irradiated sporozoites in humans, followed by controlled human malaria infection, yielded comparable results (110,111,116). However, sporozoites' mass production's difficulty led to the search for subunit vaccines. RTS, S/AS01 is the most advanced malaria subunit vaccine evaluated for efficacy in Phase III human clinical trial. RTS, S/AS01 is made up of a virus-like particle comprised of two components; 18 copies of the central repeat and the C-terminal domain of CSP fused to hepatitis B virus surface antigen (HBsAg) with extra HBsAg in a 1:4 ratio (139). In phase III clinical trial, RTS, S/AS01 failed to induce sterile immunity in endemic areas, but it showed protection from severe disease forms. The vaccine efficacy varied across malaria transmission intensity sites; protection waned within 18 months and was age-dependent (139). The mechanisms that mediated partial RTS, S/AS01 immune-protection are not fully understood. Nonetheless, existing data strongly suggest that high antibody concentrations against the NANP amino acid repeats are strongly associated with protection (140). The waning of such antibody responses is likely to be responsible for decreasing efficacy. In addition to antibody, CD8⁺ and CD4⁺ T cell responses play some role in protection (140). Different vaccination strategies reveal additional insight into mechanisms that mediate RTS, S/AS01, pointing towards the innate immune cells, early B-cell transcription signature, IgG subclass,

among others(141,142). The impairments of the different immune compartments, immune-tolerance, and exposure to multiple parasite strains in endemic areas may contribute to the vaccine's low efficacy of the vaccine observed in endemic areas.

Reviewed in (143), several design strategies to improve RTS, S/AS01 efficacy, and protection are underway. These include (i) use of improved adjuvants to enhance the longevity of high antibody titer, (ii) modification of dose and schedule that seem to affect isotope switching associated with improvement in protection in the preliminary phase II clinical trial findings (141) (iii) reduction of 4-fold excess HBsAg to increase anti-NANP IgG and reduce anti-HBsAg IgG to increase CSP antibody target epitopes per dose, (iv) use of full-length CSP containing the N-terminal non-repeat region to increase antibody targets for epitopes not present in RTS,S (144) (v) structure-based vaccine design that involve isolation of monoclonal antibodies from humans exposed to an infection or by a vaccine that shows potent neutralizing function. The structure of the epitope bound by the monoclonal antibody is determined at atomic resolution. This information is used to design immunogens to elicit antibodies with functional activity (145).

1.9.2 Whole sporozoite vaccines

In addition to subunit vaccines, exploration of whole sporozoite vaccination strategies is underway. These involve the administration of live-attenuated sporozoites that cease development at various stages before the appearance of blood-stage infection or live sporozoites that reach the blood but are eliminated by drugs. Strategies attempted in human clinical trials

under CHMI include (i) irradiated attenuated sporozoites (*Pf*SPZ vaccine) that arrest development at random points early in liver-stage development. *Pf*SPZ vaccine conferred protection in humans in CHMI trials administered by mosquito bites. Its protection was associated with tissue-resident *Pf*SPZ-specific CD8⁺ T cell responses (115,116). (ii) Genetically attenuated parasite (GAP), targeting sporozoite gene knockout like p52-/p36-/sap1, arrest early liver-stage development and was reported as fully attenuated (146–148). (iii) Wild-type sporozoites under chloroquine drug cover allow liver-stage parasite development before being killed upon entry into the blood-stage (149,150). This method was free of clinical disease in CHMI when challenged with homologous, although not heterologous parasites after two years. Overall, whole sporozoite vaccines seem to suffer from the requirement of multiple vaccination boosts, strain specificity, and short-lived protection.

1.9.3 Vaccines targeting blood-stage

Blood-stage vaccines are likely not to induce sterile immunity but to mimic naturally acquired immune phenotypes like anti-disease or anti-parasite. These vaccines will play an essential role in complementing the liver-stage vaccines. Besides, they will boost or maintain naturally acquired immunity in highly endemic areas during elimination campaigns and prevent malaria epidemics if transmission outbreaks occur. Antibodies remain the primary target for these vaccines due to their role demonstrated in naturally acquired immunity and involvement on the effector mechanisms at mediate anti-parasite immunity. In blood-stage malaria, antibodies are essential in mediating protective mechanisms such as blocking red blood cell invasion,

opsonization for phagocytosis, and complement-mediated effector mechanisms, among others (151–153).

Several blood-stage antigens have been tried for vaccine development over the decades but yielded undesirable outcomes mainly due to polymorphisms and redundant invasion pathways (154–156). Advances in high throughput antigen expression and probing technologies like microarray have improved the identification of new vaccine candidates that target highly conserved merozoite epitopes critical to parasite function (157,158).

The most advanced and promising blood-stage vaccine is the *P. falciparum* reticulocyte-binding protein homolog 5 (*PF*RH5). It is highly conserved hence overcoming the problems of polymorphism. It forms an essential interaction with Basigin (CD147), a receptor on the erythrocyte surface during the invasion; therefore, overcoming limitations associated with redundant invasion pathways (159).

Other promising vaccines include subunits against pregnancy-associated malaria using VAR2CSA (160) and chemically attenuated whole-parasite blood-stage vaccine to mimic naturally acquired immunity (161,162). Table 1.5 summarizes leading vaccine candidates in the human clinical trial.

1.9.4 Transmission-blocking Vaccine targeting the sexual Stages

These vaccines target the gametocytes and aim to induce antibodies taken up by mosquitoes during a blood meal, blocking sexual development inside the mosquito. This kind of vaccine will

Table 1.5 Summary of the malaria vaccines in human clinical trials targeting different *P. falciparum* life cycle stages and type of immunity aimed to induce (143).

Vaccine Target	Vaccine Candidate	Targeted Mode of Action	Development Phase
Killing of Infected hepatocytes, Liver Stage	PfSPZ Vaccine	T cell	Phase IIb
	PfGAP3KO	T cell	Phase I/IIa
	PfSPZ-GA1	T cell	Phase I/IIa
	ChAd63 or MVA ME-TRAP	T cell	Phase IIb
	ChAd63 or MVA ME-TRAP (IV route)	T cell	Phase Ia
	ChAdOx1-MVA LS2	T cell	Phase I/IIa
Inhibition of Merozoite, Blood Stage	ChAd63-MVA	Antibody	Phase Ia/Ib
	RH5.1/AS01	Antibody	Phase I/IIa
	PFAMA1-DiCo/Alhydrogel or GLA-SE	Antibody	Phase Ia/b
	P27A/Alhydrogel or GLA-SE	Antibody	Phase Ia/b
	BK-SE36 [PfSERA5]/Alhydrogel ± CpG	Antibody	Phase Ia/b
	PfPEBS/Alhydrogel	Antibody	Phase I/IIa
	ChAd63-MVA PvDBP_RII	Antibody	Phase I/IIa
	PvDBPII/GLA-SE	Antibody	Phase Ib
Prevention of iRBC-mediated pathology, Blood Stage	PAMVAC/Alhydrogel or GLA-SE or GLA-LSG	Antibody	Phase Ia/b
	PRIMVAC/Alhydrogel or GLA-SE	Antibody	Phase Ia/b
Inhibition of sporozoite infection, transmission blocking	RTS,S/AS01	Antibody	Pilot implementation
	RTS,S/AS01 “Fractional Dose”	Antibody	Phase IIb
	R21/Matrix-M	Antibody	Phase I/IIa and Ib
	R21/AS01	Antibody	Phase I/IIa
	FMP012 [PfCelTOS]/GLA-SE or AS01	Antibody	Phase I/IIa
Inhibition of sexual-stage development, Mosquito Stage	ChAd63-MVA Pfs25-IMX313	Antibody	Phase Ia
	Pfs25-EPA/Alhydrogel or AS01	Antibody	Phase Ia/b
	Pfs230D1M-EPA/Alhydrogel	Antibody	Phase Ia/b
	Pfs25 VLP-FhCMB/Alhydrogel	Antibody	Phase Ia

1.10 IgG structural features that determine the function

There are five immunoglobulin isotypes in humans: IgM, IgD, IgG, IgA, and IgE. IgG is the most abundant, accounting for about 10 - 20% of plasma protein (165). IgG is the primary antibody type secreted by plasma cells derived from memory B-cell and is the major isotype involved in adaptive immune responses. Like the other isotypes, IgG is a heterodimeric protein composed of two identical 50 kDa heavy and two 25kDa light chains, which are paired by both non-covalent and inter-chain disulfide bonds (Figure 1.6a). The light chain consists of either kappa (κ) or lambda (λ) chains. The N-terminal of each of the chains contains a variable region that determines the antibody's specificity (Figure 1.6a). The C-terminal consists of the constant region made up of constant (C) domains. Both light chains contain only 1 CL domain, whereas heavy chains contain 3C_H domains. The heavy chains include a spacer hinge region between the first (C_{H1}) and second (C_{H2}) constant domains. The C_{H2} and C_{H3} of the heavy chains make up the crystallizable component (Fc) of the antibody, which mediates the antibody's effector function (Figure 1.6a). The V_L, C_L, V_H, and C_{H1} make up the antibody binding fraction (Fab) that mediates the antibody's specificity.

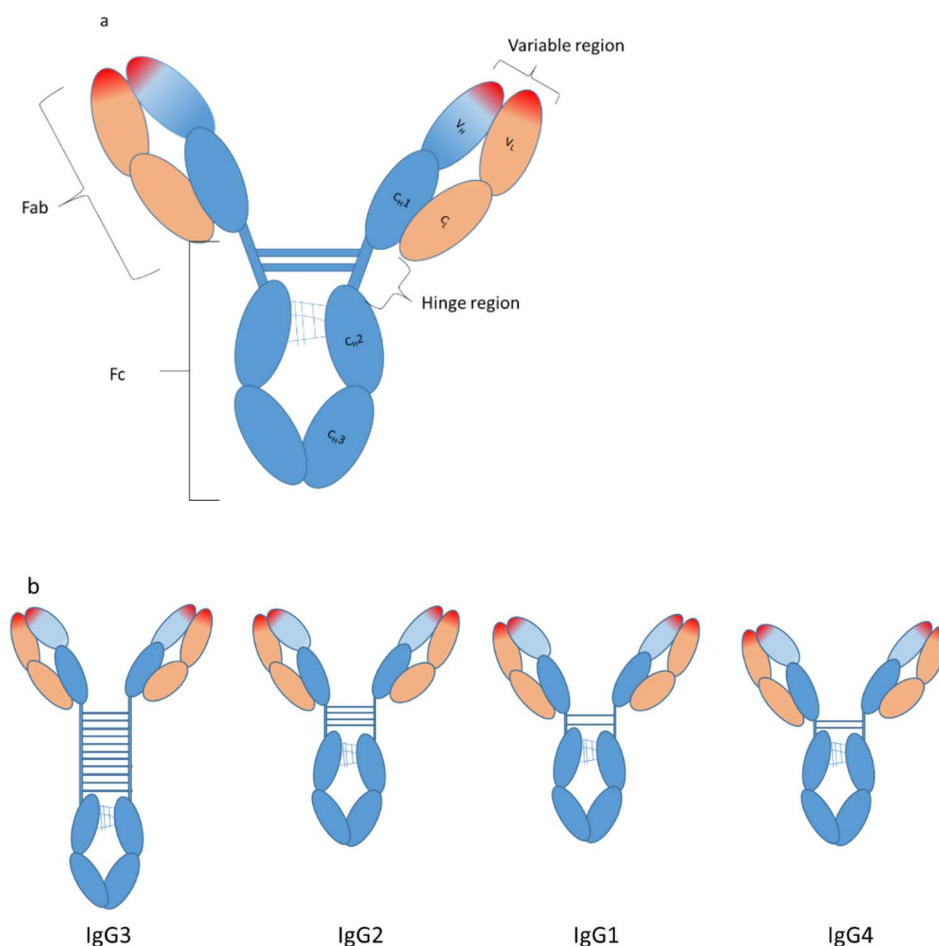
IgG can be subdivided further into subclasses that differ structurally and functionally (Figure 1.6b).

This section will highlight the different properties of IgG subclasses that are important in acquiring, function, and maintaining immunity.

1.11 Differences in IgG subclasses structures that affect half-life and function.

There are four IgG subclasses named in order of decreasing abundance IgG1 > IgG2 > IgG3 > IgG4 (166). All four subclasses have the same basic IgG structure and share more than 90% homology (165). However, there are differences in surfaces of exposed amino acid residues on the C_H1, C_H2, and C_H3 and substantially higher variation in the hinge region (165) (Figure 1.6b). These variations define the differences of IgG subclasses' unique profiles for antigen binding, immune complex formation, complement activation, triggering of antibody-mediated effector cell function, susceptibility to proteolytic enzyme activity, half-life, and placental transport. The subclasses exhibit variations in asparagine N-linked glycan composition between the C_H2-C_H3 junction (N297) that forms the overlapping regions of engagement for complement C1q and Fc-γ receptors and that result in variation in subclass effector function (167,168). The Fc region of IgG3 has the most elongate hinge region, followed by IgG1, with IgG2 and IgG4 having the shortest (Figure 1.6b). The length of the hinge confers flexibility and easy accessibility to effector function. As a result, IgG3 has the highest affinity for the Fc-γ receptors (FcγR) (169). The C_H2-C_H3 domains also contain the binding region for the neonatal Fc receptor (FcRn) responsible for recovering IgG from scavenging epithelial, endothelial, and myeloid cells, translocation of IgG at mucosal sites, and placental transfer (170). The interaction between the C_H2-C_H3 binding site and FcRn is mediated by histidine residual at amino acid position 434 at acidic pH <6.5 of the endocytic vacuoles. IgG3 allotypes (except for H434 containing g3m) with a substitution in this position have remarkably reduced half-life and placental transfer (171). The

low binding of IgG3 to the FcRn result in a shorter half-life of IgG3 of 7 days compared to other subclasses at 21 days (172) and low placental transfer (173).



3 Figure 1.6 Schematic layout of IgG features and subclasses a) Basic structure of IgG composed of two γ heavy chains and two light chains linked together by disulfide bonds. The two identical heavy chains are composed of variable regions, the constant domains CH1, CH2 joined by the hinge region and CH3. The heavy and light chains' variable regions make up the antigen binding and define the antibody's specificity. The hinge, CH2, and CH3 make up the Fc that define the subclasses and contain the Fc γ receptors C1q receptor, Fc γ R, and glycosylation sites that determine the functionality of the antibody. (b) IgG subclasses show their differences in the amino acids and disulfide bonds in hinge regions that influence receptors' subclass affinity. The hinge length is the longest in IgG3 11 disulfide bonds, followed by IgG2 with four and IgG1&4 with two bonds. *The hinge size determines the flexibility of FC than enhancing FcR binding and stability of the complex.*

Table 1.7 summarize the properties of IgG subclasses (165)

General	IgG1		IgG2		IgG3		IgG4	
Molecular mass (kD)	146		146		170		146	
Amino acids in the hinge region	15		12		62		12	
Inter-heavy chain disulfide bonds	2		4		11		2	
Mean adult serum level (g/l)	6.96		3.8		0.51		0.56	
Relative abundance (%)	60		32		4		4	
Half-life (days)	21		21		7/~2		21	
Placental transfer	++++		++		++/++++		+++	
Antibody response to:								
Proteins	++		+/-		++		++	
Polysaccharides	+		+++		+/-		+/-	
Allergens	+		(-)		(-)		++	
Complement activation								
C1q binding	++		+		+++		-	
Fc receptors								
FcγRI	+++	65	-	-	++++	61	++	34
FcγRIIaH131	+++	5.2	++	0.45	++++	0.89	++	0.71
FcγRIIaR131	+++	3.5	+	0.1	++++	0.91	++	0.21
FcγRII b/c	+	0.12	-	0.02	++	0.17	+	0.2
FcγRIIIaf168	++	1.2	-	0.03	++++	7.7	-	0.2
FcγRIIIav158	+++	2	+	0.07	++++	9.8	++	0.25
FcγRIIIb	+++	0.2	-	-	++++	1.1	-	-
FcRn(at Ph<6.5)	+++		+++		++/+++ ^a		+++	

1.12 Antibody affinity and avidity

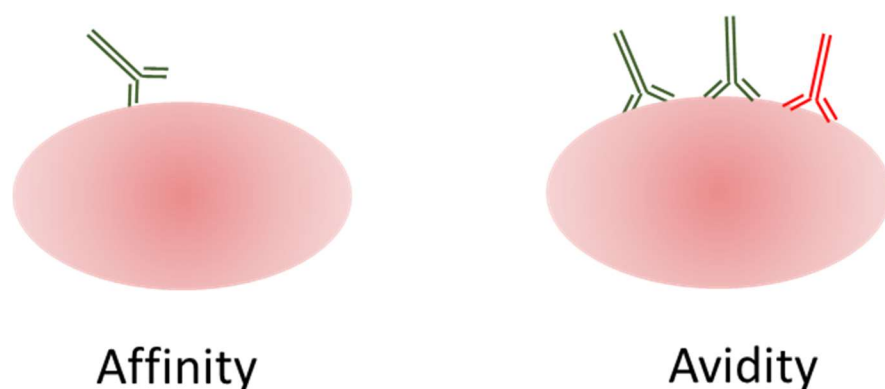
The variable region of the antibody facilitates binding with the antigen and mediates the specificity of the antibody. Binding between antibody and antigen is mediated by non-covalent forces such as Van der Waals forces, ionic force, hydrophobic force, and hydrogen bond. The strength of binding between epitope (single antigenic binding site) and paratope (single antibody binding site) is referred to as affinity. When more than one paratope binds to an antigen's multi-

epitopes, the total binding force is called avidity. Avidity can also be referred to as functional affinity and plays a critical role in the antibody's functioning. For antibodies to mediate functions such as neutralization, it must strongly bind to the antigen and long enough to prevent displacement by the pathogen's competing antigen ligand that mediates cell attachment or entry. Antibodies work in cooperation when interacting with their legends on effector receptors. For example, during complement fixing, the Cq1 molecule binds up to 6 antibodies via the FcR, which improves the complex's stability and allows time to recruit and activate the complement cascade that results in membrane attack complex (174,175). Avidity has been shown to improve following secondary exposure to infection and is associated with naturally acquired vaccines' immunity and efficacy (176–178).

Antibody avidity is commonly measured by disruption of antibody-antigen complexes on the ELISA platform by chaotropic agents (e.g., Urea, sodium thiocyanate, and guanidine hydrochloride) such that they interrupt physical binding forces without affecting the nature of the proteins. The measurement outcome is either the avidity index –the proportion of residue binding antibodies of the total, or the plasma concentration at which 50% of antibody is displaced-functional affinity index (179). This method has been successfully used to measure avidity maturation in vaccination like rubella and MUMPS that induce protective neutralizing antibodies (180–184). It has also been shown to correlate with affinity maturation and the accumulation of antigen-specific MBC populations following cholera (185), *Haemophilus influenza* (176) infections, and *Haemophilus influenzae* type b vaccinations (186). Furthermore, the avidity index

has been shown to distinguish between primary and chronic infection in cytomegalovirus (187), human herpesvirus (188), west Nile virus (189), and estimating HIV incidence (190).

More recently, antibody kinetics based assays such as surface Plasmon resonance (SPR, Biacore) and Bio-Layer Interferometry (Octet System, Pall Life Sciences) are becoming popular applications to measure antibody binding properties such as the on and off-rate constants (191,192). The differentiation constant is derived from the titrated antibody concentration and the association and dissociation constants from the kinetic equilibrium. The methods are susceptible to mass transport limitation where the antibodies can rebind on surfaces that have just dissociated, which distort the dissociation constant (191). This method has been used in HIV studies to gain insight into the function of neutralizing antibodies and the viral immune evasion mechanisms and, more recently, applied in malaria antibody affinity evaluations (193).



4 Figure 1.9 illustration of affinity and avidity.

Antibody-antigen interaction is mediated by reversible physical forces such as hydrogen bonds, hydrophobic bonds, and Van-der-Waals forces. There is a continuous association and dissociation between the epitope (antibody binding site on antigen) paratope (antigen-binding antibody site). Affinity is high when the association rate is higher than the dissociation rate at equilibrium. When more than one paratope of the same antibody or different antibodies is binding, the total association rate significantly increases at equilibrium, which increases total affinity or avidity. Avidity stabilizes antibody binding and increases Antibody cooperation in the mediation of effector functions like complement activation and phagocytosis, which require more than one antibody binding. The different antibody colors symbolize additional specificity

1.13 B-cell reaction pathways; the source of affinity and class switching

B cell responses are initiated when a specific antigen activates a B cell via the B cell receptor (BCR). BCR is a complex trans-membrane form of antibody made by the B cell and a heterodimer of Ig- α and Ig- β chains. Primary activation of the B cell results mainly in IgM and limited IgG antibody production. However, a secondary response results in class switching and affinity maturation that is characteristic of a robust, highly effective secondary response.

This section describes the B cell's alternative pathways in response and the germinal center reaction, affecting antibody affinity and isotype composition.

Upon activation by recognition of specific antigen by the BCR, B cells can take three pathways.

- (i) Directly differentiate into plasma cell in the T-independent extra-follicular response.
- (ii) Receive T-cell help, proliferate, and differentiate into plasma cells or MBC in the T-dependent extra-follicular response.
- (iii) Receive T-cell help, enter germinal center reaction in the T-dependent response.

1.13.1 T-independent extra-follicular response of B-cell

Direct differentiation into plasma cells is mainly driven by T-independent antigens (TI) that can directly activate B cells. These antigens activate the B cells via crosslinking the BCR and Toll-like receptors (TLR) (194). There are two types of TI antigens, namely TI-1 and TI-2. The TI-1 are sometimes referred to as mitogens due to their ability to stimulate B cells nonspecifically via the TLR resulting in low-affinity polyclonal IgM and, to a lesser extent, IgG antibodies. TI-1 antigens are not known to generate MBC. TI-2, on the other hand, are specific for BCR and activate B cells through cross-linking of several BCRs. These antigens are mainly polysaccharides of encapsulated bacteria and proteins that consist of highly repetitive epitopes. TI-2 antigens induce class-switched antibodies and memory B cells (195).

1.13.2 T-dependent extra-follicular B cell response

The T-dependent B cell response initiate when a B cell recognizes an antigen via its BCR undergoes activation and receives an additional signal from a T helper cell. The B cell endocytoses the antigen through their BCR processes and presents the peptides via the major

histocompatibility complex class II (MHC II) to the T helper cell. The presentation of the antigens to a specific T helper cell activates it. The activation promotes the B and T helper cells' intricate interaction via co-stimulatory signaling of the CD40 on the T cell and CD40L on the B cell(196,197). The B cell receives additional signaling via the T cell's cytokine secretion, which influences its proliferation, limited somatic mutation, isotype switching, and destiny.

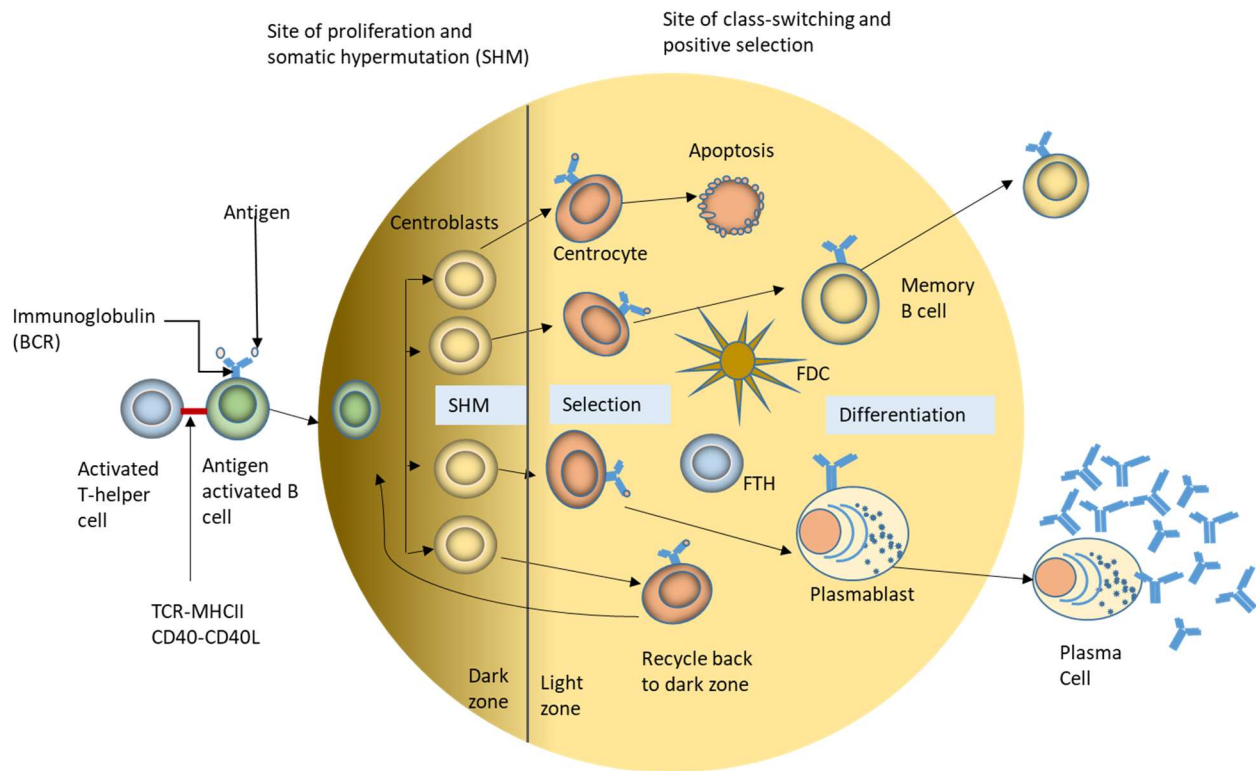
From the B: T interaction, the B cell undergoes extrafollicular proliferation (198). Its progenies differentiate into plasma cells that secrete low-affinity IgM or IgG antibodies, essential during early infection containment. The second alternative is to differentiate into early memory B cell (MBC). These early MBC have limited or no somatic mutation and mostly with IgM BCR(199–201). The third alternative is to enter the follicle, proliferate, and establish a germinal center. The drivers of these choices are not fully understood. Still, we know that B cells that commit to germinal center reaction upregulate the transcriptional factor Bcl-6, and those that commit to plasma cells upregulate transcriptional regulator BLIMP-1.

1.13.3 Germinal center reaction

A germinal center reaction is seeded when activated B cells that previously received T cell help migrate back to the follicle and undergo proliferation to form a mass of noticeable cells after 4-5 days. Other cell types like the follicular dendritic cell (FDC) and follicular helper T cell (Tfh) are an integral part of the germinal center and play a critical role in structural organization, affinity maturation, and class switching. The germinal center consists of dark and light zones (Figure 1.8). In the dark zone, cells undergo proliferation and somatic hyper-mutation in the immunoglobulin gene's variable region, resulting in varied affinities and specificities (202). Activation-induced cytidine deaminase (AID) is up-regulated in B cells located in the germinal center, mediating both isotype switching and somatic hypermutation (203,204). B cell progenies from the dark zone interact with antigens (in immune complexes) presented on FDC to select specificity and affinity in the light zone. During this process, referred to as affinity maturation, B cell progenies compete for antigens presented on FDC in antibody-antigen complex via the Fc receptor, complement receptors, or lectin receptors for positive selection survival signal (205). Because the antigen is presented in the antigen-antibody complex, a successful B cell must have a higher affinity to displace the existing antibody from the binding site. The successful B cell extracts antigen from the FDC, initiates endocytosis, and presents the peptides via the MHC II to T-follicular helper. The T-follicular helper and the B cell's intricate interaction provides signaling for survival through CD40-CD40L and cytokines such as IL-21 (202). The low-affinity B cell progeny undergo apoptosis while the high-affinity ones either migrate back to the dark

zone for additional proliferation and hyper-mutation or exit the germinal center to differentiate into MBC and plasma cells. Some plasma cells are long-lived plasma cells (LLPC) that migrate to the survival niches in the bone marrow from where they secrete antibodies for a long time. Others are short lived plasma cells (SLPC) that migrate into peripheral tissue and secrete antibodies for a short period (206).

Germinal center reactions are highly organized, thought to last for weeks to months, and demonstrated to have temporal output. SLPC exit the germinal center earliest, followed by MBC and much later LLPC with extensive mutations compared to MBC, indicating intensive somatic mutation and affinity maturation of the LLPC (199).



5 Figure 1.8 Schematic representation of Germinal center reaction (207). When activated, one B cell initiates a germinal center reaction. It receives T-cell help, undergoes proliferation, and somatic hypermutation in the B cell receptor gene to form a mass of progenies. The germinal center is a highly organized architectural structure that consists of two zones. The dark zone, densely packed with B cells that undergo proliferation and hypermutation. The light zone, where B cells interact with follicular helper cells (TFH) and follicular dendritic cells (FDC) for positive affinity selection, survival signal, and differentiation into SLPC, MBC, or LLPC. The low-affinity B cells can recirculate back into the dark zone to undergo additional proliferation and hypermutation or undergo apoptosis. The germinal center output is temporally defined. The initial output is the SLPC, followed by MBC and later LLPC. The commitment of cells to either fate is influenced by affinity, Tfh signal, and differential expression of transcriptional factors.

Chapter 2

2.1 Background and rationale

This thesis focuses on two IgG properties critical for antibody function; antibody avidity and subclasses in relation to *P. falciparum* transmission intensity. The focus of the thesis was inspired by the following observations; (i) Slow acquisition of immunity to malaria that is rarely complete (ii) Apparent failure to maintain natural or vaccine-induced immunity (iii) evidence of the critical role antibodies play in immunity to malaria. (iv) Inconsistent association of antibody titers with protection in natural and vaccine modals.

These observations lead to two major hypotheses that have generated increasing supporting evidence

1. *P. falciparum* infection interferes with acquisition and maintenance of immunity to malaria
2. The quantity together with the quality of antimalarial antibody than just the quantity provides better insight into acquisition and maintenance of immunity to malaria

For a long time, the dogma supporting hypothesis 1 was the highly polymorphic *P. falciparum* antigen repertoire (208). However, there is increasing evidence to suggest parasite interference and impairment of acquired immunity. Several observations indicate that frequent *P. falciparum* infection may interfere with the acquisition of effective immunologic memory (209). *P. falciparum* infection may detrimentally affect the generation and maintenance of an effective antibody immune response through (i) impairment of antigen presentation by dendritic cell populations (210,211), (ii) impairment of T-helper cells populations (212), (iii) interruption of B cell response and germinal center reaction (213), (iv) impairment of innate effector cells function (213–216), (v) interruption of temporal and spatial microenvironments that affect the differentiation and survival of antibody-forming cells and memory cell populations(68). The overall effects manifest in the quality of antibodies in terms of breadth of response, affinity maturation, isotypes and subclass composition, rapid antibody decay in the absence of infection and the ability of antibodies to mediate effector function.

In support of hypothesis 2, several epidemiological studies have shown inconsistent associations between antibody levels and the different forms of malaria immunity, even for leading vaccine candidates like Rh5, EBA175 RIII-V, CSP, among others. Furthermore, vaccine trials and controlled human malaria infection (CHMI) that show protection, an association of antibody titer

with malaria, protection is rarely demonstrated. Different adjuvants, vaccine vector, and immunization boost schedules of the CSP based RTS have resulted in differences in efficacy and duration of the protection(217). The different vaccine delivery models have also resulted in differences in antibody titer and antibody avidity, and subclass composition(141). This observation may imply that the differences in avidity and subclass composition may partly contribute to observed differences in efficacy and protection duration. Furthermore, in-vitro assays increasingly show antibody-mediated effector functions such as phagocytosis, complement-fixing, and respiratory bursts as correlates of protection. Antibody affinity and IgG subclass are known determinants of antibody effector function, and their composition may influence protection outcome.

2.2 Hypothesis and aim

This thesis hypothesized that frequent *P. falciparum* infections interrupt avidity maturation and IgG subclass composition, affecting the acquisition and maintenance of immunity to malaria.

2.3 Study aim

I pursued three aims to test the hypothesis.

1. To determine the associations between age and *P. falciparum* transmission intensity with *P. falciparum* specific antibody avidity.
2. To determine the effect of the interruption of exposure to *P. falciparum* infection by IRS on the avidity of antibodies against a large number of *P. falciparum* antigens.
3. To determine the effect of the interruption of exposure to *P. falciparum* infection by IRS on the IgG subclass responses against a large number of *P. falciparum* antigens.

Understanding the dynamics of antibody avidity and IgG subclass in relation to *P. falciparum* transmission intensity or during transmission interruption and with age will provide useful insight into the acquisition and maintenance of naturally acquired immunity. This information can be crucial in understanding how to define immunity and longevity, design better vaccine strategies to induce durable immunity, and use antibody kinetics to develop tools to measure recent infection for surveillance diagnostics. Serological tools can be cost-effective and robust during the malaria elimination era that requires intensive active surveillance.

Chapter 3

3.1 Methods

I performed all the laboratory experiments and data analysis included in this chapter. The PRISM study conducted cross-sectional and cohort surveys where samples for this thesis were obtained. Kigozi provided the maps in figure 3.1 that show the three study sites, Isabel Rodriguez provided figure 3.3 that summarises the cohort malaria status, Simon Peter and Lindsay Wu performed the normalization of the Luminex data in chapters 5 and 6 to adjust for inter-plate variations.

3.1.0 Study Population

3.1.1 Program for Resistance, Immunology, Surveillance, and Modeling of Malaria in Uganda

My Ph.D. was nested in a larger study titled Program for Resistance, Immunology, Surveillance, and Modeling of Malaria (PRISM) in Uganda. The PRISM program's overall strategy was to apply a comprehensive, iterative approach to malaria surveillance that aimed to generate a foundation of evidence to maximize the impact of control interventions across a wide range of epidemiological settings. The study was designed to address the complexity of interactions between the mosquito vector, malaria parasite, and human host. The study combined standard malaria surveillance techniques and metrics with cutting-edge methods, and this was aimed to improve surveillance. Also, PRISM aimed to develop human resources and infrastructure towards sustainable research capacity and help translate research findings into policy. The

project brought together a strong collaborative team, including Infectious Diseases Research Collaboration (IDRC) and Makerere University in Uganda, London School of Hygiene and Tropical Medicine, and Liverpool School of Tropical Medicine in the UK, University of California San Francisco, and the University of Florida in the USA.

Between 2010 and 2017, PRISM conducted entomological and human cross-sectional surveys and human longitudinal cohorts at three different transmission sites in Uganda. The sites included Nagongera sub-county in Tororo District, Walukuba sub-county in Jinja District, and Kihhihi sub-county in Kanungu District.

3.1.2 Cross-Sectional Surveys

Three cross-sectional surveys were conducted in 2012, 2013, and 2015 in three different sub-counties in Uganda to estimate malaria incidence among children and adults living in different epidemiological settings with varying malaria transmission intensity. Each of the three surveys enrolled 200 unique random households for each of the three rounds from a household census database. A comprehensive questionnaire was administered, and finger-prick blood samples were collected from all children under 15 years and a random selection of age-stratified adults. Thick and thin blood smear microscopy and RDT were performed for the detection of malaria infection. Dried blood spots (DBS) were collected and stored at -20 for serological and molecular tests (218). Chapter 4 of my study utilized DBS samples from the 2012 cross-sectional surveys.

3.1.3 Description of the three epidemiological settings

Walukuba is a peri-urban sub-county in the Jinja district with an estimated population of 417,243 people. It is an area of historically medium transmission with an entomologic inoculation rate (EIR) of 6 infective bites per person per year in 2002 (29). A recent estimate of transmission intensity in the region has shown a marked decrease in EIR to 2 infective bites per person per year (Figure 3.1 & Table 3.2) (30).

The second site is Kihhihi, which is a rural sub-county in Kanungu district. The district has an estimated population of 252,144 people and is an area that was historically of relatively low EIR of 2 infective bites per person per year in 2002. Recent PRISM surveillance indicated an increase in malaria transmission intensity, where EIR was estimated at 6 infective bites per person per year (Figure 3.1 & Table 3.2) (30).

The third site is Nagongera sub-county in Tororo district. This site is predominantly rural with very high malaria transmission. Entomology studies conducted in Nagongera in 2012-13 estimated EIR to be 305 infective bites per person per year (30). The total population of Nagongera sub-county is 517,082 people, with children aged 1 to 10 years constituting 37% of the population (Figure 3.1 & Table 3.2).

The study sites (shown on the map of Uganda in Figure 3.1) are summarized in Table 3.2.

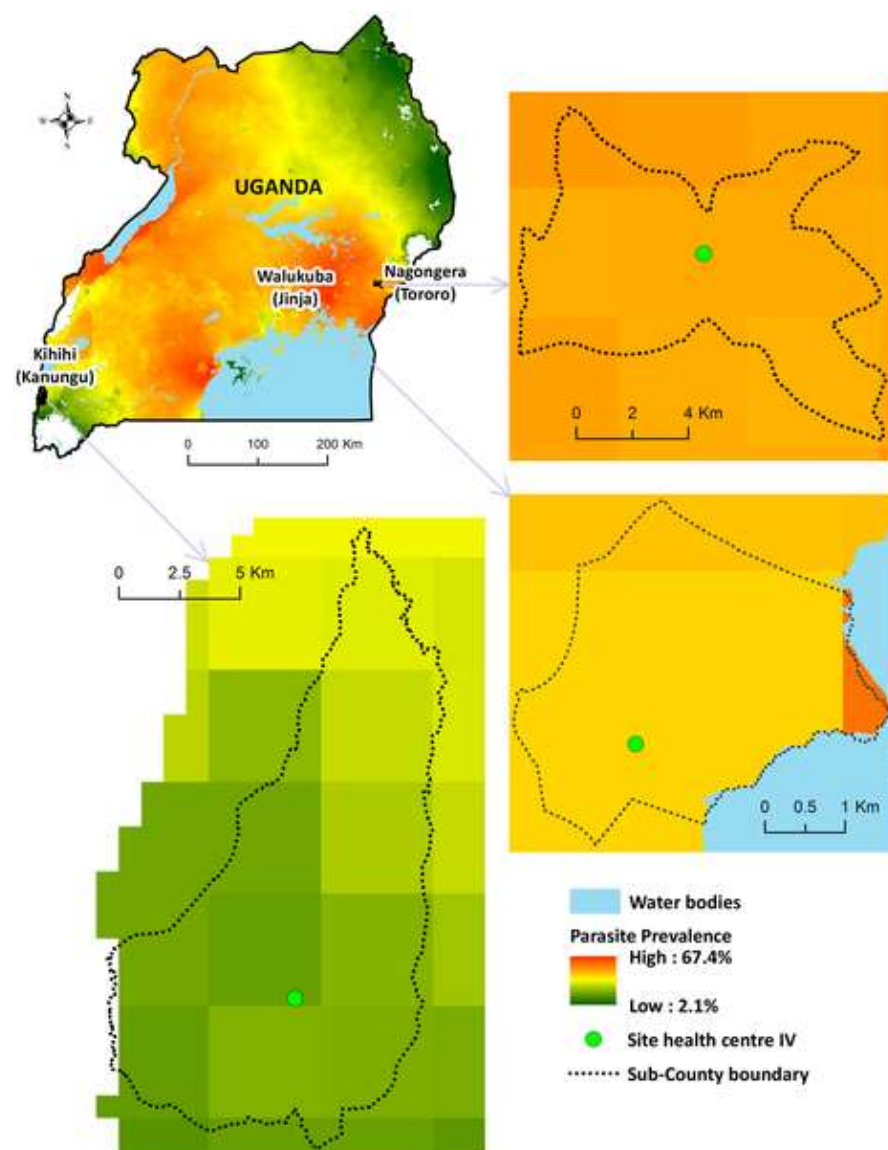


Figure 3.1. Map of Uganda showing the three study sites (219). Walukuba in Jinja (EIR; 2, population; 37,714). Nagongera in Tororo (305; population 517,082) is located further east near the border with Kenya. Kihhihi, Kanungu (EIR; 6 population 252,144). The map was provided by Simon Peter Kigozi, IDRC.

I Table 3.2. Characteristics of study Districts

District	Kanungu	Jinja	Tororo
Demographics(220)			
Location in Uganda	Southwest	East	East
Population	252,144	417,243	517,082
Urbanization level	20%	36.6%	20.3%
Number of households	55,975	105,463	102,634
Persons per household	4.5	3.9	5.0
Historical -Entomology (data collected 2001-2002)(29)			
EIR	2	6	562
Predominate vector species	<i>An. gambiae ss</i>	<i>An.gambiae ss</i>	<i>An.gambiae ss</i>
PRISM Estimated Entomology (data collected 2012-2013)(30)			
EIR	6	2	305
Predominate vector species	<i>An. gambiae ss</i>	<i>An.gambiae ss</i>	<i>An.gambiae ss</i>
PRISM Estimate Measures of infection (data collected in children 2-9 years of age,			
Parasite Rate	11.8%	13%	38.5%

3.1.4 Description of the Longitudinal Cohort at Nagongera

The main PRISM study conducted three longitudinal cohorts at the study sites described in the cross-sectional surveys above (Figure 3.1). Chapters 5 and 6 of this Ph.D. thesis utilized samples from the Nagongera longitudinal cohort that is described in this section. Enrolment included all children aged 6 months to less than 11 years and one primary caregiver above 18 years per household. Participants were enrolled from 100 randomly selected households from an earlier

household enumeration survey. The cohort was enrolled in August 2011 and was followed until September 2017. The cohort was dynamic, such that all newly eligible children were enrolled and exited those who reached 11 years. All study participants were given long-lasting insecticide-treated nets at enrollment. They were encouraged to come to a dedicated study clinic that was open 7 days a week any time they were ill.

Routine evaluations were performed on all 3 months, including blood smears and blood collection for future laboratory testing. Passive surveillance to estimate the incidence of symptomatic malaria and active surveillance to estimate parasite prevalence were used. As part of the routine 3 monthly evaluation, study participants' parasitemia status was assessed by microscopy (221). All negative microscopy samples were further tested by LAMP for submicroscopic infections (222). Blood collected in heparin tubes from routine visits was processed for plasma and DBS. In November 2014, the frequency of routine visits was reduced from 3 to 1 month for an enhanced surveillance amendment to the protocol. In addition to the routine visits, participants reported to the clinic whenever they were sick or had a fever and were diagnosed. Entomology surveillance of the households was done using CDC light traps and human landing catches. Entomological inoculation rates were determined over the follow-up period to assess malaria exposure status (221,223).

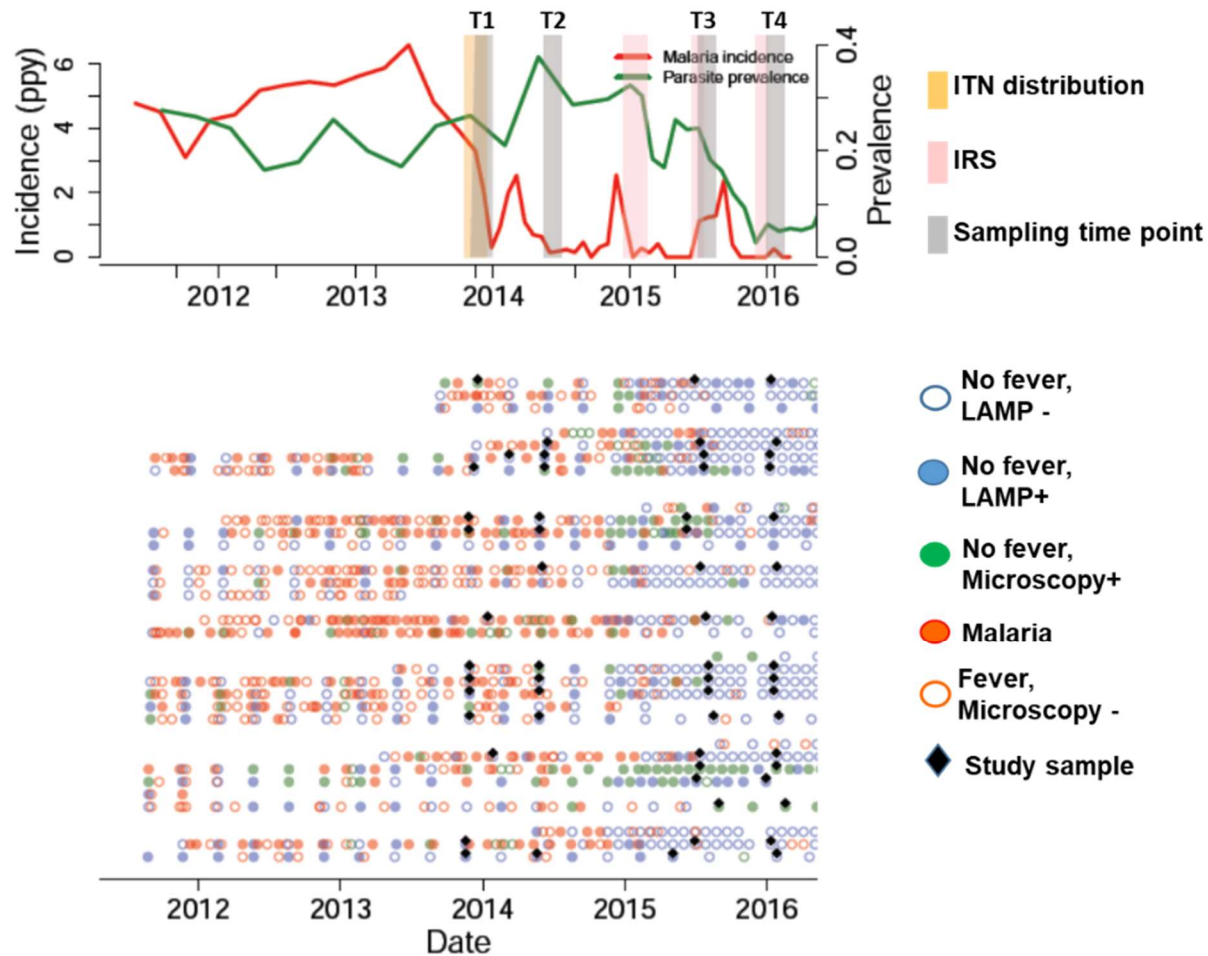
3.1.5 Interruption of transmission by IRS and Enhanced surveillance in Nagongera

Between November 2014 and January 2015, Indoor residual spraying with carbamate bendiocarb was introduced in Tororo for the first time. This intervention led to a dramatic decrease in malaria exposure and transmission rates within the cohort. Three additional IRS rounds were performed every 6 months. The sustained IRS maintained childhood malaria incidence and parasite prevalence at very low levels through the end of the PRISM cohort follow up in September 2017. The IRS introduction coincided with the increased frequency of patient follow up from 3 to 1-month interval that increased the accuracy of evaluation of parasite exposure, dynamics of infection, and the frequency with which participants acquired and cleared parasites (219). I included 160 participants from the PRISM longitudinal cohort in Nagongera in this thesis at 4-time-points.

3.1.6 IRS schedule and sampling time-points

Pre-IRS time-points; T1 and T2 were selected 12 and 6 months before the first round of IRS from routine plasma samples collected in November 2013 - January 2014 and June- July 2014, respectively (Figure3.3). Post-IRS time-points, T3 and T4, were selected at 6 and 12 months after the first and during the second round of IRS in June –July 2015 and the third round of IRS in December 2015 – January 2016, respectively. T3 coincided with the spike in malaria incidence, and T4 was taken when malaria incidence neared zero (Figure3.3).

Despite the distribution of long-lasting insecticide-treated bed nets and reported high net usage within the cohort, monthly malaria incidence in children under five and asymptomatic infection prevalence by microscopy in school going children 5-11 years was high before IRS (221). Malaria transmission intensity peaked in July 2014 at monthly malaria incidence and parasite prevalence estimation of 6 ppy and 35%, respectively (Figure 3.3). Following the introduction of the first round of IRS, monthly malaria incidence gradually reduced to 1 ppy. Also, there was a gradual decline in parasite prevalence from 35% eventually 25%. Malaria incidence spiked at the 6 months following the first IRS round, but the trend reversed after the second IRS in July 2015. Malaria incidence reduced to near 0/ppy and parasite prevalence to 10% by December 2016 when the third round of IRS was done (Figure3.3).



3.1.7 Malaria status within the study population

A total of 160 participants were enrolled from the PRISM longitudinal cohort in Nagongera, including the 4-time-points. The participants were in age categories, 1 - 4 years (40/160), 5 – 11 years (92/160), and >18 years (28/160) (Table 3.4). Within the study population, the incidence was high before the IRS. At T1, 61%, 44%, and 11% in ages 1 - 4, 5 - 11, and >18 years respectively had at least one malaria episode in the last 90 days (Table 3.4). Malaria was defined by the presence of fever and positive blood smear by microscopy. Rates of malaria peaked at T2, where 73%, 55%, and 10% of the participant in ages 1 - 4, 5 - 11, and >18 years respectively had at least 1 malaria episode in the last 90 days. Gradual reduction of malaria among participants in the previous 90 days was observed at 39% and 34% in 1-4 and 5-11 years, respectively, at T3. The highest reduction to 0% and 4% in the 1-4 and 5-11 years respectively who had at least 1 malaria episode in the last 90 days was recorded at T4. No one in the adults had any malaria episodes during the previous 90 days at T3 and T4 (Table 3.4).

The proportion of asymptomatic parasitemia at least once in the last 9 days was high before IRS peaking at T2 and gradually reduced to the lowest at T4 after introducing IRS (Table 3.4). Asymptomatic parasitemia was defined as the presence of *P. falciparum* by microscopy and LAMP (for microscopy negative) in the absence of fever. At T1, 76%, 95%, and 58% in ages 1 - 4, 5 - 11, and >18 years respectively had a positive parasitemia at least once in 90 days. Rates

of parasitemia peaked at T2, where 80%, 89%, and 70% in age 1 - 4, 5 - 11, and >18 years respectively recorded at least one parasitemia in the last 90 days. After IRS, there was some reduction to 58% and 85% and 45% in ages 1 - 4 and 5 - 11 and >18 years respectively at T3. Further reduction was recorded at T4, where 14% and 45% and 14% age categories 1-4, 5-11, and above 18 years respectively had at least one asymptomatic parasitemia episode in the last 90 days.

Other malaria transmission intensity indicators (summarized in Table 3.4) such as parasitemia today, the proportion of months free of malaria in the last 12 months, proportion of months free of parasitemia in the previous 12 months showed a similar reduction in *P. falciparum* infection intensity one-year post-IRS.

Table 3.4 Summary of the study population and malaria matrix by time-points

Malaria Matrix	Age (years)	Time Point			
		T1	T2	T3	T4
Population	1- 4	40	40	40	38
	5 - 11	93	93	91	93
	>18	28	28	28	28
The proportion with at least 1 malaria in the last 90 days (%)	1- 4	61	73	39	0
	5 - 11	44	55	34	4
	>18	11	10	0	0
Proportion parasitic at least once in the last 90 days (%)	1- 4	76	80	58	14
	5 - 11	95	89	85	45
	>18	58	70	45	14
Mean days since parasitemia	1- 4	51	40	91	240
	5 - 11	9	23	50	146
	>18	77	84	186	322
Proportion of months free of parasite in last 6 months	1- 4	0.42	0.35	0.62	0.83
	5 - 11	0.27	0.25	0.41	0.62
	>18	0.48	0.53	0.71	0.85
Proportion of months free of parasite in last 12 months	1- 4	0.45	0.40	0.51	0.75
	5 - 11	0.29	0.29	0.37	0.51
	>18	0.49	0.51	0.64	0.78

Time-points were relative to the first round of IRS. T1=12, T2=6 months before IRS. T3=6, T2=12 months after IRS. Malaria was defined by fever and positive blood smear microscopy. Parasitemia status was determined by microscopy or LAMP positive at monthly interval

3.1.8 Informed consent

Before enrollment into the cross-sectional and longitudinal surveillance studies, written informed consent was obtained from adults, parents/guardians of children, and assent from children aged 8 years and older. Informed follow-up consent was obtained when the enhanced monthly surveillance sampling in participants was introduced.

3.2 Laboratory methods

3.2.1 *P. falciparum* Recombinant Antigens

A total of 18 recombinant *P. falciparum* blood-stage antigens and Tetanus toxoid protein (TT) (non-malaria control) were used in the experiments reported in Chapters 4, 5, and 6. The antigens were mainly of three categories; (i) infected red blood cell-associated antigens, (ii) merozoite apical complex expressed proteins, and (iii) merozoite surface antigens. The antigens included leading vaccine candidates, recent exposure markers, long-term/cumulative exposure markers, and commonly studied antigens. The recombinant antigens were expressed in *Escherichia coli* either as glutathione S-transferase (GST) fusion proteins or histidine-tagged constructs. Details of the antigens included in the study are provided in Table 3.5 below

Chapter 3: Methods

3 Table 3.5 Summary of the *P. falciparum* Blood-stage antigens

Gene ID	Description	Antigen name	Allele	AA	Location	Tag
PF3D7_0501100.1	Heat Shock Protein 40, type II, Antigen1(*KT)	-	3D7	71-153	iRBC/Gam	GST
PF3D7_0423700	Early Transcribed Membrane Protein 4,	ETRAMP4Ag2	3D7	76-137	iRBC/PVM	GST
PF3D7_0532100	early transcribed membrane protein 5 Antigen1(*KT)	ETRAMP5Ag1	3D7	26-111	iRBC/PVM	GST
PF3D7_1002000	Plasmodium exported protein (hyp2), unknown	Hyp2	3D7	101-418	iRBC/PVM	GST
PF3D7_0501300	Skeleton-Binding Protein 1(*KT)	SBP1	3D7	1-239	Scht/MC	GST
PF3D7_1021800	Schizont Egress Antigen 1(*KT)	SEA	3D7	810-1083	Scht/MC	GST
PF3D7_1133400	Apical Membrane Antigen 1(153)	AMA-1	FVO	97-546	SpZ/Mer	His _{x6}
PF3D7_1301600	Erythrocyte Binding Antigen-140 Region III-V (224)	EBA140 RIII-V	3D7		Mer -M	GST
PF3D7_0731500	Erythrocyte Binding Antigen-175 Region III-V	EBA175 RIII-V	3D7	761-1298	Mer-M	GST
PF3D7_0102500	Erythrocyte Binding Antigen-181 Region III-V (224)	EBA181 RIII-V	3D7	769-1365	Mer -M	GST
PF3D7_1335400	Reticulocyte Binding Protein Homologue 2 (225)	Rh2	D10	2030-2528	Mer-Rh	GST
PF3D7_0424200	Reticulocyte Binding Protein Homologue 4 (226)	Rh4.2	3D7	28-766	Mer-Rh	His _{x6}
PF3D7_0424100	reticulocyte binding protein homologue 5 (227)	Rh5	3D7	1-526	Mer-Rh	C-tag
PF3D7_1035300	Glutamate Rich Protein R2 (228)	GLURP RII	F32	816-1091	Mer-S	n/a
PF3D7_1036000	Merozoite Surface Protein 11/H101 (229)	H103	3D7	40-243	Mer-S	GST
PF3D7_0930300	19kDa fragment of MSP1 molecule (230)	MSP1-19	Wellcome	1631-1726	Mer-S	GST
PF3D7_0206800	Merozoite surface protein 2, Dd2 allele (231)	MSP2 Dd2	Dd2	22-247	Mer-S	GST
PF3D7_0206800	Merozoite surface protein 2, CH150/9 allele (231)	MSP2 CH150/9	CH150/9	34-215	Mer-S	GST
n/a	Tetanus Toxoid (Non-adsorbed)	TT	n/a	n/a	n/a	n/a

iRBC =Infected red blood cell, Gem- Gametocyte, PVM = parasitophorous vacuole membrane, MC = Maurer's cleft, SPZ = sporozoite, Mer-S = merozoite surface, Mer-M = merozoite micronemes, Mer-Rh = merozoite Rhoptry *KT = Tetteh. K, unpublished

3.2.2 Elution of antibodies from DBS

DBS from the cross-sectional surveys were collected on Whatman 3MM filter paper and stored at -20°C. For this thesis, a 3mm diameter punch of DBS was hydrated in 200µl of phosphate-buffered saline (PBS) containing 0.005% Tween 20 and 0.01% sodium azide. The excised spot was estimated to have approximately 2µl plasma, resulting in a serum dilution factor of 1:200 (232).

3.2.3 Avidity ELISA assay

Immulon-4 microtitre plates (Thermo Labsystems, Basingstoke, UK) were coated overnight at 4°C with 0.5mg/ml of antigen in coating buffer (0.1M sodium carbonate/bicarbonate, pH 9.6), and then washed three times with wash buffer; PBS, 0.05% Tween-20. The plates were blocked for 3 hours at room temperature with 200µl/well PBS, 0.05% Tween-20, 1% skimmed dried milk, and then washed three times. For each sample, plasma was diluted to a final concentration of 1:1000 for MSP1-19 and 1:2000 for AMA1, with 50ul of diluted plasma added per well. Plates were incubated overnight at 4°C and washed 6 times. Horseradish peroxidase enzyme (HRP)-conjugated rabbit anti-human IgG (Dako Ltd, High Wycombe, UK) was diluted 1:5000 in blocking buffer, and 50ul was added per well. The plates were incubated for 3 hours at room temperature, then washed 6 times, and developed with 100µl/well of *o*-phenylenediamine (OPD)-H₂O₂. The reaction was stopped after 15 minutes with 25ul 2M sulphuric acid. Optical

densities (ODs) were measured at 492 nm using a VERSAmax plate reader with Softmax software (Molecular Devices, USA).

To evaluate antibody avidity, the standard sandwich ELISA assay described above was modified to include an antibody disassociation step before the addition of HRP-conjugated secondary antibody. Briefly, diluted plasma samples were incubated on the plates overnight at 4°C; triplicate wells were treated with 2M or 5M or PBS guanidine hydrochloride (GuHCl) for 10 minutes and then washed 6 times. PBS well was the control to measure the total antibody binding. Test samples with and without GuHCl were run on the same plate to minimize variability. The avidity index was defined as the proportion of antibodies binding after treatment with GuHCl for each dilution (Avidity Index = [OD following GuHCl treatment / OD without GuHCl treatment] X100).

Only samples with titers above a normalized OD (adjusted OD based on a positive control to correct for inter-plate variations) of 0.5 were included in the avidity index assessment to ensure detectable binding after antibody binding interruption. In each plate, hyper-immune sera (CP3) based on a Tanzanian endemic adult pool was included at a dilution of 1:3200 as a positive control.

3.2.4 Preparation of Luminex assay reagents

To prepare wash buffer (0.05% Tween20 PBS, 0.02%NaN₃), 250µl of tween20 (Croda International, UK) was added to 500ml phosphate-buffered saline (PBS). Sodium azide

(0.1gm) was added to preserve the wash buffer at 0.02%. The reagent was mixed on a magnetic stirrer (AccuPlate, Analog Magnetic Stirrer, USA) for 30 minutes and kept at 4-8°C for 2 weeks before expiry.

To prepare Buffer A (0.5% BSA, wash buffer), 2.5gm bovine serum albumin (BSA) (Sigma-Aldrich Co. LLC, USA) was added to 500ml wash buffer. Buffer A was mixed on a magnetic stirrer for 30 minutes and kept at 4-8°C for 2 weeks before expiry.

To prepare Buffer B (0.1% liquid casein, 0.5% PVA, 0.8% PVP, 1/100uL *E. coli* extract, Buffer A), 0.5gm casein, 2.5gm PVA, 4.0gm PVP, and 100ul *E.coli* extract (Chris lab, London school) was added to Buffer A. Buffer B was mixed on a magnetic stirrer overnight and kept at 4-8°C for 2 weeks before expiry or was kept for at -80°C for a longer period.

Buffer B was used to reduce background signal due to nonspecific binding and reduce risk of measuring *E.coli* specific responses since most *P. falciparum* antigens were expressed in *E.coli*.

3.25 Luminex Bead counting

The coupled beads were counted to determine the couple's quantity for small couplings and determine bead recovery after coupling.

After suspension by medium vortexing for 30 seconds, 10µl of suspension was injected into a disposable hemocytometer and counted under objective lens x100.

3.2.6 Determination of optimal antigen coupling concentration

Antigen coupling titration was done to determine the optimal concentration of antigen required to couple beads and achieve the most informative signal. The titration was done using hyperimmune sera. Briefly, 5×10^6 beads were washed twice with 100 μ l distilled water by vortexing for 30 seconds and centrifuged at 16,000g before removing the supernatant on a magnetic rack. Beads were divided into 5 aliquots of 1.0×10^6 in a 1.5ml low protein binding surface micro-centrifuge tube (Eppendorf, UK). Bead carboxyl surface activation and antigen coupling were done as per the coupling procedure in 3.34 below. The stock antigen was diluted serially from 1/10 by a factor of 5, and each concentration was coupled to one of the five tubes for 2 hours on a rotating shaker. The beads were washed and suspended in the storage buffer.

The beads were tested with hyperimmune sera at 1/1000 dilution as per the assay procedure outlined in section 3.36. The net median fluorescent intensities (MFI) were plotted against the antigen concentration. Optimal coupling concentration was selected from a mid-point on the curve's linear portion (Figure 3.6). The stock reagent volume required to couple 12.5×10^6 beads in a volume of 1ml was derived. Briefly, the optimal coupling concentration of 12.5×10^6 beads in 400 μ l was derived from the selected antigen dilution factor and the antigen stock concentration. This was scaled up to the amount of antigen required to couple 12.5×10^6 beads in 1,000 μ l (Table 3.7).

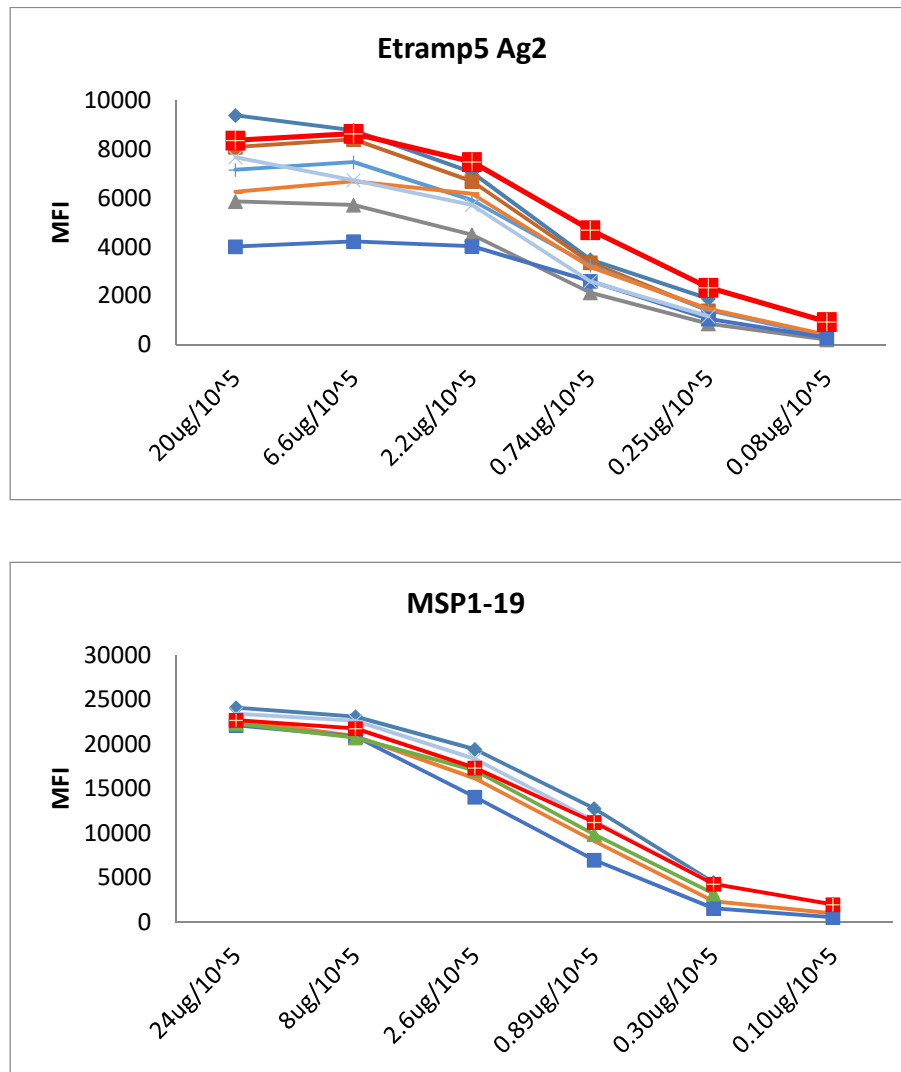


Figure 3.6 Representative Graphs showing the titration of Stock coupling concentration in Bead. The different colored curves represent different hyper-reactive serum at 1/1,000 dilution

4 Table 3.7 Summary of the antigens concentrations required for large batch coupling

Antigen	Ag stock concentration (mg/ml)	Ag coupling in 400µl (ug/1x10 ⁶)	Ag needed to couple in 400µl (ug/12.5x10 ⁶)	Vol of Ag stock to couple 12.5x10 ⁶ in 1ml	Vol of Ag stock to scale up to 1ml	Vol of PBS top-up to 1ml
HSP40 Ag1	0.681	15.0	187.5	275.3	688	311.7
ETRAMP4Ag2	0.651	5.0	62.5	96.0	240	760.0
ETRAMP5Ag1	0.539	14.0	175.0	324.7	812	188.3
Hyp2	0.785	22.0	275.0	350.3	876	124.2
SBP1	0.700	44.0	550.0	785.7	1964	-964.3
SEA	5.400	44.0	550.0	101.9	255	745.4
AMA-1	0.962	1.0	12.5	13.0	32	967.5
EBA140 RIII-V	0.113	22.0	275.0	2433.6	6084	-5084.1
EBA175 RIII-V	0.218	1.6	20.0	91.7	229	770.6
EBA181 RIII-V	1.486	22.0	275.0	185.1	463	537.3
Rh2	0.604	5.0	62.5	103.5	259	741.3
Rh 4.2	6.745	1.0	12.5	1.9	5	995.4
Rh5	1.477	20.0	250.0	169.3	423	576.8
GLURP RII	1.255	30.0	375.0	298.8	747	253.0
H103	0.980	15.0	187.5	191.3	478	521.7
MSP 1-19	2.770	22.0	275.0	99.3	248	751.8
MSP2 Dd2	7.740	44.0	550.0	71.1	178	822.4
MSP2 CH150/9	0.807	4.9	61.3	75.9	190	810.3
TT	0.364	5.0	62.5	171.7	429	570.7

3.2.7 Covalent coupling of antigens to magnetic microsphere Bead

Antigens were covalently coupled to MagPlex carboxylated magnetic microspheres (Luminex Corp, Austin, USA)(233). 12.5×10^6 beads for each bead region were suspended by sonication for 60 seconds and vortexing at medium speed for 60 seconds. The beads were transferred from the stock bottle into a 1.5ml micro-centrifuge tube with a low protein binding surface (Eppendorf, UK) to minimize bead loss and centrifuged at 16,000g for 3 minutes. The bead pellet was pulled on the tube side by placing into a magnetic rack for 1 minute before pipetting off the supernatant. The beads were washed twice by suspension in 100ul distilled water, vortexed for 30 seconds, and centrifuged at 16,000g. The supernatant was removed after settling the beads on a magnetic rack for 2 minutes. Beads were suspended in 80ul monobasic Sodium Phosphate (NaH_2PO_4 , pH 6.2 activation buffer). To activate the carboxyl surface of the beads, 10ul of 50mg/ml Hydroxysulfosuccinimide (Sulfo-NHS) (Thermo Fisher Scientific, UK) was added, vortexed briefly, and immediately followed by the addition of 10ul of 50mg/ml 1-ethyl-3-(3-dimethylaminopropyl) carbodiimide hydrochloride (EDC), (Thermo Fisher Scientific, UK).

The beads were incubated for 20 minutes at room temperature in the dark when wrapped in aluminum foil on a rotating platform. During the 10 minute incubation, the beads were vortexed for 20 seconds to ensure homogeneous activation. Beads were pelleted by centrifuging at 16,000g for 5 minutes, placed tubes in a magnetic holder for 1 minute –the supernatant carefully

removed, and washed 3 times with 250µl PBS as above. Previously determined antigens were added to each bead region in PBS to make a final volume of 500µl (Table 3.7). The appropriate amount of antigen for coupling was determined by titration in the method described (3.2.5 Determination of optimal antigen coupling concentration). The beads/antigen suspension was incubated for 2 hours on a rotating shaker in the dark and covered in aluminum foil. Coupled beads were pelleted by centrifugation at 16,000g for 3 minutes and washed of excess antigen 3 times with 250µl of phosphate-buffered saline 0.05% tween20 (PBS-TBN). The antigen coupled beads were suspended in 1ml storage buffer (PBS-TBN plus pefabloc) and stored at 4°C.

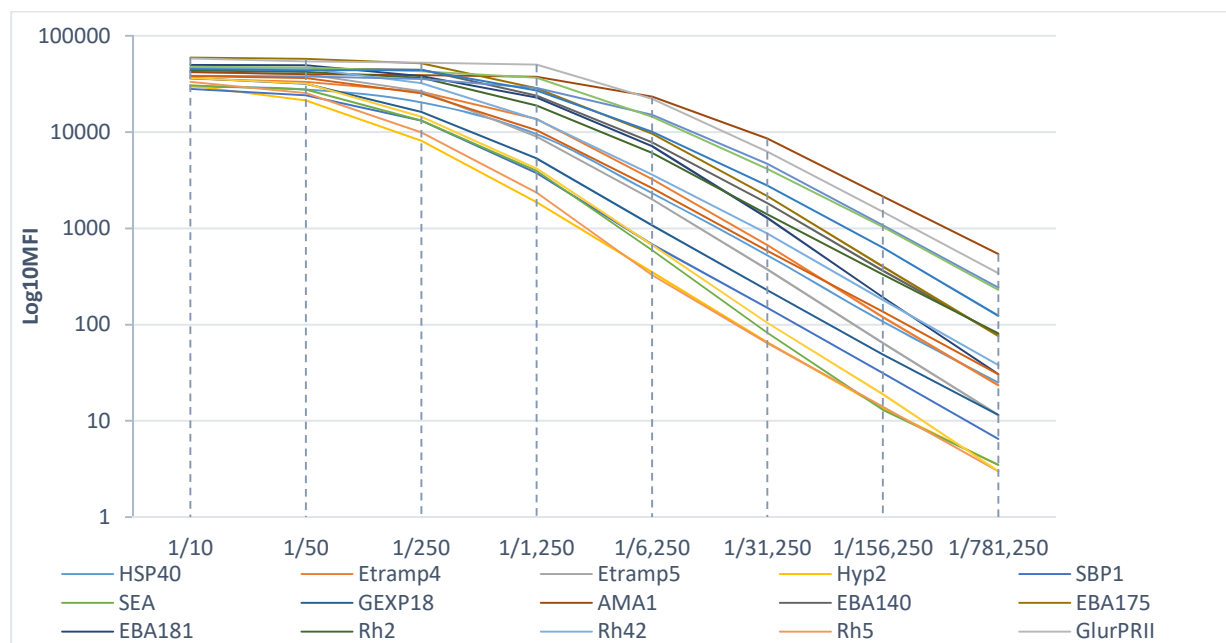
3.2.8 Plasma dilution

A volume of 10µl of plasma was added to 500µl of PBS-TBN in a deep well plate to make a 1/50 dilution. The deep well plates were stored at -20°C until use. To make the 1/100 dilution for the IgG subclass assays, 200µl of 1/50 was added to 200µl buffer B (PBS, 0.05% Tween 20, 0.1% casein, 0.02% NaN₃, 0.5% PVA, 0.8% PVP, 1/100uL *E. coli* extract. To make 1/1000 dilution for the total IgG and avidity assays, 40µl of a 1/50 sample dilution was added to 360µl of buffer B). The samples were incubated in buffer B overnight before the Luminex assay to reduce background binding (nonspecific reactivity in some individuals due to the presence of *E.coli* proteins, reflected in the high MFI in the negative controls).

3.2.9 Construction of hyperimmune control - PRISM pool 4

Plasma pool 4 (PP4) was constructed based on 22 plasma samples that were positive and broadly reactive to the antigens included on my panel. Based on the previous set of data, the samples' reactivity per antigen was divided into 5 percentiles. Each sample was assigned a percentile score of 1 to 5 (5 most reactive and 1 least reactive).

The scores were added, and the 50 top-scored samples were selected. The list was narrowed down to 22 by manually eliminating samples with low reactivity in some antigens, especially those with a low frequency of highly reactive samples or those whose maximum MFI was less than 8,000 at 1/1,000. An aliquot of 200µl of each of the 22 samples was pooled to construct PP4. The PP4 standard curve was constructed from 8 serials dilutions starting from 1/10 and a 5-fold dilution factor (Figure 3.8).



7 Figure 3.8 Representative PP4 standard curves of 18 *P. falciparum* antigens and Tetanus toxoid PP4 was able to result in a saturation curve for all the antigens on the panel

3.2.10 Luminex MagPex multiplex bead array assay to measure total IgG

Total IgG responses to 18 *P. falciparum* blood-stage antigens and TT were measured in plasma diluted Buffer Bat 1/1000 on the MagPix (Luminex Corp, Austin, Texas) multiplex bead array as previously described (234). The samples were incubated in buffer B overnight at 4-8°C before the assay. Tetanus toxoid (National Institute of Biological Service and Control (NIBSC)) was added as a positive control for both malaria-endemic and non-endemic samples.

Briefly, 10µl per region of antigen coupled bead stock (MagPex magnetic microsphere) (Luminex Corp, Austin, Texas) was added in 5ml of buffer A to make a combined pool of all the 19 regions at a concentration of 100,000 beads/region. 50µl of the bead suspension was added

to each well (~1,000 beads/region/well) of the 96-well plate (Bio-plex Pro, flat bottom) (BioRad, UK). The plate was washed, placed on a magnetic block for 2 minutes covered in aluminum foil, and the supernatant poured off with the plate still attached to the magnet and gently blotted on a paper towel. The beads were washed twice with wash buffer, rested on the magnetic separator for 2 minutes, and supernatant poured off.

Using a multichannel pipette, 50µl of prepared plasma at a dilution of 1/1,000 in Buffer B and hyperimmune control PP4 standard was added to the beads. PBS was added to two blank wells. The plate was covered with aluminum foil and incubated at room temperature on a shaker at 600rpm for 90 minutes. At the end of the incubation period, the plate was placed on a magnetic separator for 2 minutes. A rapid inversion poured off the supernatant with a sharp shake followed by a gentle blot on a paper towel. The plate was washed three times, with 100 µl wash buffer. Using a multichannel pipette, 50µl of 1/200 R-Phycoerythrin-conjugated AffiniPure F (ab') 2 goat anti-human IgG (Jackson Immuno Research Laboratories) diluted in buffer A was added. The plate was covered in aluminum foil and incubated at room temperature on a shaker at 600rpm for 90 minutes. The plate was placed on a magnetic separator for 2 minutes, and the supernatant poured off.

The plate was washed three times with wash buffer. Buffer A 50µl was added and the plate incubated at room temperature on a shaker at 600rpm for 30 minutes before washing once. The beads were suspended in 100µl of PBS pH 7.2 per well and suspended on a plate shaker for 5 minutes. The plate was read on a MagPix machine (Luminex, USA), acquiring at least 100

beads/region/ well. The results were expressed as median fluorescent intensity (MFI). The blank well MFI was deducted from each well to determine the net MFI.

The samples were tested in a single well, where 100 beads were acquired. The reproducibility data informed the choice of a single well of the MFI. I compared the MFI of duplicate samples on the same plate and across plates. The PP4 hyper-immune plasma curve was used for the inter-plate comparison (Chapter 5, Figure 5.50a & b). There was a high correlation between the duplicates expressed by the r-square within the plate (upper panel) and across plates (lower panel).

3.2.11 Luminex Multiplex bead array assay to measure total IgG avidity responses

Antibody avidity index of 18 malaria antigens was measured in a modified total IgG Luminex multiplex assay by adding the GuHCl differentiation step after antibody binding. Tetanus toxoid (National Institute of Biological Service and Control (NIBSC)) was added as a positive control for both malaria-endemic and non-endemic samples.

Briefly, stock bead regions were vortexed for ~30 minutes to resuspend the beads. The resuspension was necessary to disrupt any clumps or aggregated beads that had formed during storage. A volume of 10µl was pipetted into 5ml buffer A (~100,000 beads/region). 50µl of the bead suspension was added to each well (~1,000 beads/region/well) (BioRad). The plates were washed twice with 100µl /well of wash buffer. To minimize bead loss, the plates were placed on a magnetic block for 2 minutes to pellet the MagPix beads before removing the supernatant by a

rapid inversion of the plate with a single sharp shake. 50µl of 1/1000 plasma in Buffer B was added to duplicate wells per sample; the plate was covered in aluminum foil to protect from the light and incubated at ~22°C on a shaking platform at 600 rpm for 90 minutes. The plate was returned to the magnetic block for 2 minutes, and the supernatant was removed as before. The plates were washed two times with 100µl wash buffer.

To assay for avid antibodies, 50µl Guanidine Hydrochloride (GuHCl) was added to one of the duplicate wells per sample to dissociate weakly binding antibodies, 50µl PBS was added to the second well for total antibody. The plate was incubated at room temperature on a shaker at 600rpm for 20 minutes. The plate was placed on the magnetic block for 2 minutes, and the supernatant was poured off. The plate was washed with wash buffer 3 times. 50µl of 1/200 R-Phycoerythrin-conjugated AffiniPure F (ab')₂ goat anti-human IgG (Jackson Immuno Research Laboratories) in buffer A was added. The plate was incubated at room temperature on a shaker at 600rpm for 90 minutes. The plate was placed on the magnetic block for 2 minutes, and the supernatant poured off. The plate was washed 2 times with 100µl wash buffer. 50µl of buffer A was added and the plate incubated at room temperature on a shaker at 600rpm for 30 minutes before washing once. 100µl of PBS pH 7.2 per well was added. The beads were suspended on a shaker for 1 minute and read on a Magpix (Luminex Corp, Austin, Texas), acquiring at least 100 beads/region/well. The avidity index was defined as the percentage of antibodies that remained binding after treatment with GuHCl. (Avidity index = MFI with GuHCl/ MFI with PBS)X100.

3.2.12 Luminex Multiplex bead array assay to measure IgG1 – 4s

IgG subclass responses to 18 blood-stage *P. falciparum* antigens and TT (non-malaria positive control) were measured in plasma diluted at 1/100 on the Luminex MagPix platform and detected using a two-step biotinylated anti-human IgG subclass secondary antibody with a streptavidin-Phycoerythrin tertiary as previously described (235,236). The platform does not allow the multiplexing of labeled antibodies, so each of the IgG subclasses was assayed separately for every sample using the same plate layout.

Briefly, 10µl per region of antigen coupled bead stock (MagPlex magnetic microsphere) (Luminex Corp, Austin, Texas) stock was added in 5ml of buffer A to make a combined pool of all the 19 regions at a concentration of 100,000beads/region. 50µl of the bead suspension was added to each of the wells (~1,000 beads/region/well) of the 96-well plate (Bio-plex Pro flat bottom) (BioRad, UK). The plate was washed: placed on a magnetic block for 2 minutes covered in aluminum foil. The supernatant poured off while the plate on the magnet and gently blotted on a paper towel to remove as much residual as possible. The beads were washed twice with 100µl wash buffer, rested on the magnetic separator for 2 minutes, and supernatant poured off.

Using a multichannel pipette, 50µl of prepared plasma at a dilution of 1/100 in Buffer B overnight and PP4 standard was transferred from the deep wells into the bead wells. PBS was added to two blank wells. The plate was covered with aluminum foil and incubated at room temperature on a shaker at 600rpm for 90 minutes. The plate was placed on a magnetic separator for 2 minutes, and a rapid inversion poured off the supernatant with a sharp shake followed by a

gentle blot on a paper towel. The plate was washed three times with 100µl PBS-TBN. 50µl of biotinylated mouse anti-human IgG subtype (mouse anti-human IgG1, clone HP6069, mouse anti-human IgG2, clone HP6002, mouse anti-human IgG3, clone HP6050, and mouse anti-human IgG4, clone HP6023, Thermo Fisher Scientific, UK) in buffer A was added in dilutions of 1/400, 1/400, 1/1,000, 1/400 for IgG1 – 4, respectively. The plate was covered in aluminum foil and incubated at room temperature on a shaker at 600rpm for 90. The plate was washed three times with 100µl wash buffer. 50µl of streptavidin- phycoerythrin conjugate (Thermo Fisher Scientific, UK) was added to each well. The plate was covered in aluminum foil and incubated at room temperature on a shaker at 600rpm for 90 minutes. The plate was placed on a magnetic separator for 2 minutes before pouring off the supernatant. The plate was washed three times with 100µl wash buffer. The plate was read on a Luminex MagPix, acquiring at least 100 beads/region/ well. The results were expressed as MFI. The blank well MFI was deducted from each well to determine the net MFI.

3.3 Data Normalization to adjust for plate-to-plate variations.

Lindsay Wu, London School of Hygiene and Tropical Medicine performed the data normalization. Data were normalized to adjust for between plate variation using a loess normalization method(237). This involved inclusion of PP4 standard curve fits from the plate. A composite standard curve was computed for each antigen by calculating the mean MFI values for the reference plates for 100 concentrations between the highest and lowest concentration on

the standard curve. For each plate, the plate-to-reference standard curve MFI difference (Δ MFI) was calculated for these 100 concentration points and a loess regression fit to Δ MFI as a function of mean MFI. The raw MFI data for all samples on the plate were then adjusted by the predicted Δ MFI based on the loess regression fit. Data were not corrected for background signal given that the between plate variation was already accounted for in the loess normalization and all background MFIs were below 30 and therefore negligible.

3.4 Statistical Analysis.

Non-parametric comparison of unpaired medians across age groups within site or across sites was performed assuming a non-gaussian, using the Mann-Whitney test. Correlations were performed using the Pearson test. The sensitivity (true positive) and 100 - specificity (false positive) were determined by the receiver operating characteristic curve (ROC). The net change in total and avid IgG levels and avidity index during the highest and the lowest malaria transmission intensity was derived from a paired difference between MFI and AI at T2 and T4. The association between antibody levels (MFI) for total IgG and the subclasses 1 - 4 with days since the infection was assessed in a generalized estimating equation (GEE) model, adjusted for age (373). The MFI were log10-transformed. All 4-time-points were included, and the patient number was used to link the repeated measure. The GEE model assumed the Gaussian distribution, the correlations within a group were exchangeable, and the standard errors were robust. The GEE allowed estimation of the mean effect of days since the last infection on

antibody levels using repeated measures per individual at a population level. Infections were defined as parasite positive if the sample was microscopy positive (patent infections) or LAMP positive. The GEE model outcomes were regression coefficient and 95% confidence intervals (95%CI). Estimated antibody decay half-life was derived from the GEE model's regression coefficient of log₁₀ antibody levels with days since infection (log antibody loss per day since infection) by dividing log₁₀ of 2 by coefficient. The result was the number of days it takes to lose half the antibody levels since the last day of infection.

Analysis and Figures were performed with Stata version 14 (StataCorp LLC, USA), GraphPad Prism version 7 (Graphpad Software Inc, USA), and R studio. Changes and associations were considered statically significant when 95% confidence intervals did not overlap zero or P-values were less than 0.05. The P less than 0.05 assumed estimated differences between medians 95% not likely to have occurred by chance.

Chapter 4

As part of my Ph.D., I performed all the laboratory experiments and data analysis in this chapter.

The PRISM study conducted cross-sectional surveys where samples for this chapter were obtained. Eliza assay was performed in the main PRISM study to determine the seroprevalence of MSP-1-19 and AMA-1. I used the seroprevalence data to select the participants in this study, as described in the chapter.

Avidity of Antimalarial Antibodies Inversely Related to Transmission Intensity at Three Sites in Uganda

4.1 Introduction

4.1.1 Slow acquisition of Immunity to malaria

The striking feature of immunity to malaria in humans is the slow acquisition only after many years of continuous exposure in the endemic areas. In high transmission areas where children are exposed to infective bites daily, they continue to suffer from several malaria episodes each year, not until their early adolescence (238).

Children develop immunity to severe malaria around the age of 5 years in stable endemic areas. However, they remain susceptible to uncomplicated malaria until the age of 10 -15 years, when they manifest anti-disease immunity. During the anti-disease immunity, the children are chronically infected with high parasite load without clinical symptoms (24,54). A period of 10

to 15 years of continuous exposure to infection is way too long for malaria to acquire immunity compared to other viral and bacterial diseases. For example, the acquisition of protective immunity to measles and smallpox is very rapid—often after one or two infections or vaccinations with an attenuated virus (239,240). Thus, the acquisition of immunity to malaria in humans is slow, complicated, involving the early acquisition of anti-severe disease immunity, followed by anti-disease immunity and anti-parasite immunity but rarely leading to sterile immunity (241).

4.1.2 Role of antibodies in acquired immunity to malaria

In 1961, Cohen *et al.* demonstrated the role of antibodies in blood-stage malaria immunity. In his experiment, the transfer of purified IgG from malaria-immune adults to children with acute malaria led to rapid reductions in parasite numbers in the blood and the fever's subsequent resolution (138). Several epidemiology studies have reported the correlation of different immunity to antibody responses against several *P. falciparum* antigens (238,242–244). In a longitudinal study in Gabon and Cameroon, clinical protection was related to elevated antibody levels to schizont extract (245). In another study, antibodies against the merozoite surface protein 1-19 (MSP1-19) were shown to provide approximately 40% protection against clinical malaria in Sierra Leone children (246). Osier FH *et al.* reported that serum antibody levels to apical membrane antigen 1 (AMA-1) and merozoites surface protein antigens (MSP1 block 2, MSP2, and MSP3) were inversely associated with the probability of developing severe malaria in Kenyan children (244). Consequently, several malaria antibodies inducing vaccine candidate

formulations were based on antigens previously correlated with some form of protection or protective immunological mechanisms. Unfortunately, most of the vaccine candidates to date have not shown promising protective results in clinical trials despite evidence of inducing desirable antibody responses (247). Only the circumsporozoite protein (CSP) based RTS, S/AS01, has shown short-lived protection from severe forms of the disease with efficacy ranging between 30 -50% (139,248).

We do not fully understand the targets or the properties of antibodies against *P.falciparum* that mediate immune mechanisms to malaria. The quality of the protective antibodies and the precise mechanisms by which these antibodies affect their function are barely known. Furthermore, we do not understand why antibody-mediated immunity is acquired only after many years of exposure and why immunity is poorly maintained.

The inefficient acquisition of a protective immune response against malaria is partly attributed to the huge number of antigens rising from approximately 5,400 genes (249). In addition, there is a high degree of genetic diversity and polymorphism associated with parasite genes, including the multi-gene families like the var genes. This vast diversity and the complex expression at the different life cycle stages can partly explain why it takes an individual living in an endemic area a long time to generate a diverse repertoire of protective antibodies (250,251). Therefore, it is postulated that it takes years living in an endemic area for an individual to be exposed to a sufficient number of parasite clones to generate a protective repertoire of antibodies (243,252).

In addition, temporal variation of parasite antigen expression, as exhibited by the var genes and other antigens, contributes to successful parasite immune evasion and disease pathology (64).

Peter Crompton *et al.* and Scholzen *et al.* reviewed mounting evidence suggesting *P. falciparum* infection-induced dysregulation of B-cell function. This is thought to play a role in the inefficient acquisition and maintenance of antibody-mediated protection against malaria (253,254). It is suggested that *P. falciparum* infection preferentially induces short-lived plasma cells (SLPC) and does not reliably and efficiently induce a stable pool of long-lived plasma cells (LLPC) and typical MBC, especially in children (255,256).

Furthermore, *P. falciparum* malaria infection is associated with the expansion of atypical MBC (257,258) reported having reduced capacity to proliferate and differentiate into antibody-secreting cells upon *in vitro* stimulation (257). Their phenotype is similar to the exhausted MBC in HIV infection, but their role in malaria is not fully understood (259,258). These adverse effects on the B cells function may bear grave consequences on the critical antibody qualities such as maintenance of protective antibody levels, isotype composition, and avidity maturation.

4.1.3 Antibody affinity, avidity and the role in Antibody function

Antibodies against *P. falciparum* clear pathogens via several mechanisms. These include inhibition of pathogen invasion (neutralization), complement fixation, and opsonization of pathogens for clearance by innate immune cells (260–263). However, for antibodies to mediate function efficiently, they must bind to their target stably and long enough via the variable

antigen-binding site to cooperatively recruit effectors via their Fc receptors. **Antibody Affinity is the strength of the interaction between a single antigen site - epitope and a single antibody-binding site.** Thermodynamic principles govern the reversible bimolecular interaction between the antigen and antibody hence affinity. The sum of the binding affinities of the individual antibodies to a poly-epitope antigen is referred to as antibody avidity. Avidity is the functional affinities and reflects the degree of stability of antibody interaction with antigen (264). It is a function of the number of shared binding sites and the total binding energy of an antibody and antigen. Efficient antibodies must bind with high avidity to their target and long enough to mediate their functions effectively. For example, neutralizing or blocking antibodies must bind the pathogen antigens that mediate attachment or entry to the host cell faster than the cell receptors. Likewise, antibodies must bind stably and long enough on the pathogen or infected cells to effect opsonization and complement activation. Antibody affinity maturation during the germinal center reaction in a follicular T- dependent B cell response (205).

4.1.4 Evidence of acquisition of avidity during infection and role in immunity

Antibody avidity is an important correlate for immune memory and protection in infections such as MUMPS, rubella (183), toxoplasma (251), and vaccine efficacy such as pneumococcal polysaccharide and MUMPS vaccines. The decreased efficacy of *Haemophilus influenzae* type B vaccine that has been observed in combination with acellular pertussis vaccine was reported

to be a result of lower avidity maturation (265,176,266). Similarly, patients with MUMPS vaccine failure were associated with low antibody avidity (181,182).

4.1.5 Evidence of acquisition of avidity maturation during Malaria infection

There are very few studies that provide some useful insight into the role of antibody affinity in malaria. Ferreira *et al.* reported increased antibody avidity to *P. falciparum* -schizont extracts two months following resolution of clinical malaria, in the absence of re-infection in Brazilian adult patients (267). Higher avidity of the predominately cytophilic IgG antibody subclasses IgG1 and IgG3 was reported among the immune Senegalese adults compared to non-immune Brazilian *P. falciparum* malaria patients (267). In yet another study, higher avidity to *P. falciparum* blood-stage extract was reported among Brazilian children with uncomplicated and asymptomatic malaria, relative to their complicated malaria counterparts (268). Furthermore, high avidity antibodies to full-length VAR2CSA were associated with a reduced risk of placental malaria (269). More recently, antibody avidity to AMA-1 and MSP2 were reported to increase with age, and that individuals with the highest antibody avidity to MSP2 at the baseline of a prospective study had a prolonged time to clinical malaria (270). These findings are put together to provide insight into the acquisition of antibody avidity during malaria infection and its contribution to acquired immunity associated with *P. falciparum* antigen-specific antibodies.

4.1.6 What influences avidity maturation during Malaria infection?

In *P. falciparum* infection, avidity to whole schizont extract and several specific antigens have been shown to correlate with protection (267–270). However, the acquisition of high antibody avidity to *P. falciparum* antigens with age and exposure intensity is poorly understood. One study performed in an unstable malaria transmission setting showed increased antibody avidity following a clinical malaria episode (267). In contrast, two studies of children living in endemic areas failed to observe an increase in avidity index to a number of *P. falciparum* antigens with increasing exposure (271,272). Overall, it is unclear if repeated exposure to *P. falciparum* leads to increased avidity of antibodies directed against plasmodium antigens.

4.2 Study aim

Data presented in this Chapter aimed to determine the influence of *P. falciparum* exposure intensity on the acquisition of antibody avidity to 2 *P. falciparum* merozoite antigens; AMA-1 and MSP1-19. Avidity index was measured in individuals across a wide range of ages from cross-sectional surveys performed in 3 sites in Uganda with varying malaria transmission intensity. Antibody avidity indices were then compared between ages and sites to determine whether there were differences in antibody avidity associated with age and *P. falciparum* exposure intensity.

4.3 Methods

4.3.1 Study sites and cross-sectional surveys

This study utilized DBS samples collected from cross-sectional surveys conducted in 2012, described in Chapter 3 at three sub-counties in Uganda. The three sites had varied *P. falciparum* transmission intensity based on the entomology survey of 2012. Walukuba had relatively low transmission intensity, with EIR estimated at 2. Kihhihi had a medium transmission with an estimated EIR of 6. Nagongera had the highest transmission with an estimated EIR of 306. Malaria transmission at all three sites was perennial. In all three districts, malaria control interventions included using ITN malaria case management with artemisinin-based therapies and intermittent presumptive treatment during pregnancy with sulfadoxine-pyrimethamine.

Cross-sectional surveys were conducted between January and June 2012 at all 3 sites (218). The Survey recruited participants from 200 households randomly selected from a population-based census. A total of 2,217 participants were recruited in the 3 surveys (Walukuba – 629, Kihhihi – 786, Nagongera – 802). DBS from finger-prick samples were obtained from all children under fifteen years of age and from a random selection of age stratified adults in the following categories: 15–24 years, 25–34 years, 35–44 years, 45–54 years, and > 55 years. The median and interquartile age per site is indicated in Table 3.3. ELISA assay for AMA-1 and MSP1-19 was performed to determine seroprevalence.

4.3.2 Study population

ELISA assay for AMA-1 and MSP1-19 was performed previously, and OD values were obtained for the main study. Only samples with titers above a normalized OD (adjusted OD based on a positive control to correct for inter-plate variations) of 0.5 were included in the avidity index assessment to ensure detectable binding after antibody binding interruption. A total of 1,186 samples with OD > 0.5 for either AMA-1 or MSP1-19 were included in this study. A total of 424 were positive for both AMA-1 and MSP1-19, 605 AMA-1 only, and 157 MSP1-19 only. The total number for AMA-1 was 1029, and MSP1-19 was 581 the detailed summarised in Table 4.31a in the results section. The exact breakdown is included in figure 4.31b.

5 Table 4.31a Characteristics for the cross-sectional surveys

Characteristics of cross-sectional Survey	Walukuba	Kihihi	Nagongera	Total
Survey population	629	786	802	2217
Median Age (IQR)	12 (5 - 25)	12 (5 - 28)	11 (6 - 28)	
EIR	2	6	306	
Parasite rate	13	11	38	
Sero- prevalence AMA1	54.2	67.2	85.5	
Sero- prevalence MSP1-19	33.8	56.5	50.4	

Characteristics of the Study Population	Walukuba	Kihihi	Nagongera	Total
Study population- AMA1	183	343	503	1029
Study population- MSP1-19	92	270	219	581
Median Age (IQR)	18 (8 – 27)	19 (10 – 38)	12 (6 – 28)	
Percentage of the survey population- AMA1	29.1	43.6	62.7	
Percentage of survey population MSP1-19	14.6	34.4	27.3	

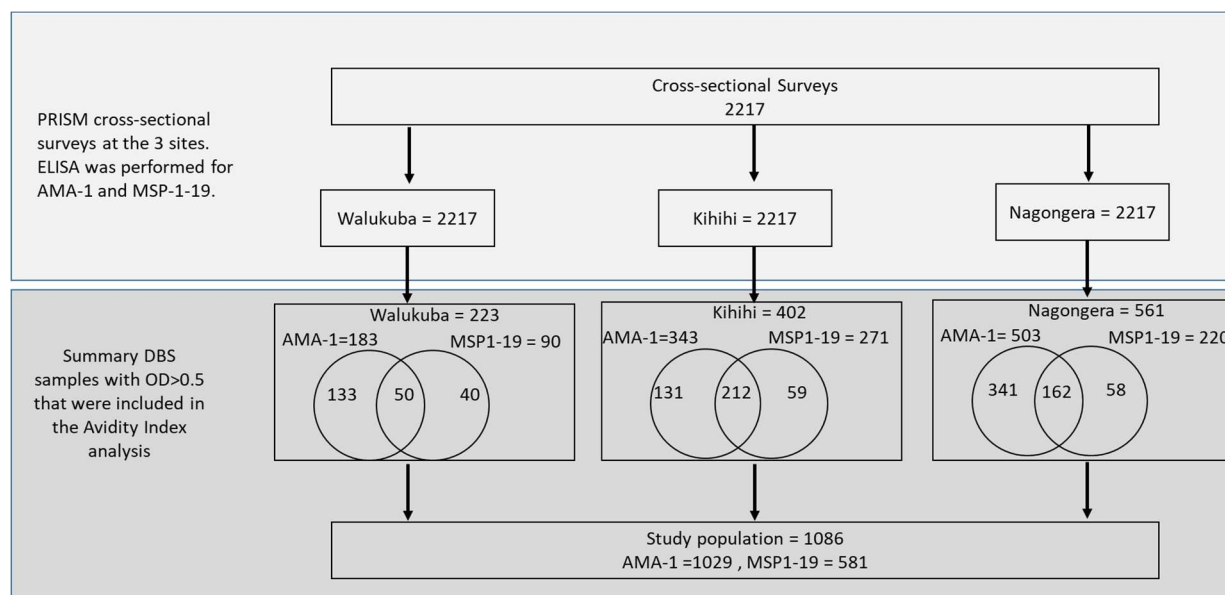


Figure 4.31b Summary of the samples selected from the PRISM cross-sectional survey based on the OD 0.5 cut off for both AMA-1 and MSP1-19

4.3.3 Modified ELISA to Measure the Avidity index

DBS collected on Whatman 3MM filter paper and stored at -20°C were eluted as described in Chapter 3 section 3.22. Antibodies to MSP1-19 and AMA-1 (3D7 strain) were measured via a modified sandwich ELISA (Chapter 3, section 3.23) at a final concentration of 1:1000 for MSP1-19 1:2000 for AMA1. For each sample, a set of two wells were treated with 2M or 5M (GuHCl) or PBC (standard ELISA to measure total antibody) to interrupt binding before the development of the plate as described in Chapter 3. The avidity index was defined as the percentage of antibodies binding after treatment with GuHCl.

4.3.4 Data Analysis

Participants were stratified into age groups 1-4, 5-15, and above 15 years. Non-parametric comparison of unpaired medians across groups within site and across sites for the different age groups was performed using the Mann-Whitney test. Correlations were performed using the Pearson test. The analysis was performed using Stata14 (Stata Corp LLC, USA) and Graphpad PRISM version 8 (Graphpad Software, USA).

4.4 Results

4.4.1 Change in age with transmission site at OD 0.5 cut off

The participants from the PRISM surveys included in this study were based on the OD of the 0.5 cut-off. Consistent with sero-prevalence observations in the same surveys, the proportion of participants included in the survey for AMA-1 increased with increasing transmission intensity (29.1%, 43.6%, and 67.7% for Walukuba, Kihhihi and Nagongera, respectively) but not MSP1-19 (14.6%, 34.5%, and 27.3% for Walukuba, Kihhihi and Nagongera respectively) (218).

Median age significantly increased between the PRISM survey and the study population for the low and medium transmission areas Walukuba (12 vs. 18 years, $P = 0.0006$), Kihhihi (12 vs. 19 years, $P > 0.0001$). Age did not change for the high transmission area of Nagongera (11 vs. 12 years, $p = 0.165$). This observation may imply a rapid sero-conversion rate at the high transmission area consistent with the previous finding (232,273,274).

4.4.2 Relationship between age and antibody avidity

Median avidity index to MSP1-19 at 2M and 5M GuHCl was not significantly different between age groups at all three sites. Median avidity index to AMA-1 at 2M was only significantly higher at 5-15 years compared to 1-4 years. AT 5M GuHCl median avidity index was not different between age groups at all three sites, with the exception of 1-4 versus 5-15-year olds in Walukuba (73.6 versus 85.1 $p=0.04$) (Figure 4.32).

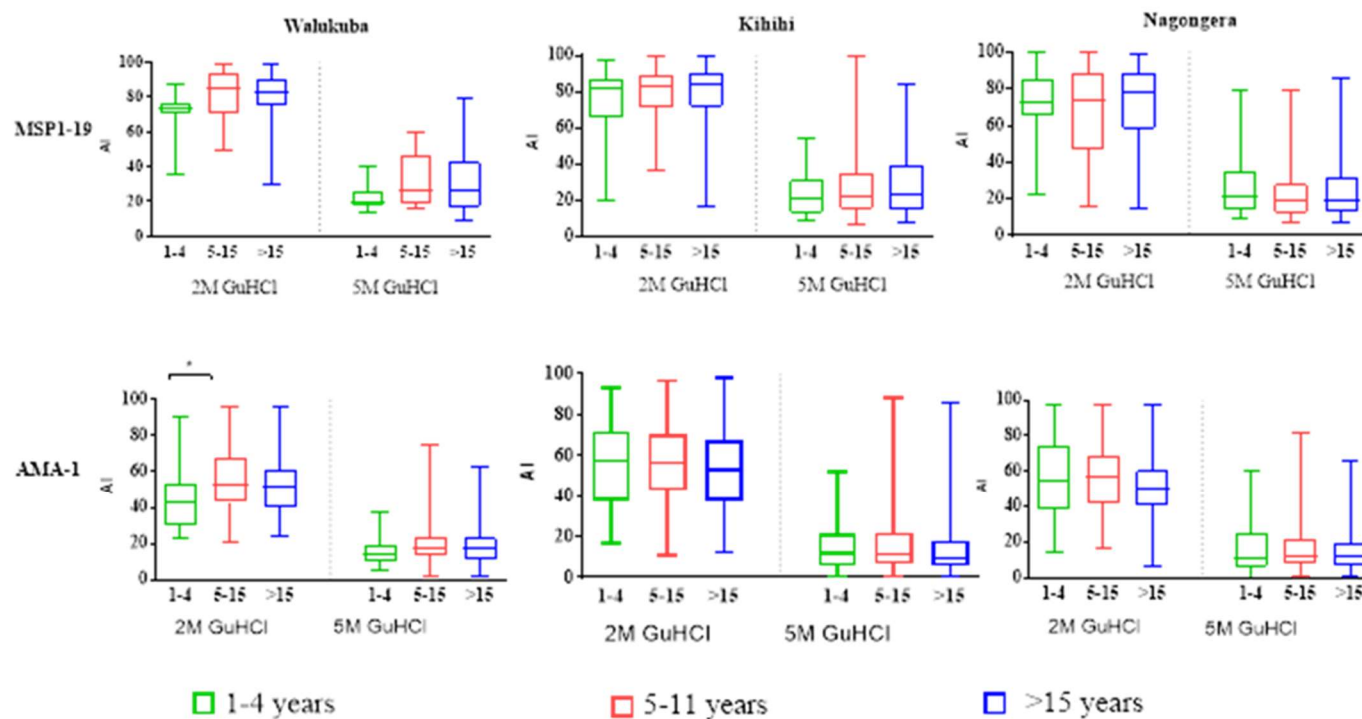
Chapter 4: Antibody Avidity at Different *P. falciparum* Transmission Sites

Figure 4.32. Avidity index to MSP1-19 and AMA-1 across age groups. Avidity index was measured as the percentage of remaining binding antibodies after 2M or 5M GuHCl treatment, of the total antibody in a modified ELISA assay. The bars represent the median and interquartile range. * = $p < 0.0$

4.4.3 Relationship between malaria transmission and antibody avidity

In contrast to the trends observed in antibody levels, the avidity index to MSP1-19 was significantly lower in the highest malaria transmission intensity site of Nagongera than Kihhi and Walukuba in those over five, at both GuHCl concentrations (2M and 5M) (Figure 4.33). There were no significant differences in avidity index between sites in children under five. Responses to AMA-1 showed a similar pattern, with avidity index lower in Nagongera and Kihhi than Walukuba in those at least five years old at 5M. There was no evidence of a correlation between the avidity index to MSP1-19 and AMA-1 at either GuHCl concentration ($r^2 < 0.002$, $p > 0.5$ at 2m and 5m GuHCl all three sites). Overall, these findings suggest an inverse relationship between the avidity index and transmission intensity and antibody response to MSP1-19 and AMA-1 across sites for those above 5 years.

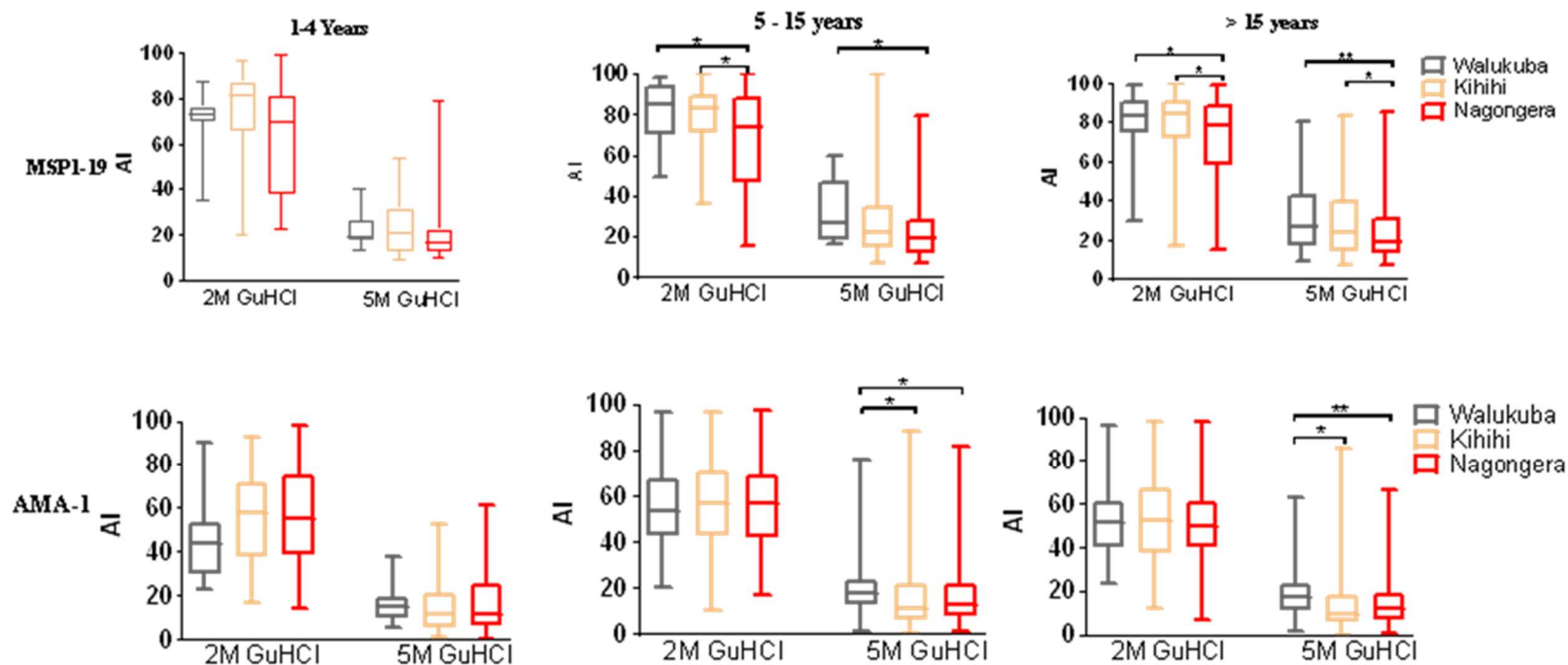


Figure 4.33. Avidity index to MSP1-19 and AMA-1 across transmission sites. Avidity index was measured as the percentage of remaining binding antibodies after 2M or 5M GuHCl treatment, of the total antibody in a modified ELISA assay. The bars represent the median and interquartile range. * = $p < 0.05$, ** = $p < 0.001$, *** = $p < 0.0001$

4.4 Discussion

4.4.1 Summary of Results

This study sought to determine the influence of *P. falciparum* exposure on the natural acquisition of high avidity antibodies. Avidity was measured to MSP1-19 and AMA-1 antigens in over 1,000 individuals encompassing a wide range of ages, from 3 sites in Uganda with transmission intensities ranging from moderate to extremely high. Our results demonstrated that age had a minimal effect on antibody avidity, consistent with previous studies using similar evaluation methods, which observed slight or inconsistent age-related differences in avidity to MSP1-19 and AMA-1 (271,272). Notably, despite higher antibody levels, both antigens' avidity was significantly lower at the site of highest *P. falciparum* transmission intensity in children ≥ 5 years and adults. These results suggest that affinity maturation to *P. falciparum* antigens may be compromised in the setting of very high, perennial exposure to this parasite.

There are at least two potential explanations for this study's main findings, which are neither exhaustive nor mutually exclusive: 1) near-constant exposure to an antigen may impair maturation/persistence of avid antibodies via several potential mechanisms; and 2) recent infection may result in the addition of low avid antibodies to the circulation, reducing the proportion which has high avidity.

4.4.2 Chronic infection may impair germinal center

Affinity maturation is acquired through somatic hypermutation during germinal center reactions, with B cell affinity to antigen driving selection that results in higher affinity antibodies (Figure 4.34) (275,276). The classical understanding of B cell biology would suggest that repeated exposure would be expected to drive several rounds of germinal center reactions, ultimately resulting in higher antibody affinities to the pathogen, hence a higher antibody avidity index. In contrast, results showed a lower avidity index in participants living in the highest *P. falciparum* transmission site, where exposure to antigen is most frequent. Animal studies suggest that germinal center development is temporally ordered, with SLPC emerging from extrafollicular differentiation and early germinal centers initially, followed by MBC. Then, weeks to months later, LLPC has undergone extensive affinity maturation (199,275). Many evidence suggests that acute and chronic infections may compromise the ultimate development of high-affinity MBC and LLPC, which are the source of high-affinity antibodies. (Summarized in Figure 4.34). Such evidence includes (i) interference of germinal center architecture in the spleen (277,278). Antigens like the CIDR- α region of the PfMP1 have a mitogenic effect that causes polyclonal activation and extrafollicular differentiation of B cells into plasma cells(254,279). In addition, antigens that have repeat domains may drive B cell extrafollicular reaction. (ii) The presence of chronically large antigen loads may result into indiscriminate survival of low-affinity B cell. (iii) Acute malaria interferes with follicular helper T cell differentiation that may affect the germinal center's integrity and interfere with the selection process (280,281). (iv) Dysregulation of B cell

differentiation factors like BAFF may result in skewed germinal center output. (v) *P. falciparum* infection is associated with dysfunction of the B cell compartment, including the accumulation of atypical memory B cells (257), which could theoretically result in the inefficient acquisition and maintenance of antibody-mediated immunity malaria due to their altered differentiation upon stimulation (254).

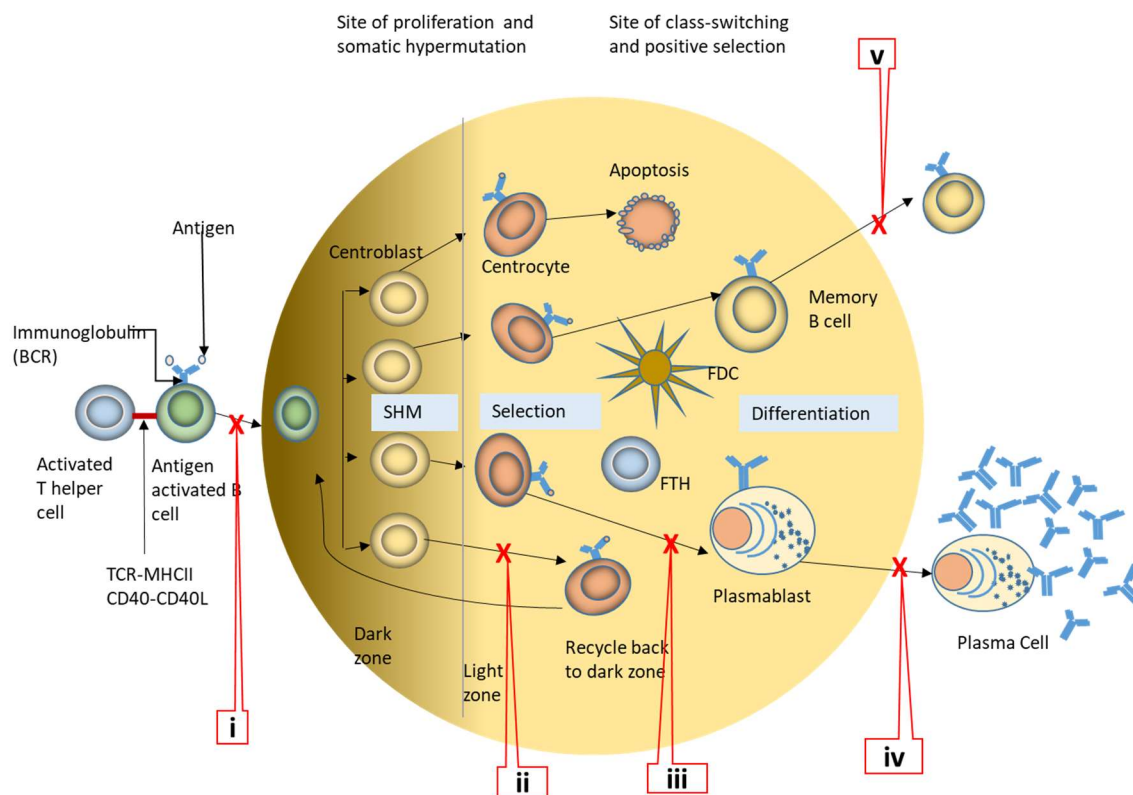


Figure 4.34 Schematic representation of Germinal center reaction showing the processes potentially interrupted by *P. falciparum* infection can result in B cell dysfunction and affinity maturation impairment. (i). Malaria antigens like CIDR- α mitogens can result in extrafollicular B cell reaction and prevent germinal center formation. (ii) Chronically large antigen load may result into a selection of B cell low-affinity B cell receptors. (iii-v) Dysregulation of follicular T helper cells and follicular dendritic cells may damage the germinal affect center architecture, survival differentiation signaling of B cell populations, and accumulation of atypical MBC.

4.2.3 Status of infection may influence Avidity index

In the presence of low antigen levels, affinity matured plasma cells that secrete high-affinity antibodies should be favored over lower affinity plasma cells for survival. These affinity matured plasma cells would, therefore, maintain the blood antibody levels. However, in the presence of frequent re-infection, a relatively large antigen load may be more likely to promote survival of poorly affinity-matured plasma cells, including T cell-independent or extra-follicular B cell reactions. Furthermore, acute *P. falciparum* infection is associated with non-specific, polyclonal B cell activation that may expand low avidity, short-lived plasma cells (282). These factors may reduce the proportion but not necessarily the titers of high avidity antibodies. In contrast, in the absence of recent infection, the antibody pool is predominantly comprised of high avidity antibodies generated by LLPC after the contraction of the SLPC. This may explain why Ugandans in lower transmission areas, who on average had a longer duration of time since their last infection, had higher proportions of highly avid antibodies.

4.3.4 Relationship between avidity index and immunity

The impact of the differences in the avidity index observed in this study on acquiring clinical or anti-parasite immunity is unknown. While antibody avidity is theoretically important in the function of an antibody response (266), there is little empiric data to support the relationship between the avidity index and immunity in malaria. Reddy et al. found that individuals with higher antibody avidity to *P. falciparum* antigens were less likely to experience malaria during

follow-up (193,283). In an RTS, S malaria vaccine trial, investigators did not find an association between antibody avidity to circumsporozoite protein and protection after the last dose of vaccination among children. Still, they did show that the change in avidity between second and third vaccination was associated with a 54% reduced risk of acquiring malaria (284,285). The relationship between avidity measurements and clinical immunity is also complex, with numerous factors other than the play's avidity index. A high antibody titer may compensate for a low avidity index; therefore, a relatively low avidity index in the presence of high antibody levels may not negatively affect naturally acquired immunity. Clinical data from this study shows that acquired immunity develops in children in Nagongera, the study site with the highest *P. falciparum* transmission, based on reductions in disease incidence with age (221). However, it is not clear whether acquired immunity would develop and be maintained more effectively by decreasing the nearly continuous exposure to blood-stage parasites at the site, e.g., via chemoprevention or reducing transmission using vector control(286).

4.3.4 Limitations

This study's cross-sectional nature limited our ability to investigate the mechanisms behind the acquisition of antibody avidity. The study looked at only one-time points that do not give information about the antibody boost and decay kinetics. Furthermore, this study only investigated responses to two of many *P. falciparum* proteins. It is not yet well established which combinations of responses are most relevant for acquiring immunity. Also, while providing an overall estimate of the proportion of the polyclonal antibody pool, which is highly avid, the

ELISA-based methods used in this study could not further dissect the antibodies' binding characteristics.

4.4 Conclusion

In conclusion, this study showed that avidity to 2 different *P. falciparum* antigens was lower in high versus low transmission intensity areas. The mechanisms behind these findings, as well as their clinical consequences, if any, are not yet clear. A more detailed investigation, ideally linked to *P. falciparum* exposure's longitudinal investigation, comprehensive analysis of the B-cell and antibody response will be valuable in further illuminating these findings.

Chapter 5

As part of my Ph.D., I performed all the laboratory experiments and data analysis in this chapter.

The PRISM study conducted the longitudinal cohort where samples for this chapter were obtained. Lindsay Wu normalized the Luminex data (Chapter 3, section 3.3) after I completed the experiments. I used the normalized data for the analysis.

***P. falciparum* infection is associated with a predominantly non-avid IgG antibody response that rapidly decays following IRS**

5.1 Introduction

Several epidemiological studies have shown a correlation between antibodies to different malaria antigens with varying forms of malaria immunity, majorly anti-disease immunity independent of age, and exposure (287–289). Furthermore, in-vitro assays have demonstrated that naturally acquired antimalarial antibodies can mediate effective effector mechanisms targeting different parasite stages in the parasite life cycle (152,290,291). The growth inhibition assays (GIA) measure antibodies' ability to interfere with parasite invasion or growth (124,291). Inhibition or reduction in growth may be a result of blockage of merozoite invasion of the red blood cell (292–294), inhibition of intra-erythrocyte parasite growth, blockage of parasite egress from infected red blood cells (295), blockage of infected red blood cell from sequestration, mediation of destruction of infected red blood cells or inhibition of schizont rupture (296). Antigens like

MSP1-19 and AMA-1 have been studied extensively in GIA and have shown an inconsistent correlation with protecting clinical disease (290,292,297,298). The GIA has revealed several other antigens like EBA175 RIII-V RIII-V and Rh5, SEA that are important targets of inhibitory antibodies and correlates well with protection and are promising vaccine candidates (123,288,299,300). Antibodies opsonize merozoites and infected red blood cells for phagocytosis via the Fc receptor (152,298,301). Naturally acquired antibody levels against merozoite surface proteins, including MSP2, MSP3, MSPDBL1, and MSPDBL2, were positively correlated with phagocytosis in-vitro assays (123,152,302,303). Merozoites opsonized by antibodies in vitro can activate neutrophils to produce reactive oxygen species, termed as an antibody-dependent respiratory burst (ADRB), and demonstrated with naturally acquired anti-MSP1-19 antibodies (304). Antibodies cooperate with monocytes and Natural killer cells (NK) to mediate antibody-dependent cellular inhibition (ADCI) (131,305). With this mechanism, antibodies mediate infected red blood cell attack indirectly through monocytes and NK cells' activation to release chemical factors that mediate parasite killing. Phase 1 vaccine trials of MSP2 and MSP3 were associated with the development of Antibody-dependent cellular inhibition (ADCI) mediating antibodies (133,306,307). Antibodies recruit the complement system to promote phagocytosis, chemotaxis, and cell lysis. Studies of naturally exposed malaria infections and vaccinated volunteers have shown that antibodies bind to merozoites, and infected red blood cells can recruit C1q and activate the classical complement cascade leading to parasite lysis (132,134). Naturally acquired antibodies to MSP1-19 and MSP2 were shown in vitro to activate the complement

classical pathway and antibodies (132). Complement activation is one of the proposed mechanisms of protection mediated by anti-sporozoite vaccine-induced antibodies (134,308).

Despite overwhelming evidence supporting the role antibodies play in malaria immunity mediated mechanisms, it is also clear that serological assays to date do not always correlate with immunity. The obvious arguments are the high polymorphisms, alternative use of different antigens for the same function/s, complex expression of antigens during a complex life cycle, all of which promote parasite immune evasion. However, there is increasing evidence to suggest malaria mediated interruption of the germinal center reaction and B-cell function (309). Antibody properties such as isotype composition and affinity play a critical role in the overall antibody functional outcome. Still, we have a poor understanding of how these properties are acquired, interrupted, or influence antibody function during malaria infection.

Antibody affinity maturation and class switching are acquired through the germinal center reaction. There is evidence discussed in Chapter 4 to indicate that the germinal center may be interrupted by *P. falciparum* infection. Although not fully understood, these interruptions of the B cell function associated with *P. falciparum* infection are strongly suspected to affect antibody avidity and maintenance of antibody-mediated immune response against malaria and, consequently, slow down acquisition and maintenance of protection against infection and disease.

We reported previously in Chapter 4 that the avidity index of antibodies against AMA-1 and MSP1-19 was inversely correlated to *P. falciparum* transmission intensity (310). The study in Chapter 4 compared the avidity index of AMA-1 and MSP1-19 in three cross-sectional surveys of different malaria transmission intensities. The study's cross-sectional nature limited our ability to gain insight into the mechanisms that drive lower avidity index at the site of highest malaria transmission intensity. Furthermore, the two antigens limited our knowledge of avidity maturation in the context of a broader antigenic profile.

5.2 Hypothesis and Aim

Based on our results from Chapter 4, where we observed lower median avidity index to AMA-1 and MAP1-19 among participants from a higher malaria transmission site compared to lower transmission sites, we hypothesize that;

1. Near constant exposure may interfere with affinity maturation
2. Recent infection may result in low avidity antibodies from short-lived plasma cells

This Chapter aimed to test the hypothesis, taking advantage of the longitudinal PRISM cohort and interruption of malaria transmission by introducing IRS to compare antibody avidity in the same individuals during high exposure and near-zero exposure, on a panel of 18 malaria antigens. A novel high throughput multiplex bead assay method was optimized and adapted to allow the simultaneous measurement of the antibody avidity profile to 18 antigenic targets, spanning different compartments of the blood-stage infection, plus a non-malaria control Tetanus toxoid

(TT). To date, there has been no method available to allow the simultaneous measurement of avidity index to a large number of *P. falciparum* antigens in a high throughput manner.

To our knowledge, this is the first study to adopt the multiplex bead assay to evaluate avidity to a large panel of 18 malaria antigens. The high throughput assay was based on the established ELISA methodology and was adapted for use on the MagPix multiplex platform (Luminex). The introduction of IRS in Tororo provided a unique opportunity to investigate the effects a reduction in *P. falciparum* infection would have on naturally acquired antibody responses following one year of IRS on a broad panel of malaria antigens from the blood-stage of infection. The avidity index, total, and avid (strongly binding antibody pool) IgG responses were analyzed to understand the driver of the humoral immune response associated with age and infection status.

5.3 Methods

5.3.1 Study population and time-points

In this study, 160 participants enrolled in a longitudinal PRISM cohort were included. These were all the children below 11 years and 20% of the adults who had plasma collected during the study period. The introduction of the IRS study informed the study period. The participants belonged to age categories 1 – 4 years (40), 5 – 11 years (92), and above 18 years (28). For each participant, 4 time-points were included; two pre-IRS time-points. T1 and T2 were taken 12 and 6 months before the first round of IRS, respectively. T3 and T4 were taken at 6 months and 1-year after the first IRS, respectively (Chapter 3, Figure 3.3).

5.3.2 Ethical consideration

Ethical approvals were obtained from the Makerere University School of Medicine Research and Ethics Committee (REC REF 2011-203), the Uganda National Council for Science and Technology (HS 1074), the LSHTM ethics committee (reference # 6012), and the University of California, San Francisco Committee on Human Research (reference 027911).

5.3.3 Multiplex bead array assay to measure total and avid IgG

Total IgG responses in diluted plasma samples as 1/1000 was measured using the MagPix (Luminex Corp, Austin, Texas) multiplex platform to 18 *P. falciparum* blood-stage antigens and TT using protocols as previously described Chapter 3, section 3.29.

The Luminex assay was modified to measure avid antibody responses, as described in Chapter 3, section 3.2.11. Basically, one of the two bead wells per sample was reacted with plasma for 90 minutes at room temp followed by treatment with 2M Guanidine Hydrochloride (GuHCl) for 20 minutes to displace weakly binding antibodies. The beads were reacted with a secondary mouse anti-human IgG antibody labeled with phycoerythrin (PE) to detect antigen-specific antibodies present in plasma. The antibodies that remained bound to the bead coupled antigen after treatment with 2M GuHCl was referred to as avid IgG pool. The second well followed the standard assay to measure total IgG. The difference between the total IgG and avid IgG pool was referred to as the non-avid antibody pool. The avidity index was defined as the percentage of avid antibody remaining after treatment and is calculated as follows:

Equation 1

$$AI = \left(\frac{\text{MFI with GuHCl (avid)}}{\text{MFI without GuHCl (Total)}} \right) \times 100$$

5.3.4 Statistical analysis

The net change in total and avid IgG levels and avidity index during the highest and lowest malaria transmission intensity was derived from a paired difference between MFI and AI at T2 and T4, respectively.

The association between antibody levels (MFI) for both the total and high avidity IgG with days since the last infection or proportion of months free from infection was assessed using the generalized estimation equation (GEE) model. GEE allows regression of repeated measures of all 4-time-points per subject, adjusted for age. Infection was defined as positive if blood smear microscopy positive or LAMP positive. The proportion of months free from infection was defined as the months out of 12 that a participant was infection-free. The GEE model analysis outcome was regression coefficient (coef) and the 95% confidence intervals (change in log₁₀ MFI for every day since the last infection).

Association between total IgG, avid IgG, and avidity index with age was assessed in a GEE model, adjusted for days since infection. Age category 1-4 years was the reference, and the

outcome was coef and 95% confidence interval (log10 change in antibody levels as you transition from age category 1-4 to 5-11 or above 18 years).

Analysis and Figures were performed with Stata version 14 (StataCorp LLC, USA) and GraphPad Prism version 7 (Graphpad Software Inc, USA). Changes and associations were considered statically significant when 95% confidence intervals did not overlap with zero or P-values were less than 0.05.

5.4 Results

5.4.1 Validation of an antibody avidity assay MagPix multiplex platform

The first part of the results describes the validation of the Luminex platform to determine suitability and reproducibility to measure antibody avidity for malaria antigens. To achieve this, we evaluated the impact of the GuHCl chaotropic agent on bead integrity and each of the coupled antigens. Once this was established, I focused on defining the optimal conditions for the assay.

5.4.2 Assay reproducibility to inform use if single well

The Luminex platform measures every bead's fluorescent intensity, which can be equated to a single ELISA well OD. Since at least 100 beads are acquired and the median fluorescence intensity (MFI) taken, this can be equivalent to a median of 100 ELISA wells. To test if the platform was indeed reproducible, we tested 20 samples duplicated and compared their MFI. A high degree of agreement between two duplicate wells on the same plate was observed (Figure

5.50a). This data-informed use of one well per sample for the assays. A standard curve constructed from hyperimmune plasma pp4 was included on every plate to monitor inter-plate variations over time. Figure 5.50b confirmed a high degree of reproducibility of the method.

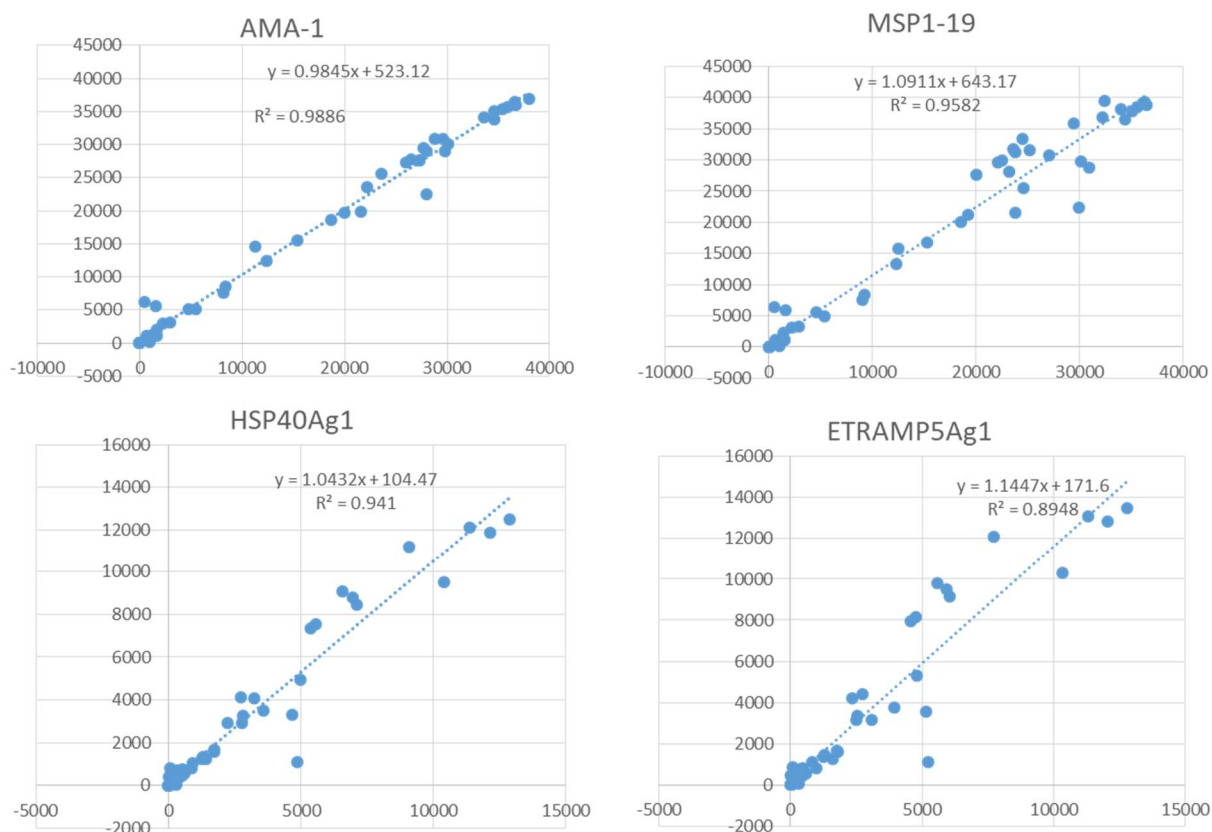


Figure 5.50a Graph showing MFI of representative antigens tested in duplicate on one plate. A total of 40 sampled at a dilution of 1/1000 were included.

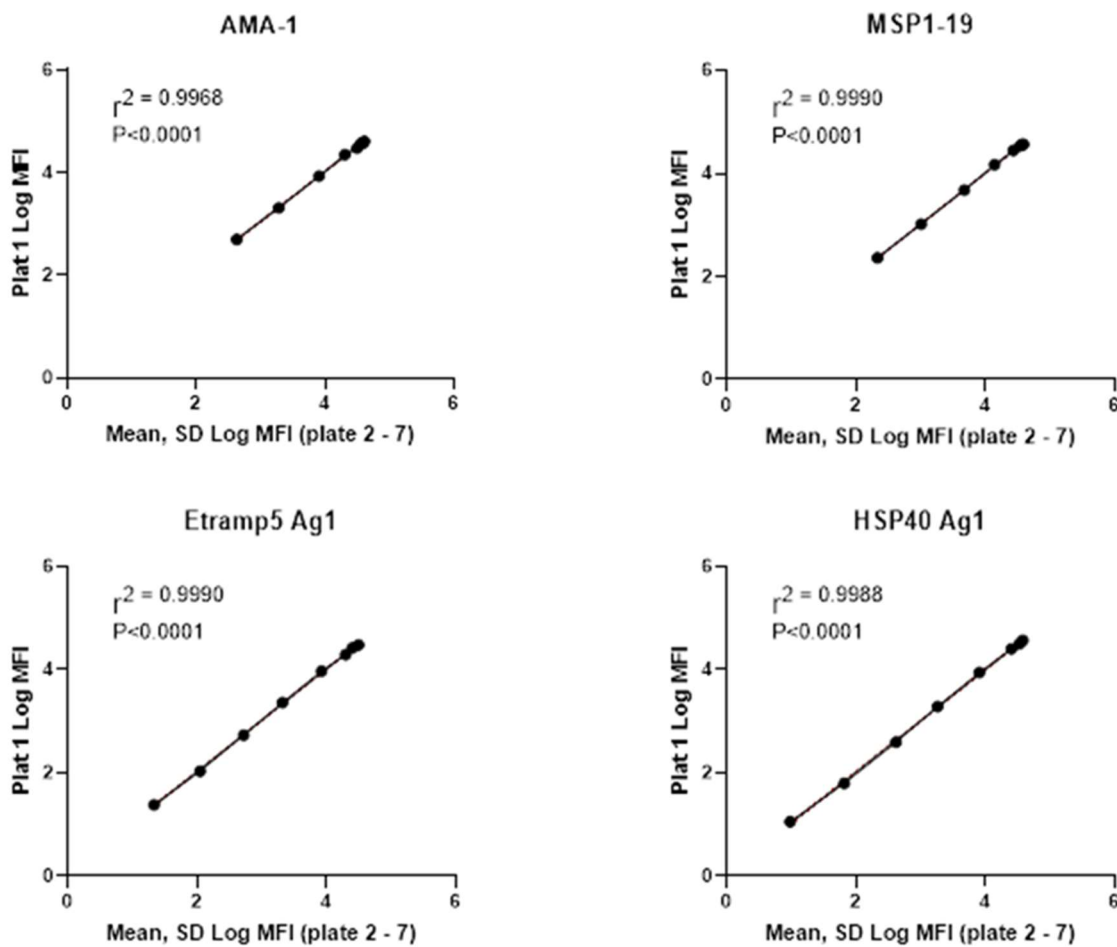


Figure 5.50b Graph showing MFI of representative antigens plate 1 PP4 curve plotted against the 7 plates. PP4 standard curve at 8, 5X dilution points included on every plate. The standard curve was used to normalize variation across plates.

5.4.3 Effect of GuHCl on the properties of magnetic beads

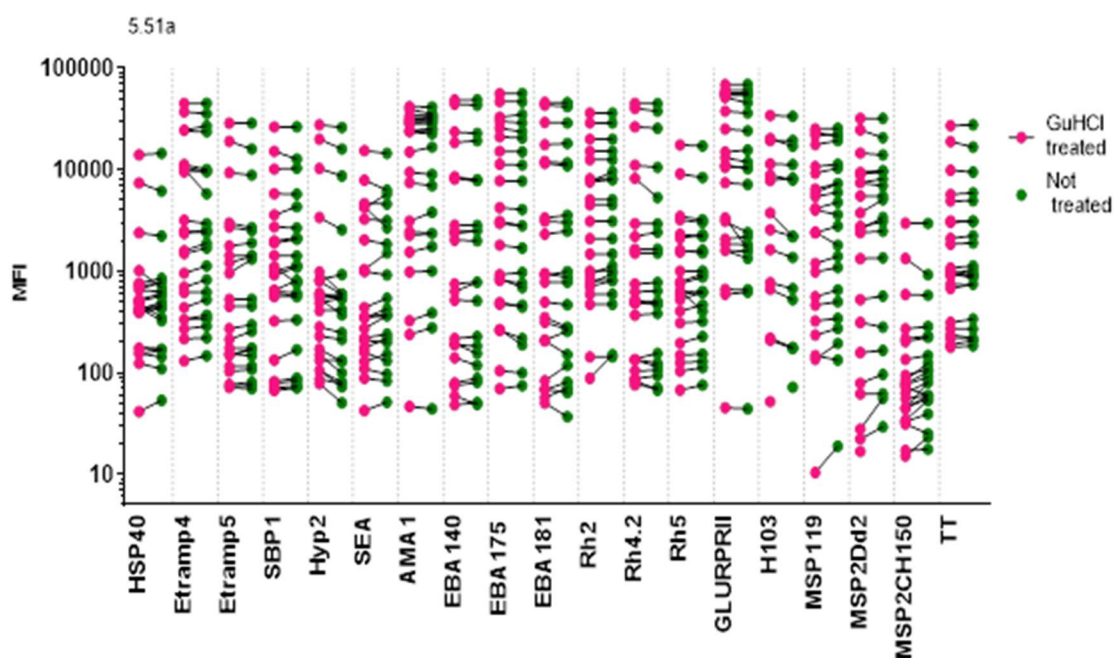
To perform the avidity assay on the Luminex platform, it was necessary to establish the effect of GuHCl on the properties of MagPex microsphere beads. Uncoupled MagPlex microsphere beads were treated with 0.5, 1, 2, and 5M GuHCl for 20 minutes at room temperature. The beads were

then washed as per the protocol and acquired using the Magpix machine. All the tested beads behaved normally, with each bead detectable in the correct bin. This result implied that GuHCl did not affect the core spectral signature or the beads' magnetic properties. A follow-up monoplex assay was then performed. In this, 1000 beads representing 5 distinct bead regions in separate duplicate wells were treated with 5M GuHCl (highest concentration previously used on the ELISA platform(310)) for 20 minutes in one well with the second well treated with PBS, and acquired on the Magpix machine. As before, the beads performed normally, with beads only detected in their assigned bins and not in other non-assigned regions. Counts were comparable between the GuHCl treated and non-treated wells. These results supported the previous conclusion, suggesting that the GuHCl at 5M did not affect the beads' spectral or magnetic properties and hence did not affect bead region identification and recovery.

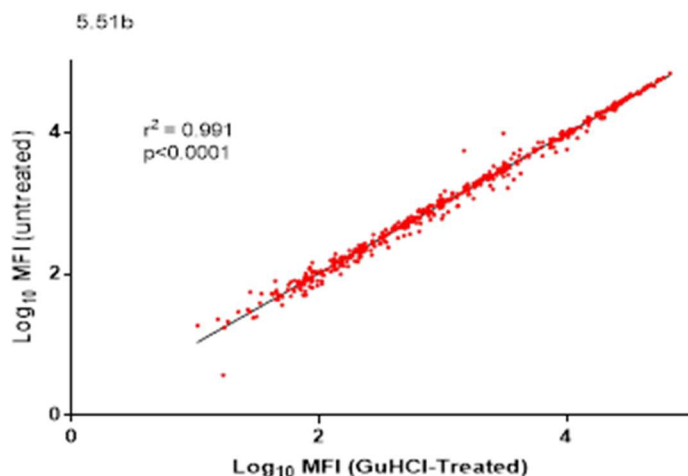
5.4.3 Effect of GuHCl on the antigens coupled to beads

Due to the chemical coupling of antigens to the microsphere and for the potential for the GuHCl to disrupt this link or damage the bound proteins, it was necessary to determine whether 5M GuHCl had an adverse effect on antigens coupled to beads, 20 samples including the positive control PP4 were assayed in duplicate. The duplicate wells containing the coupled beads, including all the 18 antigens and TT in a multiplex, were incubated with either 5M GuHCl or PBS for 30 minutes. The beads were washed, and the assay was completed following the standard method previously described. There was no difference in the MFI between the wells pre-treated with GuHCl and the wells treated with PBS (Figure 5.51a). There was a high positive correlation

between the paired wells (Figure 5.512b). This observation confirmed that GuHCl did not uncouple antigens from the beads or affect the coupled antigens' antibody-antibody binding properties.



8 **Figure 5.51a** Graph showing MFI for samples tested using GuHCl-treated and untreated antigen coupled MagPix microsphere beads. A total of 20 samples were included in this experiment. The results are displayed per antigen. One set of the beads were pre-treated with 5M GuHCl for 30 minutes before performing the standard assay, and MFI was compared to untreated beads.

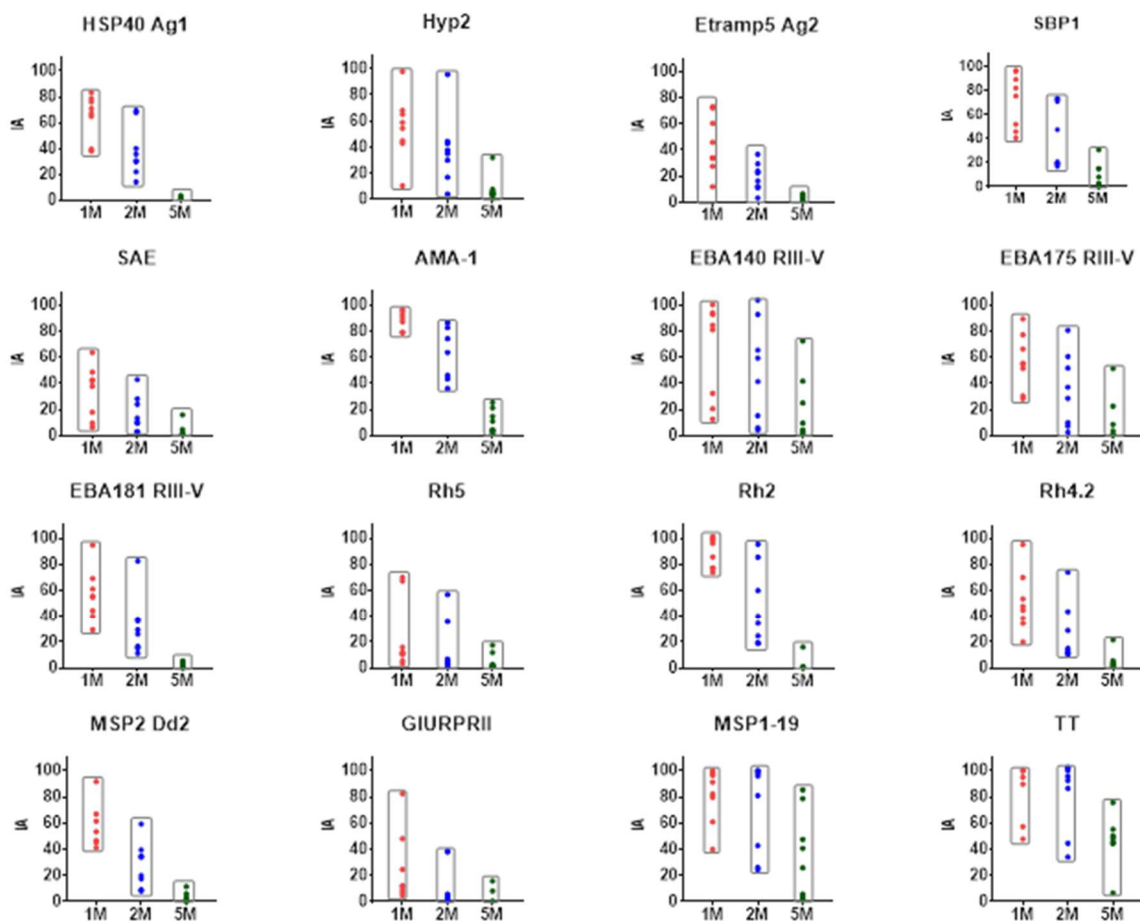


9 Figure 5.51b Scatterplot is showing the correlation between GuHCl-treated and untreated antigen-coupled MagPlex Microsphere beads. Based on the combined data of 20 samples for all 18 antigens and TT. One of the paired wells was pre-treated with GuHCl, and the second one with PBS for 30 minutes and washed before plasma was added. $r^2 = 0.991$, $P < 0.0001$.

5.4.4 Optimal GuHCl concentration and dissociation time

To further test the avidity assay's performance in the presence of serum, 7 samples with wide-ranging antibody responses across the antigen panel were selected based on the total IgG data. The GuHCl concentration was titrated at 1, 2, and 5M. All three concentrations resulted in the dissociation of antigen-specific bound antibodies. The concentration of 2M was selected for use in the main assay due to its wider dynamic range than 5M in most antigens (Figure 5.52).

5.52



10 Figure 5.52. Dot plots of avidity index at three GuHCl concentrations. 8 plasma samples were included at 1/1000. Concentrations 1M (red) and 2M (blue) had a wide dynamic range in most of the antigens compared to 5M (green).

To determine the optimal dissociation time, a total of 7 samples were included in a time-series experiment where GuHCl at 2M was added to a set of 6 wells per sample and incubated on a

shaking platform for 0, 10, 15, 20, 25, and 30 minutes. The assay was terminated as described above, and the samples were assayed and acquired on the MagPix machine as per the described methods. The avidity index was plotted against the incubation time for each of the samples (Figure 5.53).

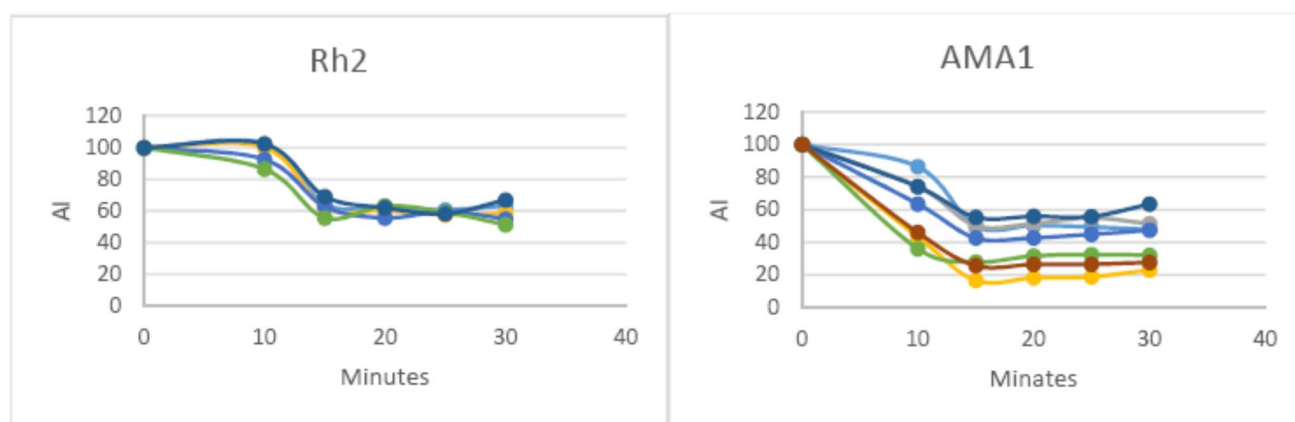


Figure 5.53. Representative graphs to show a change in the avidity index over incubation time. Antibody dissociation maximum at 2M GuHCl for 8 plasma at 1/1,000 was achieved at 15 minutes, beyond which there was no change in avidity index. 20 minutes incubation time was selected for the main assay to minimize inter-well and inter-plate

Maximum dissociation was achieved at 15 minutes, beyond which there was no appreciable decrease in MFI or increase in avidity index (Figure 5.53). An incubation period of 20 minutes was selected for the main assay as optimal dissociation time. The 20 minutes optimal time would allow for differences of up to 5 minutes in timing within wells of the same plate during pipetting without affecting the avidity index. This implied that up to five minutes difference in the GuHCl dissociation incubation period would have minimal effect on the plate's avidity index or between plates.

5.4.5 Heterogeneity in Avidity Index

The avidity index was calculated as the percentage of the avid antibody (MFI with GuHCl) of the total (MFI without GuHCl). Only samples whose MFI without GuHCl was between 50 (1.69 log 10) and 27,000 (4.43 log 10) (Figure 5.54a) were included in the analysis to allow detection of changes in MFI after dissociation at the low and high ends. Including all-time-points, there was a high heterogeneity in the antigen's avidity index, ranging from near zero to 100 (Figure 5.54b). There was minimum or no correlation between avidity index total antibody except for AMA-1 (Spearman rho 0.67 $p < 0.0001$), Rh2 (Spearman rho 0.51 $p < 0.0001$), and TT (Spearman rho 0.67 $p < 0.0001$). There was a negative correlation between the avidity index and total antibody for antigens H103 (-0.39, $p < 0.0001$) and MSP2-CH150/9 (-0.33, $p < 0.0001$). The rest of the antigen spearman rho were below 0.28 (Figure 5.54b). Furthermore, there was no apparent trend in avidity index or total antibody levels between iRBC antigens, merozoite surface antigens, or merozoite apical complex antigens. There were differences in median avidity index across antigens without considering the antigens' size, protein folding, or epitope valence. Only three antigens, AMA-1, MSP1-19, and H103, had their avidity index above 50, similar to the non-malaria antigen TT. Some antigens such as Rh4.2, Rh5, SEA, and GLURP RII had their median avidity index below 20 (Figure 5.54b). At the individual level, there were trend patterns of avidity index across the time-points ranging from steady increase to steady decreasing with several patterns from time point to time point (Figure 5.54c). At the individual level, the avidity index to TT was relatively similar across time-points,

12

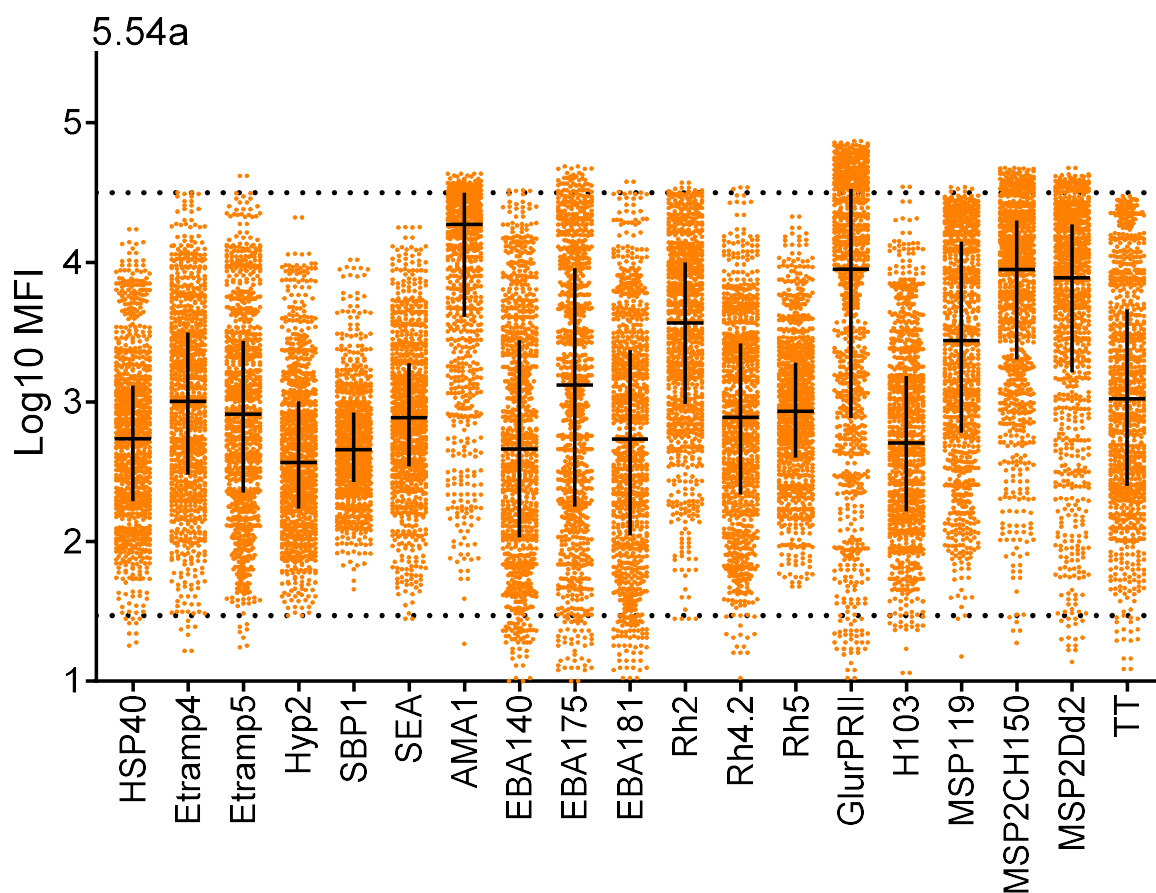


Figure 5.54a Scatter plot of Log10 MFI by antigens. MFI is representative of antibody levels measured by MagPix Luminex in a multiplex assay. All data from 4-time-points were included. The bars indicate the median and interquartile range. The dash lines indicate the data range (1.69 and 4.43 lower and upper cutoff, respectively) included in the calculation of the avidity index

13

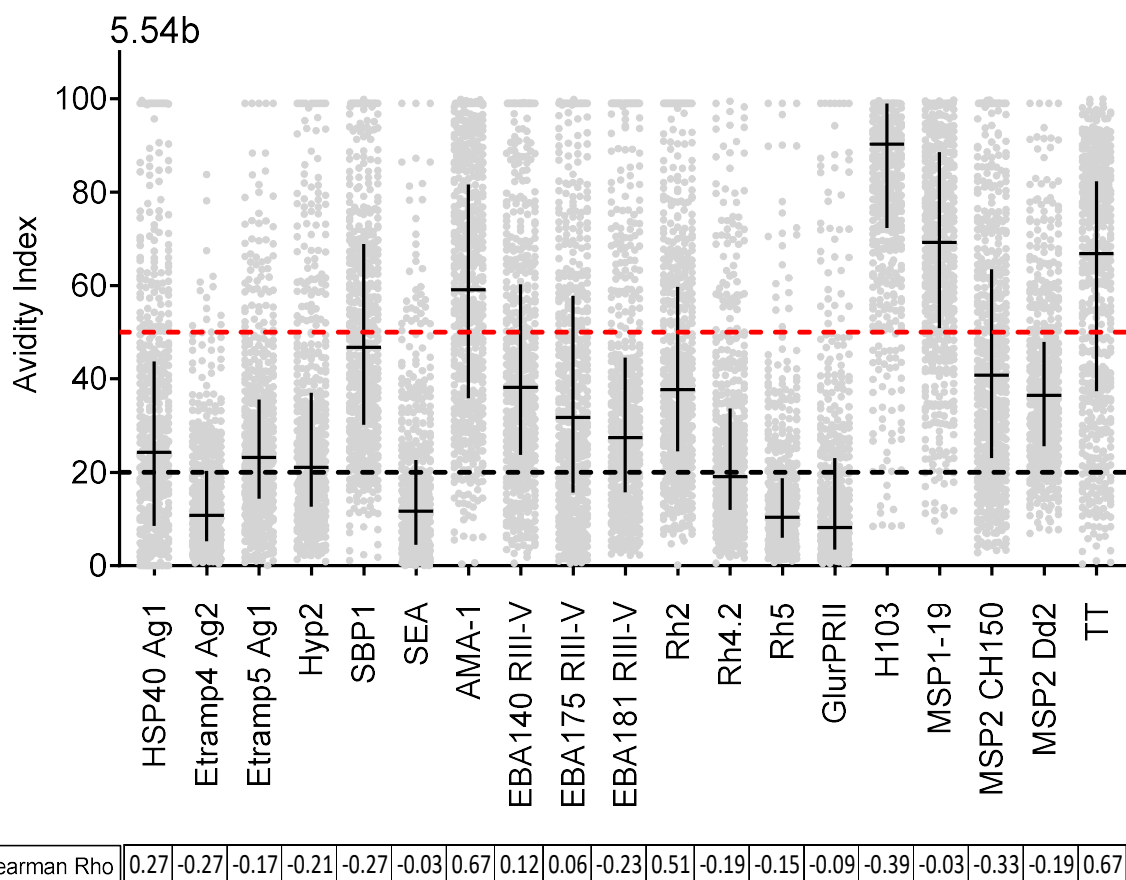


Figure 5.54b Scatter plot of avidity index by antigens. AI is the percentage of the avid antibody of the total measured by MagPix Luminex in a multiplex assay. All data from 4-time-points were included. The bars indicate the median and interquartile range. The red dash line is the 50-mark, and the black dash line the 20-mark. The bars indicate the median and interquartile range. The spearman rho shows the Spearman correlation between the avidity index and total antibody MFI.

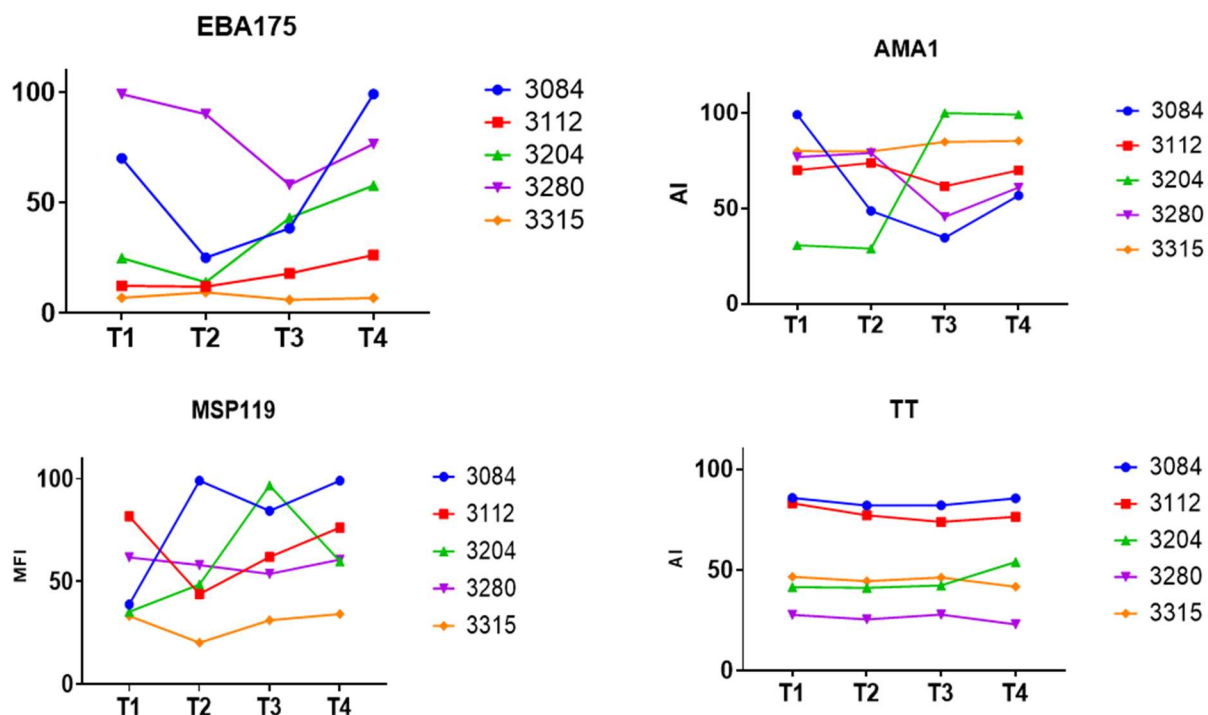
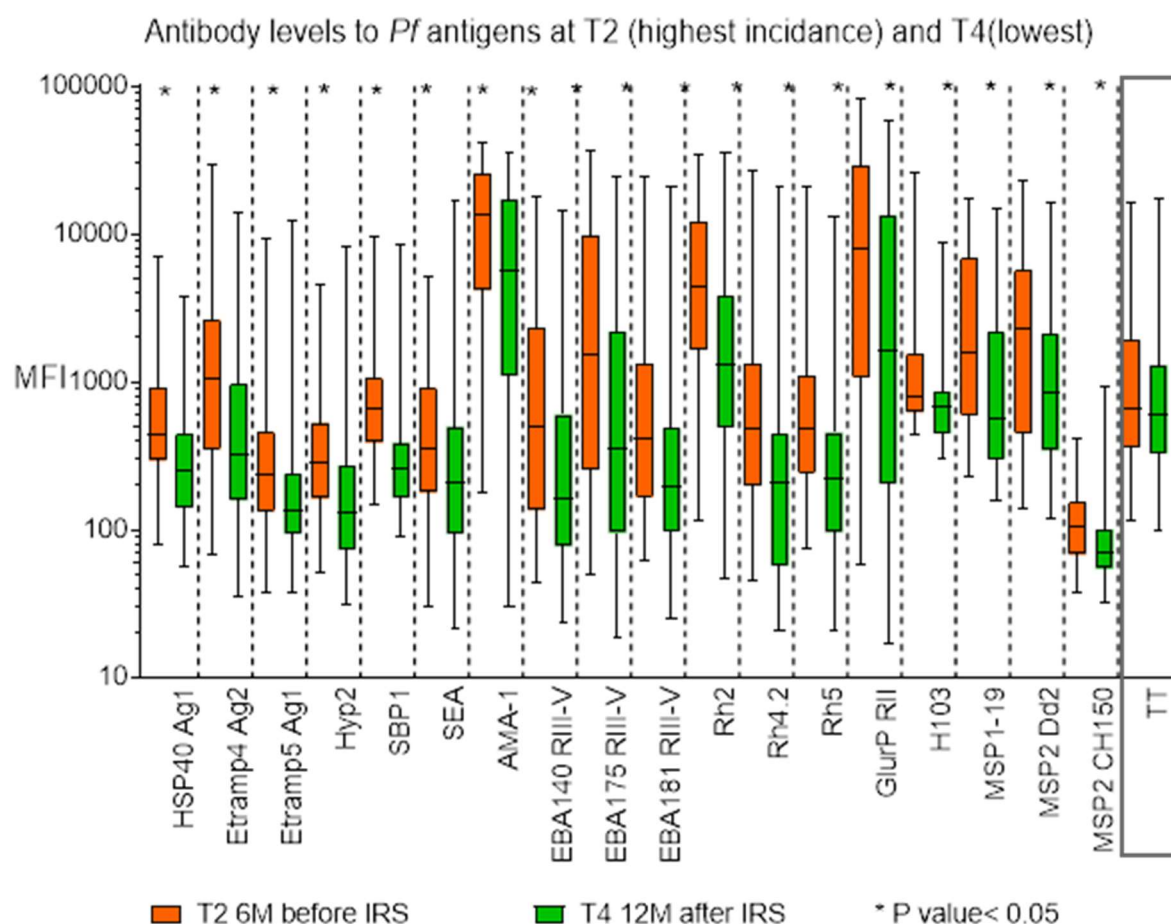


Figure 5.54c Avidity index of representative antigen for representative participants across time-points. T1 and T2 are 6 and 12 months before IRS. T3 and T4 are 6 and 12 months after the first round of IRS, respectively.

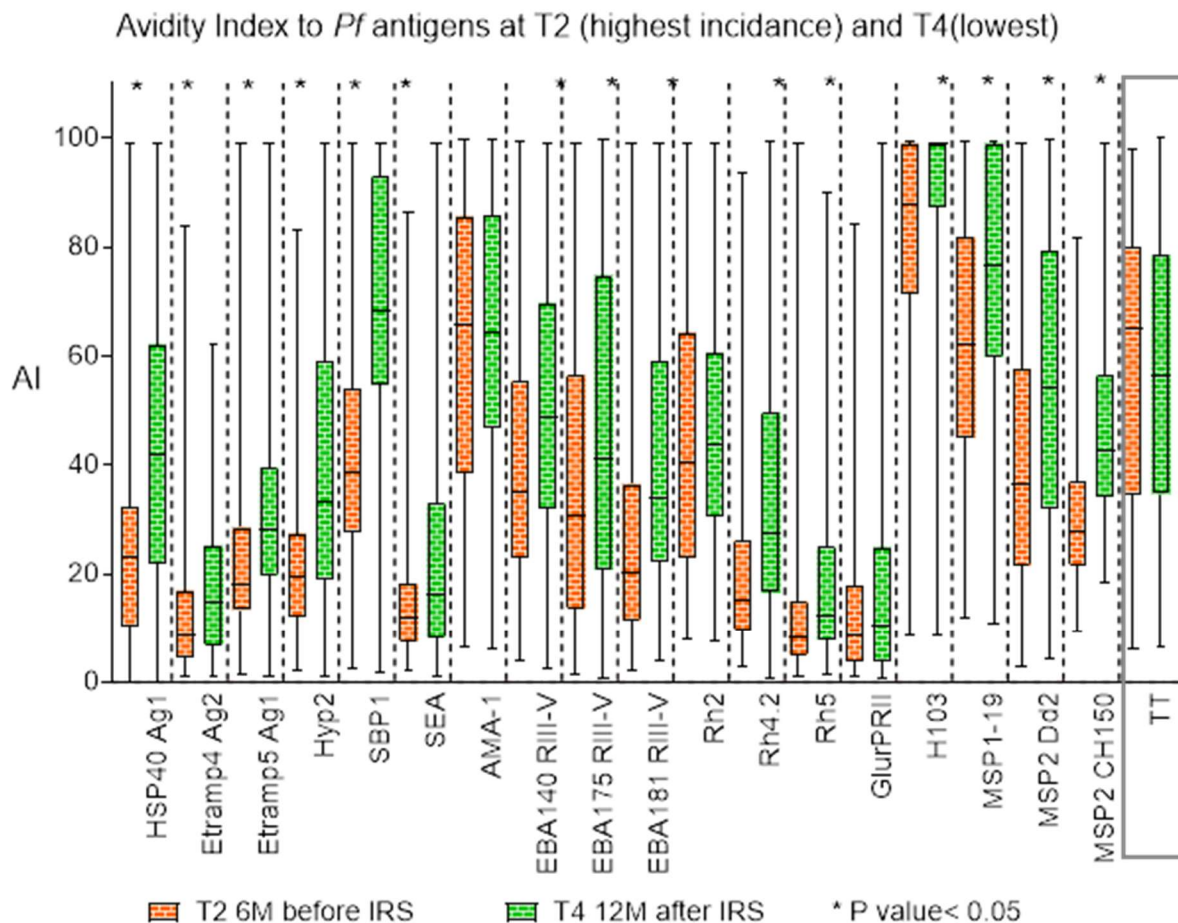
5.4.6 Decreased total antibody levels and Increased avidity index between 6 months before and 12 after IRS

To test the hypothesis that reduction in malaria transmission results in increased avidity index due to contraction of SPLC that secrete non-avid antibodies, antibody levels were compared between T2 when malaria incidence was highest (6 ppy), 6 months before the introduction of IRS, and T4 when malaria incidence declined to near zero, 12 months after the first round of IRS. Median antibody levels significantly decreased across all malaria antigens (Figure 5.55a).

Conversely, there was a significant net increase in median avidity index between T2 and T4 across most blood-stage malaria antigens except for AMA1, Rh5, and GEXP18 (Figure 5.55b). There were no noticeable trends across the infected red blood cell-associated antigens, merozoite apical complex, or merozoite surface antigens. There was no difference in TT's antibody levels and avidity index, the non-malaria positive control, between T2 and T4. Overall, these results imply that a dramatic reduction in malaria transmission intensity resulted in a general loss of antibodies against blood-stage malaria antigens and a general increased avidity index. The change in malaria transmission intensity did not affect antibody levels or avidity index of TT.



15 Figure 5.55a Comparison of median MFI between T2 and T4. Malaria incidence decreased from a peak of 6 episodes per person per year at T2 to near zero at T4 following the IRS introduction. MFI represents antibody levels measured by a MagPix Luminex multiplex assay for 18 malaria blood-stage antigens and non-malaria TT control (in a box). Medians were compared using the nonparametric Mann-Whitney U test. $P > 0.05$ was considered significant and represented by *.



16 **Figure 5.55b** Comparison of median avidity index between T2 and T4. Malaria incidence decreased from a peak of 6 episodes per person per year at T2 to near zero at T4 following the IRS introduction, 6 months before T2, and 12 months after T4. The avidity index represents the percentage of avid antibodies of the total. Medians were compared using the nonparametric Mann-Whitney U test. $P > 0.05$ was considered significant and represented by *.

5.4.7 Increased avidity index was due to differential net loss in the total pool versus avid antibody at 6 months PRE and 12 post-IRS

To try and understand the factors behind the difference in avidity index between the two-time-points, changes in total and avid antibody levels were evaluated separately. There was a significant general reduction in the total antibody's medians across all antigens (Figure 5.56). Similarly, there was a significant reduction in the medians of avid antibody levels in all the antigens except for MSP2-CH50/9 that increased. HSP40Ag1, H101, and Hyp2 had a minimal decrease in the medians of their avid antibody pools between T2 and T4 (Figure 5.56). There was no change observed in both the total and the TT's avid antibody levels, between T2 and T4 (Figure 5.56). Since the avid antibody pool was a component of the total, the differences in antibody reductions between the total and avid antibody pools were the indirect measure of the non-avid antibody pool. In summary, these findings implied a reduction in both avid and non-avid antibody pools between T2 when malaria transmission was highest and T4 when it reduced to near zero after the impact of IRS. However, the non-avid pool reduced at a greater magnitude than the avid, and this preferential loss of the non-avid antibody resulted in an increased avidity index. The net antibody reduction between the two-time-points was not observed in TT responses. The results agreed with the hypothesis that decreased malaria transmission resulted in an increased malaria-specific avidity index.

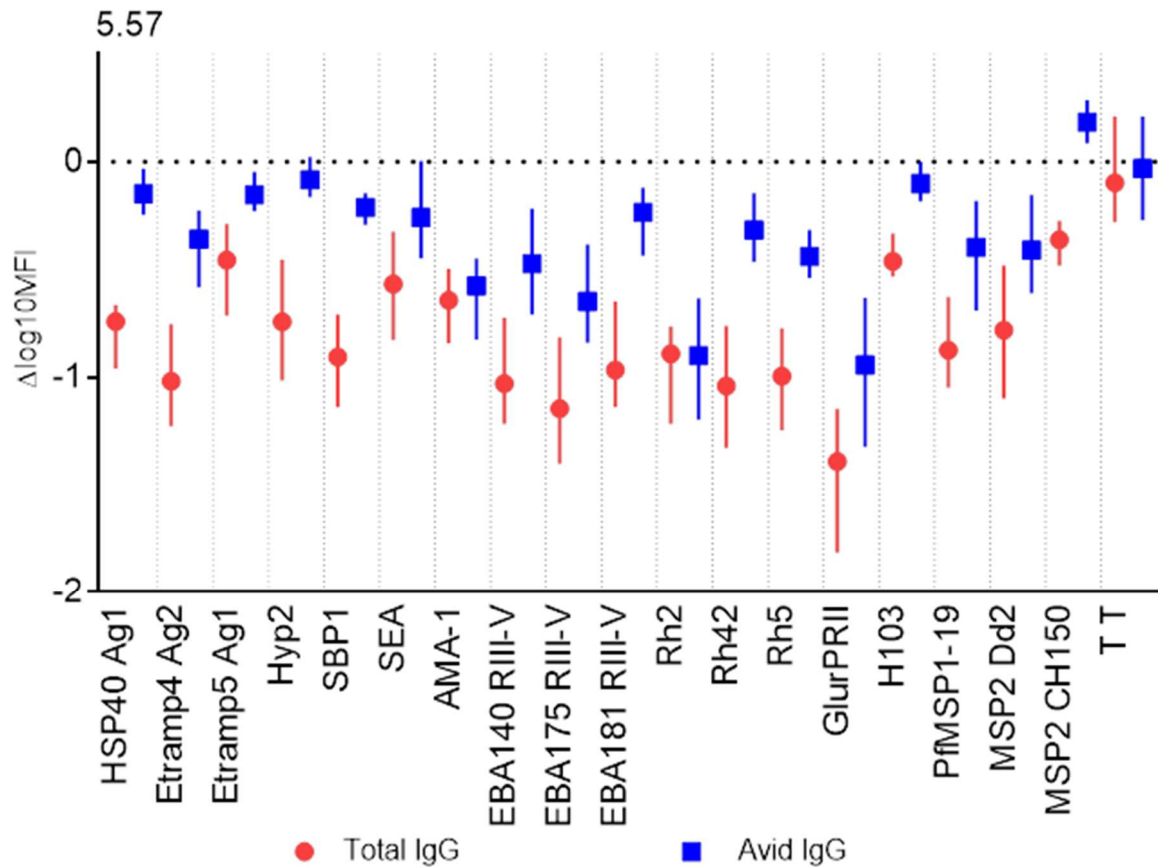


Figure 5.56. A plot of the net change in MFI between T2 and T4. Malaria incidence decreased from a peak of 6 episodes per person per year at T2 to near zero at T4. ΔLog_{10} MFI is the difference in log antibody levels between T2 and T4. The data is represented as the median with 95% CI. The horizontal line represents zero. Below the line is a loss, and above again in antibody levels between T2 and T4. Overlapping the zero line is a non-significant difference (p value > 0.05). The analysis included 160 participants at T2 and T4

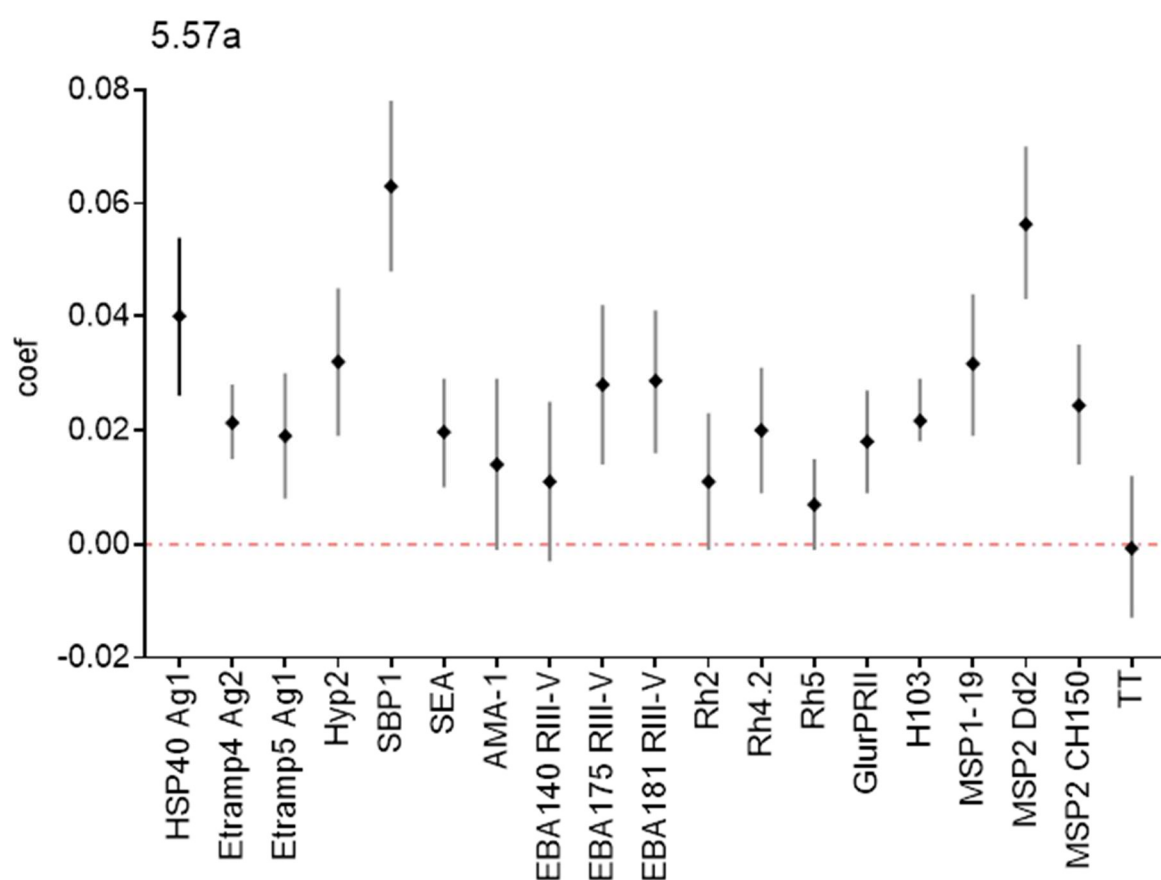
5.4.8 Avidity index was positively associated with prior malaria infection

All 4 time-points were included in the GEE to determine the association of avidity index and recent infection. The GEE fitted repeated avidity index measures of individuals in a regression model to determine linear relationships between avidity index and days since *P. falciparum* infection or the proportion of months free of *P. falciparum* infection the last 12 months. The analysis model included adjustment for age categories 1-4 years, 5-11 years, and above 18 years. Infection included both microscopic positive and sub-microscopic positive (LAMP+).

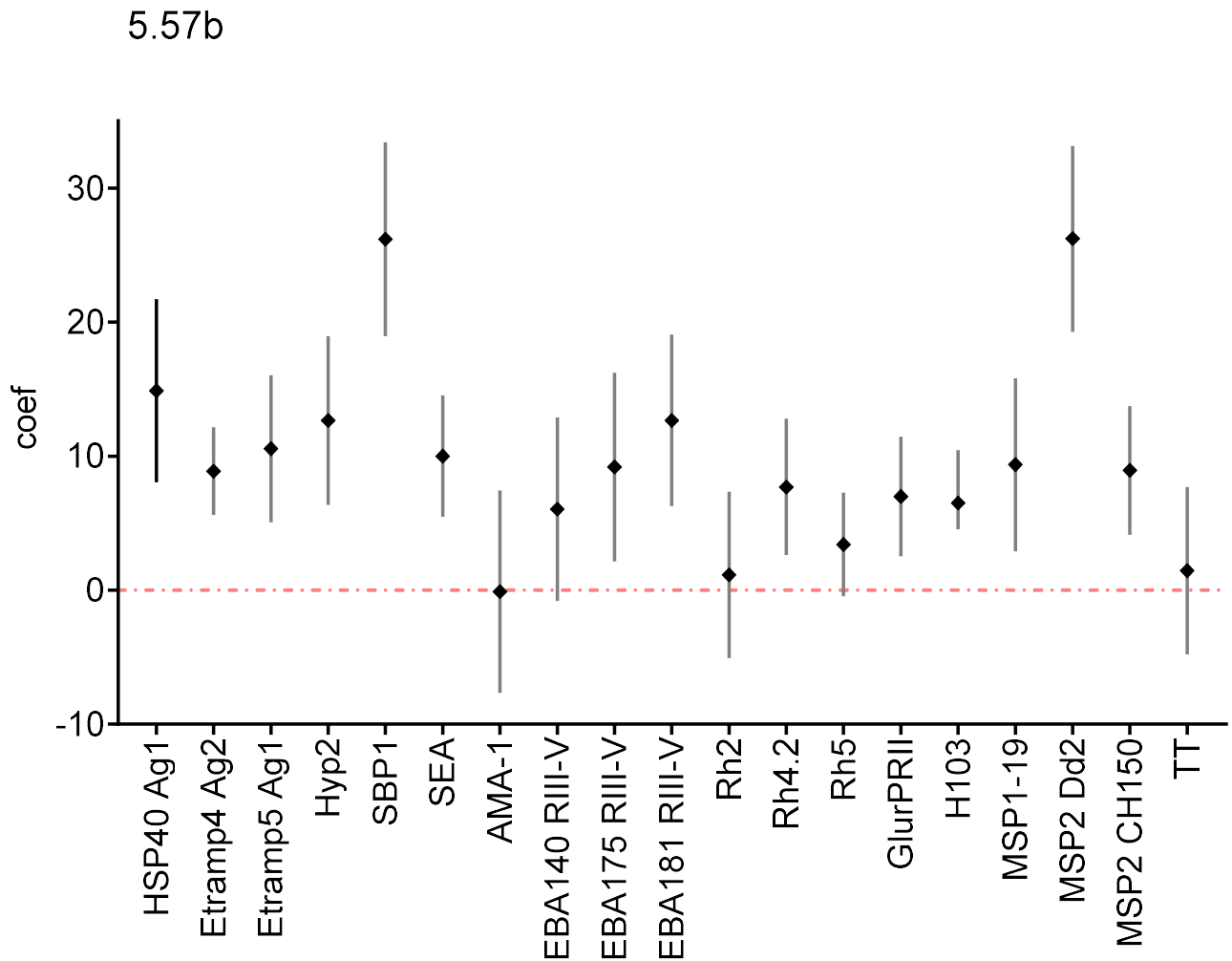
In general, there was a significant increase in avidity index associated with days since infection (Figure 5.57a). The strongest significant positive association was observed in antigens like SBP1, MSP2-Dd2, HSP40Ag1 (Figure 5.57a). Take an example, the coef of SBP1 0.06 (0.05 – 0.07), the result implied that increase on avidity index by 6.0% (5.0 – 7.0) was independently associated with 100 days since last *P. falciparum* infection. Some antigens like Rh5, Rh2-2030, and AMA-1 did not show significant associations but maintained a similar positive trend.

Similarly, avidity index was positively associated with the proportion of months free *P. falciparum* infection in the last 12 months, another measure of recent infection, ranging from a large significant association in antigens like SBP1, MSP2 Dd2 HSP40Ag1 to antigens with no significant association like Rh5, Rh2, and AMA-1(Figure 5.57b). Take a similar example of SBP1 coef of 26.2 (18.9 – 33.4), and the result implied that an increase in avidity index by 26.2% (95% CI; 18.9 – 33.4) was associated with every month free of infection in the last 12 months. Antigens with the largest differences in antibody changes between total and high avidity

antibody pool had the largest coef in the avidity index. There was no observed association between avidity index to TT and prior *P. falciparum* infection.



18 Figure 5.57a Association of avidity index with days since parasitemia adjusted for age. The Coef (diamonds) and 95% CI (bars) represents a change in the avidity index every day since the last infection. Below the zero red line is a net loss, and above is a net gain in the avidity index associated with days since the last infection. Confidence interval overlapping with zero (red dash line) is statistically non-significant. A total of 160 participants at 4 time-points were included in this analysis

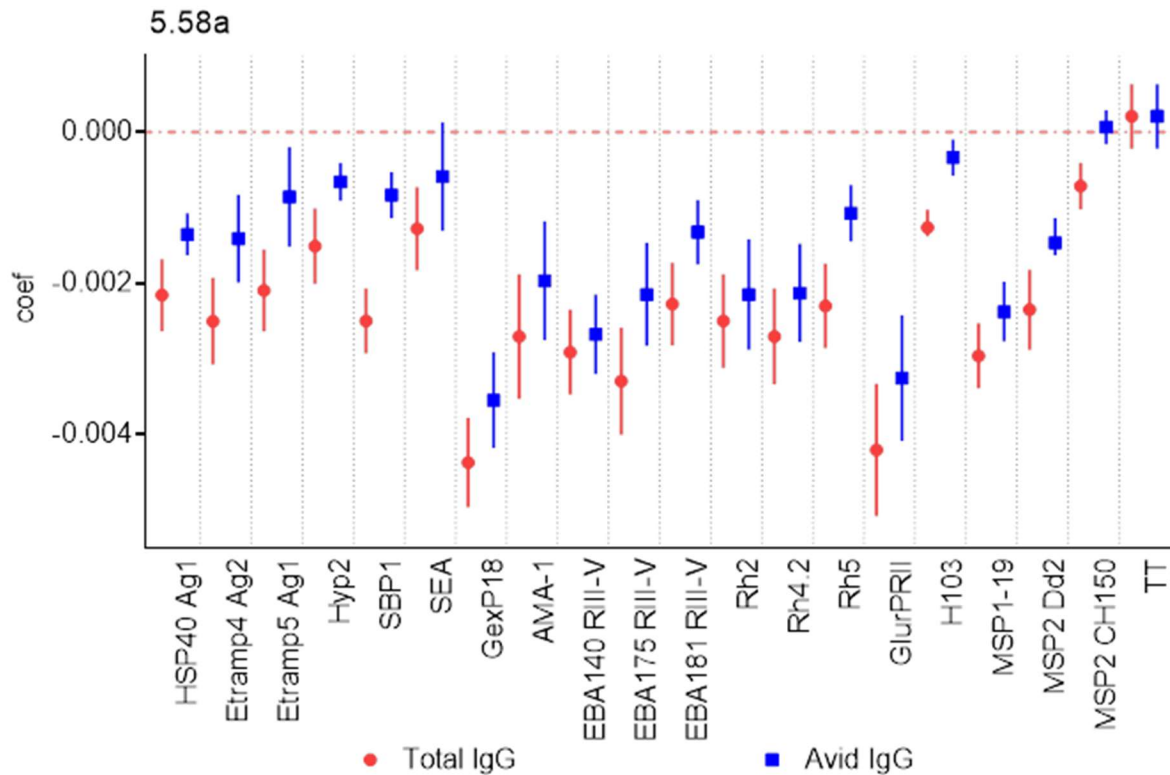


19 Figure 5.57b Association of avidity index with the proportion of months free of infection in the last 12 months, adjusted for age. The Coef (diamonds) and 95% CI (bars) represent the change in the avidity index with the proportion of months free of infection. Below the zero red dash line is a net loss, and above is a net gain. The confidence interval overlapping with zero is statistically non-significant. The analysis included 160 participants at 4 time-points.

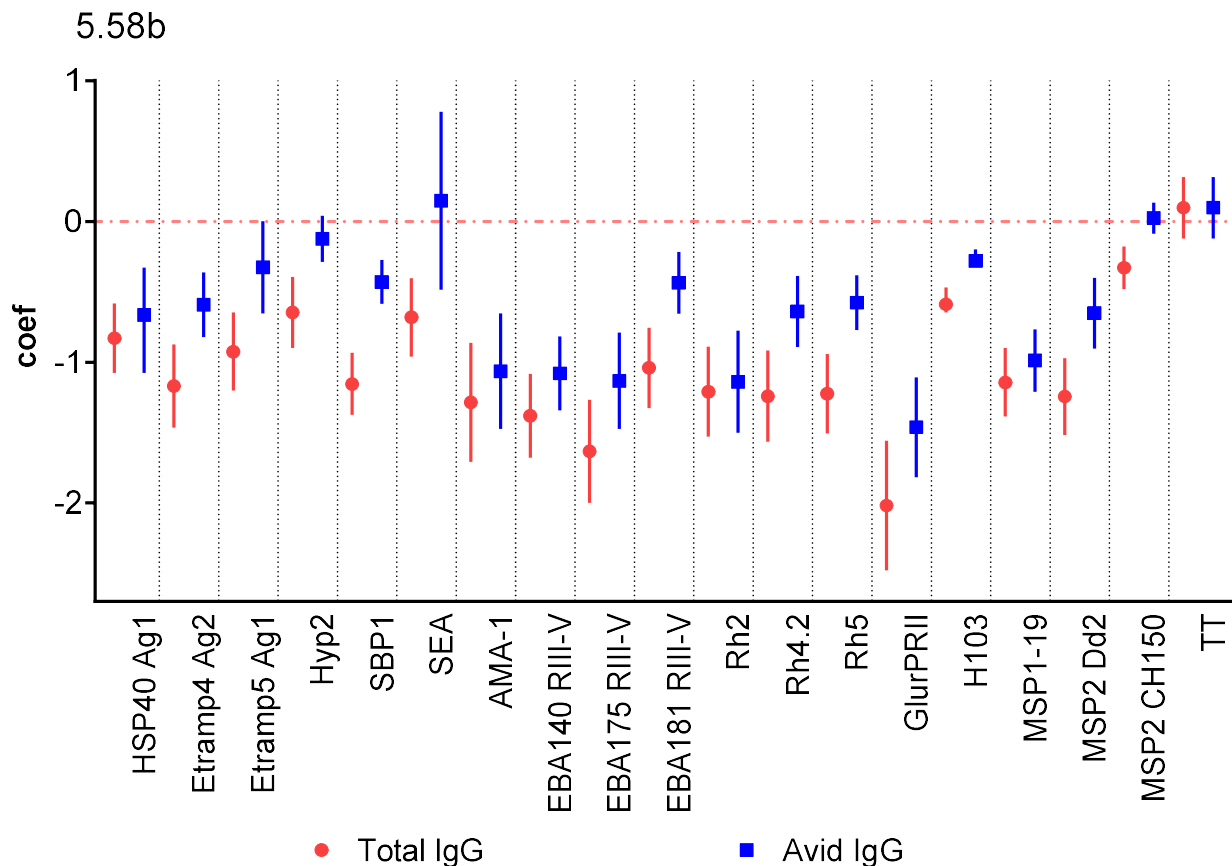
5.4.9 Total and avid antibody levels inversely associated with prior malaria infection

Overall, there was a significant inverse association of total antibody levels associated with days since infection across all the *P. falciparum* antigens from the GEE analysis modal. The highest coef was observed in GLURPRII and lowest in MSP2_CH150 (Figure 5.58a). Similarly, there was a significant inverse association between avid antibody levels with days since infection. The inverse association with days since *P. falciparum* infection was more pronounced in total than the avid antibodies in all *P. falciparum* antigens. There was an exception for antigens, AMA1, and Rh4.2, whose coef of total and avid antibody were largely overlapping (Figure 5.58a). Similar trends of an inverse association of the total and the avid antibody with a proportion of months free of infection in the last 12 months were observed, as shown in (Figure 5.58b). There was no association for total and high avidity antibodies, with days since the last infection, in TT.

Taken together, these observations implied that the loss of antibodies observed independent of age was associated with days since the last infection or with the proportion of months free of infection in the last 12 months. The antibodies lost were mainly from the non-avid than avid antibody pools. The observations supported the hypothesis that the increased avidity index associated with prior infection was due to the differences in antibody decay rates of the avid versus non-avid.



20 Figure 5.58a Association of $\text{Log}_{10}\text{MFI}$ with Days since parasitemia. Coef and 95% CI of the total (red), and the avid antibody (blue). Below the zero line is a net loss, and above is a net gain in antibody levels associated with days since the last infection. The confidence interval overlapping with zero is statistically non-significant. The analysis included 160 participants at 4 time-points.



21 **Figure 5.58b** Association of MFI with the proportion of months free of infection in the last 12 months. Coef represents the change in MFI associated with every month free of infection. The error bars indicate 95% CI. Below the zero line is a net loss. Above is a net avidity index in antibody levels associated with the proportion of months free of infection in the last 12 months. The confidence interval overlapping with zero is statistically non-significant. The analysis included 160 participants at 4 time-points.

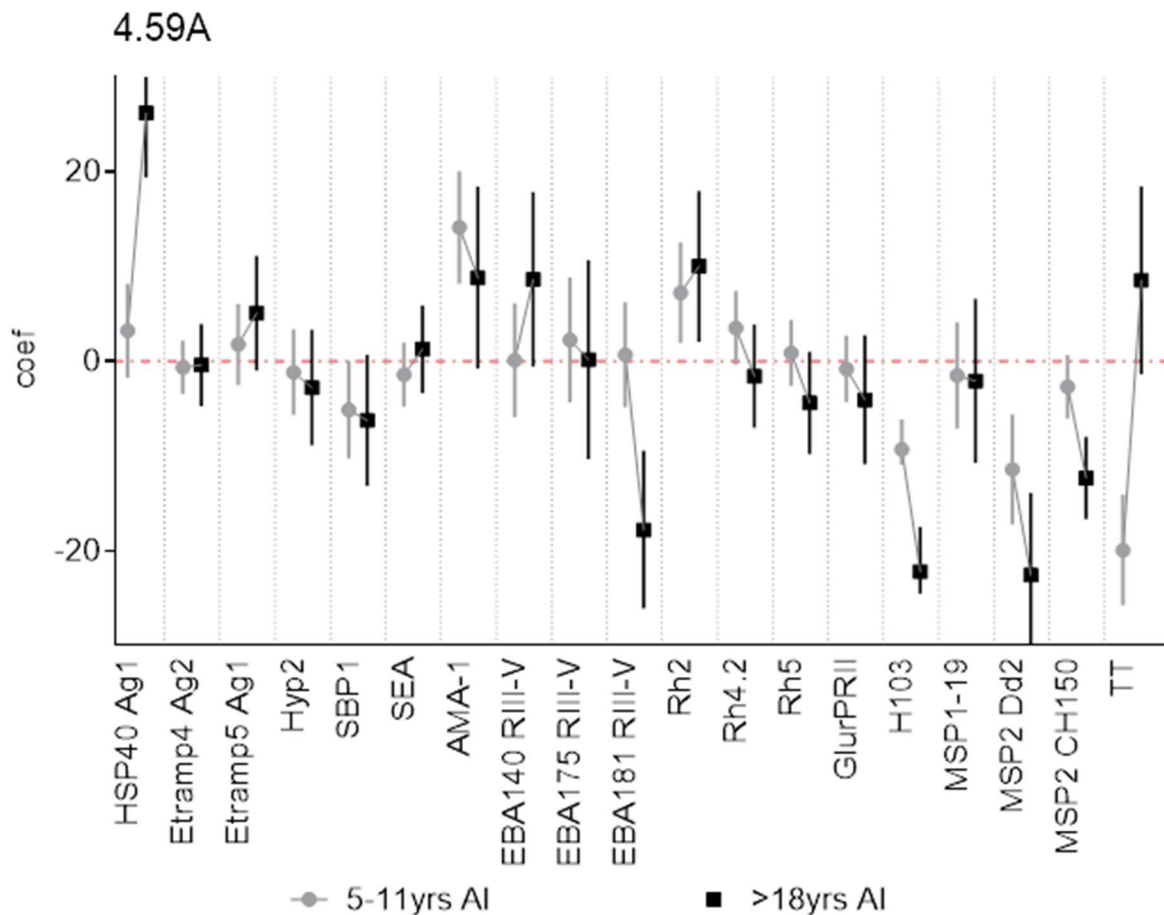
5.50 Changes in avidity index with Age

Age categories 1-4, 5 – 11, and above 18 years were fitted in a generalized estimation equation to determine the association of age with total and avid and avidity index. The model was adjusted for days since parasite infection, and 1 – 4 years was the reference age category.

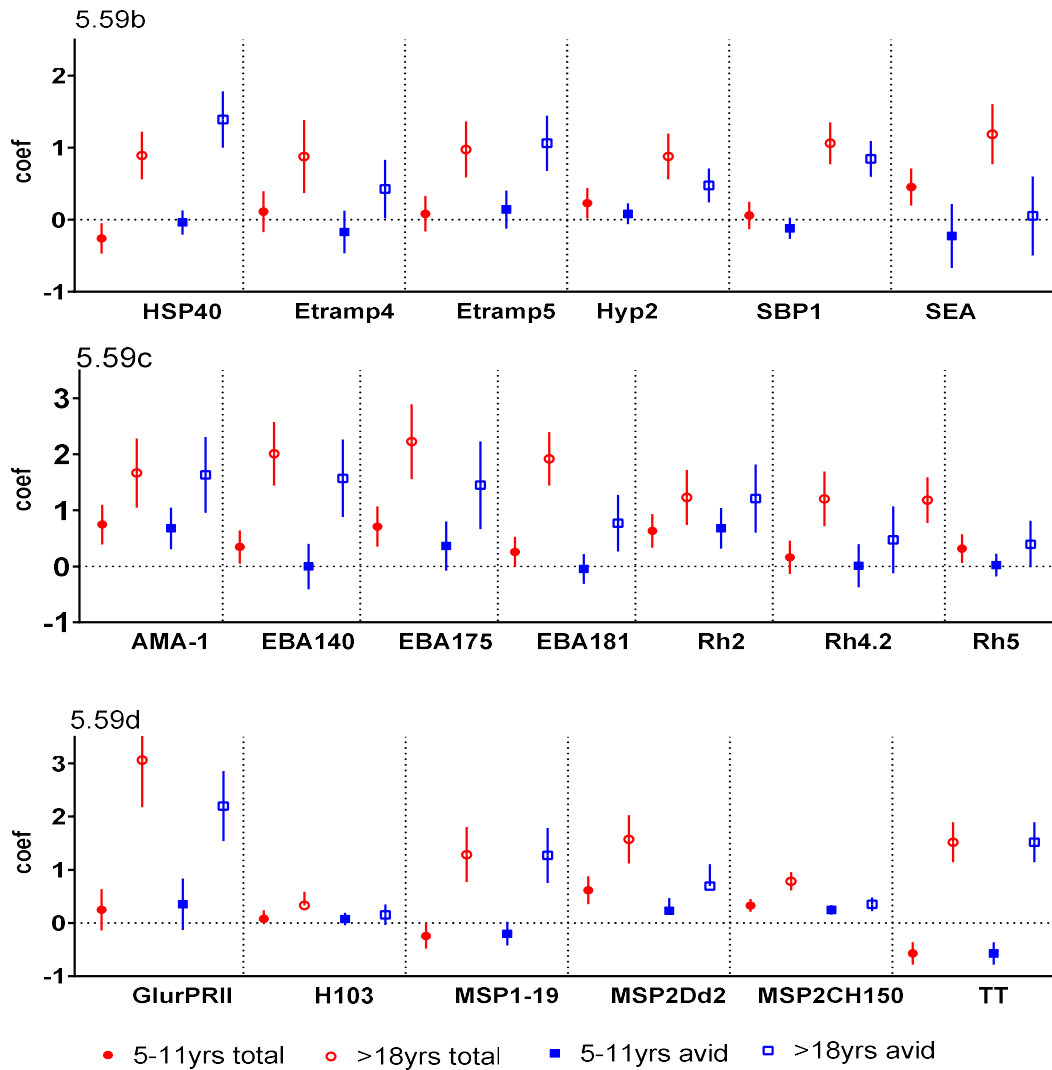
Overall, relative to 1- 4 years, both total and avid antibody levels significantly increased in the above 18 years age category, in association with days since the last infection, in all the malaria antigens. There was minimal change between under 5 and the 5 – 11 age categories (Figure 5.59a). The magnitude of association with age varied between the total and the avid antibody pools. In some antigens, the total coefficient was higher than the avid pools' coefficient, and in some other antigens, the total was lower than the avid pool. In some antigens, the magnitudes were similar for both total and high avidity. (Figure 5.59a)

There was high heterogeneity in high avidity index association with age independent of days since the last infection. In some antigens, age was positively associated with an avidity index with significant association observed above 18 years relative to 1 – 4 years. In other antigens, age was inversely associated with an avidity index with significant association observed above 18 years relative to 1 - 4 years. Yet, in some antigens, age was not associated with the avidity index. All observations taken together, the data implied that both the total and high avidity antibody pools expanded gradually with age, and significant differences only apparent in the adults relative to the 1 – 4 years. However, the two antibody pools expanded at different rates in

the different antigens. The deferential expansion of the non-avid versus avid pools resulted in the high heterogeneity associated with age with an avidity index. (Figures 5.59b-d)



22 Figure 5.59a Association of avidity index with age. GEE model adjusted for days since the last infection, 1-4 years was reference age. The zero line (dotted line) is a change in avidity index as age transition from 1-4 years. Coef and 95%CI represent the change in the avidity index relative to 1-4 years. Overlap with the confidence interval with zero red line is not a significant change in the avidity index relative to 1-4yrs. A total of 160 participants in 3 age groups at 4 time-points were included in the analysis.



23 Figure 5.59b-d Association of the total and the avid antibody with age category in a GEE model adjusted for days since the last infection. Age 1-4 years was the reference. The zero (dotted line) difference is in antibody levels as age transition from 1-4 years. Overlap coef and 95% CI overlap with zero is not a significant change in avidity index relative to 1-4years. A total of 160 participants in 3 age groups at 4 time-points were included in the analysis.

5.6 Discussion

5.6.1 Results summary

This study is thought to understand the effect of reducing *P. falciparum* transmission intensity on malaria blood-stage-specific antibody avidity. Measurement of the avidity index was adopted and optimized on the MagPix Luminex multiplex platform to simultaneously measure 18 malaria blood-stage antigens' avidity index. To our knowledge, this is the first for such a description of a multiplex avidity assay, which allows the simultaneous evaluation of the IgG avidity index of a large panel of *P. falciparum* antigens.

For the first time, I demonstrated in a simple yet informative approach two anti-malarial antibody pools, the avid and the non-avid, that had differences in decay rates in the absence of infection and acquisition rates with age. The avid antibody pool was the antibody that remained binding to an antigen after the GuHCl dissociation treatment step. The non-avid antibody pool was indirectly inferred by comparing the differences between total and avid antibody pools. Since the avid antibody pool was a subset of the total, any differences between the total and the avid pools were attributed to the non-avid antibody pool. Looking at changes in avid antibody pool and total antibody and not just avidity index provided additional insight into the effect of malaria infection on antibody acquisition and maintenance in the absence of infection. The avid and non-avid pools were of different relative compositions within antigens, decayed at different rates associated with days since the last infection, and gradually acquainted to varying ages within the different antigens.

The results showed that when IRS reduced malaria transmission, there was a net loss of both non-avid and avid pools of antibodies specific to malaria blood-stage antigens independently associated with days since the last infection duration free of disease within 12 months. Compared to the avid antibody pool, the preferential loss of the non-avid antibody pool resulted in an increased avidity index that was independently associated with time since the last infection or duration free of infection in the previous 12 months. Increased avidity index following a reduction in infection is consistent with previous findings in malaria infection (311), other infections (177,187,312), and vaccination boosts (284,284,313).

Furthermore, the results showed that both the non-avid and avid antibody pools expanded gradually with age. However, the two antibody pools expanded at different rates in the different *P. falciparum* blood-stage antigens resulting in either increased or decreased or no change in avidity index with age, consistent with our previous finding in malaria infection(272,310,314).

5.6.2 Rapid decay of non-avid antibody pool is due to rapid contraction of SLPC in the absence of infection

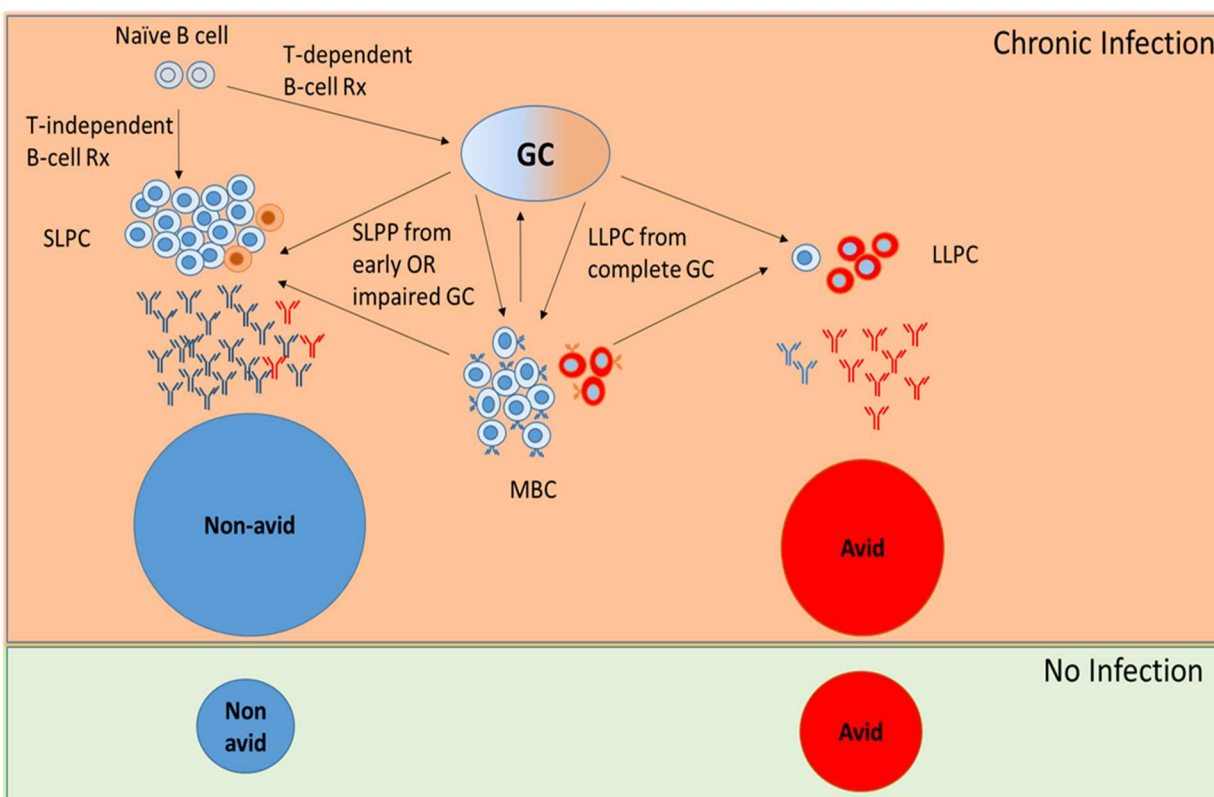
There are potential but not exclusive explanations to the observations of distinctive avid and non-avid antibody pool composition, and their decay rates associated with days since last infection or proportion of months free of infection, and acquisition with age.

LLPC produces the avid antibody pool and late germinal center class-switched typical MBC that have acquired extensive somatic mutation and affinity selection. On the other hand, the non-

avid antibody pool is produced mainly by SLPC from the T-independent extra-follicular reaction or the early stages and or impaired germinal center reaction output.

High avidity index is a result of affinity maturation, a function of somatic mutations, and positive selection for high affinity during the germinal center reaction (198,202,315,316). LLPC is the terminal output of the temporally ordered germinal center, and residents in the bone marrow were maintained for a long time and continuously secrete high-affinity antibodies (317,318). LLPC mainly maintains circulating antibody levels long after clearance of infection, hence the slower decay rate associated with days since the last infection. On the other hand, SLPC is either derived from T-independent B-cell reaction or early germinal center MBC with minimal isotope switching and limited somatic hyper-mutations (319). SLPC resides in secondary lymphoid tissue and is programmed for mass production of antibodies and short life. To maintain a pool of SLPC requires constant production of new ones from continuous B cell activation in response to active or chronic infection. Elimination of infection results in the termination of B cell reaction and the rapid contraction of the SLPC hence the fast decay rate of non-avid antibody pool associated with days since the last infection or the proportion of months free of infection. Alternative source of SLPC is the early output of the germinal center or impaired germinal center that has undergone minimal or no somatic mutation and therefore resulting mostly into lower affinity maturation. A proportion of the SLPC may be of high avidity intrinsically or from affinity matured MBC and these may contribute to the decay of the avid pool in absence of infection. Figure 5.10 summarizes the dynamics of the B cell population contribution to the antibody pool during

infection and in absence of infection. The changes in the activity of the B cell populations lead to changes in avidity index as a result of changes in the relative composition of the avid and the non-avid pools.



24 Figure 5.510 Summary of the B cell reaction demonstrating the potential cause of low avidity index during chronic infection and high avidity index in the absence of infection. The T-independent extra-follicular B cells reaction and early GC reaction result in SLPC that produce non-avid antibodies. On the other hand, the LLPC from the late GC output produces avid antibodies. In the absence of infection, the SLPC population rapidly contract, and the non-avid antibody pool decays faster than the avid pool. The result is the increased avidity index.

5.6.3 *P. falciparum* infection promotes the expansion of predominantly SLPC that result in short-lived responses

The median avidity index within malaria antigens was below 50% for all antigens except for AMA-1, H103, and MSP1-19 at 2M GuHCl. Although there were individual participants with high avidity index per antigen, implying that a large proportion of their antibodies are of the avid pool, most individuals were categorized to have non-avid antibodies. This observation may imply that most participants had SLPC driven antibody responses predominantly or that many LLPC is also non-avid. The differential expansion of both the avid and non-avid antibody pools with age may imply relative accumulation of both the high-affinity LLPC and low-affinity MBC that rapidly differentiate into SLLC. Even in the classic germinal center function where somatic hypermutations and positive selection for affinity occurs, antigenic variation may limit the expansion of the avid antibody pool. Significant loss of *P. falciparum*-specific antibody titers, mostly in children, has been reported in populations in the absence of infection (314,320,321). Most recent advances in microarray assay that allow simultaneous probing of many malaria antigens reveal a significant loss in the breadth of response to malaria antigens in the absence of age-dependent infection, implying inefficient acquisition of LLPC (255). On the other hand, MBC is reported to be more stably maintained in the absence of infection (322,323). This disproportionate acquisition of the memory compartments may contribute to the heterogeneity

in expanding the avid antibody pool and the slow acquisition of immunity to malaria. Therefore, measuring the avid antibody pool in relation to malaria-specific MBC phenotypes may provide further insight into memory acquisition and serve as a biomarker of vaccine efficacy. Secondly, understanding the mechanisms that drive responses towards the avid antibody pool will inform better vaccine design.

The presence of a low avidity index may not imply that antibodies are not functional. However, based on the thermodynamic principle, high titers of non-avid antibodies may be required to mediate function compared to avid. Therefore, the observation of predominantly non-avid antibodies may imply the requirement of very high antibody titers to achieve antibody-mediated protection from malaria as previously observed (324,325).

5.6.4 Intrinsic antigen properties may affect affinity maturation and antigen suitability for use in vaccine designs

There were differences in avidity index among the *P. falciparum* antigens. The differences could be due to the properties that can affect the number of epitopes, including size, protein folding, and conformation. However, the differences between avidity indexes among antigens could as well be due to other intrinsic properties. An example is GLURP RII, which is highly immunogenic, yet it had a very low avidity index. The poor avidity may be attributed to the glutamine repeat, affecting the diversity of binding forces. In such a case, there can be few binding options against which affinity can be selected. Rh5, a promising vaccine candidate, is another example of an antigen where the avid pool did not expand with age. Failure to induce

avid antibodies may indicate short-lived protection that has already been reported in other vaccine candidates like irradiated sporozoite and controlled human malaria infection (CHMI). CSP based RTS, S vaccine trials (139,285). Low avidity index was shown to define failure to acquire long term immunity in other infections like Mumps and *Vibrio cholerae* (182,185). Therefore, understanding the mechanisms that drive the acquisition of an avid antibody pool may improve our understanding of the acquisition of long-term protective immunity and the design of better vaccines.

5.6.5 Limitations

The study was limited because different GuHCl concentrations can result in different avidity index. Therefore, the concentration that is relevant to the antibodies' physiological properties is not known. There is likely a wide spectrum of affinities for antibodies to the same epitope that is not shown by using one GuHCl concentration. Therefore, the designation of avid and non-avid is an overly simplistic though still useful way of categorizing responses. Because treatment was only for symptomatic malaria as per the Uganda guideline for the standard of care, the period post-IRS was not long enough to allow most chronically parasitemic participants to clear the infection. Days since parasitemia, especially for time-points T1-3, were mainly from participants who were treated for malaria. We included very few symptomatic infection cases, and yet the kinetics of participants with frequent symptomatic infections may differ from those who were chronically infected. It is also important to note that the single sequence of the recombinant

proteins used in the in vitro assay may not reflect the true in vivo responses to parasites with multiple variable antigen sequences.

The MFI is reflective of antibody concentration in the linear zone on the saturation curve. At the saturation curve's plateau, antibody concentration differences can not be detected due to the maximum MFI limit. The same limitation applies to the measurement of the avidity index. A large dissociation may not be detected in MFI changes. I used a high plasma dilution factor of 1/1000 to minimize the high antibody concentrations that fall under the curve's plateau for this work.

The avidity assay on the Luminex platform was based on the long-standing ELISA assay. The assay was not validated against the 'gold standard' surface plasmon resonance (SPR) because of the two techniques' fundamental differences. SPR measures the average dissociation constant (K_d) of antibodies, including the low/medium affinity antibodies. In contrast, the chaotropic based method measures the proportion of the high-affinity antibodies that resist dissociation. Reddy et al. and Kimudu et al. did not find an association between the K_d from SPR and the avidity index from the chaotropic method suggesting that the two methods likely measured different antibody affinity (270,326). I did not have the budget or ready access to the platform to design appropriate comparison experiments.

5.66 Conclusion

This study demonstrated two malaria antibody pools distinguished by their avidity, decay rates in the absence of infection, and acquisition rate with age. The avid and non-avid composition that defines the avidity index was highly heterogynous among individuals and across antigens.

Based on these results, I hypothesize that the avid antibody pool is produced primarily by LLPC and the non-avid primarily by the SLPC. Therefore, it is critical to understand the mechanisms that drive the acquisition and maintenance of the avid antibody titers above the protective threshold and the design of better vaccines that induce long-term protection.

Chapter 6

As part of my Ph.D., I performed all the laboratory experiments and data analysis in this chapter. The PRISM study conducted the longitudinal cohort where samples for this chapter were obtained. Lindsay Wu normalized the Luminex data (Chapter 3, section 3.3) after I completed the experiments. I used the normalized data for the analysis. Isabel Rodriguez provided the R script I used to produce the antibody decay curves in figure 6-52.

Differences in the half-life of *P. falciparum* antigen-specific IgG subclasses are associated with age following interruption of exposure by IRS.**6.1 Introduction****6.1.1 Malaria challenges in the pre-elimination era**

WHO malaria elimination strategy calls for a reduction in malaria mortality rates by 40% and 90% by 2020 and 2030, respectively, compared to 2015 before global elimination can be realized (327). Many countries have accelerated efforts towards implementing this strategy. As a result, several of them are transitioning from high to medium or low malaria transmission through vector control, active case identification, treatment, and tracking index cases (27). As transmission reduces, timely identification of any form of new infections and not just malaria cases becomes difficult. Secondly, there is a risk of resurgent epidemics in non-immune populations, especially when control measures are relaxed before elimination is achieved (328–

330). Therefore, surveillance tools for the early detection of new infections or transmission foci to inform directed interventions become critical. Furthermore, vaccinations to boost population immunity will be critical elements to sustain malaria elimination gains, especially in endemic regions where countries or areas within a country will progress at different rates. Serological tools are promising surveillance tools due to their low cost and ease of application in remote settings (274,331,332). However, a better understanding of the properties of the antibody responses measured to the different *P. falciparum* antigens is required to improve both the design and malaria serology products' efficacy.

Furthermore, the RTS, S vaccine (Mosquirix™), the only malaria vaccine to have progressed to phase three clinical trials, did not yield the desired level of efficacy (139,248,333), and correlates of the short-lived protection observed are poorly understood (334–337).

6.1.2 Role of anti-malarial IgG antibodies in immunity to malaria

In high transmission settings, severe malaria cases are concentrated in children generally under 5 years, who gradually become less susceptible to disease despite chronic infection with high parasite densities compared to adults (209). The adults rarely get symptomatic but continue to acquire and sustain very low parasite densities for long periods, most times, sub-microscopic infection (53,338,339). This epidemiological observation of the different malaria immunity phenotypes supports the held idea that the acquisition of immunity to malaria is slow and is rarely, if at all, sterile (338,340). IgG is the most abundant antibody isotype and the major

contributor to acquired immunity to infections including malaria (138,341). Using purified IgG from malaria exposed adults, the malaria-ridden recipients recovered from fever and greatly reduce the parasite load (138). Based on these observations, the last 50 years have been a race for a humoral immunity-based vaccine. Studies investigated malaria-specific IgG responses either as markers of exposure (331,342,343), correlates of protection or risk of infection (344,345).

6.1.3 IgG subclasses can influence the outcome of immunity to infections

There are four subclasses: IgG1, IgG2, IgG3, and IgG4 (IgG1-4) that have differences in their constant region (Fc), particularly in their hinges and upper CH2 domains (165,346). The structural differences in IgG subclasses govern their longevity in circulation, translocation across mucosal sites, placental transfer, and effector functional properties.

The IgG subclasses have different affinities to the different variants of Fc gamma receptors (FcγR; FcγRI, FcγRII, and FcγRIII) that are expressed on B cells, the different innate effector cells as well as the complement activators C1q (165). The differential interaction of IgG subclasses with the Fcγ receptors and C1q, which act as adapters between the acquired immunity and the innate effector mechanism, influence their functional outcome.

IgG1 and IgG3 are referred to as cytophilic antibodies because of their high affinity for activating Fcγ receptors that are expressed on monocytes, macrophages, neutrophils, and natural killer cells(347). As a result, they mediate effector mechanisms such as phagocytosis (152,348), antibody-dependent cellular inhibition (ADCI), and direct parasite killing by effector cells (349).

The cytophilic subclasses also have a high affinity for C1q, a component of the complement system that initiates activation of the classical pathway, which results in the assembly of the membrane attack complex and complement-mediated phagocytosis (350).

IgG2 is commonly induced against polysaccharide antigens known to play a critical role in immunity to bacterial and viral infections (351). IgG2 is important in immunity to encapsulated bacterial infections. Deficiency of IgG2 has been associated with susceptibility to some bacterial infections (352,353).

IgG4 subclass is mainly associated with immune-modulatory mechanisms and is known as a regulatory antibody due to its ability to modulate the allergic and inflammatory responses mediated by IgE. IgG4 is also reported to be associated with protection from autoimmune diseases (354). IgG4 has the poorest affinity for Cq1 and activator Fc γ receptors compared to other subclasses. Instead, IgG4 has a relatively better affinity for the inhibitory Fc γ receptors, an important feature of IgG4 that contributes to its low inflammatory capacity (355). IgG4 has mainly been studied in allergy and worm infections, where it is shown to alleviate IgE's inflammatory effect (356,357). An increase in the tolerance to bee stings by beekeepers was associated with elevated levels of IgG4 (358)

The effector functions IgG1 and IgG3 have been elegantly demonstrated in vitro assay and correlated with immunity. But very little is known about the role of IgG2 and IgG4 in malaria immunity or immune dysfunction.

6.14 IgG subclasses, placental transfer, glycosylation and longevity in circulation

IgG subclasses have different affinities to the neonatal Fc receptor (FcRn) in the acidic endocytic vacuole that protects antibodies from degradation and modify their decay half-life and mediate placental and gut translocation of maternal antibodies (170,359).

Recent studies in autoimmunity and allergy mediated disease indicate that glycosylation of the Fc region of the IgG subclasses further modify affinities to their receptors and hence their stability and function (360,361). In HIV, IgG glycosylation is associated with Fc mediated reduction in viral replication and the abnormal glycosylation associated with chronic infection (362,363). IgG glycosylation was observed in influenza and tetanus toxoid vaccinations (364). However, there is limited knowledge about glycosylation in malaria-specific antibodies and their influence on function.

6.1.5 Evidence IgG subclasses in the immunity to malaria

The importance of IgG subclasses has been demonstrated in several infections. Many immunology studies have shown a positive association between levels of cytophilic antibodies, IgG1 and IgG3, with naturally acquired immunity (126,128,314,365–368). High IgG2 and low IgG4 response to the ring-stage infected erythrocyte surface antigen and the MSP2 alleles were associated with reduced infection risk. But this was in individuals possessing the H131 allele of FcγRII that has a high affinity for IgG2 (351). In Cameron, high levels of anti-schizont extract IgG2 were associated with reduced *P. falciparum* infection risk in infants below 2 months of age

(369). However, in-vitro functional assays have implicated interference of IgG4 in the opsonizing function of IgG1 and IgG3 in competition assay (301). The role of IgG2 and IgG4 in the protection against malaria is limited and, as such, poorly understood.

It is also possible that IgG subclasses' relative composition or ratio can affect the immune response's protective outcome. In a Kenyan cohort, high levels of IgG1 antibodies related to IgG2 and IgG4 were associated with protection from severe malaria. In contrast, high IgG2 to IgG1 ratio and IgG3 antibodies were associated with a higher risk of developing severe malaria (370). But this kind of IgG subclass combination in immunity to malaria is not well studied and could provide more insight on the immunity and immune dysfunction in malaria.

6.1.6 Evidence of differential malaria-specific IgG subclass switching

IgG subclasses result from B-cell secondary response to infection mainly in T-dependent response in germinal center reaction (202,371,372) and to a lesser extent during extrafollicular T-independent B cell reaction (319). Antigens are thought to play a role in influencing subclass switching profiles. Inflammatory and regulatory cytokines and innate signaling have been suggested to influence class switching (204,373). Malaria antigens induce mainly IgG1, and IgG3, which can skew towards either IgG1 (AMA-1) or IgG3 (MSP2) or co-dominant, like in the case of MSP1-19 (374).

6.2 Rationale and aim

IgG class switching is a function of the germinal center reaction similar to affinity maturation, and the germinal center reaction is susceptible to interruption by *P. falciparum* infection. In Chapter 5, we observed preferential expansion of non-avid antibodies that resulted in a low avidity index during high malaria transmission intensity that rapidly contracted when the IRS implementation interrupted transmission. However, we do not fully understand the effect of chronic *P. falciparum* infection on IgG subclasses' acquisition and maintenance. Assessment of longitudinal antimalarial antibody subclass responses during high malaria transmission and after the drastic reduction of transmission using highly effective intervention like IRS provides a unique opportunity to gain some insight into how IgG subclasses are acquired maintained. Several studies have looked at a few malaria antigens, mainly in cross-sectional studies. The few studies have limited our ability to understand the broader picture of the IgG subclasses' dynamics with age and exposure changes. Furthermore, understanding the IgG subclasses' kinetics to a large panel of *P. falciparum* antigens during chronic or near-constant exposure to infection and in the absence of infection can improve our knowledge on how to improve serological diagnostic and surveillance tools.

This chapter explored a large panel of (18) blood-stage *P. falciparum* antigens to provide a broader insight into specific IgG subclasses' acquisition and maintenance. Antigen-specific total IgG and subclasses 1-4 were evaluated on the MagPix (Luminex) multiplex assay, including 18 recombinant antigens from the malaria blood-stage antigens described in Chapter 3, section 3.21.

Plasma samples from 160 participants from the PRISM cohort at 4 time-points; two before introducing the IRS and two time-points after introducing the IRS, were assayed (Figure 3.3). The IRS introduction offered us a unique opportunity to investigate the effect of a reduction in *P. falciparum* infection to the naturally acquired IgG subclass antibody responses following one year of IRS on a broad panel of malaria blood-stage antigens. Total IgG and subclasses antibody decay half-lives were estimated and compared. The total IgG and subclasses' sensitivity and specificity were compared to determine their potential utilization to improve serological diagnostic tool performance to measure recent infection exposure.

6.3 Methods

6.3 1 Study population and description of PRISM cohort at Nagongera

In this study, 160 participants enrolled in longitudinal PRISM were included. The participants include all children with plasma stored at the four study periods and 20% adults. The participants belonged to age categories 1-4 years (40), 5 – 11 years (92), and above 18 years (28). The first IRS determined the study period. For each participant, 4 time-points were included; two pre-IRS time-points (T1&2) were taken 12 and 6 months before the first round of IRS and T3 and T4 at 6 months and one year post the first round of IRS (Figure 3.3).

6.3.2 Ethical consideration

Ethical approval was obtained from the Makerere University School of Medicine Research and Ethics Committee (REC REF 2011-203), the Uganda National Council for Science and Technology (HS 1074), the LSHTM ethics committee (reference # 6012), and the University of California, San Francisco Committee on Human Research (reference 027911).

Before enrolment into the study, written informed consent was obtained from adult parents/guardians of children, and assent from children aged 8 years and older; informed Re-consent was obtained when enhanced surveillance monthly sampling in participants was introduced.

6.3.3 Luminex Multiplex bead array assay to measure Total IgG

Total IgG responses to 18 *P. falciparum* blood-stage antigens and non-malaria positive control TT was measured in plasma diluted at 1/1000 on the MagPix (Luminex Corp, Austin, Texas) multiplex bead assay described in Chapter 3 and as previously described elsewhere (234).

6.3.4 Luminex Multiplex bead array assay to measure IgG1 - 4

IgG subclass antibody responses to 18 *P. falciparum* blood-stage antigens and TT were measured in plasma diluted at 1/100 on the Luminex MagPix multiplex platform and detected using a two-step biotinylated anti-human IgG subclass secondary antibody and streptavidin-phycoerythrin tertiary as previously described (235,236). Each of the IgG subclasses was assayed separately for every sample using the same plate layout described in Chapter 3.

The read on a Luminex MagPix, after acquiring at least 100 beads/region/ was the median MFI. The blank well MFI was deducted from each well to determine the net MFI. Net MFI was representative of relative antibody concentration.

6.3.5 Statistical analysis

The association between antibody levels (MFI) for total IgG and the subclasses 1 - 4 with days since infection were assessed in a generalized estimating equation (GEE) model, adjusted for age (375). The GEE allowed estimation of the mean effect of days since the last infection on antibody levels using repeated measures per individual at a population level. All four time-points were included in the GEE model. Infections were defined as parasite positive if the sample was microscopy positive (patent infections) or LAMP+. The GEE model outcomes were regression coefficient and 95% confidence intervals (95%CI). Estimated antibody decay half-life was derived from the GEE model's coefficient of antibody levels with days since infection (log antibody loss per day since infection) by dividing \log_{10} of 2 by coefficient. The result was the number of days it takes to lose half the antibody levels since the last day of infection. This half-life estimation model assumes the decay function without accounting for varying production kinetics.

Equation 2

$$\text{Antibody half-life} = \left(\frac{\log_{10} 2}{\text{Regression Coef}} \right)$$

Association between antibody levels for both total and the IgG1 - 4 subclasses with the following age categories, 1- 4, 5 -11, and above 18 years, were assessed GEE model and adjusted for days since infection. Age category 1- 4 years was the reference, and the outcome was coefficient and 95% confidence interval (log10 change in antibody levels when transitioning from age categories 1-4 to 5-11 or above 18 years).

Comparison of the medians was non-parametric Mann-Whitney T-test. A P-value below 0.05 was considered a significant difference in medians.

The sensitivity (true positive) and 100 - specificity (false positive) were determined by the receiver operating characteristic curve (ROC) (376,377). Samples were scored as positive if they had at least one infection in the last 90 or 180 days or negative if there was no infection in the last 90 or 180 days. The outcome was presented as the area under the curve (AUC) and 95%CI.

Analysis and Figures were performed with Stata version 14 (StataCorp LLC, USA), GraphPad Prism version 7 (Graphpad Software Inc, USA), and R studio. Changes and associations were considered statically significant when 95% confidence intervals did not overlap zero or P-values were less than 0.05.

6.4 Results

6.4.1 Relative responses of total and IgG subclasses

Antibody responses were detected to all 18 *P. falciparum* antigens to all 4 IgG subclasses. Overall, there was a wide dynamic range in all IgG subclasses responses from the negative response towards maximum detection Log_{10} MFI of 4.61 ($\sim 40,700$ MFI) towards the assay's saturation limit. Total IgG was tested at a higher dilution of 1/1,000 compared to the IgG subclasses at 1/100, but total IgG had higher Log_{10} MFI than the subclasses (Figure 6.51a - c).

Although not directly comparable, the median responses were predominantly higher in IgG3 than the other subclasses in the respective antigens. The exception to this was in AMA1 and Rh2, where median responses were higher in IgG1 compared to IgG3 (Figure 6.51b). Maximum detectable magnitude of responses in IgG3 was observed in many of the antigens, for example, ETRAMP4 Ag2, ETRAMP5 Ag1, EBA140 RIII-V, MSP2 Dd2, and MSP2 CH150/9, where all IgG subclass responses were low (Figure 6.51c).

In general, IgG1 responses were moderate compared to IgG3 in most antigens. The medium log_{10} MFI responses were lowest in both IgG2 and IgG4 across all antigens. Still, their maximum responses were reaching the maximum detection limit in some antigens like in ETRAMP5Ag1, EBA175 RIII-V, GLURP RII, and MSP1-19 (Figure 6.52a - c).

In TT non-malaria control, the subclasses' highest responses were IgG1 and 4 and lowest in IgG2 and IgG3.

There were no noticeable response patterns in different antigen categories of infected red blood cells, merozoite apical complex, and merozoite surface antigens (Figure 6.51a-c).

The observations taken together indicated that the assay conditions were adequate for detecting the response across the method's maximum dynamic range. The relatively higher reactivity of total IgG than the subclasses can be attributed to the secondary goat anti-human IgG polyclonal nature compared to the monoclonal anti-human IgG subclasses. In addition, the differences in reactivity between total IgG and the subclasses could be the competition for identical epitopes between the subclasses that reduce the detection signal seen.

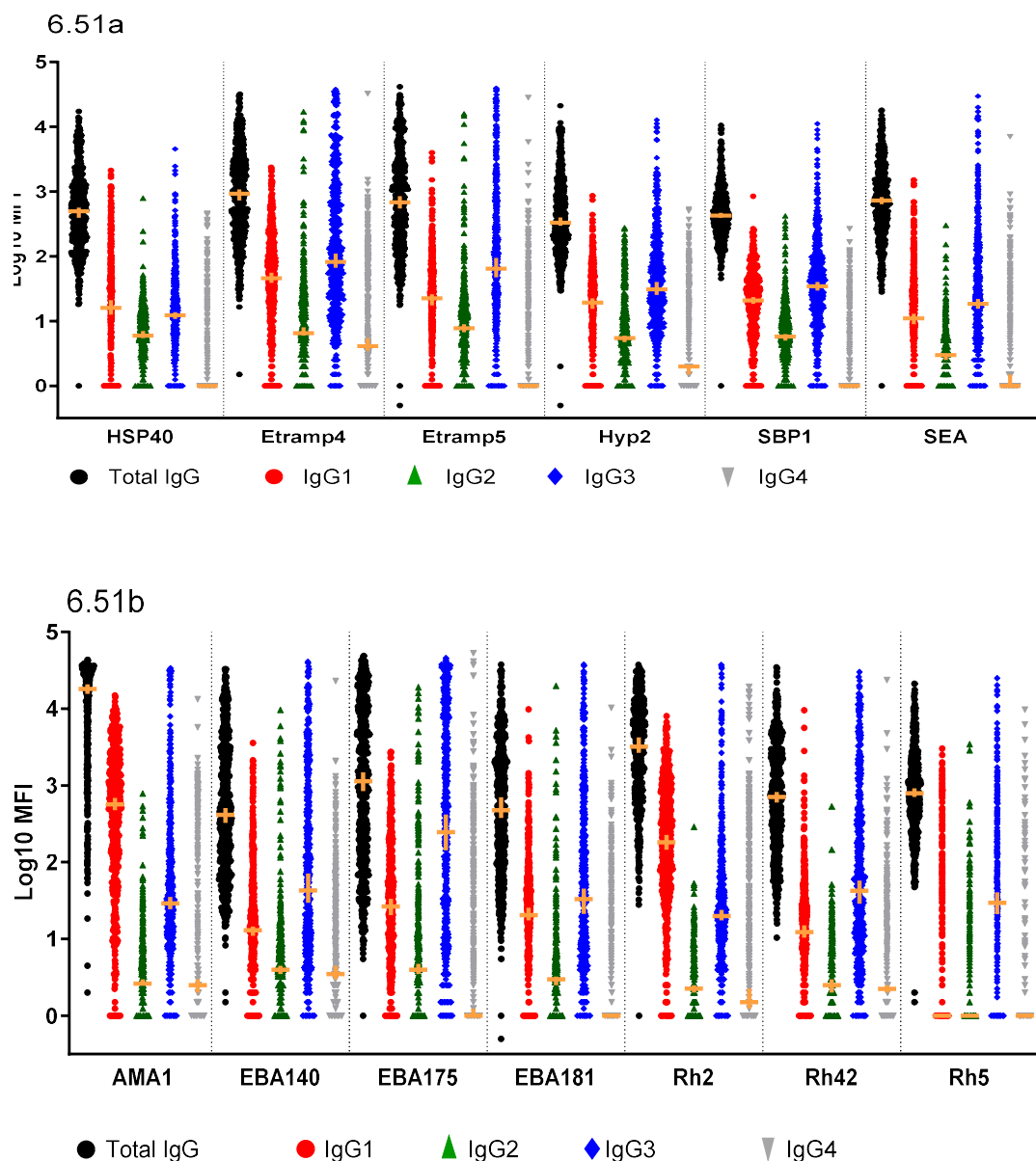
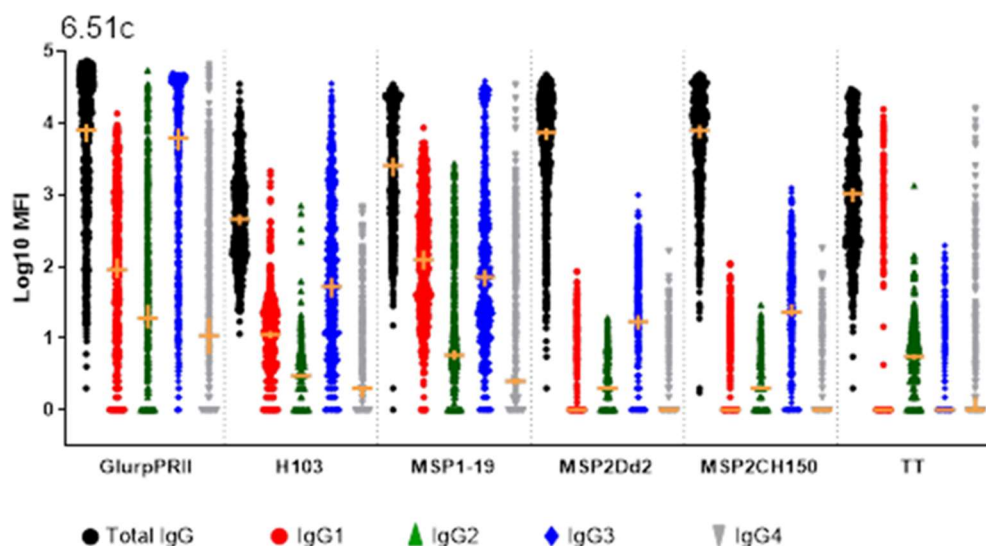
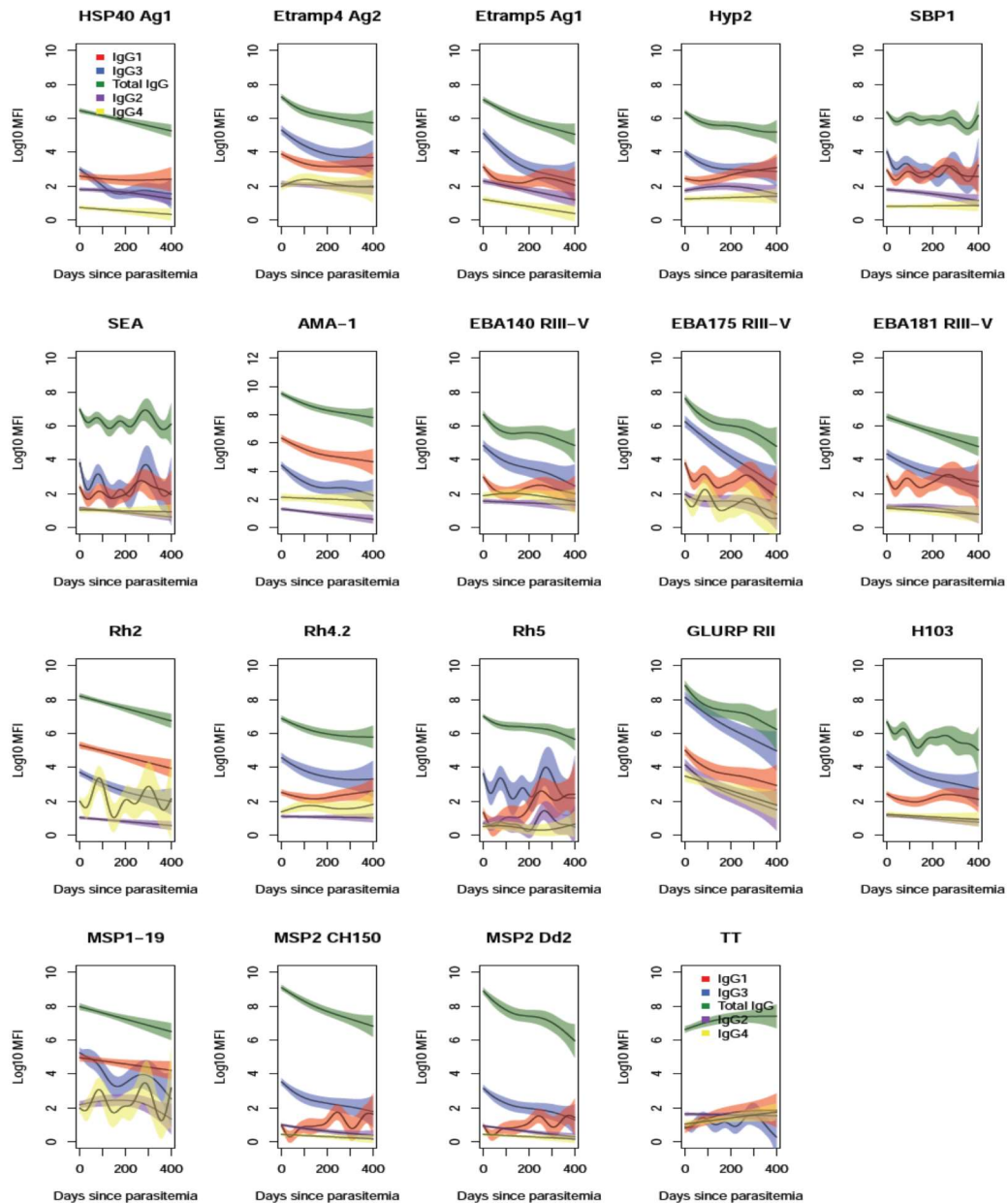


Figure 6.51a&b. Dot Plot of \log_{10} MFI for by malaria blood-stage antigens categories. Antibody levels were measured using a MagPix (Luminex) multiplex assay including 18 *P. falciparum* blood-stage antigens and TT. Each dot represents a single sample from 160 participants at 4 time-points. The horizontal bar represents the median and 95% CI. (a) Infected red blood cell antigens, (b) Merozoite apical complex antigens.



25 **Figure 6.5c.** Dot Plot of log₁₀MFI of Merozoite apical complex. Antibody levels were measured using a MagPix (Luminex) multiplex assay, including 18 malaria blood-stage antigens and TT. Each dot represents a single sample from 160 participants at 4 time-points. The horizontal bar represents the median and 95% CI.

When the data were fitted in gam plots (Figure 6.52) for MFI responses against days since the last infection, all antigens showed a clear decline in antibody responses. All antigens except for AMA1 and Rh2 showed IgG3 predominance, and the difference between IgG3 and IgG1 narrowed with days since the last infection. GLURP RII showed relatively co-dominant responses across all 4 subclasses, compared to total IgG. In the longer days since the last infection, IgG1 and IgG3 overlapped, implying co-dominance of IgG1 and IgG3 in the absence of infection.



26 Figure 6.52. GAM plots of estimated best fit Log10MFI responses against days since the last infection. The black line represents mean and the colored bands 95%CI. 160 participants at 4 time-points were included.

6.4.2 Association of total IgG and IgG subclasses responses with days since the last infection.

In a GEE model to allow repeated measures per participant, including four time-points and adjusting for age category, total IgG and subclasses levels were inversely associated with days since the last infection in all the 19 antigens (Figure 6.53a-c). There were differences observed in the IgG subclasses' regression coef values that signified the differences in the magnitude of association with days since the last infection. The highest negative coefficient values were mainly IgG3 compared to total IgG and the other IgG subclasses, across all antigens (Figure 6.53a-c). Within IgG3, responses against ETRAMP5 Ag1, EBA175 RIII-V, and MSP1-19 had the highest negative coefficient values. This observation implied that IgG3 to the *P. falciparum* blood-stage antigens, compared to the total IgG other IgG subclasses, decreased faster in association with days since the last infection the decreasing rates were highest in antigens; ETRAMP5Ag1, EBA175 RIII-V, and MSP1-19.

Despite IgG1 levels being lower than IgG3 and much higher than IgG2 and IgG4 by comparing median Log₁₀ MFI (Figures 6.51 and 6.52), IgG1 had the least negative coefficient values of the four subclasses in most antigens, tending towards or above zero. This observation was consistent in AMA-1 and Rh2, where IgG1 was the predominant subclass. This observation implied IgG1 levels decreased slower than other subclasses in association with days since infection in all antigens. The subclass's predominant abundance status did not affect the slower rate of IgG1 decrease in association with days since the last infection.

IgG2 and IgG4 levels were associated with days since the last infection was either weakly or not significantly inversely associated with days since the last infection (Figure 6.53a-c).

Strikingly, GLURP RII had relatively high \log_{10} MFI in IgG2 and IgG4 compared to other antigens (Figure 6.52), and the coefficient values were comparable in all the subclasses and total IgG. The observation implied that all IgG subclasses to GLURP RII decreased at the same rate in association with the last infection days.

Tetanus toxoid (TT) was included as a non-malaria control, and as expected, there was no significant association between antibodies to TT and days since the last infections.

In summary, these results indicated a reduction in antibody levels for total IgG and subclasses that were associated with days since the last *P. falciparum* infection independent of age, and the reductions were specific to antibodies against *P. falciparum* antigens. The rate of antibody reduction associated with days since the last infection was highest in IgG3 compared to other subclasses, even in antigens that were predominantly IgG1. GLURP RII was unique because it had co-dominance of all 4 subclasses that reduced at a relatively similar rate associated with days since the last infection.

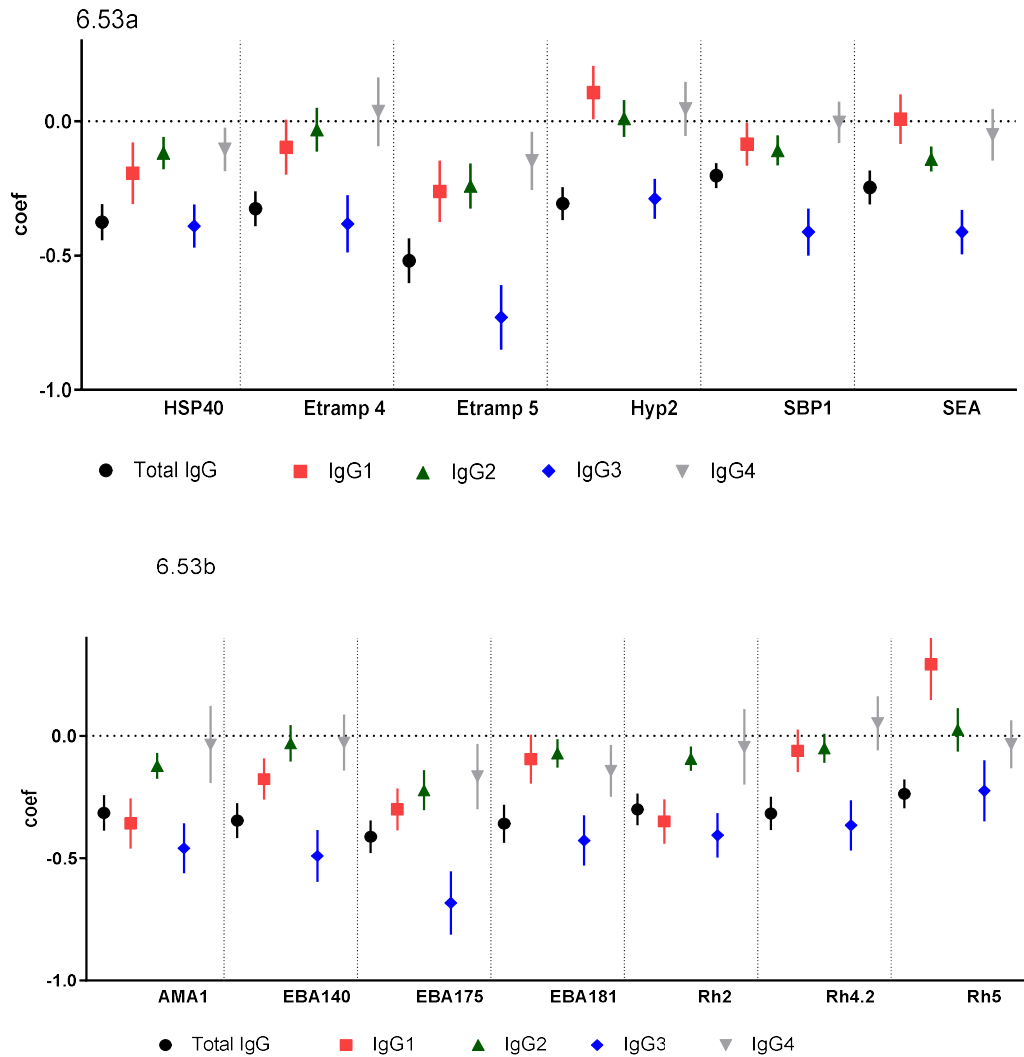
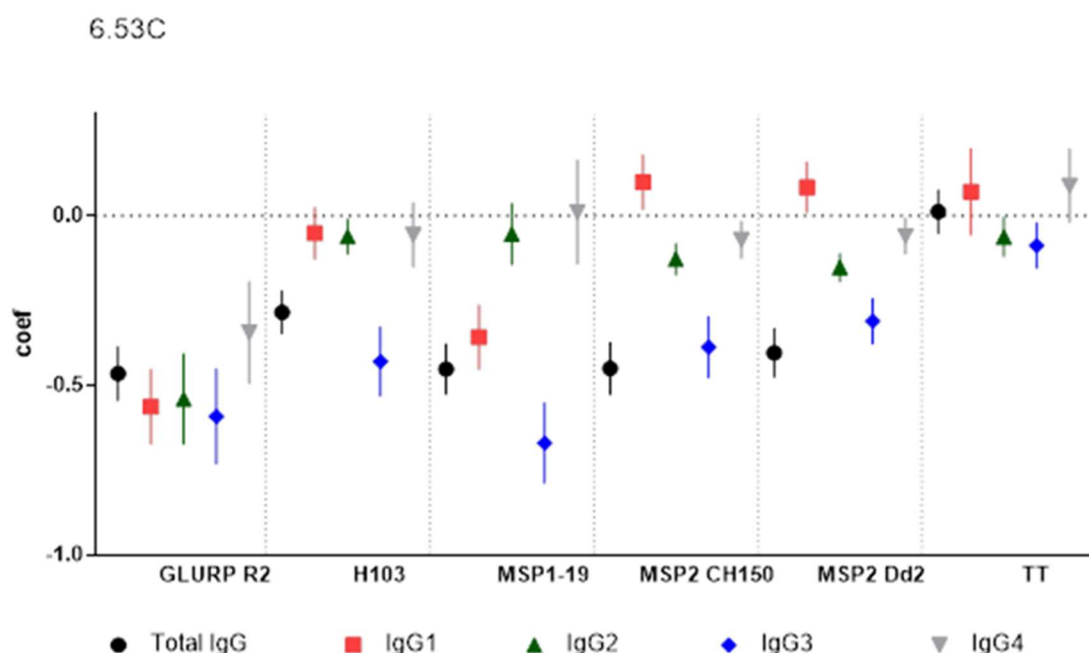


Figure 6.53a&b Association of Log_{10} MFI with days since the last infection. Total IgG and IgG subclass was measured using MagPix(Luminex) multiplex assay including 18 *P. falciparum* blood-stage antigens and TT, including 160 participants at 12 and 5 months pre-IRS and 6 and 12 months post-IRS. Malaria incidence decreased from 6ppy to near zero. Four time-points were fitted in the GEE model, adjusted for age. The lines show regression coefficient, median, and 95% CI of the total (black), IgG1 (red) IgG2 (green), IgG3 (blue), and IgG4 (grey). Infection was determined by microscopy+ or LAMP+. Below the zero lines is an inverse association, and above is a positive association. The confidence interval overlapping with zero was statistically non-significant.



27 Figure 6.53c Association of MFI with days since the last infection. Total IgG and IgG subclass was measured using MagPix(Luminex) multiplex assay including 18 *P. falciparum* blood-stage antigens and TT, including 160 participants at 12 and 5 months pre-IRS and 6 and 12 months post-IRS. Malaria incidence decreased from 6ppy to near zero. Four time-points were fitted in the GEE model, adjusted for age. The lines show regression coefficient, median, and 95% CI of the total (black), IgG1 (red) IgG2 (green), IgG3 (blue), and IgG4 (grey). Infection was determined by microscopy+ or LAMP+. Below the zero lines is an inverse association, and above is a positive association. The confidence interval overlapping with zero was statistically non-significant.

6.4.3 Association of total IgG and IgG subclasses with age in the absence of infection

To determine the relationship between antibody levels maintained in the absence of infection with age, median MFI for a total of 129 sample time-points was compared across three age categories of 1 -4 years (37), 5 – 11 years (57), and >18 years (40). 180 days without infection was the longest period where all age groups had representative samples. The period of 180 days

with no infection was thought to provide an approximate indication of the amount of antibody maintained in the absence of infection. Overall the median antibody levels maintained increased significantly from the young age category; 1- 4, 5 – 11, and > 18 years in all *P. falciparum* antigens (Figure 6.54).

IgG1 was the dominant or co-dominant with IgG3 at 1- 4 years and 5-11 years in the absence after 180 days since the last infection (Figure 6.54). The trend reversed in adults >18 years, where the dominant subclass was IgG3. In antigens, AMA1, and Rh2, IgG1 was the dominant subclass in all age groups, including adults >18 years, despite an observed steady increase in IgG3 with age (Figure 6.54).

In summary, these results indicated that malaria-specific IgG1 and IgG3 antibody levels that were maintained in the absence of infection in the last 180 days gradually increased with age in all 18 antigens. IgG1 was acquired at relatively faster rates at an early age, but the IgG3 pool was preferentially expanded faster than IgG1 in adults above 18 years compared to 1- 4 years. There were exceptions with HSP40 Ag1, AMA-1, and Rh2, where the IgG1 pool remained dominant and preferentially expanded at 5-11 years of age relative to 1-4 years.

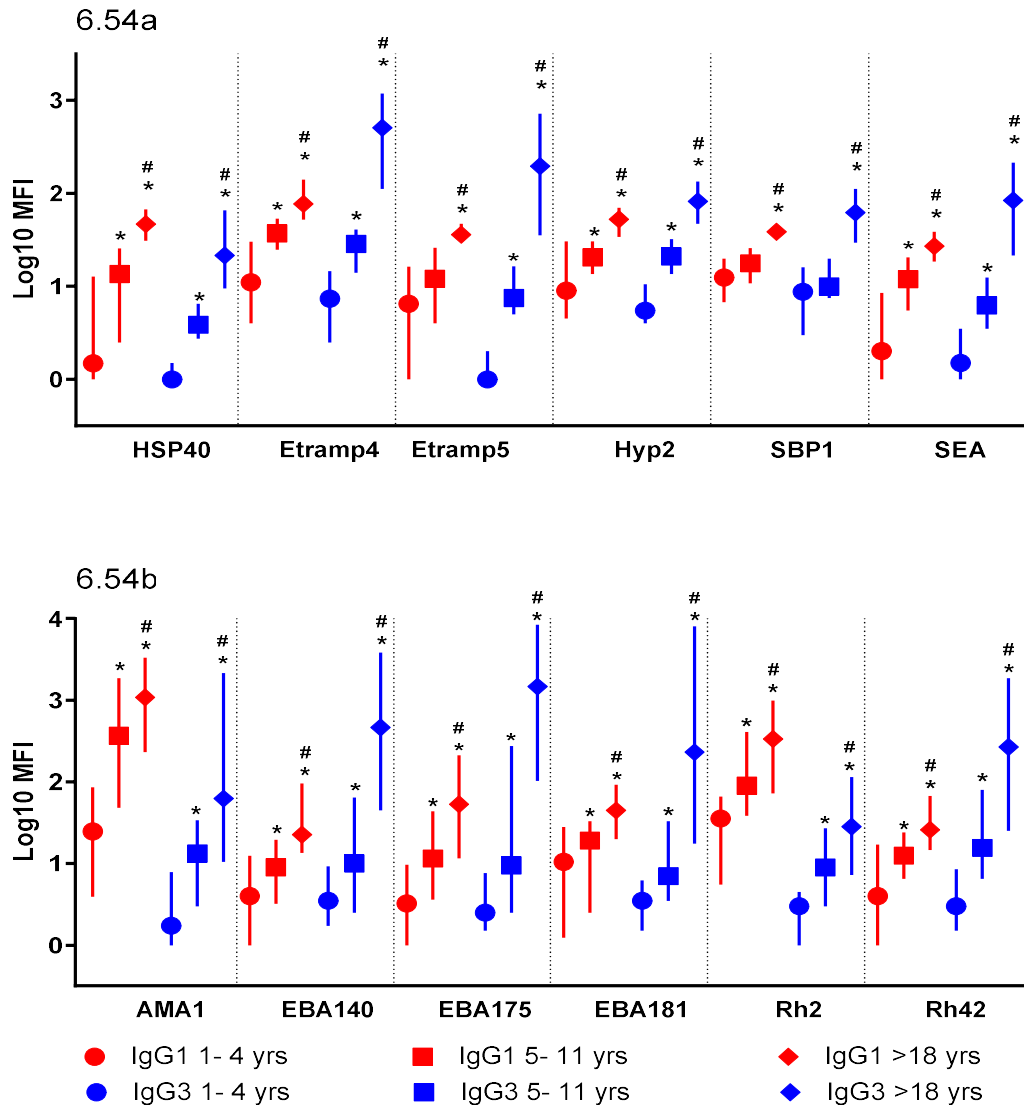
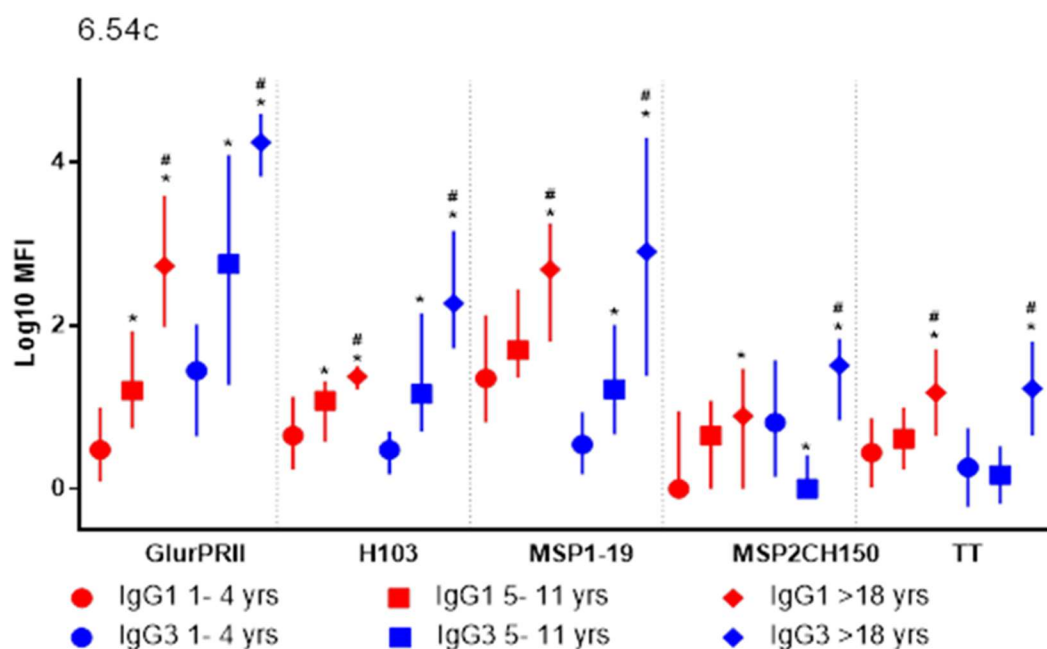


Figure 6.54a&b. Comparison of IgG1 and IgG3 across age categories. IgG1 and IgG3 of 129 samples from all time-points with no infection in at least 180 days were compared across age categories 1- 4, 5- 11, and >18 years. Infection was defined as microscopy+ or LAMP+. The median log₁₀MFI were compared between age groups in a non-parametric Mann Whitney test.

P-value <0.05 was considered significant. * = significant difference between MFI medians 1-4 and 5-11years or 1-4 and >18years. # = significant difference of MFI medians between 5-11 years and >18years.



28 Figure 6.54c. Log₁₀ MFI IgG1 and IgG3 by age categories. IgG1 and IgG3 of 129 samples from all time-points with no infection in at least 180 days were compared across age categories 1- 4, 5- 11, and >18 years. Infection was defined as microscopy+ or LAMP+. The median log₁₀MFI were compared between age groups in a non-parametric Mann Whitney test.

P-value <0.05 was considered significant. * = significant difference between of MFI medians 1-4 and 5-11years or 1-4 and >18years. # = significant difference of MFI medians between 5-11years and >18 years.

6.4.4 Differences in antibody half-life among IgG subclasses in the absence of infection.

Antibody half-life was calculated from the regression coefficient values of the GEE model of log₁₀ MFI and days since the last infection, adjusted for age categories of 0 – 4, 5 – 11, and >18 years. The coefficient represented log₁₀ antibody loss (for negative coefficient values) or gained (for positive coefficient values) each day after the last infection. The number of days to lose or

gain 50% of the antibody level after the infection was derived (section 6.35, Equation 2). The outcome was the population-level estimate of antibody decay half-life.

In general, antibodies decayed since the last day of infection. The half-life for total IgG was different across the *P. falciparum* antigens, ranging between 57 days for ETRAMP5 Ag1 and 148 days for SBP1 (Table 6.55). IgG3 had the shortest half-life compared to total IgG and the other subclasses within all *P. falciparum* blood-stage antigens, including AMA-1 and Rh2 that were predominantly IgG1 (Figure 6.53 and Table 6.55).

Among antigens that had the lowest decay half-life for IgG3 below 50 days included ETRAMP5 Ag1 (mean; 41, 95% CI; 35 - 49), EBA175 RIII-V (mean: 44, 95% CI; 37 - 54), MSP1-19 (mean; 44, 95% CI; 38 - 54).

Other IgG subclasses 1, 2, and 4 had longer population-based estimated decay half-life above 100 days with very wide confidence intervals suggesting high heterogeneity in half-life over time since the last infection.

Interestingly, GLURP RII antibody decay half-life was comparable across subclasses and means IgG1 (mean; 55, 95% CI; 45 – 66), IgG2 (mean; 55, 95% CI; 45 – 74), IgG3 (mean; 51, 95% CI; 41 – 67), IgG4 (mean 87, 95% CI; 61 – 67), total IgG (mean 65, 95% CI; 55 – 78).

6 Table 6.55 Summary of population-based estimates of half-life

Antigen	Total IgG	IgG1	IgG2	IgG3	IgG4
HSP40 Ag 1	80 (67 - 97)	155 (97 - 385)	254 (168 - 515)	77 (63 - 97)	286 (161 - 1290)
Etramp4 Ag2	92 (77 - 115)	310 (150 - -4770)	952 (266 - -605)	78 (61 - 109)	-846 (326 - -184)
Etramp5Ag1	57 (49 - 68)	115 (80 - 205)	124 (92 - 191)	41 (35 - 49)	203 (117 - 766)
Hyp2	98 (81 - 122)	-283 (-4547 - -146)	-2945 (519 - -383)	104 (82 - 140)	-651 (550 - -204)
SBP1	148 (120 - 192)	352 (182 - 5337)	277 (183 - 569)	72 (60 - 92)	7640 (374 - -415)
SEA1	136 (102 - 186)	-524 (921 - -204)	266 (182 - 341)	85 (69 - 112)	-2229 (352 - -341)
AMA-1	95 (77 - 123)	83 (65 - 117)	245 (171 - 433)	65 (53 - 84)	854 (155 - -245)
EBA140 RIII-V	86 (72 - 109)	170 (115 - 325)	998 (286 - -674)	61 (50 - 78)	1085 (211 - -347)
EBA175 RIII-V	73 (62 - 87)	100 (77 - 139)	135 (98 - 214)	44 (37 - 54)	180 (100 - 910)
EBA181 RIII-V	83 (68 - 107)	315 (154 - -6194)	419 (231 - 2243)	70 (56 - 92)	210 (121 - 815)
Rh2	100 (82 - 127)	85 (68 - 116)	321 (209 - 690)	74 (60 - 95)	668 (150 - -274)
Rh4.2	94 (78 - 121)	492 (202 - -1144)	589 (272 - -3545)	82 (64 - 114)	-581 (513 - -185)
Rh5	126 (101 - 168)	-103 (-205 - -68)	-1210 (466 - -263)	133 (86 - 301)	882 (227 - -470)
GLURP RII	64 (55 - 77)	53 (44 - 66)	55 (44 - 73)	50 (41 - 66)	87 (60 - 154)
H103	105 (86 - 135)	581 (234 - -1227)	487 (265 - 3031)	69 (56 - 91)	529 (199 - -807)
MSP1-19	66 (57 - 79)	83 (66 - 113)	554 (208 - -839)	44 (38 - 54)	-2839 (211 - -184)
MSP2 CH150/9	96 (79 - 123)	-304 (-1587 - -168)	234 (172 - 365)	77 (63 - 101)	422 (239 - 1783)
MSP2 Dd2	74 (63 - 90)	-359 (-3168 - -190)	197 (155 - 269)	96 (79 - 123)	503 (267 - 4169)
TT	-259(577 - -397)	-426 (531 - -152)	480 (248 - 7201)	342(194 - 1420)	-340 (1510 - -152)

Half-life was derived from the GEE model's coefficient of Log_{10} MFI and days since the last infection. The positive value indicates the number of days it takes for antibody decay by 50%, a negative value indicates the antibody takes to boost by 50%. A 95% confidence interval that overlap negative and positive values indicate a non-significant change. A total of 160 participants at 4-time points were included in the analysis.

6.4.5 IgG subclass stratify into distinct clusters

When total IgG was plotted against the subclasses, scatter plots revealed clustering of unique subpopulations. When subclasses were plotted against each other, two main distinctive clusters were observed in some antigens. When IgG1 was plotted against IgG3, (i) high IgG1 and low/or no IgG3 responses (IgG1^{H3L}), and (ii) both high IgG1 and high IgG3 (IgG1^{H3H}). Because the clustering was not consistent in all antigens, I ruled out assay artifacts due to anti-human IgG1 or 3 to bind to some allotypes. A clear example of clustering can be seen in Rh2, MSP2 CH150/9, and MSP2 Dd2 (Figure 6.57). When samples that were IgG1^{H3L} were selected for an antigen, individual participants were categorized in the same clusters for all 4 time-points, implying individual dependent factors driving the response pattern.

When IgG1 or IgG3 was plotted against IgG4, 3 distinct clusters were observed; IgG1^{H4H} , IgG1^{L4H} , and IgG1^{H4L} example, in Hyp2 (in Figure 6.58). For both AMA1 and Rh2, where IgG1 is the predominant subclass, the IgG1^{L4H} phenotype was missing.

Overall, our data indicated that there are cluster expressions based on IgG subclasses, and they can be characteristic to individuals and antigen. The definition of the clusters in the study was arbitrary. Further work is required to define the clusters using unsupervised models like random forest e analysis and investigate antibody function among the distinct phenotypes.

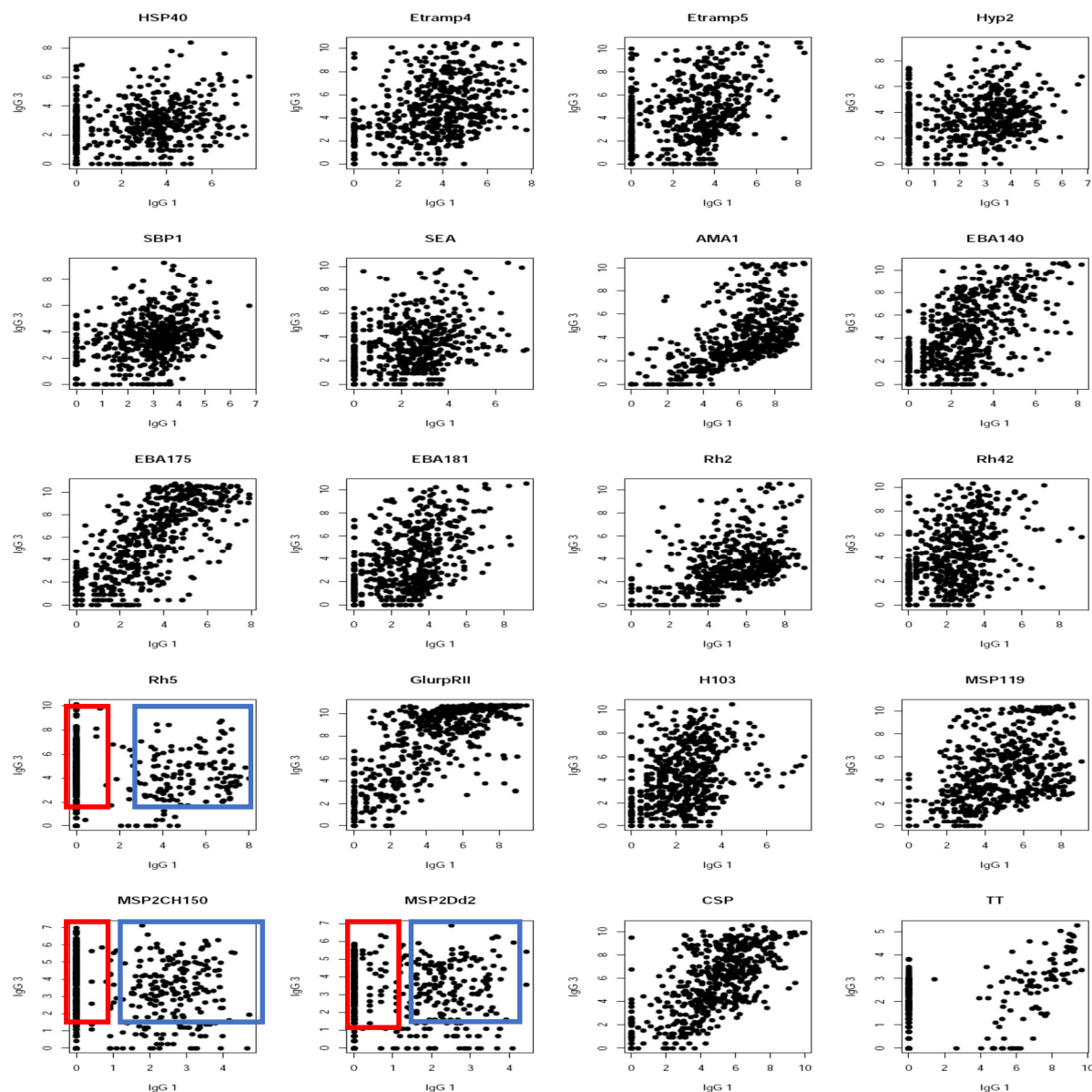


Figure 6.57 Scatter plots of IgG1 against IgG3. IgG1 and IgG3 antibodies against 18 malaria blood-stage antigens were measured on the MagPix (Luminex) multiplex assay. All 4 time-points for each of the 160 participants were included. The red gate is a cluster of samples with low IgG1 and high IgG3 responses. Blue gate is a cluster of samples with both high IgG1 IgG3 responses. The gates were arbitrary based on visual observation.

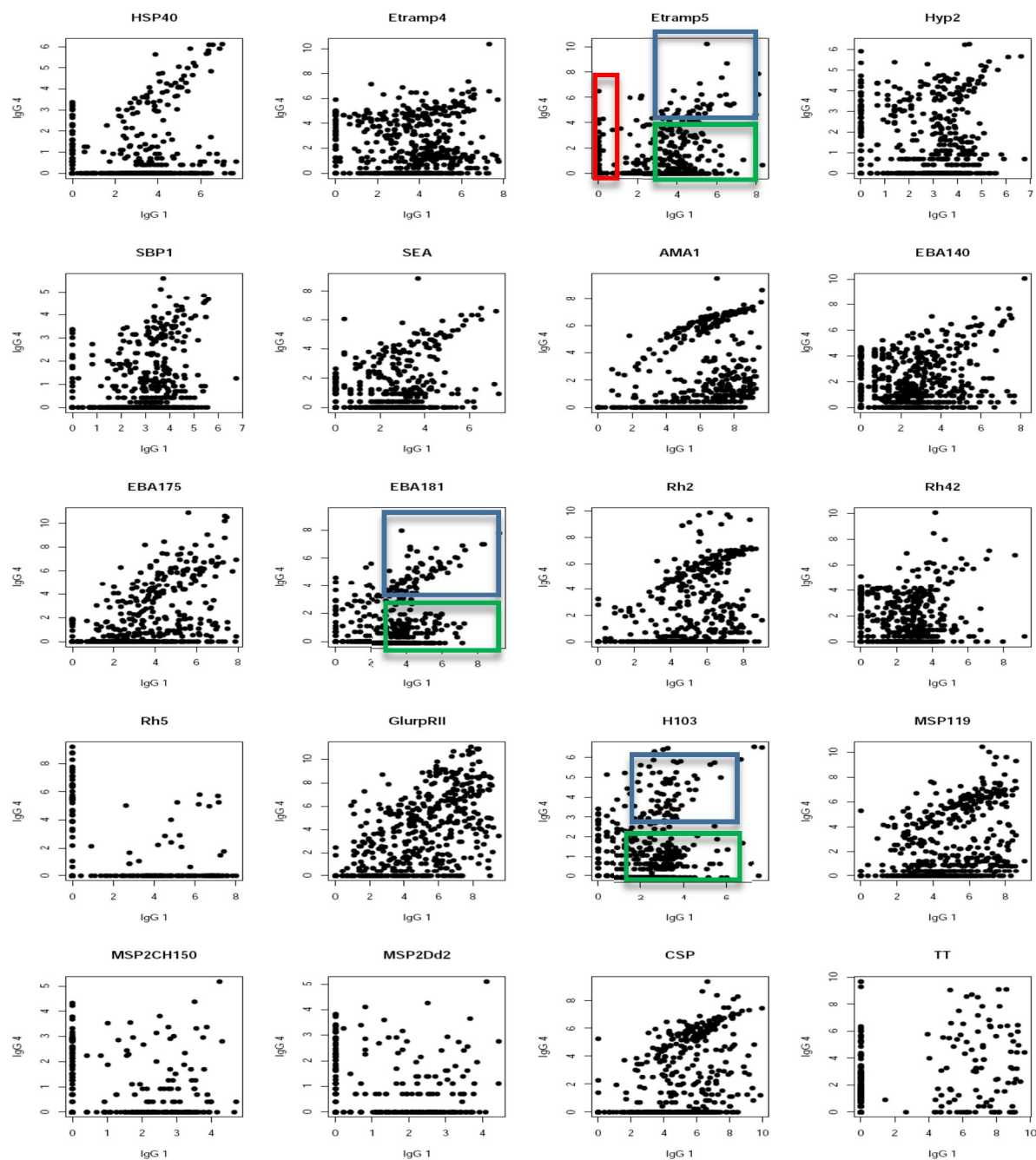


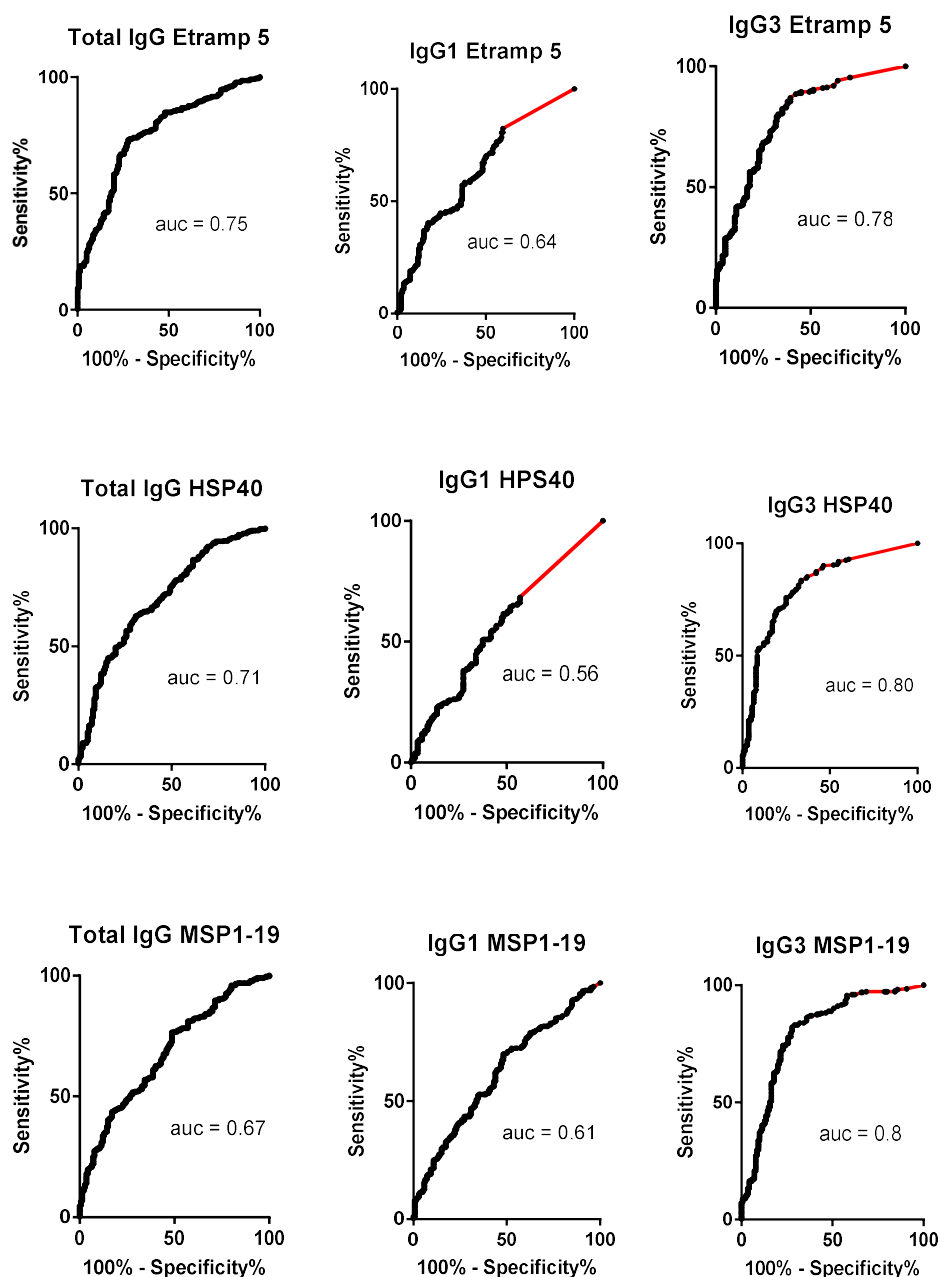
Figure 6.58 Scatter plots of IgG1 against IgG3. IgG1 and IgG4 antibodies against 18 malaria blood-stage antigens were measured on the MagPix (Luminex) multiplex assay. All 4 time-points for each of the 160 participants were included. The red gate includes a cluster of samples with low IgG1 and low IgG4 responses. Blue gate is a cluster of samples with both high IgG1 IgG4 responses. Green is high IgG1 and low IgG4.

6.4.6 IgG3 showed improved specificity of antigens to predict recent infection compared to total and IgG1

IgG3 was predicted to improve antigens' performance as markers of recent infection due to its shorter half-life than total and IgG1 (Table 6.54). ROC curve analysis was performed to evaluate the antibody response's ability to antigens to classify an individual by their infection status in the last 90 or 180 days since the last infection. Infection definition included both patent and sub-patent infection (LAMP positive) samples from all four time-points were stratified into either infected at least once in the last 90 or 180 days or not infected during the same period.

Overall, IgG3 had the highest estimated AUC across antigens, IgG1 had the lowest, and total IgG fell between IgG3 and IgG1 (Table 6.59). There was a significant negative correlation between AUC and estimated half-life. Antigens that had the shortest IgG3 half-life such as ETRAMP5Ag1 (Median half-life: 44; AUC: 77), HSP40 AG1 (Median half-life: 77; AUC: 79) MSP1-19 (Median half-life: 41; AUC: 79) and EBA175 RIII-V (Median half-life: 45; AUC: 75), had the highest AUC (Figure 6.510). Antigens like GLURP RII had a similar half-life between total, IgG3 and IgG1 had comparable AUC (Table 6.59). AUC values did not improve significantly at 180 days' time point. Similar results are observed when only T4 is included in the analysis but with wider 95% confidence intervals due to the smaller numbers.

Overall, the results implied that IgG3, even in highly immunogenic antigens like MSP1-19 and EBA175 RIII-V, improved antigens' sensitivity to predict recent infections in the last 90 days



29 Figure 6.510 ROC curves for antigens ETRAMP5 Ag1, HSP40 Ag1, MSP1-19 for total IgG, IgG1, and IgG3. Samples from 160 participants at 4 time-points were defined as *P. falciparum* positive if the participant was microscopic positive or LAMP positive, and negative if the participant was LMAP negative in the last 90 days. Each analysis includes 232 negative and 408 positive samples.

7 Table 6.511 Summary of AUC for defining infection status at 90 days

Antigen	Total IgG AUC (95% CI)	IgG1 AUC (95% CI)	IgG3 AUC (95% CI)
HSP40 Ag1	0.71 (0.64 - 0.75)	0.56 (0.48 - 0.60)	0.80 (0.75 - 0.84)
Etramp 4 Ag2	0.73 (0.69 - 0.78)	0.63 (0.57 - 0.68)	0.70 (0.64 - 0.76)
Etramp 5 Ag1	0.75 (0.70 - 0.80)	0.60 (0.55 - 0.66)	0.77 (0.73 - 0.82)
Hyp2	0.72 (0.70 - 0.79)	0.45 (0.40 - 0.50)	0.68 (0.62 - 0.73)
SBP1	0.63 (0.58 - 0.68)	0.53 (0.48 - 0.59)	0.73 (0.68 - 0.79)
SA-1	0.65 (0.60 - 0.71)	0.53 (0.47 - 0.58)	0.75 (0.71 - 0.80)
AMA-1	0.73 (0.68 - 0.78)	0.70 (0.65 - 0.76)	0.76 (0.71 - 0.82)
EBA140 RIII-V	0.70 (0.65 - 0.75)	0.62 (0.57 - 0.68)	0.72 (0.67 - 0.77)
EBA175 RIII-V	0.75 (0.70 - 0.80)	0.69 (0.64 - 0.76)	0.75 (0.70 - 0.80)
EBA181 RIII-V	0.71 (0.67 - 0.76)	0.56 (0.51 - 0.62)	0.74 (0.69 - 0.80)
Rh2	0.70 (0.65 - 0.75)	0.68 (0.63 - 0.76)	0.74 (0.70 - 0.80)
Rh4.2	0.71 (0.66 - 0.76)	0.58 (0.52 - 0.63)	0.71 (0.65 - 0.76)
Rh5	0.69 (0.64 - 0.74)	0.63 (0.57 - 0.68)	0.59 (0.54 - 0.65)
GRURP RII	0.73 (0.69 - 0.78)	0.72 (0.67 - 0.77)	0.72 (0.67 - 0.77)
H103	0.73 (0.68 - 0.78)	0.57 (0.52 - 0.63)	0.73 (0.68 - 0.79)
PfMSP1-19	0.67 (0.62 - 0.72)	0.61 (0.56 - 0.70)	0.80 (0.75 - 0.84)
MSP2 CH150/9	0.78 (0.74 - 0.83)	0.20 (0.21 - 0.29)	0.70 (0.65 - 0.76)
MSP2 Dd2	0.78 (0.73 - 0.82)	0.30 (0.25 - 0.35)	0.71 (0.67 - 0.76)
Tet Tox	0.39 (0.33 - 0.45)	0.06 (0.03 - 0.08)	0.33 (0.28 - 0.38)

Area under curve (AUC) values were estimated by the receiver operating characteristic curve (ROC). Samples from 160 participants at 4 time-points were defined as *P. falciparum* positive if the participant was microscopic positive or LAMP positive, and negative if the participant was LAMP negative in the last 90 days. Each analysis includes 232 negative and 408 positive samples. The sample was defined as *P. falciparum* negative if the participant was LAMP negative in the last 90 days.

6.5 Discussion

6.5.1 Summary of results

This study sought insight into how total IgG and subclasses are acquired with age during high malaria transmission intensity and maintained when the transmission was interrupted by the IRS. Longitudinal samples from 160 participants from three age categories (1-4, 5-11 and >18 years) were included from a larger PRISM cohort (219,221), at two time-points during high malaria transmission (12 and 6 months before IRS) and at two time-points after the transmission was interrupted to near-zero incidence. (6 and 12 months after the first round of IRS). Malaria transmission intensity did not decrease appreciatively to near-zero incidence until 12 months after the IRS's first round. (Chapter3, Figure 3.3). Total IgG and IgG1 - 4 antibody responses to 18 *P. falciparum* antigens were measured using the MagPix (Lumimex) multiplex assay. The antigens were from the *P. falciparum* life cycle's blood-stage, including infected red blood cells, the merozoite apical complex, and merozoite surface.

Total IgG and subclass antibody responses were observed in all antigens spanning the method's full dynamic range. IgG3 was the most dominant antibody relative to the other subclasses except for AMA-1 and Rh2, where IgG1 was the dominant subclass. IgG2 and IgG4 had relatively lower reactivity to the malaria antigens than the IgG1 and IgG3 subclasses, consistent with the previous findings (370,374,378).

Total IgG and IgG subclass antibody levels were inversely associated with days since the last infection, independent of age categories. Generally, IgG3 was observed to have the lowest

population level estimated antibody half-life than total IgG and the other subclasses within the antigen. In some antigens like HSP40 Ag1, ETRAMP5 Ag1, MSP1-19, IgG3 half-life was lower than 50 days. The shorter half-life of *P. falciparum* specific IgG3 compared to IgG1 was previously reported in children (379), and intravenous administration of immunoglobulin (380). Antibody levels maintained after 180 days since the last infection was thought to indicate memory antibody levels. Furthermore, the dominant subclass antibody memory pool shifted from IgG1 in children to IgG3 in the adults except for AMA-1 and Rh2. The antigen-dependent subclass dominance and skewing of IgG subclass towards IgG3 with age were observed in antigens like MSP1-19, MSP2 Dd2 (374). These observations implied; (i) antigen intrinsic factors that influence subclass switching, (ii) early establishment of a predominantly IgG1 memory, (iii) differential expansion of both IgG1 and IgG3 memory pools with age and or exposure that skew towards IgG3 in adulthood.

Because of the shorter antibody half-life observed, it was hypothesized that IgG3 could improve the ability of antibody responses to antigens to measure recent infection. The results presented supported this hypothesis. IgG3 improved the sensitivity antigens, outstandingly in ETRAMP5Ag1, MSP1-19, and HSP40 AG1, to define if a participant was infected *P. falciparum* in the last 90 days. Infection was defined by a sensitive molecular test (LAMP) to include sub patent infections. Overall, this finding boosts the prospects of using antigens to develop effective serology surveillance tools.

6.5.2 Determinants of antibody decay Half-life

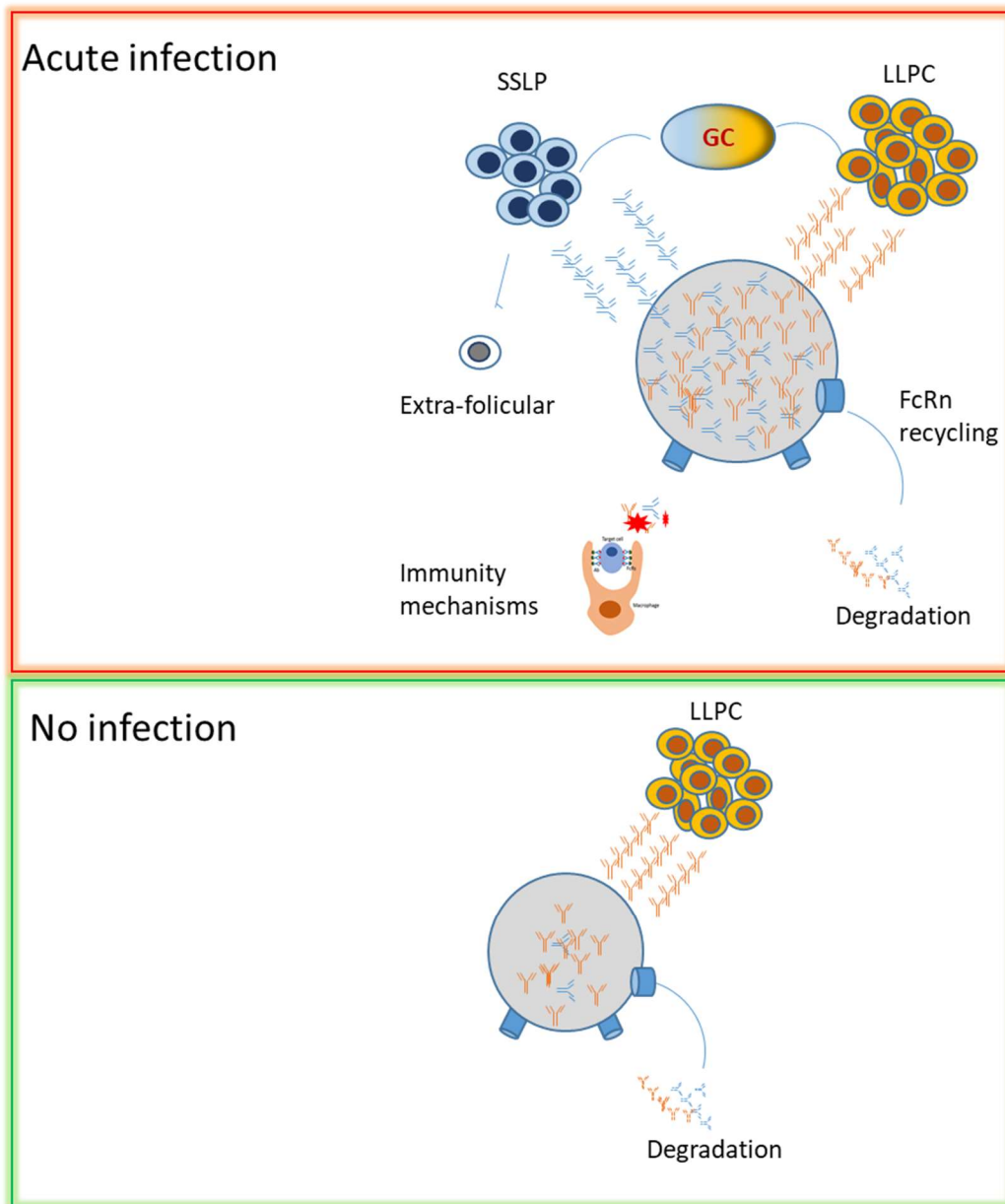
The differences in antibody half-life between antigens and subclasses and the predominance of subclass IgG1 and IgG3 between antigens and the shift with age were intriguing. The half-life of antibodies transfused into naïve patients are short-lived. IgG3 is reported to have the shortest decay half-life 7 days and about 21 days for the other subclasses (381). The classical half-life in intravenous transfusion is mainly due to catabolic processes and immunological mechanisms. However, in this study, the IgG subclass half-lives observed were longer than the classical ones, up to 6 times longer in the shortest half-life observed in IgG3. The difference between the classical and observed half-life can be attributed to the secondary nature of the immune response that is influenced by several factors including but not limited to pool sizes of (i) LLPC, (ii) SLPC, (ii) phenotype composition of MBC, (iv) frequency and or duration of infection, (v) subclass interaction with FcRn receptor.

During acute infection, extrafollicular B cell reaction, MBC activation, and early germinal center output result in a pool of SLPC that secrete antibodies, increasing the overall antibody levels (Figure 6.511) (319,382). However, SLPC declined rapidly in the absence of infection due to intrinsic survival mechanisms and cessation of new ones (383). Also, part of the germinal center output is the LLPC that migrate to the bone marrow, where they continuously secrete antibodies in the absence of infection (317,318). The size of the MBC and the phenotype composition influence the accumulation of both the SPLC and LLPC. MBC can directly differentiate into SLPC or initiate a new germinal center reaction upon activation (384). For example, switched

IgG⁺MBC are reported to differentiate into plasma cells preferentially, and the unstitched IgM⁺ MBC rapidly-produce SLPC and readily initiates CG (385). Furthermore, the accumulation of atypical MBC that express exhaustion and are difficult to transform into plasma cells in vitro is likely to affect the number of MBC that either form GC or plasma cells.

On the other hand, homeostatic mechanisms remove antibodies via the Fc receptor-mediated catabolic process. In addition, target binding effector mechanisms such as phagocytosis, complement activation, the formation of immune complexes consumes antibodies (Figure 6.511).

The FcRn increases half-life through its antibody recycling property (170). In the absence of infection, the half-life depends on the size of the SLPC, LLPC, and the ability FcRn to recycle antibodies. Figure 6.511 summarizes the different contributors that determine the antibody pool's size during and in the absence of infection.



30 **Figure 6.511** Illustrate the antibody source and destruction during acute infection and no infection. The net balance between the catabolic destruction and production source determines the size of the antibody pool. SLPC from the extrafollicular B cell and GC reaction, and the LLPC secrete antibody. In the no infection state, the LLPC and catabolic process determine the size of the antibody pool.

6.5.3 *P. falciparum* antigens may induce differential expansion of SLPC, LLPC, and MBC phenotypes

Antigens included in this study had differing total IgG and subclass half-lives. The differences in total IgG half-life can be attributed to the composition of the IgG subclasses, the size of the LLPC, and the recent boosting of SLPC. For example, AMA-1 and Rh2, which had IgG1 predominantly, were not necessarily with the longest half-life. Antigens like SBP1, Rh5, and SEA had lower antibody levels and longer half-life. The seemingly longer half-life of such antigens (Figure 6.511, green) may be due to a general lack of antibody boosting (failure to induce new SLPC) during infection. The lack of antigen boosting may be due to the transient and or limited expression of antigen quantity above a threshold to trigger a response. The alternative explanation could be the establishment of dysfunctional atypical MBC.

Some antigens like GLURP RII had high antibody levels but with a shorter half-life. Such antigens are likely to elicit a large SLPC pool, a large MBC pool, and a small LLPC pool. Antibodies against this kind of antigens will have a large difference between the peak antibody levels during infection and the memory level maintained in the absence of infection (Figure 6.511, red).

On the other hand, there were antigens like AMA-1, whose antibody response has a high titer and a longer half-life. Such antigens are likely to elicit both large pools of LLPC and SLPC, resulting in boosting during infection but decay much slower due to the minimum difference

between the peak boost and the memory level maintained in the absence of infection (Figure 6.511, blue).

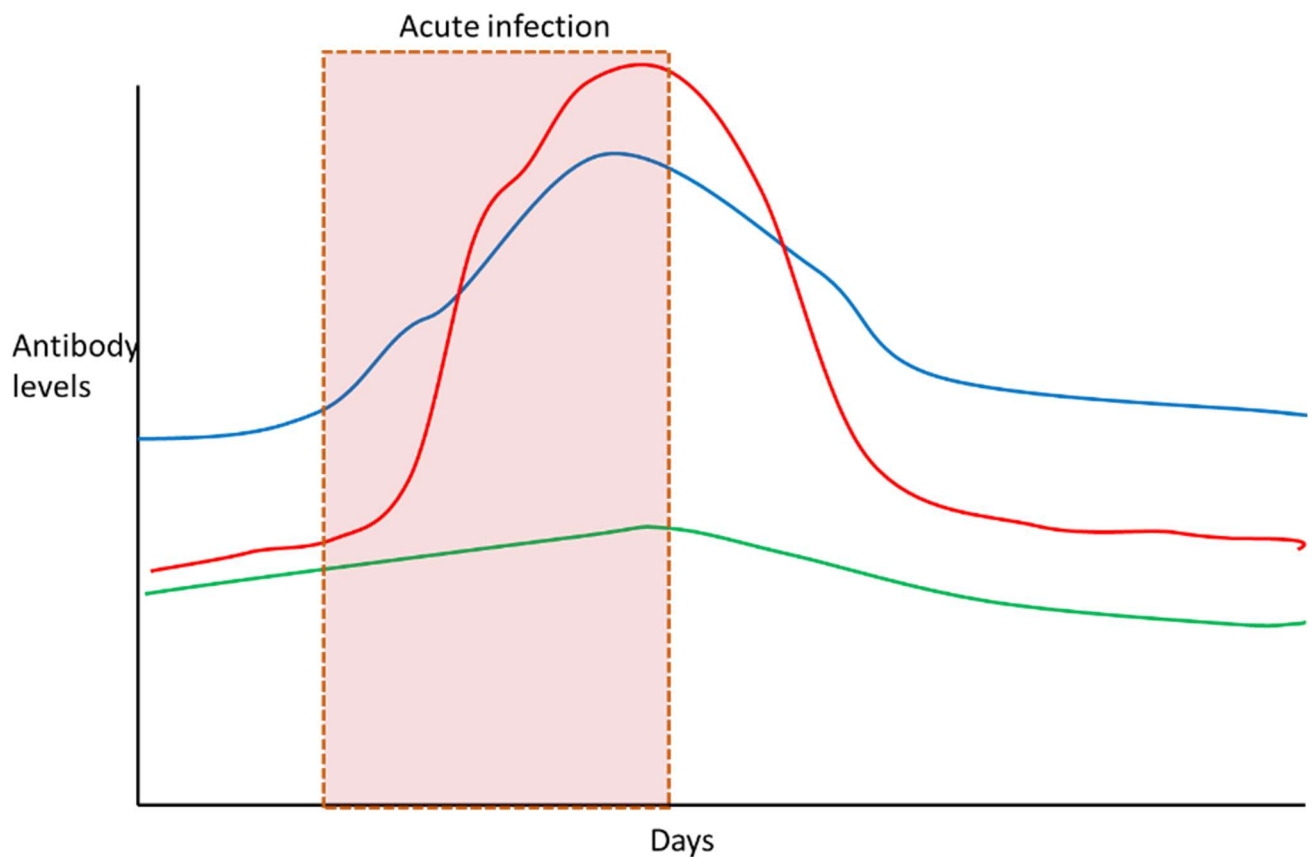
The differences observed among antigens support the notion that *P. falciparum* antigens differentially influence the B cell responses towards divergent memory compartments may bear consequences to the short-lived acquired immunity to malaria thought to require continuous exposure (340,386). Malaria-specific MBC were detected in the absence of antibodies implying inefficient accumulation of LLPC (322,387). MBC response is important to boost antibody response within 3 to 7 days of infection. However, highly invasive merozoites are released in large numbers from the liver stage. Maintaining antibody levels is important for the initial control of the parasite load and alleviation of disease before the antibody boost from extrafollicular MBC response and later germinal center reaction (324).

Therefore, it is important to understand the factors that influence the memory compartment's outcome and antigens' role to inform better malaria vaccine designs that induce antibody titers sustained at high concentration and provide durable protection.

6.5.4 FcRn may influence half-lives of IgG3 compared to IgG1

This study showed differences in the half-life among subclasses within antigen, and IgG3 decayed relatively faster than the other subclasses. The faster decay of IgG3 may be attributed to its poor binding to the FcRn in acidic conditions (171,388). This property is critical for

protecting IgG from degradation in the endocytotic vacuoles (170). The FcRn receptor is also responsible for the placental maternal antibodies.



3/ 6.511 Illustration of the three scenarios of antibody boost and decay profiles. Red has a short half-life. Predominantly from SLPC antibody and very small LLPC pool. Maintain low antibody levels, highly boosted during infection, and rapidly decay in the absence of infection. Blue has a long half-life due to a large pool of LLPC boosted with a large pool of SSLP and accumulated additional LLPC in the absence of infection. Green has a small LLPC pool and does not boost SLPC effectively during infection.

6.5.5 Slowed acquisition of IgG3 memory

Cytophilic subclasses IgG1 and IgG3 are thought to play a critical role in antibody-mediated protective mechanisms against blood-stage malaria. IgG3 is thought to play a greater role than IgG1 due to IgG3 high affinity for the Fc γ receptors and C1q compared to IgG1. Maintenance of predominantly IgG1 in the absence of infection in children and IgG3 in adults may imply impaired or slowed acquisition of IgG3 LLPC. IgG class switching follows a one-way direction (IgG3, 1, 2 to 4) due to its nature of the Fc region's CH domains. IgG2 and IgG4 are referred to as terminal subclasses and are thought to have more somatic hypermutation implying extensive affinity maturation (389). IgG1 switched MBC will not switch to IgG3, but the results showed a shift from IgG1 in children towards IgG3 in adults. Likely, MBC that eventually give rise to IgG3+ LLPC is not the early ones that switched to IgG1, IgM+ MBC is most likely the source of late IgG3 LLPC, and this may underscore their importance in the slow acquisition of immunity to malaria. In some antigens, some adults express only IgG3 without IgG1. In this scenario, the absence of IgG1 may imply a total deletion of IgG1 switched MBC or their impairment with age or continued exposure. Although cytokines, intrinsic properties of antigens, the toll-like receptors (TLR), and microenvironment are implicated in switching (390), it remains unclear why switching is biased to IgG1 in children and shifted towards IgG3 in adults. The alternative explanation may be the preferential affinity maturation and acquisition of LLPC in the IgG3 than IgG1. Because of the common epitopes' competitive binding, IgG1 is the most prevalent competitively binds epitopes and is therefore quantified in the Luminex assay. However, as IgG3

accumulates affinity maturation and the titer increases, IgG1 is outcompeted for the binding sites and therefore under quantified. Therefore, the shift from IgG1 to Ig3 with age may be due to the preferential affinity maturation in the IgG3 subclass .

6.5.6 Prospects on using IgG3 as a marker of recent infection

Results showed early expansion of IgG1 at an early age and a gradual expansion of IgG1 and IgG3 with age, biased towards IgG3. Similarly, our results demonstrated that IgG3 decayed with a shorter half-life than total IgG and IgG1 in the absence of infection. These two features may partly explain the better performance of IgG3 as a marker of recent infection compared to total IgG. Infection was defined to include both patent and sub-patent infections, and IgG3 improved specificity of a highly reactive protein like MSP1-1 from 67% for total IgG to 80% for IgG3. This existing finding increases the prospects of designing superior malaria serological diagnostic or surveillance tools. The limitation of serological malaria diagnostic tools has always been the accumulation of memory with age and exposure that dampens the method's specificity. This limitation is likely to continue with IgG3, especially based on the generally increasing accumulation of IgG3 with age maintained after 180 days since the last infection. However, heterogeneity in the acquisition and maintenance of antibody responses by various malaria antigens has been previously observed and explored to identify recent exposure markers (331). Using similar microarray and bioinformatics approaches, focusing on IgG3 and exploring combination of antigens may result in the discovery of superior tools.

6.5.7 Drivers of distinctive antibody clusters

Previously, a linear relationship, especially between IgG1 and IgG3, was assumed and reported. Surprisingly our data revealed distinct clustering when IgG subclasses were plotted against each other. Outdating clusters were observed in IgG1 versus IgG3 and IgG4 versus IgG1 or IgG3. Some phenotypes like the IgG1^{13^h} and co-dominant IgG1^{h3^h} seemed to be consistent in some individuals at all four time-points. However, after highly stratifying the subpopulations at the participant level, the numbers were too small to make any meaningful deductions. Phenotypic expression of cell markers and cytokine secretion of T cells, especially T helper, including Tfh cells, has been extensively elaborated. T helper cells influence B cell reaction and class switching. IgG subclass ratios were previously associated with severe disease. More recently, a delayed boost in RTS, S resulted in increased IgG4 and improved efficacy(141). Likely, exposure timing and duration, T cell help, and other factors may influence IgG subclass composition, which can bear consequences on the immunity phenotype and maintenance. More work is required to understand the dynamics and drivers of IgG subclass phenotypes.

6.5.8 Limitations

Compared to total IgG, subclass signals were lower even at a higher plasma concentration. The low signal was due to monoclonal secondary anti-subclass use compared to the polyclonal anti-IgG for total antibody. The competitive binding epitopes further compounded subclasses' detection levels relative to each other by the different subclasses, resulting in under quantification of especially subclass with low affinity and concentration. The estimation

method of decay half-life assumed a constant linear reduction in antibody levels instead of a diphasic decay, which may result in the estimation of shorter half-lives. Also, the estimation method did not put into account antibody boosting.

6.6 Conclusions

This study demonstrated the acquisition of all four IgG subclasses against malaria antigens and IgG1 and 3 being the dominant ones, similar to other findings. The IgG subclasses decayed at different rates; IgG3 had the shortest decay half-life. IgG3 memory pool maintained in the absence of infection was relatively smaller than IgG1 but expanded preferentially with age to become dominant or co-dominant subclass in adults. As a result of a shorter half-life and slow accumulation of memory pool, IgG3 demonstrated improved specificity performance as a recent infection marker compared to total IgG. Furthermore, a combination of IgG subclasses revealed phenotypes. Additional work is required to explore IgG3 as a diagnostic tool for recent exposure and to understand the cause and implication of IgG subclass phenotype.

Chapter 7

7.1 Discussion

7.1.1 Summary of results

This thesis's first aim (Chapter 4) was to determine the association between *P. falciparum* transmission intensity with *P. falciparum* specific antibody avidity. To achieve this objective, 1,029 and 582 samples from three cross-sectional surveys from low (EIR= 2) medium (EIR=6) to very high (EIR = 305) transmission intensity were utilized to compare avidity index to AMA-1 and MSP1-19 across the sites, respectively. The avidity index was measured as a proportion of highly binding antibodies that remained after treatment with a chaotropic agent in the modified ELISA assay. Results demonstrated that despite higher antibody levels, avidity to both AMA-1 and MSP1-19 was significantly lower at the site of highest *P. falciparum* transmission intensity in children above 5 years and adults. Age had a minimal effect on antibody avidity. These observations suggest that affinity maturation to *P. falciparum* antigens may be compromised in the setting of high *P. falciparum* transmission. This observation led to the hypothesis; (i) Recent infection may result in low avidity antibodies from predominately SLPC (ii) Near constant exposure may interfere with affinity maturation. However, the cross-sectional nature of the study limited the ability to explore the two hypotheses. Secondly, only two malaria antigens were included, which limited our ability to generalize the findings.

The second objective was inspired by hypotheses derived from the first aim's results (Chapter 4). I took advantage of the PRISM longitudinal cohort at Nagongera, a high transmission site, in Chapter 4. IRS was introduced and interrupted transmission drastically to near-zero incidence within one year. The interruption of transmission provided the opportunity to measure antibody avidity within the same individuals during high *P. falciparum* prevalence, and malaria prevalence was nearly zero. The objective was to determine the effect of interruption in *P. falciparum* transmission by IRS on antibody avidity to a panel of 18 *P. falciparum* blood-stage antigens. The PRISM cohort's uniqueness provided accurate *P. falciparum* infection documentation, up to intervals of one-month active surveillance for patent and sub patent infection using light microscopy and LAMP, respectively. The detailed intensive surveillance allowed estimation of days since last infection or proportion of months free of infection for each of the 4 time-points; 6 and 12 months pre-IRS and 6- and 12-months post-IRS. The chaotropic interruption of antibody binding technique previously established for ELISA was adopted for use on the MagPix (Luminex) platform to allow multiplexing. To our knowledge, this was the first such description of a multiplex avidity assay that allows the simultaneous evaluation of the IgG avidity index of a large panel of *P. falciparum* antigens. On top of the multiplexing, the method's high dynamic range allowed detection of subtle differences and inclusion of samples with low reactivity compared to the ELISA method.

Generally, across all 18 malaria antigens explored, the avidity index was below 50% for all antigens except for AMA1 and Rh2 in most participants. However, there were a few participants

with an avidity index above 80% to near 100%. Secondly, the avidity index increased significantly after the IRS, and the increase was associated with days since the last infection or proportion of months free of infection, independent of age. The increase in avidity index was found to be due to the differential decay of the predominantly non-avid antibody pool compared to the avid pool. Thirdly, there was high heterogeneity in the avidity index in association with age independent of days since the last infection. Avidity index increased in some antigens, decreased or remained the same in other antigens in association with age. The heterogeneity was due to the differential expansion of both the avid and the non-avid antibody pools in association with age.

Based on the observation of low avidity index, faster decay rates of non-avid compared to avid pool in the absence of infection, I postulated that (i) The non-avid pool was produced primarily by SLPC that rapidly wane in the absence of infection. (ii) The avid pool is produced primarily by LLPC that survive and continually produce antibodies in the absence of infection. These findings supported the hypothesis derived from Chapter 4; recent or near-constant exposure promotes low avidity antibodies from SLPC. Because most of the individuals had a predominantly low avidity index for most antigens, these results strengthen the second hypothesis, stating that frequent *P. falciparum* infection may impair affinity maturation.

Both affinity maturation and class switching occur during the germinal center reaction. Both properties impact antibody-mediated immunity to malaria. The third objective sought to determine the effect of interruption of malaria transmission by IRS on the IgG subclass response

on a large number of blood-stage malaria antigens. The same cohort samples used in objective 2 in Chapter 5 were utilized. Total IgG and IgG1-4 antibodies against 18 malaria blood-stage antigens were measured on the MagPix (Luminex) multiplex assay. All four IgG subclasses were detected in all antigens with no clear pattern between iRBC associated antigens, apical complex, or merozoite surface antigens. IgG subclasses decayed at different rates, and IgG3 half-life was the shortest of the four subclasses, consistent with previous findings. There was a general preferential early acquisition IgG1 maintained after 180 days since infection (antibody memory) at the early age, and the antibody memory expansion with age was skewed towards IgG3, resulting in a memory predominance of IgG3 over IgG1 in adults for most of the antigens except for AMA-1 and Rh2. Due to its shorter half-life, IgG3 improved antigens' specificity as a marker of recent infection compared to total IgG or IgG1, even for highly immunogenic antigens like MSP1-19. When plotted against each other, IgG subclasses formed distinctive clusters instead of linear associations previously reported.

7.1.2 Does *P. falciparum* infection interfere with affinity maturation?

Chapter 4 (Objective 1) showed that malaria antigens' avidity index was inversely associated with malaria transmission intensity. Results from Chapter 5 (Objective 2) showed that most individuals from a high malaria transmission intensity had low avidity index generally across 18 blood-stage malaria antigens. The avidity index improved after one year of interrupting malaria transmission. Although an overly simplified designation, the results revealed differences in decay rates of avid compared to non-avid antibody pools in the absence of infection, implying a

difference in sources, primarily LLPC and SLPC, respectively. Furthermore, the accumulation of both avid and non-avid pools hence avidity index with age varied across antigens. In a highly endemic setting where an individual suffers hundreds of infections in the early years of age, the avid pool's accumulation should have been acquired and saturated very early in life. However, age had little effect on the avidity index in Chapter 4, and the avid pool only significantly increased in adults compared with children 1 - 4 years for most antigens in Chapter 5. Expansion of the avid pool happened alongside the expansion of the non-avid pool, and in some antigens, the non-avid pool expanding preferentially. Also, results from Chapter 6 showed later acquisition of the memory IgG3 subclass compared to IgG1. IgG3 is thought to be superior to IgG1 at mediating effector function mechanisms due to a higher affinity for Fc γ R and flexibility of the long hinge that improves the binding complex (132,391). The delayed acquisition of the germinal center output features like avid antibody pool and IgG3 may imply interruption of B cell reaction in *P. falciparum* infection.

These findings contribute to the growing evidence of malaria interference of the germinal center reaction at different stages, including (i) skewed T-independent extrafollicular B cell response, (ii) impairment of the T follicular helper cells population, (iii) disruption of germinal center architecture, (iv) interruption of antigen presentation by dendritic and other antigen-presenting cells (v) presence of a large chronic volume of antigens that affect affinity selection (vi) chronic immune activation. The consequence of these impairments results in (i) skewed memory compartments, (ii) accumulation of atypical MBC, (iii) accumulation of IgM⁺ MBC, (iv) low

antibody avidity, (v) poor maintenance of high antibody titers due to short half-life (vi) delayed IgG3 memory.

7.1.3 What is the implication of low antibody avidity (predominantly non-avid antibodies)?

The presence of a predominantly non-avid antibody pool may reflect the dynamics in the acquisition and maintenance of SLPC, LLPC, and MBC phenotypes. Class switched MBC has been widely studied in malaria, but most recently non switched IgM⁺ MBC have been described and reported in malaria (385,392). Non-switched IgM⁺ MBC characterized by fewer somatic hypermutations rapidly respond to malaria infection and give rise to IgM and IgG plasmablasts within three days of infection(392,393). Their rapid response in the extrafollicular T independent response can be critical in the early boosting of antibody titers and, subsequently, control parasite density to alleviate disease outcomes. Secondly, these IgM⁺ MBC may be important in maintaining a large non-avid pool with a high breadth of recognition or wide cross reactivity. This attribute of cross-reactivity allows for rapid recognition of high antigenic variation and prevents parasite immune evasion. However, the broad reactivity comes at a low avidity cost and requires a high antibody titer to mediate function. Therefore, a predominantly non-avid antibody pool may reflect the plasticity of the IgM⁺ MBC or extrafollicular IgG+MBC, a host adaptation to counteract the high polymorphism and genetic diversity of the parasite antigens. This IgM⁺ MBC and extrafollicular IgG+MBC plasticity may be an adaptation that comes at the cost of delayed and poor maintenance of acquired immunity. However, whether there is a skewed expansion of IgM⁺ MBC and extrafollicular IgG+MBC in malaria infection and if it affects the

acquisition of avid antibody and long-term memory is unknown. In addition, there are germinal center independent IgG+MBC (315) that are of low somatic hypermutation. How these contribute to the pool of non-avid antibodies is also not known.

The PRISM cohort provides an opportunity to study malaria-specific MBC phenotypes kinetics from the same individuals during high exposure to infection. In the absence of infection, properties of MBC such as surface marker phenotypes, class/subclass switching, mutations in the V-gene region, their ability to proliferate and differentiate into antibody-forming cells, and the relative avidity of the secreted antibodies can be studied. Tetramers can be used to sort malaria-specific B cells. To increase the yield, tetramers of several malaria antigens can be used to harvest a polyclonal population. B cell receptor class switching, surface markers, can be associated with age, malaria exposure history, state of infection, pre and post-IRS, among other factors

The B cells may be sorted further by surface marker phenotypes or B cell receptor subclass, sequence the v-gene region, and culture for proliferation and differentiation into antibody-forming cells. Avidity of the antibodies secreted in culture can be associated with the V-gene mutations and the different phenotypes. These features can be related to age, immunity status, history of exposure, and effective elimination of IRS exposure. While peripheral blood MBC may not fully tell the full story of the different memory compartment acquisition and maintenance, we can gain useful insight into drivers and nature of secondary antibody responses.

7.1.4 Does malaria induce short-lived memory compared to other infections?

The amount of antibody maintained in the absence of infection is the net difference between antibody production by LLPC and antibody decay. Therefore, the increased antibody half-life can indicate memory since the catabolic decay is a constant in the absence of infection. The rate of production from LLPC or differentiating MBC into SLPC determines the rate for decay. Chapter 6 results showed that the total IgG half-life for the malaria blood-stage antigens ranged between 57 to 120 days compared to a double boost within 259 for TT. While IgG1, 2, and 4 indicated longer decay half-life with some trends of boosting in some antigens, IgG3 had the lowest decay half-life, to as low as 41 days for ETRAMP5 Ag1, for example. This observation implied that total antibody decay was majorly contributed to by IgG3. Other studies have reported shorter half-life of antibodies to malaria blood-stage antigens from as low as 6 and 7 days for IgG1 and IgG3, respectively (379,394), and as high as 157 years for total IgG to *Pf* VAR2CSA (151). The wide differences in half-life could be due to several factors, including the methodology and assumption of a constant linear decay than diphasic decay, antigen type, population age, and time from infection. All these factors can influence the estimation outcome. However, not even the longest half-life estimation of malaria antibodies is comparable to estimates for other diseases like measles (over 369 years), MUMPS (124 years), Rubella (over 85 years), among others (395). Therefore, a question remains whether malaria impairs memory acquisition or alters the acquisition of the memory compartments that bear consequences to protective immunity? Studies in African migrants who return to malaria-endemic areas after a

long time have increased susceptibility to malaria, although not to the extent seen in malaria naïve (396,397).

Furthermore, the resurgence of malaria and severe forms in adults have been reported in areas where effective interventions like IRS and ITN have been discontinued (329,398). Other studies have demonstrated maintenance of malaria MBC in the absence of detectable antibodies (387,399), implying that the MBC compartment can be acquired and maintained without the LLPC compartment. Failure to maintain antibodies may affect immunity due to failure to contain the infection within the first 3 to 5 days before secondary B cell reaction results in antibody boost. According to our results, IgG1, 2, and 4 are maintained better than IgG3 in the absence of infection. Therefore, the IgG subclasses' composition is likely to alter, and because IgG4, for example, can have an antagonistic effect on IgG1 and IgG3 effector function, this alteration may affect the potency and effectiveness of the maintaining antibody in the absence of infection. IgG subclasses are associated with graft rejection implying their role in modifying the immunity outcome (346). More work is required to determine IgG subclass composition's effect on effector function like antibody-dependent phagocytosis, cytotoxicity, complement-fixing, or parasite growth inhibition.

7.1.5 IgG subclass phenotypes and implication in immunity to malaria

Results in Chapter 6 revealed clustering of IgG subclasses when plotted against each other, more clearly in IgG1 VS IgG3 and IgG4 VS IgG1 or IgG3. The results also indicated differences in decay half-life as well as acquisition rates with age. These two features can result in clustering. Other factors like T-follicular phenotypes, pro-inflammatory versus non-inflammatory cytokine environment, and innate signaling can influence IgG subclass switching patterns among individuals(373,390,400,401). However, we already know that IgG subclasses have different abilities to mediate the different effector mechanisms. Secondly, the different malaria immunity profiles like anti-disease and anti-parasites are mediated by different mechanisms. Therefore, the IgG subclass phenotypes are likely important surrogate markers of immunity profiles, historical exposure, or predictors of maintenance of immunity or risk of disease. Further work must understand the relationship between IgG subclass phenotypes and malaria exposure and immunity status.

7.1.6 Prospects of IgG3 as a diagnostic tool for malaria in the elimination era

The new UN Sustainable Development Goal 3C calls for reducing malaria mortality and morbidity by at least 90%, eliminating malaria in 35 countries by 2030. To achieve this goal, intensive surveillance and timely identification of any infection will be required to target treatment. Serology tools provide prospects due to the ease of use in the fields and quick turnaround time. These tools may not serve as diagnostic tools, but they will play a big role in detecting recent exposure. Results from Chapter 6 showed that IgG3 had a shorter half-life and

delayed accumulation of memory antibody pool maintained in the absence of infection with age compared to IgG1 and total IgG. These observations implied that despite IgG3 having a shorter half-life, it also suffers from the delayed acquisition of LLPC relative to IgG1. Because IgG1 and IgG3 are the most prevalent subclasses in malaria immune responses, as shown by our results and others, detecting only IgG3 can improve malaria antigens' performance to measure recent infection. Results in Chapter 6 supported this postulation where IgG3 showed better specificity to predict infection on the last 90 days compared to total IgG and IgG1. The results indicated that the performance of IgG3 could be equally as good for highly immunogenic antigens like MSP1-19 even when infection was defined at the sub-patent level. Because antigens such as MSP1-19 are universally reactive, IgG3 offers the prospects of overcoming specificity limitations that come with antigens that are not universally reactive. However, our results are from a highly endemic area where the infection was drastically interrupted; the kinetics of memory compartments and subclasses may be different in such a high perennial transmission setting compared to seasonal malaria, low transmission, or near elimination areas. Additional work is required, exploring more malaria antigens and different transmission settings.

7.2 Significance

This thesis showed that frequent infection-induced predominantly non-avid antibodies with shorter half-lives supported the hypothesis that chronic near-constant infection may interrupt affinity maturation. This bears consequence on the quality of antibody-mediated immunity against *P. falciparum* infection and its longevity. Poor and short-lived efficacy of RTS, S was

reported in endemic areas, and this could have been due to the vaccine inducing mainly SLPC. If our hypothesis is true, vaccine outcome will improve if vaccination is conducted under chemoprophylaxis to allow vaccination to induce complete germinal center reaction and produce LLPC. Secondly, a simple intervention involving intensive malaria prophylaxis following a malaria episode may improve avidity maturation and early acquire an effective protective immune response. Our results clearly show that measuring IgG3 increases the prospects of using serology tools to measure recent infection. Finally, our results indicate that measuring antibody quality and quantity instead of quantity alone may provide better correlates of naturally acquired or vaccine-induced immunity and its longevity.

7.3 Conclusions

This thesis aimed to determine the effect of malaria transmission intensity on the antibodies against blood-stage malaria properties, namely antibody avidity, and IgG subclasses' composition. This was driven by the observation of antibodies' roles in acquired immunity to malaria, the slow acquisition of immunity with age, and the increasing evidence supporting the interruption of immunity acquisition. *P. falciparum* is thought to interrupt immunity acquisition partly through the interruption of the germinal center reaction, which is the source of both affinity maturation and class switching. We compared the avidity index to AMA-1 and MSP1-19 in three different transmission settings and observed that the avidity index was inversely associated with transmission intensity. We further compared avidity index and IgG

subclasses to 18 blood-stage malaria antigens in a longitudinal study where IRS interrupted high transmission intensity to near zero after one year. We observed that the increase in avidity index with days since the last infection was due to the differential rates of decay of the non-avid antibody pool compared to the avid pool. The non-avid pool was postulated to be majorly produced by SLPC that contracts rapidly in the absence of infection. The avid pool by LLPC was maintained in the absence of infection. Heterogeneity in avidity index with age across antigens was observed due to differences in expansion of both the avid and non-avid pool with association with age. Furthermore, IgG subclasses decayed at different half-lives, with IgG3 generally having the shortest half-life. IgG1 pool maintained in the absence of infection was preferentially acquired early in age, but IgG3 was preferentially accumulated with age, thus explaining the shift in dominance from IgG1 to IgG3. Consequently, IgG3 performed with better specificity as a recent infection marker compared to total IgG and IgG1. When plotted against each other, IgG subclasses revealed conspicuous clustering that requires further investigation. This thesis supports the existing notion that *P. falciparum* interrupts the acquisition and maintenance of immunity to malaria. We provide further evidence of predominant production of non-avid antibodies that rapidly decay in the absence of infection and the slow accumulation of the avid pools that majorly maintain circulating antibodies in the absence of infection.

7.4 Future Direction

The thesis further shows the disproportionate acquisition and maintenance of IgG3 subclasses. Further work is required to determine functional differences between IgG1 and IgG3 in malaria immunity to understand the implication of the IgG3 memory pool's delayed accumulation. This can be done by affinity purification of IgG1 and IgG3 from plasma. The purified antibodies can be used in functional antibody assays like parasite growth inhibition and antibody-mediated complement-fixing. It is also important to understand if IgG1 is functionally comparable to IgG3 and their synergy in combination and with IgG subclasses.

Furthermore, IgG3 showed improved *P. falciparum* antigen performance as a recent infection marker, especially with highly immunogenic antigens like MSP1-19. Further investigation is needed to validate this finding in a larger study and to explore additional antigens and a combination of antigens. A serology tool can greatly impact malaria surveillance due to the ease of use and cost-effectiveness.

For the first time, I showed distinct clustering of individuals based on their IgG1, IgG3, and IgG4 profiles. This observation needs to be validated in a larger sample size. Also, factors associated with the clusters should be determined to understand the impact on immunity and its maintenance.

Further work is required to investigate malaria-specific MBC population phenotypes, class-switching, and SHM patterns. Characterization of antibody avidity, subclass, and functional assays for the antibodies secreted by the MBC in-vitro with age and exposure is required to gain more knowledge in antibody memory acquisition dynamics.

Publications

The publication that resulted from the Ph.D. work

The candidate took the lead role in the publication listed in this section. The roles included the design of the studies, performed all the laboratory experiments, data analysis results interpretation, and writing the first manuscript draft. The candidate compiled the revisions from all contributors produce the final versions that were submitted to journals for publication.

1. Avidity of anti-malarial antibodies inversely related to transmission intensity at three sites in Uganda.

Ssewanyana I, Arinaitwe E, Nankabirwa JI, Yeka A, Sullivan R, Kamya MR, Rosenthal PJ, Dorsey G, Mayanja-Kizza H, Drakeley C, Greenhouse B, Tetteh KK.

Malar J. 2017 Feb 10;16(1):67. doi:10.1186/s12936-017-1721-3. PMID: 28183299; PMCID: PMC5301436.

2. Impact Q1 of a Rapid Decline in Malaria Transmission on Antimalarial IgG Subclasses and Avidity.

Isaac Ssewanyana, John Rek, Isabel Rodriguez, Lindsey Wu, Emmanuel Arinaitwe, Joaniter I. Nankabirwa, James G. Beeson, Harriet Mayanja-Kizza⁴, Philip J. Rosenthal, Grant Dorsey, Moses Kamya, Chris Drakeley, Bryan Greenhouse, and Kevin K. A. Tetteh
Accepted for publication the Frontier in Immunology, Microbial

Other Relevant work published from projects I significantly contributed

The candidate contributed significantly to publication in this section including design of the studies, lab experiments, data analysis and interpretation, and writing.

1. Quantification of anti-parasite and anti-disease immunity to malaria as a function of age and exposure.

Rodriguez-Barraquer I, Arinaitwe E, Jagannathan P, Kamya MR, Rosenthal PJ, Rek J, Dorsey G, Nankabirwa J, Staedke SG, Kilama M, Drakeley C, **Ssewanyana I**, Smith DL, Greenhouse B. Elife. 2018 Jul25;7:e35832. doi: 10.7554/eLife.35832. PMID: 30044224; PMCID: PMC6103767.

2. Elevated plasma abscisic acid is associated with asymptomatic falciparum malaria and with IgG-/caspase-1-dependent immunity in Plasmodium yoelii-infected mice.

Glennon EKK, Megawati D, Torrevillas BK, **Ssewanyana I**, Huang L, Aweeka F, Greenhouse B, Adams LG, Luckhart S.
Sci Rep. 2018 Jun 11;8(1):8896. doi:10.1038/s41598-018-27073-1. PMID: 29891920; PMCID: PMC5995817.

3. Dihydroartemisinin-piperaquine for intermittent preventive treatment of malaria during pregnancy and risk of malaria in early childhood: A randomized controlled trial.

Jagannathan P, Kakuru A, Okiring J, Muhindo MK, Natureeba P, Nakalembe M, Opira B, Olwoch P, Nankya F, **Ssewanyana I**, Tetteh K, Drakeley C, Beeson J, Reiling L, Clark TD, Rodriguez-Barraquer I, Greenhouse B, Wallender E, Aweeka F, Prah M, Charlebois ED, Feeney ME, Havlir DV, Kamya MR, Dorsey G.
PLoS Med. 2018 Jul 17;15(7):e1002606. doi: 10.1371/journal.pmed.1002606. PMID: 30016328; PMCID: PMC6049882.

4. B cell sub-types following acute malaria and associations with clinical immunity.

Sullivan RT, **Ssewanyana I**, Wamala S, Nankya F, Jagannathan P, Tappero JW, Mayanja-Kizza H, Muhindo MK, Arinaitwe E, Kamya M, Dorsey G, Feeney ME, Riley EM, Drakeley CJ, Greenhouse B, Sullivan R
Malar J. 2016 Mar 3;15:139. doi: 10.1186/s12936-016-1190-0. Erratum in: Malar J. 2016;15(1):188. PMID: 26939776; PMCID: PMC4778296.

5. Quantifying Heterogeneous Malaria Exposure and Clinical Protection in a Cohort of Ugandan Children.

Rodriguez-Barraquer I, Arinaitwe E, Jagannathan P, Boyle MJ, Tappero J, Muhindo M, Kamya MR, Dorsey G, Drakeley C, **Ssewanyana I**, Smith DL, Greenhouse B.
J Infect Dis. 2016 Oct 1;214(7):1072-80. doi:10.1093/infdis/jiw301. Epub 2016 Aug 1. PMID: 27481862; PMCID: PMC5021229.

6. Examination of Antibody Responses as a Measure of Exposure to Malaria in the Indigenous Batwa and Their Non-Indigenous Neighbors in Southwestern Uganda.

Kulkarni MA, Garrod G, Berrang-Ford L, **Ssewanyana I**, Harper SL, Baraheberwa N, Donnelly B, Patterson K, Namanya DB, Lwasa S, Drakeley C.
Am J Trop Med Hyg. 2017 Feb 8;96(2):330-334. doi: 10.4269/ajtmh.16-0559. Epub 2016 Nov 28. PMID: 27895271; PMCID: PMC5303031.

7. Novel serologic biomarkers provide accurate estimates of recent Plasmodium falciparum exposure for individuals and communities.

Helb DA, Tetteh KK, Felgner PL, Skinner J, Hubbard A, Arinaitwe E, Mayanja-Kizza H, **Ssewanyana I**, Kamya MR, Beeson JG, Tappero J, Smith DL, Crompton PD, Rosenthal PJ, Dorsey G, Drakeley CJ, Greenhouse B
 Proc Natl Acad Sci U S A. 2015 Aug 11;112(32):E4438-47. doi: 10.1073/pnas.1501705112. Epub 2015 Jul 27. PMID: 26216993; PMCID: PMC4538641.

Reference

1. Crompton PD, Moebius J, Portugal S, Waisberg M, Hart G, Garver LS, et al. Malaria immunity in man and mosquito: insights into unsolved mysteries of a deadly infectious disease. *Annu Rev Immunol*. 2014;32:157–87.
2. Cox-Singh J, Singh B. Knowlesi malaria: newly emergent and of public health importance? *Trends Parasitol*. 2008 Sep 1;24(9):406–10.
3. Kantele A, Jokiranta TS. Review of Cases With the Emerging Fifth Human Malaria Parasite, *Plasmodium knowlesi*. *Clin Infect Dis*. 2011 Jun 1;52(11):1356–62.
4. WHO | World Malaria Report 2016 [Internet]. WHO. [cited 2017 Nov 2]. Available from: <http://www.who.int/malaria/publications/world-malaria-report-2016/report/en/>
5. Coetzee M, Craig M, le Sueur D. Distribution of African Malaria Mosquitoes Belonging to the *Anopheles gambiae* Complex. *Parasitol Today*. 2000 Feb 1;16(2):74–7.
6. White GB. *Anopheles gambiae* complex and disease transmission in Africa. *Trans R Soc Trop Med Hyg*. 1974 Jan 1;68(4):278–98.
7. Zheng L, Benedict MQ, Cornel AJ, Collins FH, Kafatos FC. An Integrated Genetic Map of the African Human Malaria Vector Mosquito, *Anopheles gambiae*. *Genetics*. 1996 Jun 1;143(2):941–52.
8. Gratz NG. Emerging and Resurging Vector-Borne Diseases. *Annu Rev Entomol*. 1999;44(1):51–75.
9. Rosenberg R, Wirtz RA, Schneider I, Burge R. An estimation of the number of malaria sporozoites ejected by a feeding mosquito. *Trans R Soc Trop Med Hyg*. 1990 Mar 1;84(2):209–12.
10. Ishino T, Yano K, Chinzei Y, Yuda M. Cell-Passage Activity Is Required for the Malarial Parasite to Cross the Liver Sinusoidal Cell Layer. *PLoS Biol*. 2004 Jan 20;2(1):e4.

11. Mota MM, Hafalla JCR, Rodriguez A. Migration through host cells activates Plasmodium sporozoites for infection. *Nat Med*. 2002 Nov;8(11):1318–22.
12. Fujioka H, Aikawa M. Structure and Life Cycle. In: Perlmann P, Troye-Blomberg M, editors. *Chemical Immunology and Allergy* [Internet]. Basel: KARGER; 2002 [cited 2014 Nov 24]. p. 1–26. Available from: <http://www.karger.com/Article/Abstract/58837>
13. Sturm A, Amino R, van de Sand C, Regen T, Retzlaff S, Rennenberg A, et al. Manipulation of host hepatocytes by the malaria parasite for delivery into liver sinusoids. *Science*. 2006 Sep 1;313(5791):1287–90.
14. Beeson JG, Drew DR, Boyle MJ, Feng G, Fowkes FJI, Richards JS. Merozoite surface proteins in red blood cell invasion, immunity and vaccines against malaria. *FEMS Microbiol Rev*. 2016 May 1;40(3):343–72.
15. Cowman AF, Berry D, Baum J. The cellular and molecular basis for malaria parasite invasion of the human red blood cell. *J Cell Biol*. 2012 Sep 17;198(6):961–71.
16. Urban BC, Hien TT, Day NP, Phu NH, Roberts R, Pongponratn E, et al. Fatal Plasmodium falciparum Malaria Causes Specific Patterns of Splenic Architectural Disorganization. *Infect Immun*. 2005 Apr 1;73(4):1986–94.
17. Cowman AF, Crabb BS. Invasion of Red Blood Cells by Malaria Parasites. *Cell*. 2006 Feb 24;124(4):755–66.
18. Kafsack BFC, Rovira-Graells N, Clark TG, Bancells C, Crowley VM, Campino SG, et al. A transcriptional switch underlies commitment to sexual development in malaria parasites. *Nature* [Internet]. 2014 Feb 23 [cited 2014 Mar 5];advance online publication. Available from: <http://www.nature.com.ez.lshtm.ac.uk/nature/journal/vaop/ncurrent/full/nature12920.html>
19. Drakeley C, Sutherland C, Bousema JT, Sauerwein RW, Targett GAT. The epidemiology of Plasmodium falciparum gametocytes: weapons of mass dispersion. *Trends Parasitol*. 2006 Sep;22(9):424–30.
20. Busula AO, Verhulst NO, Bousema T, Takken W, de Boer JG. Mechanisms of Plasmodium-Enhanced Attraction of Mosquito Vectors. *Trends Parasitol*. 2017 Dec 1;33(12):961–73.
21. Cator L. Malaria Altering Host Attractiveness and Mosquito Feeding. *Trends Parasitol*. 2017 May 1;33(5):338–9.
22. Baton LA, Ranford-Cartwright LC. Spreading the seeds of million-murdering death: metamorphoses of malaria in the mosquito. *Trends Parasitol*. 2005 Dec;21(12):573–80.

23. Ghosh A, Edwards MJ, Jacobs-Lorena M. The Journey of the Malaria Parasite in the Mosquito: Hopes for the New Century. *Parasitol Today*. 2000 May 1;16(5):196–201.
24. Doolan DL, Dobano C, Baird JK. Acquired Immunity to Malaria. *Clin Microbiol Rev*. 2009 Jan;22(1):13–36.
25. Malaria | Carter Center Malaria Control Program [Internet]. [cited 2014 Nov 27]. Available from: http://www.cartercenter.org/health/malaria_control/index.html
26. Bhatt S, Weiss DJ, Cameron E, Bisanzio D, Mappin B, Dalrymple U, et al. The effect of malaria control on *Plasmodium falciparum* in Africa between 2000 and 2015. *Nature*. 2015 Oct 8;526(7572):207–11.
27. WHO | World malaria report 2017 [Internet]. WHO. [cited 2018 Jun 30]. Available from: <http://www.who.int/malaria/publications/world-malaria-report-2017/en/>
28. Yeka A, Gasasira A, Mpimbaza A, Achan J, Nankabirwa J, Nsoby S, et al. Malaria in Uganda: challenges to control on the long road to elimination: I. Epidemiology and current control efforts. *Acta Trop*. 2012 Mar;121(3):184–95.
29. Okello PE, Van Bortel W, Byaruhanga AM, Correwyn A, Roelants P, Talisuna A, et al. Variation in malaria transmission intensity in seven sites throughout Uganda. *Am J Trop Med Hyg*. 2006 Aug;75(2):219–25.
30. Kilama M, Smith DL, Hutchinson R, Kigozi R, Yeka A, Lavoy G, et al. Estimating the annual entomological inoculation rate for *Plasmodium falciparum* transmitted by *Anopheles gambiae* s.l. using three sampling methods in three sites in Uganda. *Malar J*. 2014;13:111.
31. Nabarro D. Roll Back Malaria. *Parassitologia*. 1999 Sep;41(1–3):501–4.
32. Pogge T. The First United Nations Millennium Development Goal: A cause for celebration? *J Hum Dev*. 2004 Nov 1;5(3):377–97.
33. Tatem AJ, Gething PW, Smith DL, Hay SI. Urbanization and the global malaria recession. *Malar J*. 2013 Apr 17;12:133.
34. Qi Q, Guerra CA, Moyes CL, Elyazar IAF, Gething PW, Hay SI, et al. The effects of urbanization on global *Plasmodium vivax* malaria transmission. *Malar J*. 2012 Dec 5;11:403.
35. Tusting LS, Ippolito MM, Willey BA, Kleinschmidt I, Dorsey G, Gosling RD, et al. The evidence for improving housing to reduce malaria: a systematic review and meta-analysis. *Malar J*. 2015 Jun 9;14:209.

36. Carter R, Mendis KN. Evolutionary and historical aspects of the burden of malaria. *Clin Microbiol Rev.* 2002 Oct;15(4):564–94.
37. Feachem RG, Phillips AA, Hwang J, Cotter C, Wielgosz B, Greenwood BM, et al. Shrinking the malaria map: progress and prospects. *The Lancet.* 2010 Nov 6;376(9752):1566–78.
38. Tanner M, Savigny D de. Malaria eradication back on the table. *Bull World Health Organ.* 2008 Feb;86:82–82.
39. Sachs JD. From Millennium Development Goals to Sustainable Development Goals. *The Lancet.* 2012 Jun 9;379(9832):2206–11.
40. WHO | Global Technical Strategy for Malaria 2016–2030 [Internet]. [cited 2017 Nov 3]. Available from: <http://www.who.int/malaria/publications/atoz/9789241564991/en/>
41. Myint MK, Rasmussen C, Thi A, Bustos D, Ringwald P, Lin K. Therapeutic efficacy and artemisinin resistance in northern Myanmar: evidence from in vivo and molecular marker studies. *Malar J* [Internet]. 2017 Apr 7 [cited 2018 Sep 25];16. Available from: <https://www.ncbi.nlm.nih.gov/pmc/articles/PMC5383981/>
42. Peatey CL, Leroy D, Gardiner DL, Trenholme KR. Anti-malarial drugs: how effective are they against *Plasmodium falciparum* gametocytes? *Malar J.* 2012 Feb 6;11(1):34.
43. Wadi I, Anvikar AR, Nath M, Pillai CR, Sinha A, Valecha N. Critical examination of approaches exploited to assess the effectiveness of transmission-blocking drugs for malaria. *Future Med Chem.* 2018 Nov 1;10(22):2619–39.
44. Ondeto BM, Nyundo C, Kamau L, Muriu SM, Mwangangi JM, Njagi K, et al. Current status of insecticide resistance among malaria vectors in Kenya. *Parasit Vectors.* 2017 Sep 19;10(1):429.
45. Protopopoff N, Mosha JF, Lukole E, Charlwood JD, Wright A, Mwalimu CD, et al. Effectiveness of a long-lasting piperonyl butoxide-treated insecticidal net and indoor residual spray interventions, separately and together, against malaria transmitted by pyrethroid-resistant mosquitoes: a cluster, randomised controlled, two-by-two factorial design trial. *Lancet Lond Engl.* 2018 Apr 21;391(10130):1577–88.
46. Killeen GF, Ranson H. Insecticide-resistant malaria vectors must be tackled. *The Lancet.* 2018 Apr 21;391(10130):1551–2.
47. Lin Ouédraogo A, Gonçalves BP, Gnémé A, Wenger EA, Guelbeogo MW, Ouédraogo A, et al. Dynamics of the Human Infectious Reservoir for Malaria Determined by Mosquito Feeding Assays and Ultrasensitive Malaria Diagnosis in Burkina Faso. *J Infect Dis.* 2016 Jan 1;213(1):90–9.

48. Stone W, Gonçalves BP, Bousema T, Drakeley C. Assessing the infectious reservoir of falciparum malaria: past and future. *Trends Parasitol.* 2015 Jul;31(7):287–96.
49. Miller LH, Good MF, Milon G. Malaria pathogenesis. *Science.* 1994 Jun 24;264(5167):1878–83.
50. Schofield L, Grau GE. Immunological processes in malaria pathogenesis. *Nat Rev Immunol.* 2005 Sep 1;5(9):722–35.
51. Gatton ML, Cheng Q. Evaluation of the pyrogenic threshold for *Plasmodium falciparum* malaria in naive individuals. *Am J Trop Med Hyg.* 2002 May 1;66(5):467–73.
52. Rogier C, Commenges D, Trape J-F. Evidence for an Age-Dependent Pyrogenic Threshold of *Plasmodium falciparum* Parasitemia in Highly Endemic Populations. *Am J Trop Med Hyg.* 1996 Jun 1;54(6):613–9.
53. Schwartz E, Sadetzki S, Murad H, Raveh D. Age as a Risk Factor for Severe *Plasmodium falciparum* Malaria in Nonimmune Patients. *Clin Infect Dis.* 2001 Nov 15;33(10):1774–7.
54. Snow RW, Omumbo JA, Lowe B, Molyneux CS, Obiero J-O, Palmer A, et al. Relation between severe malaria morbidity in children and level of *Plasmodium falciparum* transmission in Africa. *The Lancet.* 1997 Jun 7;349(9066):1650–4.
55. Menendez C, Ordi J, Ismail MR, Ventura PJ, Aponte JJ, Kahigwa E, et al. The Impact of Placental Malaria on Gestational Age and Birth Weight. *J Infect Dis.* 2000 May 1;181(5):1740–5.
56. Jensen ATR, Magistrado P, Sharp S, Joergensen L, Lavstsen T, Chiucchiuini A, et al. *Plasmodium falciparum* Associated with Severe Childhood Malaria Preferentially Expresses PfEMP1 Encoded by Group A var Genes. *J Exp Med.* 2004 May 3;199(9):1179–90.
57. Cooke BM, Berendt AR, Craig AG, MacGregor J, Newbold CI, Nash GB. Rolling and stationary cytoadhesion of red blood cells parasitized by *Plasmodium falciparum*: separate roles for ICAM-1, CD36 and thrombospondin. *Br J Haematol.* 1994 May 1;87(1):162–70.
58. Newbold C, Craig A, Kyes S, Rowe A, Fernandez-Reyes D, Fagan T. Cytoadherence, pathogenesis and the infected red cell surface in *Plasmodium falciparum*. *Int J Parasitol.* 1999 Jun 1;29(6):927–37.
59. Liu EW, Skinner J, Tran TM, Kumar K, Narum DL, Jain A, et al. Protein-Specific Features Associated with Variability in Human Antibody Responses to *Plasmodium falciparum* Malaria Antigens. *Am J Trop Med Hyg.* 2018 Jan;98(1):57–66.

60. Su X, Heatwole VM, Wertheimer SP, Guinet F, Herrfeldt JA, Peterson DS, et al. The large diverse gene family var encodes proteins involved in cytoadherence and antigenic variation of plasmodium falciparum-infected erythrocytes. *Cell*. 1995 Jul 14;82(1):89–100.
61. Valmaseda A, Macete E, Nhabomba A, Guinovart C, Aide P, Bardají A, et al. Identifying Immune Correlates of Protection Against Plasmodium falciparum Through a Novel Approach to Account for Heterogeneity in Malaria Exposure. *Clin Infect Dis*. 2018 Feb 1;66(4):586–93.
62. Buffet PA, Safeukui I, Deplaine G, Brousse V, Prendki V, Thellier M, et al. The pathogenesis of Plasmodium falciparum malaria in humans: insights from splenic physiology. *Blood*. 2010 Jan 1;blood-2010-04-202911.
63. Dondorp AM, Kager PA, Vreeken J, White NJ. Abnormal Blood Flow and Red Blood Cell Deformability in Severe Malaria. *Parasitol Today*. 2000 Jun 1;16(6):228–32.
64. Kraemer SM, Smith JD. A family affair: var genes, PfEMP1 binding, and malaria disease. *Curr Opin Microbiol*. 2006 Aug;9(4):374–80.
65. Tutterrow YL, Salanti A, Avril M, Smith JD, Pagano IS, Ako S, et al. High Avidity Antibodies to Full-Length VAR2CSA Correlate with Absence of Placental Malaria. *PLoS ONE*. 2012 Jun 26;7(6):e40049.
66. Tutterrow YL, Salanti A, Avril M, Smith JD, Pagano IS, Ako S, et al. High Avidity Antibodies to Full-Length VAR2CSA Correlate with Absence of Placental Malaria. *PLoS ONE* [Internet]. 2012 Jun 26 [cited 2018 May 17];7(6). Available from: <https://www.ncbi.nlm.nih.gov/pmc/articles/PMC3383675/>
67. Steketee RW, Wirima JJ, Hightower AW, Slutsker L, Heymann DL, Breman JG. The effect of malaria and malaria prevention in pregnancy on offspring birthweight, prematurity, and intrauterine growth retardation in rural Malawi. *Am J Trop Med Hyg*. 1996 Jul 1;55(1_Suppl):33–41.
68. Wickramasinghe SN, Abdalla SH. Blood and bone marrow changes in malaria. *Best Pract Res Clin Haematol*. 2000 Jun 1;13(2):277–99.
69. Abdalla SH, Wickramasinghe SN. A study of erythroid progenitor cells in the bone marrow of Gambian children with falciparum malaria. *Clin Lab Haematol*. 1988;10(1):33–40.
70. Goheen MM, Wegmüller R, Bah A, Darboe B, Danso E, Affara M, et al. Anemia Offers Stronger Protection Than Sick Cell Trait Against the Erythrocytic Stage of Falciparum Malaria and This Protection Is Reversed by Iron Supplementation. *EBioMedicine*. 2016 Dec 1;14:123–30.

71. Payne D. Use and limitations of light microscopy for diagnosing malaria at the primary health care level. *Bull World Health Organ.* 1988;66(5):621–6.
72. Koita OA, Doumbo OK, Ouattara A, Tall LK, Konaré A, Diakité M, et al. False-Negative Rapid Diagnostic Tests for Malaria and Deletion of the Histidine-Rich Repeat Region of the hrp2 Gene†. *Am J Trop Med Hyg.* 2012 Feb 1;86(2):194–8.
73. Kumar N, Pande V, Bhatt RM, Shah NK, Mishra N, Srivastava B, et al. Genetic deletion of HRP2 and HRP3 in Indian *Plasmodium falciparum* population and false negative malaria rapid diagnostic test. *Acta Trop.* 2013 Jan 1;125(1):119–21.
74. Menegon M, L'Episcopia M, Nurahmed AM, Talha AA, Nour BYM, Severini C. Identification of *Plasmodium falciparum* isolates lacking histidine-rich protein 2 and 3 in Eritrea. *Infect Genet Evol.* 2017 Nov 1;55:131–4.
75. Beshir KB, Sepúlveda N, Bharmal J, Robinson A, Mwanguzi J, Busula AO, et al. *Plasmodium falciparum* parasites with histidine-rich protein 2 (pfhrp2) and pfhrp3 gene deletions in two endemic regions of Kenya. *Sci Rep.* 2017 Nov 7;7(1):14718.
76. Kozycki CT, Umulisa N, Rulisa S, Mwikarago EI, Musabyimana JP, Habimana JP, et al. False-negative malaria rapid diagnostic tests in Rwanda: impact of *Plasmodium falciparum* isolates lacking hrp2 and declining malaria transmission. *Malar J.* 2017 Mar 20;16(1):123.
77. Gatton ML, Dunn J, Chaudhry A, Ciketic S, Cunningham J, Cheng Q. Use of PfHRP2-only RDTs rapidly select for PfHRP2-negative parasites with serious implications for malaria case management and control. *J Infect Dis.* 2017 Apr 12;215:1156–66.
78. Dalrymple U, Arambepola R, Gething PW, Cameron E. How long do rapid diagnostic tests remain positive after anti-malarial treatment? *Malar J.* 2018 Jun 8;17(1):228.
79. Sirichaisinthop J, Buates S, Watanabe R, Han E-T, Suktawonjaroenpon W, Krassaesub S, et al. Evaluation of Loop-Mediated Isothermal Amplification (LAMP) for Malaria Diagnosis in a Field Setting. *Am J Trop Med Hyg.* 2011 Oct 1;85(4):594–6.
80. Sattabongkot J, Tsuboi T, Han E-T, Bantuchai S, Buates S. Loop-Mediated Isothermal Amplification Assay for Rapid Diagnosis of Malaria Infections in an Area of Endemicity in Thailand. *J Clin Microbiol.* 2014 May 1;52(5):1471–7.
81. Gupta S, Snow RW, Donnelly CA, Marsh K, Newbold C. Immunity to non-cerebral severe malaria is acquired after one or two infections. *Nat Med.* 1999 Mar;5(3):340–3.
82. Chan J-A, Boyle MJ, Moore KA, Reiling L, Lin Z, Hasang W, et al. Antibody Targets on the Surface of *Plasmodium falciparum*-Infected Erythrocytes That Are Associated With Immunity to Severe

- Malaria in Young Children. J Infect Dis [Internet]. [cited 2018 Nov 8]; Available from: <https://academic.oup.com/jid/advance-article/doi/10.1093/infdis/jiy580/5145051>
83. MacPherson GG, Warrell MJ, White NJ, Looareesuwan S, Warrell DA. Human cerebral malaria. A quantitative ultrastructural analysis of parasitized erythrocyte sequestration. Am J Pathol. 1985 Jun;119(3):385–401.
 84. Miller LH, Baruch DI, Marsh K, Doumbo OK. The pathogenic basis of malaria [Internet]. Nature. 2002 [cited 2018 Aug 23]. Available from: <http://www.nature.com/articles/415673a>
 85. Sullivan DJ. A Single Human Cerebral Malaria Histopathologic Study Can Be Worth a Thousand Experiments. mBio. 2015 Dec 31;6(6):e01818-15.
 86. Marquet S. Overview of human genetic susceptibility to malaria: From parasitemia control to severe disease. Infect Genet Evol. 2018 Dec 1;66:399–409.
 87. Kwiatkowski D. Genetic susceptibility to malaria getting complex. Curr Opin Genet Dev. 2000 Jun 1;10(3):320–4.
 88. McGuire W, Hill AVS, Allsopp CEM, Greenwood BM, Kwiatkowski D. Variation in the TNF- α promoter region associated with susceptibility to cerebral malaria. Nature. 1994 Oct;371(6497):508–11.
 89. Hill AVS, Allsopp CEM, Kwiatkowski D, Anstey NM, Twumasi P, Rowe PA, et al. Common West African HLA antigens are associated with protection from severe malaria. Nature. 1991 Aug;352(6336):595–600.
 90. Mockenhaupt FP, Cramer JP, Hamann L, Stegemann MS, Eckert J, Oh N-R, et al. Toll-like receptor (TLR) polymorphisms in African children: Common TLR-4 variants predispose to severe malaria. Proc Natl Acad Sci. 2006 Jan 3;103(1):177–82.
 91. Ravenhall M, Campino S, Sepúlveda N, Manjurano A, Nadjm B, Mtove G, et al. Novel genetic polymorphisms associated with severe malaria and under selective pressure in North-eastern Tanzania. PLOS Genet. 2018 Jan 30;14(1):e1007172.
 92. Rodriguez-Barraquer I, Arinaitwe E, Jagannathan P, Kamya MR, Rosenthal PJ, Rek J, et al. Quantification of anti-parasite and anti-disease immunity to malaria as a function of age and exposure [Internet]. eLife. 2018 [cited 2018 Jul 26]. Available from: <https://elifesciences.org/articles/35832>
 93. Lyke KE, Burges R, Cissoko Y, Sangare L, Dao M, Diarra I, et al. Serum Levels of the Proinflammatory Cytokines Interleukin-1 Beta (IL-1 β), IL-6, IL-8, IL-10, Tumor Necrosis Factor

- Alpha, and IL-12(p70) in Malian Children with Severe *Plasmodium falciparum* Malaria and Matched Uncomplicated Malaria or Healthy Controls. *Infect Immun*. 2004 Oct 1;72(10):5630–7.
94. Doodoo D, Omer FM, Todd J, Akanmori BD, Koram KA, Riley EM. Absolute Levels and Ratios of Proinflammatory and Anti-inflammatory Cytokine Production In Vitro Predict Clinical Immunity to *Plasmodium falciparum* Malaria. *J Infect Dis*. 2002 Apr 1;185(7):971–9.
 95. Portugal S, Moebius J, Skinner J, Doumbo S, Doumtabe D, Kone Y, et al. Exposure-Dependent Control of Malaria-Induced Inflammation in Children. *PLOS Pathog*. 2014 Apr 17;10(4):e1004079.
 96. Ademolue TW, Aniweh Y, Kusi KA, Awandare GA. Patterns of inflammatory responses and parasite tolerance vary with malaria transmission intensity. *Malar J*. 2017 Apr 11;16(1):145.
 97. Hirunpetcharat C, Finkelman F, Clark IA, Good MF. Malaria parasite-specific Th1-like T cells simultaneously reduce parasitemia and promote disease. *Parasite Immunol*. 1999 Jun 1;21(6):319–29.
 98. Kwiatkowski D. Cytokines and anti-disease immunity to malaria. *Res Immunol*. 1991 Jan 1;142(8):707–12.
 99. Jagannathan P, Kim CC, Greenhouse B, Nankya F, Bowen K, Eccles-James I, et al. Loss and dysfunction of V δ 2+ $\gamma\delta$ T cells are associated with clinical tolerance to malaria. *Sci Transl Med*. 2014 Aug 27;6(251):251ra117-251ra117.
 100. Koepfli C, Ome-Kaius M, Jally S, Malau E, Maripal S, Ginny J, et al. Sustained Malaria Control Over an 8-Year Period in Papua New Guinea: The Challenge of Low-Density Asymptomatic *Plasmodium* Infections. *J Infect Dis*. 2017 Dec 12;216(11):1434–43.
 101. Miller MJ. Observations on the natural history of malaria in the semi-resistant West African. *Trans R Soc Trop Med Hyg*. 1958 Mar 1;52(2):152–68.
 102. Rek J, Katrak S, Obasi H, Nayebare P, Katureebe A, Kakande E, et al. Characterizing microscopic and submicroscopic malaria parasitaemia at three sites with varied transmission intensity in Uganda. *Malar J*. 2016 Sep 15;15(1):470.
 103. Iwasaki A, Medzhitov R. Control of adaptive immunity by the innate immune system. *Nat Immunol*. 2015 Apr;16(4):343–53.
 104. Stevenson MM, Riley EM. Innate immunity to malaria. *Nat Rev Immunol*. 2004 Mar;4(3):169–80.

105. Cook J, Grignard L, Al-Eryani S, Al-Selwei M, Mnzava A, Al-Yarie H, et al. High heterogeneity of malaria transmission and a large sub-patent and diverse reservoir of infection in Wusab As Safil district, Republic of Yemen. *Malar J*. 2016 Apr 8;15(1):193.
106. Buchwald AG, Sorkin JD, Sixpence A, Chimenya M, Damson M, Wilson ML, et al. Association Between Age and Plasmodium falciparum Infection Dynamics. *Am J Epidemiol* [Internet]. [cited 2018 Nov 6]; Available from: <https://academic.oup.com/aje/advance-article/doi/10.1093/aje/kwy213/5106630>
107. Djimdé AA, Doumbo OK, Traore O, Guindo AB, Kayentao K, Diourte Y, et al. CLEARANCE OF DRUG-RESISTANT PARASITES AS A MODEL FOR PROTECTIVE IMMUNITY IN PLASMODIUM FALCIPARUM MALARIA. *Am J Trop Med Hyg*. 2003 Nov 1;69(5):558–63.
108. Walther M, Tongren JE, Andrews L, Korbel D, King E, Fletcher H, et al. Upregulation of TGF- β , FOXP3, and CD4+CD25+ Regulatory T Cells Correlates with More Rapid Parasite Growth in Human Malaria Infection. *Immunity*. 2005 Sep 1;23(3):287–96.
109. Boutlis CS, Gowda DC, Naik RS, Maguire GP, Mgone CS, Bockarie MJ, et al. Antibodies to Plasmodium falciparum Glycosylphosphatidylinositols: Inverse Association with Tolerance of Parasitemia in Papua New Guinean Children and Adults. *Infect Immun*. 2002 Sep 1;70(9):5052–7.
110. Kumar KA, Sano G, Boscardin S, Nussenzweig RS, Nussenzweig MC, Zavala F, et al. The circumsporozoite protein is an immunodominant protective antigen in irradiated sporozoites. *Nature*. 2006 Dec 14;444(7121):937–40.
111. Hoffman SL, Goh LML, Luke TC, Schneider I, Le TP, Doolan DL, et al. Protection of humans against malaria by immunization with radiation-attenuated Plasmodium falciparum sporozoites. *J Infect Dis*. 2002 Apr 15;185(8):1155–64.
112. Mordmüller B, Surat G, Lagler H, Chakravarty S, Ishizuka AS, Lalremruata A, et al. Sterile protection against human malaria by chemoattenuated PfSPZ vaccine. *Nature*. 2017 Feb;542(7642):445–9.
113. Zaidi I, Diallo H, Conteh S, Robbins Y, Kolasny J, Orr-Gonzalez S, et al. $\gamma\delta$ T Cells Are Required for the Induction of Sterile Immunity during Irradiated Sporozoite Vaccinations. *J Immunol*. 2017 Oct 27;ji1700314.
114. Zhou J, Kaiser A, Ng C, Karcher R, McConnell T, Paczkowski P, et al. CD8+ T-cell mediated anti-malaria protection induced by malaria vaccines; assessment of hepatic CD8+ T cells by SCBC assay. *Hum Vaccines Immunother*. 2017 Jul 3;13(7):1625–9.

115. Lyke KE, Ishizuka AS, Berry AA, Chakravarty S, DeZure A, Enama ME, et al. Attenuated PfSPZ Vaccine induces strain-transcending T cells and durable protection against heterologous controlled human malaria infection. *Proc Natl Acad Sci*. 2017 Feb 15;201615324.
116. Epstein JE, Paolino KM, Richie TL, Sedegah M, Singer A, Ruben AJ, et al. Protection against *Plasmodium falciparum* malaria by PfSPZ Vaccine. *JCI Insight* [Internet]. [cited 2018 Aug 23];2(1). Available from: <https://www.ncbi.nlm.nih.gov/pmc/articles/PMC5214067/>
117. McGregor IA, Carrington SP, Cohen S. Treatment of east african *P. falciparum* malaria with west african human γ -globulin. *Trans R Soc Trop Med Hyg*. 1963 May;57(3):170–5.
118. McGregor IA. The Passive Transfer of Human Malarial Immunity. *Am J Trop Med Hyg*. 1964 Jan 1;13(1 Part 2):237–9.
119. Kitua AY, Smith TA, Alonso PL, Urassa H, Masanja H, Kimario J, et al. The role of low level *Plasmodium falciparum* parasitaemia in anaemia among infants living in an area of intense and perennial transmission. *Trop Med Int Health*. 1997 Apr 1;2(4):325–33.
120. Riley EM, Wagner GE, Akanmori BD, Koram KA. Do maternally acquired antibodies protect infants from malaria infection? *Parasite Immunol*. 2001 Feb 1;23(2):51–9.
121. Murungi LM, Sondén K, Odera D, Oduor LB, Guleid F, Nkumama IN, et al. Cord blood IgG and the risk of severe *Plasmodium falciparum* malaria in the first year of life. *Int J Parasitol*. 2017 Feb;47(2–3):153–62.
122. Chan J-A, Stanisic DI, Duffy MF, Robinson LJ, Lin E, Kazura JW, et al. Patterns of protective associations differ for antibodies to *P.falciparum*-infected erythrocytes and merozoites in immunity against malaria in children. *Eur J Immunol*. :n/a-n/a.
123. Chiu CYH, Healer J, Thompson JK, Chen L, Kaul A, Savergave L, et al. Association of antibodies to *Plasmodium falciparum* reticulocyte binding protein homolog 5 with protection from clinical malaria. *Front Microbiol* [Internet]. 2014 Jun 30 [cited 2014 Nov 11];5. Available from: <http://www.ncbi.nlm.nih.gov/pmc/articles/PMC4074990/>
124. Chiu CYH, Hodder AN, Lin CS, Hill DL, Li Wai Suen CSN, Schofield L, et al. Antibodies to the *Plasmodium falciparum* Proteins MSPDBL1 and MSPDBL2 Opsonize Merozoites, Inhibit Parasite Growth, and Predict Protection From Clinical Malaria. *J Infect Dis*. 2015 Aug 1;212(3):406–15.
125. Medeiros MM, Fotoran WL, dalla Martha RC, Katsuragawa TH, Pereira da Silva LH, Wunderlich G. Natural antibody response to *Plasmodium falciparum* merozoite antigens MSP5, MSP9 and EBA175 is associated to clinical protection in the Brazilian Amazon. *BMC Infect Dis*. 2013 Dec 28;13:608.

126. Osier FHA, Fegan G, Polley SD, Murungi L, Verra F, Tetteh KKA, et al. Breadth and Magnitude of Antibody Responses to Multiple Plasmodium falciparum Merozoite Antigens Are Associated with Protection from Clinical Malaria. *Infect Immun*. 2008 May 1;76(5):2240–8.
127. Dodoo D, Aikins A, Kusi KA, Lamptey H, Remarque E, Milligan P, et al. Cohort study of the association of antibody levels to AMA1, MSP119, MSP3 and GLURP with protection from clinical malaria in Ghanaian children. *Malar J*. 2008 Jul 29;7(1):142.
128. Oeuvray C, Theisen M, Rogier C, Trape JF, Jepsen S, Druilhe P. Cytophilic immunoglobulin responses to Plasmodium falciparum glutamate-rich protein are correlated with protection against clinical malaria in Dielmo, Senegal. *Infect Immun*. 2000 May;68(5):2617–20.
129. Pratt-Riccio LR, Bianco C Jr, Totino PRR, Perce-Da-Silva DDS, Silva LA, Riccio EKP, et al. Antibodies against the Plasmodium falciparum glutamate-rich protein from naturally exposed individuals living in a Brazilian malaria-endemic area can inhibit in vitro parasite growth. *Mem Inst Oswaldo Cruz*. 2011 Aug;106 Suppl 1:34–43.
130. Oeuvray C, Bouharoun-Tayoun H, Gras-Masse H, Bottius E, Kaidoh T, Aikawa M, et al. Merozoite surface protein-3: a malaria protein inducing antibodies that promote Plasmodium falciparum killing by cooperation with blood monocytes. *Blood*. 1994 Sep 1;84(5):1594–602.
131. Arora G, Hart GT, Manzella-Lapeira J, Doritchamou JY, Narum DL, Thomas LM, et al. NK cells inhibit Plasmodium falciparum growth in red blood cells via antibody-dependent cellular cytotoxicity. *eLife*. 2018 Jun 26;7.
132. Boyle MJ, Reiling L, Feng G, Langer C, Osier FH, Aspelung-Jones H, et al. Human antibodies fix complement to inhibit Plasmodium falciparum invasion of erythrocytes and are associated with protection against malaria. *Immunity*. 2015 Mar 17;42(3):580–90.
133. Stubbs J, Olugbile S, Saidou B, Simpore J, Corradin G, Lanzavecchia A. Strain-transcending Fc-dependent killing of Plasmodium falciparum by merozoite surface protein 2 allele-specific human antibodies. *Infect Immun*. 2011 Mar;79(3):1143–52.
134. Behet MC, Kurtovic L, van Gemert G-J, Haukes CM, Siebelink-Stoter R, Graumans W, et al. The complement system contributes to functional antibody-mediated responses induced by immunization with Plasmodium falciparum malaria sporozoites. *Infect Immun*. 2018 May 7;
135. Nussenzweig RS, Vanderberg JP, Most H, Orton C. Specificity of Protective Immunity produced by X-irradiated Plasmodium berghei Sporozoites. *Publ Online* 03 May 1969
Doi101038222488a0. 1969 May 3;222(5192):488–9.

136. Henderson DA. Principles and lessons from the smallpox eradication programme. *Bull World Health Organ.* 1987;65(4):535–46.
137. Minor PD. The polio-eradication programme and issues of the end game. *J Gen Virol.* 2012;93(3):457–74.
138. Cohen S, McGREGOR IA, Carrington S. Gamma-globulin and acquired immunity to human malaria. *Nature.* 1961 Nov 25;192:733–7.
139. Alonso PL, Sacarlal J, Aponte JJ, Leach A, Macete E, Aide P, et al. Duration of protection with RTS,S/AS02A malaria vaccine in prevention of *Plasmodium falciparum* disease in Mozambican children: single-blind extended follow-up of a randomised controlled trial. *The Lancet.* 2005 Dec 16;366(9502):2012–8.
140. Moorthy VS, Ballou WR. Immunological mechanisms underlying protection mediated by RTS,S: a review of the available data. *Malar J.* 2009 Dec 30;8(1):312.
141. Chaudhury S, Regules JA, Darko CA, Dutta S, Wallqvist A, Waters NC, et al. Delayed fractional dose regimen of the RTS,S/AS01 malaria vaccine candidate enhances an IgG4 response that inhibits serum opsonophagocytosis. *Sci Rep [Internet].* 2017 Aug 11 [cited 2018 Apr 2];7. Available from: <https://www.ncbi.nlm.nih.gov/pmc/articles/PMC5554171/>
142. Kazmin D, Nakaya HI, Lee EK, Johnson MJ, van der Most R, van den Berg RA, et al. Systems analysis of protective immune responses to RTS,S malaria vaccination in humans. *Proc Natl Acad Sci U S A.* 2017 Feb 28;114(9):2425–30.
143. Draper SJ, Sack BK, King CR, Nielsen CM, Rayner JC, Higgins MK, et al. Malaria Vaccines: Recent Advances and New Horizons. *Cell Host Microbe.* 2018 Jul;24(1):43–56.
144. Kastenmüller K, Espinosa DA, Trager L, Stoyanov C, Salazar AM, Pokalwar S, et al. Full-Length *Plasmodium falciparum* Circumsporozoite Protein Administered with Long-Chain Poly(I-C) or the Toll-Like Receptor 4 Agonist Glucopyranosyl Lipid Adjuvant-Stable Emulsion Elicits Potent Antibody and CD4+ T Cell Immunity and Protection in Mice. *Infect Immun.* 2013 Mar 1;81(3):789–800.
145. Wardemann H, Murugan R. From human antibody structure and function towards the design of a novel *Plasmodium falciparum* circumsporozoite protein malaria vaccine. *Curr Opin Immunol.* 2018 Aug 1;53:119–23.
146. Kublin JG, Mikolajczak SA, Sack BK, Fishbaugher ME, Seilie A, Shelton L, et al. Complete attenuation of genetically engineered *Plasmodium falciparum* sporozoites in human subjects. *Sci Transl Med.* 2017 Jan 4;9(371):eaad9099.

147. Mikolajczak SA, Lakshmanan V, Fishbaugher M, Camargo N, Harupa A, Kaushansky A, et al. A Next-generation Genetically Attenuated *Plasmodium falciparum* Parasite Created by Triple Gene Deletion. *Mol Ther*. 2014 Sep 1;22(9):1707–15.
148. Jobe O, Lumsden J, Mueller A-K, Williams J, Silva-Rivera H, Kappe SHI, et al. Genetically Attenuated *Plasmodium berghei* Liver Stages Induce Sterile Protracted Protection That Is Mediated by Major Histocompatibility Complex Class I-Dependent Interferon- γ -Producing CD8+ T Cells. *J Infect Dis*. 2007 Aug 15;196(4):599–607.
149. Walk J, Reuling IJ, Behet MC, Meerstein-Kessel L, Graumans W, van Gemert G-J, et al. Modest heterologous protection after *Plasmodium falciparum* sporozoite immunization: a double-blind randomized controlled clinical trial. *BMC Med*. 2017 Sep 13;15(1):168.
150. Roestenberg M, McCall M, Hopman J, Wiersma J, Luty AJF, van Gemert GJ, et al. Protection against a Malaria Challenge by Sporozoite Inoculation. *N Engl J Med*. 2009 Jul 30;361(5):468–77.
151. Boyle MJ, Reiling L, Osier FH, Fowkes FJI. Recent insights into humoral immunity targeting *Plasmodium falciparum* and *Plasmodium vivax* malaria. *Int J Parasitol*. 2016 Jul 20;
152. Osier FH, Feng G, Boyle MJ, Langer C, Zhou J, Richards JS, et al. Opsonic phagocytosis of *Plasmodium falciparum* merozoites: mechanism in human immunity and a correlate of protection against malaria. *BMC Med*. 2014 Jul 1;12:108.
153. Collins CR, Withers-Martinez C, Bentley GA, Batchelor AH, Thomas AW, Blackman MJ. Fine mapping of an epitope recognized by an invasion-inhibitory monoclonal antibody on the malaria vaccine candidate apical membrane antigen 1. *J Biol Chem*. 2007 Mar 9;282(10):7431–41.
154. Alaganan A, Singh P, Chitnis CE. Molecular mechanisms that mediate invasion and egress of malaria parasites from red blood cells. *Curr Opin Hematol*. 2017 May;24(3):208–14.
155. Wright GJ, Rayner JC. *Plasmodium falciparum* Erythrocyte Invasion: Combining Function with Immune Evasion. *PLoS Pathog* [Internet]. 2014 Mar 20 [cited 2014 Nov 27];10(3). Available from: <http://www.ncbi.nlm.nih.gov/pmc/articles/PMC3961354/>
156. Gaur D, Chitnis CE. Molecular interactions and signaling mechanisms during erythrocyte invasion by malaria parasites. *Curr Opin Microbiol*. 2011 Aug 1;14(4):422–8.
157. Kamuyu G, Tuju J, Kimathi R, Mwai K, Mburu J, Kibinge N, et al. KILchip v1.0: A Novel *Plasmodium falciparum* Merozoite Protein Microarray to Facilitate Malaria Vaccine Candidate

- Prioritization. *Front Immunol* [Internet]. 2018 [cited 2018 Dec 13];9. Available from: <https://www.frontiersin.org/articles/10.3389/fimmu.2018.02866/full>
158. Morita M, Takashima E, Ito D, Miura K, Thongkukiatkul A, Diouf A, et al. Immunoscreening of *Plasmodium falciparum* proteins expressed in a wheat germ cell-free system reveals a novel malaria vaccine candidate. *Sci Rep*. 2017 Apr 5;7:46086.
 159. Crosnier C, Bustamante LY, Bartholdson SJ, Bei AK, Theron M, Uchikawa M, et al. BASIGIN is a receptor essential for erythrocyte invasion by *Plasmodium falciparum*. *Nature*. 2011 Nov 9;480(7378):534–7.
 160. Gbédandé K, Fievet N, Viwami F, Ezinmegnon S, Issifou S, Chippaux J-P, et al. Clinical development of a VAR2CSA-based placental malaria vaccine PAMVAC: Quantifying vaccine antigen-specific memory B & T cell activity in Beninese primigravidae. *Vaccine*. 2017 Jun 14;35(27):3474–81.
 161. Stanisic DI, Fink J, Mayer J, Coghill S, Gore L, Liu XQ, et al. Vaccination with chemically attenuated *Plasmodium falciparum* asexual blood-stage parasites induces parasite-specific cellular immune responses in malaria-naïve volunteers: a pilot study. *BMC Med*. 2018 Oct 8;16(1):184.
 162. Stanisic DI, Good MF. Whole organism blood stage vaccines against malaria. *Vaccine*. 2015 Dec 22;33(52):7469–75.
 163. Patra KP, Li F, Carter D, Gregory JA, Baga S, Reed SG, et al. Alga-produced malaria transmission-blocking vaccine candidate Pfs25 formulated with a human use-compatible potent adjuvant induces high-affinity antibodies that block *Plasmodium falciparum* infection of mosquitoes. *Infect Immun*. 2015 May;83(5):1799–808.
 164. Carter R. Transmission blocking malaria vaccines. *Vaccine*. 2001 Mar 21;19(17):2309–14.
 165. Vidarsson G, Dekkers G, Rispens T. IgG Subclasses and Allotypes: From Structure to Effector Functions. *Front Immunol* [Internet]. 2014 Oct 20 [cited 2017 Aug 10];5. Available from: <http://www.ncbi.nlm.nih.gov/pmc/articles/PMC4202688/>
 166. Schur PH. IgG subclasses. A historical perspective. *Monogr Allergy*. 1988;23:1–11.
 167. Nimmerjahn F, Ravetch JV. Divergent Immunoglobulin G Subclass Activity Through Selective Fc Receptor Binding. *Science*. 2005 Dec 2;310(5753):1510–2.
 168. Alter G, Ottenhoff THM, Joosten SA. Antibody glycosylation in inflammation, disease and vaccination. *Semin Immunol*. 2018 Oct 1;39:102–10.

169. Bruhns P, Iannascoli B, England P, Mancardi DA, Fernandez N, Jorieux S, et al. Specificity and affinity of human Fc γ receptors and their polymorphic variants for human IgG subclasses. *Blood*. 2009 Apr 16;113(16):3716–25.
170. FcRn: the neonatal Fc receptor comes of age | *Nature Reviews Immunology* [Internet]. [cited 2018 Jul 2]. Available from: <https://www-nature-com.ez.ishtm.ac.uk/articles/nri2155>
171. Dechavanne C, Dechavanne S, Sadissou I, Lokossou AG, Alvarado F, Dambrun M, et al. Associations between an IgG3 polymorphism in the binding domain for FcRn, transplacental transfer of malaria-specific IgG3, and protection against *Plasmodium falciparum* malaria during infancy: A birth cohort study in Benin. *PLoS Med* [Internet]. 2017 Oct 9 [cited 2018 Apr 20];14(10). Available from: <https://www.ncbi.nlm.nih.gov/pmc/articles/PMC5633139/>
172. Brambell FWR, Hemmings WA, Morris IG. A Theoretical Model of γ -Globulin Catabolism. *Nature*. 1964 Sep;203(4952):1352–5.
173. Brambell FWR. THE TRANSMISSION OF IMMUNITY FROM MOTHER TO YOUNG AND THE CATABOLISM OF IMMUNOGLOBULINS. *The Lancet*. 1966 Nov 19;288(7473):1087–93.
174. Duncan AR, Winter G. The binding site for C1q on IgG. *Nature*. 1988 Apr;332(6166):738–40.
175. Kishore U, Reid KB. C1q: structure, function, and receptors. *Immunopharmacology*. 2000 Aug;49(1–2):159–70.
176. Goldblatt D, Vaz AR, Miller E. Antibody avidity as a surrogate marker of successful priming by *Haemophilus influenzae* type b conjugate vaccines following infant immunization. *J Infect Dis*. 1998 Apr;177(4):1112–5.
177. Böttiger B, Jensen IP. Maturation of rubella IgG avidity over time after acute rubella infection. *Clin Diagn Virol*. 1997 Aug 1;8(2):105–11.
178. Anttila M, Eskola J, Åhman H, Käyhty H. Differences in the avidity of antibodies evoked by four different pneumococcal conjugate vaccines in early childhood1In the study the European guidelines for Good Clinical Practice (based on directive no. 91/507/EEC) were followed. The protocol of the study was approved by the Ethics Committee of the National Public Health Institute, Helsinki, Finland. Written informed consent was obtained from the parents prior to enrolment of their children.1. *Vaccine*. 1999 Apr 9;17(15):1970–7.
179. Dimitrov JD, Lacroix-Desmazes S, Kaveri SV. Important parameters for evaluation of antibody avidity by immunosorbent assay. *Anal Biochem*. 2011 Nov;418(1):149–51.

180. Narita M, Matsuzono Y, Takekoshi Y, Yamada S, Itakura O, Kubota M, et al. Analysis of Mumps Vaccine Failure by Means of Avidity Testing for Mumps Virus-Specific Immunoglobulin G. *Clin Diagn Lab Immunol*. 1998 Nov;5(6):799–803.
181. Park DW, Nam M-H, Kim JY, Kim HJ, Sohn JW, Cho Y, et al. Mumps outbreak in a highly vaccinated school population: assessment of secondary vaccine failure using IgG avidity measurements. *Vaccine*. 2007 Jun 11;25(24):4665–70.
182. Sanz-Moreno JC, Limia-Sánchez A, García-Comas L, Mosquera-Gutiérrez MM, Echevarria-Mayo JE, Castellanos-Nadal A, et al. Detection of secondary mumps vaccine failure by means of avidity testing for specific immunoglobulin G. *Vaccine*. 2005 Sep 30;23(41):4921–5.
183. Hedman K, Rousseau SA. Measurement of avidity of specific IgG for verification of recent primary rubella. *J Med Virol*. 1989 Apr;27(4):288–92.
184. Reis MM, Tessaro MM, Cruz e Silva J, Giordano SA, d’Azevedo PA. Avidity of IgG for rubella: an evaluation of the need for implementation at the Materno-Infantil Presidente Vargas Hospital in Porto Alegre, Rio Grande do Sul, Brazil. *Braz J Infect Dis*. 2004 Jun;8(3):249–54.
185. Alam MM, Arifuzzaman M, Ahmad SM, Hosen MI, Rahman MA, Rashu R, et al. Study of Avidity of Antigen-Specific Antibody as a Means of Understanding Development of Long-Term Immunological Memory after *Vibrio cholerae* O1 Infection. *Clin Vaccine Immunol*. 2013 Jan 1;20(1):17–23.
186. Lee YC, Kelly DF, Yu L-M, Slack MPE, Booy R, Heath PT, et al. Haemophilus influenzae Type b Vaccine Failure in Children Is Associated with Inadequate Production of High-Quality Antibody. *Clin Infect Dis*. 2008 Jan 15;46(2):186–92.
187. Prince HE, Lapé-Nixon M. Role of Cytomegalovirus (CMV) IgG Avidity Testing in Diagnosing Primary CMV Infection during Pregnancy. *Clin Vaccine Immunol*. 2014 Oct;21(10):1377–84.
188. Ward KN, Gray JJ, Joslin ME, Sheldon MJ. Avidity of IgG antibodies to human herpesvirus-6 distinguishes primary from recurrent infection in organ transplant recipients and excludes cross-reactivity with other herpesviruses. *J Med Virol*. 1993 Jan;39(1):44–9.
189. Fox JL, Hazell SL, Tobler LH, Busch MP. Immunoglobulin G Avidity in Differentiation between Early and Late Antibody Responses to West Nile Virus. *Clin Vaccine Immunol*. 2006 Jan;13(1):33–6.
190. Duong YT, Qiu M, De AK, Jackson K, Dobbs T, Kim AA, et al. Detection of Recent HIV-1 Infection Using a New Limiting-Antigen Avidity Assay: Potential for HIV-1 Incidence Estimates and Avidity Maturation Studies. *PLOS ONE*. 2012 Mar 27;7(3):e33328.

191. Malmqvist M. Surface plasmon resonance for detection and measurement of antibody-antigen affinity and kinetics. *Curr Opin Immunol*. 1993;5(2):282–6.
192. Lad L, Clancy S, Kovalenko M, Liu C, Hui T, Smith V, et al. High-Throughput Kinetic Screening of Hybridomas to Identify High-Affinity Antibodies Using Bio-Layer Interferometry. *J Biomol Screen*. 2015 Apr 1;20(4):498–507.
193. Reddy SB, Anders RF, Cross N, Mueller I, Senn N, Stanisic DI, et al. Differences in affinity of monoclonal and naturally acquired polyclonal antibodies against *Plasmodium falciparum* merozoite antigens. *BMC Microbiol* [Internet]. 2015 Jul 3 [cited 2015 Sep 30];15. Available from: <http://www.ncbi.nlm.nih.gov/pmc/articles/PMC4491891/>
194. Fagarasan S, Honjo T. T-Independent Immune Response: New Aspects of B Cell Biology. *Science*. 2000 Oct 6;290(5489):89–92.
195. Obukhanych TV, Nussenzweig MC. T-independent type II immune responses generate memory B cells. *J Exp Med*. 2006 Feb 20;203(2):305–10.
196. Grewal IS, Flavell RA. The role of CD40 ligand in costimulation and T-cell activation. *Immunol Rev*. 1996 Oct;153:85–106.
197. Foy TM, Shepherd DM, Durie FH, Aruffo A, Ledbetter JA, Noelle RJ. In vivo CD40-gp39 interactions are essential for thymus-dependent humoral immunity. II. Prolonged suppression of the humoral immune response by an antibody to the ligand for CD40, gp39. *J Exp Med*. 1993 Nov 1;178(5):1567–75.
198. DeFranco AL. The germinal center antibody response in health and disease. *F1000Research* [Internet]. 2016 May 25 [cited 2018 Jul 9];5. Available from: <https://www.ncbi.nlm.nih.gov/pmc/articles/PMC4882753/>
199. Weisel FJ, Zuccarino-Catania GV, Chikina M, Shlomchik MJ. A Temporal Switch in the Germinal Center Determines Differential Output of Memory B and Plasma Cells. *Immunity*. 2016 Jan 19;44(1):116–30.
200. Stone SL, Lund FE. IgM Memory Cells: First Responders in Malaria. *Immunity*. 2016 Aug 16;45(2):235–7.
201. Pupovac A, Good-Jacobson KL. An antigen to remember: regulation of B cell memory in health and disease. *Curr Opin Immunol*. 2017 Apr 1;45:89–96.
202. Gatto D, Brink R. The germinal center reaction. *J Allergy Clin Immunol*. 2010 Nov;126(5):898–907; quiz 908–9.

203. Methot SP, Di Noia JM. Chapter Two - Molecular Mechanisms of Somatic Hypermutation and Class Switch Recombination. In: Alt FW, editor. *Advances in Immunology* [Internet]. Academic Press; 2017 [cited 2018 Sep 14]. p. 37–87. Available from: <http://www.sciencedirect.com/science/article/pii/S0065277616300530>
204. Honjo T, Kinoshita K, Muramatsu M. MOLECULAR MECHANISM OF CLASS SWITCH RECOMBINATION: Linkage with Somatic Hypermutation. *Annu Rev Immunol*. 2002;20(1):165–96.
205. Tarlinton DM, Smith KGC. Dissecting affinity maturation: a model explaining selection of antibody-forming cells and memory B cells in the germinal centre. *Trends Immunol*. 2000 Sep 1;21(9):436–41.
206. O'Connor BP, Cascalho M, Noelle RJ. Short-lived and Long-lived Bone Marrow Plasma Cells Are Derived from a Novel Precursor Population. *J Exp Med*. 2002 Mar 18;195(6):737–45.
207. Klein U, Dalla-Favera R. Germinal centres: role in B-cell physiology and malignancy. *Nat Rev Immunol*. 2008 Jan;8(1):22–33.
208. Mendis KN, David PH, Carter R. Antigenic polymorphism in malaria: is it an important mechanism for immune evasion? *Immunol Today*. 1991 Mar;12(3):A34-37.
209. Langhorne J, Ndungu FM, Sponaas A-M, Marsh K. Immunity to malaria: more questions than answers. *Nat Immunol*. 2008;9(7):725–32.
210. Cockburn IA, Zavala F. Dendritic cell function and antigen presentation in malaria. *Curr Opin Immunol*. 2016 Jun 1;40:1–6.
211. Urban BC, Todryk S. Malaria pigment paralyzes dendritic cells. *J Biol*. 2006 Apr 12;5:4.
212. Obeng-Adjei N, Portugal S, Tran TM, Yazew TB, Skinner J, Li S, et al. Circulating Th1 cell-type Tfh cells that exhibit impaired B cell help are preferentially activated during acute malaria in children. *Cell Rep*. 2015 Oct 13;13(2):425–39.
213. Carvalho LJ, Ferreira-da-Cruz MF, Daniel-Ribeiro CT, Pelajo-Machado M, Lenzi HL. Germinal center architecture disturbance during *Plasmodium berghei* ANKA infection in CBA mice. *Malar J*. 2007 May 16;6(1):59.
214. Babatunde KA, Walch M, Fellay I, Kharoubi-Hess S, Filgueira L, Ghiran I, et al. Malaria derived extracellular vesicles influence human neutrophils function. *FASEB J*. 2017 Apr 1;31(1_supplement):391.2-391.2.
215. Aitken EH, Alemu A, Rogerson SJ. Neutrophils and Malaria. *Front Immunol*. 2018;9:3005.

216. Eriksson EM, Schofield L. Dysfunctional $\gamma\delta$ T cells: a contributing factor for clinical tolerance to malaria? *Ann Transl Med* [Internet]. 2015 May [cited 2019 Apr 2];3(Suppl 1). Available from: <https://www.ncbi.nlm.nih.gov/pmc/articles/PMC4437952/>
217. Regules JA, Cicatelli SB, Bennett JW, Paolino KM, Twomey PS, Moon JE, et al. Fractional Third and Fourth Dose of RTS,S/AS01 Malaria Candidate Vaccine: A Phase 2a Controlled Human Malaria Parasite Infection and Immunogenicity Study. *J Infect Dis*. 2016 Sep 1;214(5):762–71.
218. Yeka A, Nankabirwa J, Mpimbaza A, Kigozi R, Arinaitwe E, Drakeley C, et al. Factors Associated with Malaria Parasitemia, Anemia and Serological Responses in a Spectrum of Epidemiological Settings in Uganda. *PLoS ONE* [Internet]. 2015 Mar 13 [cited 2015 Jun 26];10(3). Available from: <http://www.ncbi.nlm.nih.gov/pmc/articles/PMC4358889/>
219. Katureebe A, Zinszer K, Arinaitwe E, Rek J, Kakande E, Charland K, et al. Measures of Malaria Burden after Long-Lasting Insecticidal Net Distribution and Indoor Residual Spraying at Three Sites in Uganda: A Prospective Observational Study. *PLoS Med* [Internet]. 2016 Nov 8 [cited 2018 Apr 10];13(11). Available from: <https://www.ncbi.nlm.nih.gov/pmc/articles/PMC5100985/>
220. National Population and Housing Census Final Report 2014 | Knowledge Management Portal [Internet]. [cited 2018 Jul 26]. Available from: <http://library.health.go.ug/publications/leadership-and-governance-monitoring-and-evaluation/population/national-population-an-0>
221. Kanya MR, Arinaitwe E, Wanzira H, Katureebe A, Barusya C, Kigozi SP, et al. Malaria Transmission, Infection, and Disease at Three Sites with Varied Transmission Intensity in Uganda: Implications for Malaria Control. *Am J Trop Med Hyg*. 2015 May 6;92(5):903–12.
222. Katrak S, Murphy M, Nayebara P, Rek J, Smith M, Arinaitwe E, et al. Performance of Loop-Mediated Isothermal Amplification for the Identification of Submicroscopic *Plasmodium falciparum* Infection in Uganda. *Am J Trop Med Hyg*. 2017 Dec 6;97(6):1777–81.
223. Alegana VA, Kigozi SP, Nankabirwa J, Arinaitwe E, Kigozi R, Mawejje H, et al. Spatio-temporal analysis of malaria vector density from baseline through intervention in a high transmission setting. *Parasit Vectors*. 2016;9(1):637.
224. Richards JS, Stanisic DI, Fowkes FJI, Tavul L, Dabod E, Thompson JK, et al. Association between naturally acquired antibodies to erythrocyte-binding antigens of *Plasmodium falciparum* and protection from malaria and high-density parasitemia. *Clin Infect Dis Off Publ Infect Dis Soc Am*. 2010 Oct 15;51(8):e50-60.

225. Triglia T, Thompson J, Caruana SR, Delorenzi M, Speed T, Cowman AF. Identification of Proteins from *Plasmodium falciparum* That Are Homologous to Reticulocyte Binding Proteins in *Plasmodium vivax*. *Infect Immun*. 2001 Feb 1;69(2):1084–92.
226. Reiling L, Richards JS, Fowkes FJL, Wilson DW, Chokejindachai W, Barry AE, et al. The *Plasmodium falciparum* Erythrocyte Invasion Ligand Pfrh4 as a Target of Functional and Protective Human Antibodies against Malaria. *PLOS ONE*. 2012 Sep 20;7(9):e45253.
227. Hjerrild KA, Jin J, Wright KE, Brown RE, Marshall JM, Labbé GM, et al. Production of full-length soluble *Plasmodium falciparum* RH5 protein vaccine using a *Drosophila melanogaster* Schneider 2 stable cell line system. *Sci Rep*. 2016 Jul 26;6:30357.
228. Theisen M, Vuust J, Gottschau A, Jepsen S, Høgh B. Antigenicity and immunogenicity of recombinant glutamate-rich protein of *Plasmodium falciparum* expressed in *Escherichia coli*. *Clin Diagn Lab Immunol*. 1995 Jan 1;2(1):30–4.
229. Pearce JA, Mills K, Triglia T, Cowman AF, Anders RF. Characterisation of two novel proteins from the asexual stage of *Plasmodium falciparum*, H101 and H103. *Mol Biochem Parasitol*. 2005 Feb 1;139(2):141–51.
230. Burghaus PA, Holder AA. Expression of the 19-kilodalton carboxy-terminal fragment of the *Plasmodium falciparum* merozoite surface protein-1 in *Escherichia coli* as a correctly folded protein. *Mol Biochem Parasitol*. 1994 Mar;64(1):165–9.
231. Polley SD, Conway DJ, Cavanagh DR, McBride JS, Lowe BS, Williams TN, et al. High levels of serum antibodies to merozoite surface protein 2 of *Plasmodium falciparum* are associated with reduced risk of clinical malaria in coastal Kenya. *Vaccine*. 2006 May 8;24(19):4233–46.
232. Corran PH, Cook J, Lynch C, Leendertse H, Manjurano A, Griffin J, et al. Dried blood spots as a source of anti-malarial antibodies for epidemiological studies. *Malar J*. 2008 Sep 30;7:195.
233. xMAP Cookbook 4th Edition | Thanks for Downloading [Internet]. [cited 2018 Aug 19]. Available from: <http://info.luminexcorp.com/research/thank-you-xmap-cookbook?submissionGuid=5c61b69a-ad98-4908-b6a4-7cb3adf5e75c>
234. Ondigo BN, Park GS, Gose SO, Ho BM, Ochola LA, Ayodo GO, et al. Standardization and validation of a cytometric bead assay to assess antibodies to multiple *Plasmodium falciparum* recombinant antigens. *Malar J*. 2012 Dec 21;11:427.
235. Cham GK, Kurtis J, Lusingu J, Theander TG, Jensen AT, Turner L. A semi-automated multiplex high-throughput assay for measuring IgG antibodies against *Plasmodium falciparum*

- erythrocyte membrane protein 1 (PfEMP1) domains in small volumes of plasma. *Malar J.* 2008;7(1):108.
236. Fernandez-Becerra C, Sanz S, Brucet M, Stanisic DI, Alves FP, Camargo EP, et al. Naturally-acquired humoral immune responses against the N- and C-termini of the Plasmodium vivax MSP1 protein in endemic regions of Brazil and Papua New Guinea using a multiplex assay. *Malar J.* 2010;9(1):29.
 237. Smyth GK, Speed T. Normalization of cDNA microarray data. *Methods.* 2003 Dec 1;31(4):265–73.
 238. Druilhe P, Khusmith S. Epidemiological correlation between levels of antibodies promoting merozoite phagocytosis of Plasmodium falciparum and malaria-immune status. *Infect Immun.* 1987 Apr 1;55(4):888–91.
 239. Krugman S, Giles JP, Friedman H, Stone S. Studies on immunity to measles. *J Pediatr.* 1965 Mar 1;66(3):471–88.
 240. Hammarlund E, Lewis MW, Hansen SG, Strelow LI, Nelson JA, Sexton GJ, et al. Duration of antiviral immunity after smallpox vaccination. *Nat Med.* 2003 Sep;9(9):1131–7.
 241. Crompton PD, Moebius J, Portugal S, Waisberg M, Hart G, Garver LS, et al. Malaria Immunity in Man and Mosquito: Insights into Unsolved Mysteries of a Deadly Infectious Disease. *Annu Rev Immunol.* 2014;32(1):157–87.
 242. John CC, Moormann AM, Pregibon DC, Sumba PO, Mchugh MM, Narum DL, et al. Correlation of High Levels of Antibodies to Multiple Pre-Erythrocytic Plasmodium Falciparum Antigens and Protection from Infection. *Am J Trop Med Hyg.* 2005 Jul 1;73(1):222–8.
 243. Bull PC, Lowe BS, Kortok M, Molyneux CS, Newbold CI, Marsh K. Parasite antigens on the infected red cell surface are targets for naturally acquired immunity to malaria. *Nat Med.* 1998 Mar;4(3):358–60.
 244. Osier FHA, Fegan G, Polley SD, Murungi L, Verra F, Tetteh KKA, et al. Breadth and magnitude of antibody responses to multiple Plasmodium falciparum merozoite antigens are associated with protection from clinical malaria. *Infect Immun.* 2008 May;76(5):2240–8.
 245. Migot-Nabias F, Luty AJ, Ringwald P, Vaillant M, Dubois B, Renaut A, et al. Immune responses against Plasmodium falciparum asexual blood-stage antigens and disease susceptibility in Gabonese and Cameroonian children. *Am J Trop Med Hyg.* 1999 Sep;61(3):488–94.

246. Egan AF, Morris J, Barnish G, Allen S, Greenwood BM, Kaslow DC, et al. Clinical Immunity to *Plasmodium falciparum* Malaria Is Associated with Serum Antibodies to the 19-kDa C-Terminal Fragment of the Merozoite Surface Antigen, PfMSP-I. *J Infect Dis*. 1996 Mar 1;173(3):765–8.
247. Schwartz L, Brown GV, Genton B, Moorthy VS. A review of malaria vaccine clinical projects based on the WHO rainbow table. *Malar J*. 2012 Jan 9;11:11.
248. RTS,S Clinical Trials Partnership. Efficacy and safety of the RTS,S/AS01 malaria vaccine during 18 months after vaccination: a phase 3 randomized, controlled trial in children and young infants at 11 African sites. *PLoS Med*. 2014 Jul;11(7):e1001685.
249. Gardner MJ, Hall N, Fung E, White O, Berriman M, Hyman RW, et al. Genome sequence of the human malaria parasite *Plasmodium falciparum*. *Nature*. 2002 Oct 3;419(6906):498–511.
250. Hviid L. Clinical disease, immunity and protection against *Plasmodium falciparum* malaria in populations living in endemic areas. *Expert Rev Mol Med*. 1998 Jun;null(04):1–10.
251. Pour Abolghasem S, Bonyadi MR, Babaloo Z, Porhasan A, Nagili B, Gardashkhani OA, et al. IgG avidity test for the diagnosis of acute *Toxoplasma gondii* infection in early pregnancy. *Iran J Immunol IJI*. 2011 Dec;8(4):251–5.
252. Barfod L, Dalgaard MB, Pleman ST, Ofori MF, Pleass RJ, Hviid L. Evasion of immunity to *Plasmodium falciparum* malaria by IgM masking of protective IgG epitopes in infected erythrocyte surface-exposed PfEMP1. *Proc Natl Acad Sci*. 2011 Jul 11;201103708.
253. Portugal S, Pierce SK, Crompton PD. Young lives lost as B cells falter: what we are learning about antibody responses in malaria. *J Immunol Baltim Md 1950*. 2013 Apr 1;190(7):3039–46.
254. Scholzen A, Sauerwein RW. How malaria modulates memory: activation and dysregulation of B cells in *Plasmodium* infection. *Trends Parasitol*. 2013 May;29(5):252–62.
255. Crompton PD, Kayala MA, Traore B, Kayentao K, Ongoiba A, Weiss GE, et al. A prospective analysis of the Ab response to *Plasmodium falciparum* before and after a malaria season by protein microarray. *Proc Natl Acad Sci*. 2010 Apr 13;107(15):6958–63.
256. Weiss GE, Clark EH, Li S, Traore B, Kayentao K, Ongoiba A, et al. A Positive Correlation between Atypical Memory B Cells and *Plasmodium falciparum* Transmission Intensity in Cross-Sectional Studies in Peru and Mali. *PLoS ONE*. 2011 Jan 14;6(1):e15983.
257. Weiss GE, Crompton PD, Li S, Walsh LA, Moir S, Traore B, et al. Atypical Memory B Cells Are Greatly Expanded in Individuals Living in a Malaria-Endemic Area. *J Immunol*. 2009 Aug 1;183(3):2176–82.

258. Portugal S, Doumtabe D, Traore B, Miller LH, Troye-Blomberg M, Doumbo OK, et al. B cell analysis of ethnic groups in Mali with differential susceptibility to malaria. *Malar J.* 2012 May 11;11(1):162.
259. Illingworth J, Butler NS, Roetynck S, Mwacharo J, Pierce SK, Bejon P, et al. Chronic Exposure to *Plasmodium falciparum* Is Associated with Phenotypic Evidence of B and T Cell Exhaustion. *J Immunol.* 2013 Feb 1;190(3):1038–47.
260. Groux H, Gysin J. Opsonization as an effector mechanism in human protection against asexual blood stages of *Plasmodium falciparum*: Functional role of IgG subclasses. *Res Immunol.* 1990;141(5):529–42.
261. Epstein N, Miller LH, Kaushel DC, Udeinya JJ, Renner J, Howard RJ, et al. Monoclonal antibodies against a specific surface determinant on malarial (*Plasmodium knowlesi*) merozoites block erythrocyte invasion. *J Immunol.* 1981 Jul 1;127(1):212–7.
262. Patiño JAG, Holder AA, McBride JS, Blackman MJ. Antibodies that Inhibit Malaria Merozoite Surface Protein–1 Processing and Erythrocyte Invasion Are Blocked by Naturally Acquired Human Antibodies. *J Exp Med.* 1997 Nov 17;186(10):1689–99.
263. Marsh K, Kinyanjui S. Immune effector mechanisms in malaria. *Parasite Immunol.* 2006 Jan 1;28(1–2):51–60.
264. Karush F. Affinity and the Immune Response*. *Ann N Y Acad Sci.* 1970 Feb 1;169(1):56–64.
265. Schlesinger Y, Granoff DM, Murphy TV, et al. Avidity and bactericidal activity of antibody elicited by different haemophilus influenzae type b conjugate vaccines. *JAMA.* 1992 Mar 18;267(11):1489–94.
266. Cremers AJH, Lut J, Hermans PWM, Meis JF, Jonge MI de, Ferwerda G. Avidity of Antibodies against Infecting Pneumococcal Serotypes Increases with Age and Severity of Disease. *Clin Vaccine Immunol.* 2014 Jun 1;21(6):904–7.
267. Ferreira MU, Kimura EAS, Souza JM de, Katzin AM. The Isotype Composition and Avidity of Naturally Acquired Anti-*Plasmodium falciparum* Antibodies: Differential Patterns in Clinically Immune Africans and Amazonian Patients. *Am J Trop Med Hyg.* 1996 Sep 1;55(3):315–23.
268. Leoratti FM, Durlacher RR, Lacerda MV, Alecrim MG, Ferreira AW, Sanchez MC, et al. Pattern of humoral immune response to *Plasmodium falciparum* blood stages in individuals presenting different clinical expressions of malaria. *Malar J.* 2008 Sep 24;7:186.
269. Tutterrow YL, Salanti A, Avril M, Smith JD, Pagano IS, Ako S, et al. High Avidity Antibodies to Full-Length VAR2CSA Correlate with Absence of Placental Malaria. *PLoS ONE [Internet].* 2012

- Jun 26 [cited 2014 Jul 22];7(6). Available from:
<http://www.ncbi.nlm.nih.gov/pmc/articles/PMC3383675/>
270. Reddy SB, Anders RF, Beeson JG, Farnert A, Kironde F, Berenzon SK, et al. High Affinity Antibodies to Plasmodium falciparum Merozoite Antigens Are Associated with Protection from Malaria. PLoS ONE [Internet]. 2012 Feb 21 [cited 2014 Jan 8];7(2). Available from:
<http://www.ncbi.nlm.nih.gov/pmc/articles/PMC3283742/>
 271. AKPOGHENETA OJ, DUNYO S, PINDER M, CONWAY DJ. Boosting antibody responses to Plasmodium falciparum merozoite antigens in children with highly seasonal exposure to infection. Parasite Immunol. 2010 Apr;32(4):296–304.
 272. Ibison F, Olotu A, Muema DM, Mwacharo J, Ohuma E, Kimani D, et al. Lack of Avidity Maturation of Merozoite Antigen-Specific Antibodies with Increasing Exposure to Plasmodium falciparum amongst Children and Adults Exposed to Endemic Malaria in Kenya. PLoS ONE. 2012 Dec 26;7(12):e52939.
 273. Stewart L, Gosling R, Griffin J, Gesase S, Campo J, Hashim R, et al. Rapid Assessment of Malaria Transmission Using Age-Specific Sero-Conversion Rates. PLoS ONE. 2009 Jun 29;4(6):e6083.
 274. Nyunt MH, Soe TN, Shein T, Zaw NN, Han SS, Muh F, et al. Estimation on local transmission of malaria by serological approach under low transmission setting in Myanmar. Malar J. 2018 Jan 5;17:6.
 275. Shlomchik MJ, Weisel F. Germinal center selection and the development of memory B and plasma cells. Immunol Rev. 2012 May;247(1):52–63.
 276. Liu Y-J, Joshua DE, Williams GT, Smith CA, Gordon J, MacLennan ICM. Mechanism of antigen-driven selection in germinal centres. Nature. 1989 Dec 28;342(6252):929–31.
 277. Cadman ET, Abdallah AY, Voisine C, Sponaas A-M, Corran P, Lamb T, et al. Alterations of Splenic Architecture in Malaria Are Induced Independently of Toll-Like Receptors 2, 4, and 9 or MyD88 and May Affect Antibody Affinity. Infect Immun. 2008 Sep 1;76(9):3924–31.
 278. Alves FA, Pelajo-Machado M, Totino PR, Souza MT, Gonçalves EC, Schneider MP, et al. Splenic architecture disruption and parasite-induced splenocyte activation and anergy in Plasmodium falciparum-infected Saimiri sciureus monkeys. Malar J. 2015 Mar 25;14(1):128.
 279. Donati D, Zhang LP, Chen Q, Chêne A, Flick K, Nyström M, et al. Identification of a Polyclonal B-Cell Activator in Plasmodium falciparum. Infect Immun. 2004 Sep 1;72(9):5412–8.

280. Ryg-Cornejo V, Ioannidis LJ, Ly A, Chiu CY, Tellier J, Hill DL, et al. Severe Malaria Infections Impair Germinal Center Responses by Inhibiting T Follicular Helper Cell Differentiation. *Cell Rep*. 2015 Dec 22;
281. Emerging concepts in T follicular helper cell responses to malaria. *Int J Parasitol*. 2017 Feb 1;47(2–3):105–10.
282. Donati D, Mok B, Chêne A, Xu H, Thangarajh M, Glas R, et al. Increased B Cell Survival and Preferential Activation of the Memory Compartment by a Malaria Polyclonal B Cell Activator. *J Immunol*. 2006 Sep 1;177(5):3035–44.
283. Reddy SB, Anders RF, Beeson JG, Färnert A, Kironde F, Berenzon SK, et al. *PLoS ONE*. 2012 Feb 21;7(2):e32242.
284. Ajua A, Lell B, Agnandji ST, Asante KP, Owusu-Agyei S, Mwangoka G, et al. The effect of immunization schedule with the malaria vaccine candidate RTS,S/AS01E on protective efficacy and anti-circumsporozoite protein antibody avidity in African infants. *Malar J*. 2015;14:72.
285. Olotu A, Clement F, Jongert E, Vekemans J, Njuguna P, Ndungu FM, et al. Avidity of Anti-Circumsporozoite Antibodies following Vaccination with RTS,S/AS01E in Young Children. *PLoS ONE*. 2014 Dec 15;9(12):e115126.
286. Jagannathan P, Bowen K, Nankya F, McIntyre TI, Auma A, Wamala S, et al. Effective Antimalarial Chemoprevention in Childhood Enhances the Quality of CD4+ T Cells and Limits Their Production of Immunoregulatory Interleukin 10. *J Infect Dis*. 2016 Jul 15;214(2):329–38.
287. Al-Yaman F, Genton B, Kramer KJ, Chang SP, Hui GS, Baisor M, et al. Assessment of the Role of Naturally Acquired Antibody Levels to *Plasmodium falciparum* Merozoite Surface Protein-1 in Protecting Papua New Guinean Children from Malaria Morbidity. *Am J Trop Med Hyg*. 1996 May 1;54(5):443–8.
288. Dobaño C, Quelhas D, Quintó L, Puyol L, Serra-Casas E, Mayor A, et al. Age-dependent IgG subclass responses to *Plasmodium falciparum* EBA-175 are differentially associated with incidence of malaria in Mozambican children. *Clin Vaccine Immunol CVI*. 2012 Feb;19(2):157–66.
289. Tetteh KKA, Osier FHA, Salanti A, Kamuyu G, Drought L, Failly M, et al. Analysis of antibodies to newly described *Plasmodium falciparum* merozoite antigens supports MSPDBL2 as a predicted target of naturally acquired immunity. *Infect Immun*. 2013 Oct;81(10):3835–42.

290. Mugenyi CK, Elliott SR, McCallum FJ, Anders RF, Marsh K, Beeson JG. Antibodies to polymorphic invasion-inhibitory and non-Inhibitory epitopes of *Plasmodium falciparum* apical membrane antigen 1 in human malaria. *PloS One*. 2013;8(7):e68304.
291. Tran TM, Ongoiba A, Coursen J, Crosnier C, Diouf A, Huang C-Y, et al. Naturally Acquired Antibodies Specific for *Plasmodium falciparum* RH5 Inhibit Parasite Growth and Predict Protection From Malaria. *J Infect Dis*. 2013 Oct 16;jit553.
292. O'Donnell RA, de Koning-Ward TF, Burt RA, Bockarie M, Reeder JC, Cowman AF, et al. Antibodies against merozoite surface protein (MSP)-1(19) are a major component of the invasion-inhibitory response in individuals immune to malaria. *J Exp Med*. 2001 Jun 18;193(12):1403–12.
293. Patiño JAG, Holder AA, McBride JS, Blackman MJ. Antibodies that Inhibit Malaria Merozoite Surface Protein–1 Processing and Erythrocyte Invasion Are Blocked by Naturally Acquired Human Antibodies. *J Exp Med*. 1997 Nov 17;186(10):1689–99.
294. Persson KEM. Erythrocyte invasion and functionally inhibitory antibodies in *Plasmodium falciparum* malaria. *Acta Trop*. 2010 Jun;114(3):138–43.
295. Raj DK, Nixon CP, Nixon CE, Dvorin JD, DiPetrillo CG, Pond-Tor S, et al. Antibodies to PfSEA-1 block parasite egress from RBCs and protect against malaria infection. *Science*. 2014 May 23;344(6186):871–7.
296. Teo A, Feng G, Brown GV, Beeson JG, Rogerson SJ. Functional Antibodies and Protection against Blood-stage Malaria. *Trends Parasitol*. 2016 Nov;32(11):887–98.
297. Okech BA, Corran PH, Todd J, Joynson-Hicks A, Uthaipibull C, Egwang TG, et al. Fine specificity of serum antibodies to *Plasmodium falciparum* merozoite surface protein, PfMSP-1(19), predicts protection from malaria infection and high-density parasitemia. *Infect Immun*. 2004 Mar;72(3):1557–67.
298. Jäschke A, Coulibaly B, Remarque EJ, Bujard H, Epp C. Merozoite Surface Protein 1 from *Plasmodium falciparum* Is a Major Target of Opsonizing Antibodies in Individuals with Acquired Immunity against Malaria. *Clin Vaccine Immunol CVI*. 2017 Nov;24(11).
299. Weaver R, Reiling L, Feng G, Drew DR, Mueller I, Siba PM, et al. The association between naturally acquired IgG subclass specific antibodies to the PfRH5 invasion complex and protection from *Plasmodium falciparum* malaria. *Sci Rep [Internet]*. 2016 Sep 8 [cited 2018 Apr 24];6. Available from: <https://www.ncbi.nlm.nih.gov/pmc/articles/PMC5015043/>

300. Richards JS, Stanisic DI, Fowkes FJI, Tavul L, Dabod E, Thompson JK, et al. Association between naturally acquired antibodies to erythrocyte-binding antigens of *Plasmodium falciparum* and protection from malaria and high-density parasitemia. *Clin Infect Dis Off Publ Infect Dis Soc Am*. 2010 Oct 15;51(8):e50-60.
301. Groux H, Gysin J. Opsonization as an effector mechanism in human protection against asexual blood stages of *Plasmodium falciparum*: Functional role of IgG subclasses. *Res Immunol*. 1990;141(5):529–42.
302. Sakamoto H, Takeo S, Takashima E, Miura K, Kanoi BN, Kaneko T, et al. Identification of target proteins of clinical immunity to *Plasmodium falciparum* in a region of low malaria transmission. *Parasitol Int*. 2017 Dec 4;
303. Hill DL, Wilson DW, Sampaio NG, Eriksson EM, Ryg-Cornejo V, Harrison GLA, et al. Merozoite Antigens of *Plasmodium falciparum* Elicit Strain-Transcending Opsonizing Immunity. *Infect Immun*. 2016;84(8):2175–84.
304. Joos C, Varela M-L, Mbengue B, Mansourou A, Marrama L, Sokhna C, et al. Antibodies to *Plasmodium falciparum* merozoite surface protein-1p19 malaria vaccine candidate induce antibody-dependent respiratory burst in human neutrophils. *Malar J*. 2015 Oct 15;14:409.
305. Tiendrebeogo RW, Adu B, Singh SK, Dziegiel MH, Nébié I, Sirima SB, et al. Antibody-Dependent Cellular Inhibition Is Associated With Reduced Risk Against Febrile Malaria in a Longitudinal Cohort Study Involving Ghanaian Children. *Open Forum Infect Dis* [Internet]. 2015 Apr 1 [cited 2018 Jul 27];2(2). Available from: <https://academic.oup.com/ofid/article/2/2/ofv044/1411648>
306. McCarthy JS, Marjason J, Elliott S, Fahey P, Bang G, Malkin E, et al. A phase 1 trial of MSP2-C1, a blood-stage malaria vaccine containing 2 isoforms of MSP2 formulated with Montanide® ISA 720. *PloS One*. 2011;6(9):e24413.
307. Jepsen MPG, Jogdand PS, Singh SK, Esen M, Christiansen M, Issifou S, et al. The malaria vaccine candidate GMZ2 elicits functional antibodies in individuals from malaria endemic and non-endemic areas. *J Infect Dis*. 2013 Aug 1;208(3):479–88.
308. Zenklusen I, Jongo S, Abdulla S, Ramadhani K, Lee Sim BK, Cardamone H, et al. Immunization of Malaria-Preexposed Volunteers With PfSPZ Vaccine Elicits Long-Lived IgM Invasion-Inhibitory and Complement-Fixing Antibodies. *J Infect Dis*. 2018 Apr 23;217(10):1569–78.
309. How malaria modulates memory: activation and dysregulation of B cells in *Plasmodium* infection. *Trends Parasitol*. 2013 May 1;29(5):252–62.

310. Ssewanyana I, Arinaitwe E, Nankabirwa JI, Yeka A, Sullivan R, Kamya MR, et al. Avidity of anti-malarial antibodies inversely related to transmission intensity at three sites in Uganda. *Malar J* [Internet]. 2017 Feb 10 [cited 2018 Jan 23];16. Available from: <https://www.ncbi.nlm.nih.gov/pmc/articles/PMC5301436/>
311. Ferreira MU, Katzin AM. The assessment of antibody affinity distribution by thiocyanate elution: a simple dose-response approach. *J Immunol Methods*. 1995 Dec 1;187(2):297–305.
312. Lau L, Green AM, Balmaseda A, Harris E. Antibody Avidity Following Secondary Dengue Virus Type 2 Infection Across a Range of Disease Severity. *J Clin Virol Off Publ Pan Am Soc Clin Virol*. 2015 Aug;69:63–7.
313. Khurana S, Verma N, Yewdell JW, Hilbert AK, Castellino F, Lattanzi M, et al. MF59 Adjuvant Enhances Diversity and Affinity of Antibody-Mediated Immune Response to Pandemic Influenza Vaccines. *Sci Transl Med*. 2011 Jun 1;3(85):85ra48-85ra48.
314. Akpogheneta OJ, Duah NO, Tetteh KKA, Dunyo S, Lanar DE, Pinder M, et al. Duration of Naturally Acquired Antibody Responses to Blood-Stage *Plasmodium falciparum* Is Age Dependent and Antigen Specific. *Infect Immun*. 2008 Apr;76(4):1748–55.
315. Corcoran LM, Tarlinton DM. Regulation of germinal center responses, memory B cells and plasma cell formation — an update. *Curr Opin Immunol*. 2016 Apr;39:59–67.
316. Silva M, Nguyen TH, Philbrook P, Chu M, Sears O, Hatfield S, et al. Targeted Elimination of Immunodominant B Cells Drives the Germinal Center Reaction toward Subdominant Epitopes. *Cell Rep*. 2017 Dec 26;21(13):3672–80.
317. Chu VT, Berek C. The establishment of the plasma cell survival niche in the bone marrow. *Immunol Rev*. 2013;251(1):177–88.
318. Chernova I, Jones DD, Wilmore JR, Bortnick A, Yucel M, Hershberg U, et al. Lasting antibody responses are mediated by a combination of newly formed and established bone marrow plasma cells drawn from clonally distinct precursors. *J Immunol Baltim Md 1950*. 2014 Nov 15;193(10):4971–9.
319. MacLennan ICM, Toellner K-M, Cunningham AF, Serre K, Sze DM-Y, Zúñiga E, et al. Extrafollicular antibody responses. *Immunol Rev*. 194(1):8–18.
320. van den Hoogen LL, Griffin JT, Cook J, Sepúlveda N, Corran P, Conway DJ, et al. Serology describes a profile of declining malaria transmission in Farafenni, The Gambia. *Malar J*. 2015 Oct 22;14(1):416.

321. Mugenyi CK, Elliott SR, Yap XZ, Feng G, Boeuf P, Fegan G, et al. Declining Malaria Transmission Differentially Impacts the Maintenance of Humoral Immunity to *Plasmodium falciparum* in Children. *J Infect Dis*. 2017 Oct 17;216(7):887–98.
322. Ndungu FM, Lundblom K, Rono J, Illingworth J, Eriksson S, Färnert A. Long-lived *Plasmodium falciparum* specific memory B cells in naturally exposed Swedish travelers. *Eur J Immunol*. 2013 Nov 1;43(11):2919–29.
323. Ndungu FM, Olotu A, Mwacharo J, Nyonda M, Apfeld J, Mramba LK, et al. Memory B cells are a more reliable archive for historical antimalarial responses than plasma antibodies in no-longer exposed children. *Proc Natl Acad Sci*. 2012 May 22;109(21):8247–52.
324. Murungi LM, Kamuyu G, Lowe B, Bejon P, Theisen M, Kinyanjui SM, et al. A threshold concentration of anti-merozoite antibodies is required for protection from clinical episodes of malaria. *Vaccine*. 2013 Aug 20;31(37):3936–42.
325. Offeddu V, Olotu A, Osier F, Marsh K, Matuschewski K, Thathy V. High Sporozoite Antibody Titers in Conjunction with Microscopically Detectable Blood Infection Display Signatures of Protection from Clinical Malaria. *Front Immunol* [Internet]. 2017 [cited 2018 Nov 27];8. Available from: <https://www.frontiersin.org/articles/10.3389/fimmu.2017.00488/full>
326. Kimuda SG, Biraro IA, Bagaya BS, Raynes JG, Cose S. Characterising antibody avidity in individuals of varied *Mycobacterium tuberculosis* infection status using surface plasmon resonance. *PLOS ONE*. 2018 Oct 12;13(10):e0205102.
327. WHO. WHO | Malaria elimination [Internet]. WHO. [cited 2018 Jun 30]. Available from: <http://www.who.int/malaria/areas/elimination/en/>
328. Cohen JM, Smith DL, Cotter C, Ward A, Yamey G, Sabot OJ, et al. Malaria resurgence: a systematic review and assessment of its causes. *Malar J*. 2012;11(1):122.
329. Raouf S, Mpimbaza A, Kigozi R, Sserwanga A, Rubahika D, Katamba H, et al. Resurgence of Malaria Following Discontinuation of Indoor Residual Spraying of Insecticide in an Area of Uganda With Previously High-Transmission Intensity. *Clin Infect Dis*. 2017 Aug 1;65(3):453–60.
330. Liu H, Xu J-W, Yang H-L, Li M, Sun C-D, Yin Y-J, et al. Investigation and control of a *Plasmodium falciparum* malaria outbreak in Shan Special Region II of Myanmar along the China-Myanmar Border from June to December 2014. *Infect Dis Poverty*. 2016 Apr 25;5:32.
331. Helb DA, Tetteh KKA, Felgner PL, Skinner J, Hubbard A, Arinaitwe E, et al. Novel serologic biomarkers provide accurate estimates of recent *Plasmodium falciparum* exposure for individuals and communities. *Proc Natl Acad Sci U S A*. 2015 Jul 27;

332. Kerkhof K, Sluydts V, Willen L, Kim S, Canier L, Heng S, et al. Serological markers to measure recent changes in malaria at population level in Cambodia. *Malar J* [Internet]. 2016 Nov 4 [cited 2016 Nov 9];15. Available from: <http://www.ncbi.nlm.nih.gov/pmc/articles/PMC5096337/>
333. Kester KE, Cummings JF, Ofori-Anyinam O, Ockenhouse CF, Krzych U, Moris P, et al. Randomized, Double-Blind, Phase 2a Trial of Falciparum Malaria Vaccines RTS,S/AS01B and RTS,S/AS02A in Malaria-Naive Adults: Safety, Efficacy, and Immunologic Associates of Protection. *J Infect Dis*. 2009 Aug 1;200(3):337–46.
334. Chaudhury S, Ockenhouse CF, Regules JA, Dutta S, Wallqvist A, Jongert E, et al. The biological function of antibodies induced by the RTS,S/AS01 malaria vaccine candidate is determined by their fine specificity. *Malar J* [Internet]. 2016 May 31 [cited 2018 Apr 6];15. Available from: <https://www.ncbi.nlm.nih.gov/pmc/articles/PMC4886414/>
335. Lalvani A, Moris P, Voss G, Pathan AA, Kester KE, Brookes R, et al. Potent Induction of Focused Th1-Type Cellular and Humoral Immune Responses by RTS,S/SBAS2, a Recombinant Plasmodium falciparum Malaria Vaccine. *J Infect Dis*. 1999 Nov 1;180(5):1656–64.
336. Olotu A, Clement F, Jongert E, Vekemans J, Njuguna P, Ndungu FM, et al. Avidity of Anti-Circumsporozoite Antibodies following Vaccination with RTS,S/AS01E in Young Children. *PLoS ONE* [Internet]. 2014 Dec 15 [cited 2016 Mar 12];9(12). Available from: <http://www.ncbi.nlm.nih.gov/pmc/articles/PMC4266636/>
337. White MT, Bejon P, Olotu A, Griffin JT, Bojang K, Lusingu J, et al. A combined analysis of immunogenicity, antibody kinetics and vaccine efficacy from phase 2 trials of the RTS,S malaria vaccine. *BMC Med*. 2014 Jul 10;12(1):117.
338. Ryg-Cornejo V, Ly A, Hansen DS. Immunological processes underlying the slow acquisition of humoral immunity to malaria. *Parasitology*. 2016 Feb;143(Special Issue 02):199–207.
339. Horata N, Choowongkamon K, Ratanabunyong S, Tongshoob J, Khusmith S. Acquisition of naturally acquired antibody response to Plasmodium falciparum erythrocyte membrane protein 1-DBL α and differential regulation of IgG subclasses in severe and uncomplicated malaria. *Asian Pac J Trop Biomed*. 2017 Dec 1;7(12):1055–61.
340. Deloron P, Chougnet C. Is immunity to malaria really short-lived? *Parasitol Today Pers Ed*. 1992 Nov;8(11):375–8.
341. Cohen S, Butcher GA. Properties of protective malarial antibody. *Immunology*. 1970 Aug;19(2):369–83.

342. M. P, Poinsignon A, Marie A, Noukpo H, Doucoure S, Cornelié S, et al. New Salivary Biomarkers of Human Exposure to Malaria Vector Bites. In: Manguin S, editor. *Anopheles mosquitoes - New insights into malaria vectors* [Internet]. InTech; 2013 [cited 2013 Dec 10]. Available from: <http://www.intechopen.com/books/anopheles-mosquitoes-new-insights-into-malaria-vectors/new-salivary-biomarkers-of-human-exposure-to-malaria-vector-bites>
343. Mayor A, Dobaño C, Nhabomba A, Guinovart C, Jiménez A, Manaca MN, et al. IgM and IgG against *Plasmodium falciparum* lysate as surrogates of malaria exposure and protection during pregnancy. *Malar J*. 2018 May 10;17(1):182.
344. Dent AE, Nakajima R, Liang L, Baum E, Moormann AM, Sumba PO, et al. *Plasmodium falciparum* Protein Microarray Antibody Profiles Correlate With Protection From Symptomatic Malaria in Kenya. *J Infect Dis*. 2015 Apr 15;
345. Kanoi BN, Takashima E, Morita M, White MT, Palacpac NMQ, Ntege EH, et al. Antibody profiles to wheat germ cell-free system synthesized *Plasmodium falciparum* proteins correlate with protection from symptomatic malaria in Uganda. *Vaccine* [Internet]. [cited 2017 Jan 17]; Available from: <http://www.sciencedirect.com/science/article/pii/S0264410X17300038>
346. Valenzuela NM, Schaub S. The Biology of IgG Subclasses and Their Clinical Relevance to Transplantation. *Transplantation* [Internet]. 2018 Jan 1 [cited 2018 Mar 23];102(1S). Available from: <https://insights-ovid-com.ez.lshrm.ac.uk/pubmed/?pmid=29266057>
347. Kana IH, Garcia-Senosai A, Singh SK, Tiendrebeogo RW, Chourasia BK, Malhotra P, et al. Cytophilic Antibodies Against Key *Plasmodium falciparum* Blood Stage Antigens Contribute to Protection Against Clinical Malaria in a High Transmission Region of Eastern India. *J Infect Dis* [Internet]. 2018 May 4 [cited 2018 Jun 27]; Available from: <https://academic.oup.com/jid/advance-article/doi/10.1093/infdis/jiy258/4992614>
348. Celada A, Cruchaud A, Perrin LH. Opsonic activity of human immune serum on in vitro phagocytosis of *Plasmodium falciparum* infected red blood cells by monocytes. *Clin Exp Immunol*. 1982 Mar;47(3):635–44.
349. Bouharoun-Tayoun H, Attanath P, Sabchareon A, Chongsuphajaisiddhi T, Druilhe P. Antibodies that protect humans against *Plasmodium falciparum* blood stages do not on their own inhibit parasite growth and invasion in vitro, but act in cooperation with monocytes. *J Exp Med*. 1990 Dec 1;172(6):1633–41.
350. Biryukov S, Angov E, Landmesser ME, Spring MD, Ockenhouse CF, Stoute JA. Complement and Antibody-mediated Enhancement of Red Blood Cell Invasion and Growth of Malaria Parasites. *EBioMedicine*. 2016 Jul 1;9:207–16.

351. Aucan C, Traoré Y, Tall F, Nacro B, Traoré-Leroux T, Fumoux F, et al. High Immunoglobulin G2 (IgG2) and Low IgG4 Levels Are Associated with Human Resistance to *Plasmodium falciparum* Malaria. *Infect Immun*. 2000 Mar;68(3):1252–8.
352. Oxelius V-A. Chronic infections in a family with hereditary deficiency of IgG2 and IgG4. *Clin Exp Immunol*. 1974 May;17(1):19–27.
353. Spectrum of IgG2 subclass deficiency in children with recurrent infections: Prospective study - *The Journal of Pediatrics* [Internet]. [cited 2018 Jul 2]. Available from: [https://www.jpeds.com/article/S0022-3476\(86\)81035-6/abstract](https://www.jpeds.com/article/S0022-3476(86)81035-6/abstract)
354. Zuo Y, Evangelista F, Culton D, Guilabert A, Lin L, Li N, et al. IgG4 autoantibodies are inhibitory in the autoimmune disease bullous pemphigoid. *J Autoimmun*. 2016 Sep 1;73:111–9.
355. Lighaam LC, Rispens T. The Immunobiology of Immunoglobulin G4. *Semin Liver Dis*. 2016 Aug;36(3):200–15.
356. van de Veen W, Akdis M. Role of IgG4 in IgE-mediated allergic responses. *J Allergy Clin Immunol*. 2016 Nov;138(5):1434–5.
357. A comparison between IgE and IgG4 as markers of allergy in children: an experimental trial in a model of natural antigen avoidance. - PubMed - NCBI [Internet]. [cited 2018 Jul 2]. Available from: <https://www.ncbi.nlm.nih.gov/pubmed/22230410>
358. Varga E-M, Kausar F, Aberer W, Zach M, Eber E, Durham SR, et al. Tolerant beekeepers display venom-specific functional IgG4 antibodies in the absence of specific IgE. *J Allergy Clin Immunol*. 2013 May;131(5):1419–21.
359. Israel EJ, Taylor S, Wu Z, Mizoguchi E, Blumberg RS, Bhan A, et al. Expression of the neonatal Fc receptor, FcRn, on human intestinal epithelial cells. *Immunology*. 92(1):69–74.
360. Li T, DiLillo DJ, Bournazos S, Giddens JP, Ravetch JV, Wang L-X. Modulating IgG effector function by Fc glycan engineering. *Proc Natl Acad Sci*. 2017 Mar 28;114(13):3485–90.
361. Plomp R, Ruhaak LR, Uh H-W, Reiding KR, Selman M, Houwing-Duistermaat JJ, et al. Subclass-specific IgG glycosylation is associated with markers of inflammation and metabolic health. *Sci Rep* [Internet]. 2017 Dec [cited 2018 Jul 17];7(1). Available from: <http://www.nature.com/articles/s41598-017-12495-0>
362. Ackerman ME, Crispin M, Yu X, Baruah K, Boesch AW, Harvey DJ, et al. Natural variation in Fc glycosylation of HIV-specific antibodies impacts antiviral activity. *J Clin Invest*. 2013 May 1;123(5):2183–92.

363. Tomana M, Schrohenloher RE, Koopman WJ, Alarc n GS, Paul WA. Abnormal glycosylation of serum igg from patients with chronic inflammatory diseases. *Arthritis Rheum*. 1988 Mar 1;31(3):333–8.
364. Selman MHJ, Jong SE de, Soonawala D, Kroon FP, Adegnika AA, Deelder AM, et al. Changes in antigen-specific IgG1 Fc N-glycosylation upon influenza and tetanus vaccination. *Mol Cell Proteomics*. 2011 Dec 19;mcp.M111.014563.
365. Aribot G, Rogier C, Sarthou JL, Trape JF, Balde AT, Druilhe P, et al. Pattern of immunoglobulin isotype response to *Plasmodium falciparum* blood-stage antigens in individuals living in a holoendemic area of Senegal (Dielmo, west Africa). *Am J Trop Med Hyg*. 1996 May;54(5):449–57.
366. Taylor RR, Allen SJ, Greenwood BM, Riley EM. IgG3 antibodies to *Plasmodium falciparum* merozoite surface protein 2 (MSP2): increasing prevalence with age and association with clinical immunity to malaria. *Am J Trop Med Hyg*. 1998 Apr 1;58(4):406–13.
367. Metzger WG, Okenu DMN, Cavanagh DR, Robinson JV, Bojang KA, Weiss HA, et al. Serum IgG3 to the *Plasmodium falciparum* merozoite surface protein 2 is strongly associated with a reduced prospective risk of malaria. *Parasite Immunol*. 25(6):307–12.
368. DUAH NO, MILES DJC, WHITTLE HC, CONWAY DJ. Acquisition of antibody isotypes against *Plasmodium falciparum* blood stage antigens in a birth cohort. *Parasite Immunol*. 2010 Feb;32(2):125–34.
369. Isotypic analysis of maternally transmitted *Plasmodium falciparum*-specific antibodies in Cameroon, and relationship with risk of *P. falciparum* infection - DELORON - 1997 - Clinical & Experimental Immunology - Wiley Online Library [Internet]. [cited 2018 Jul 17]. Available from: <https://onlinelibrary-wiley-com.ez.lshtm.ac.uk/doi/abs/10.1111/j.1365-2249.1997.tb08319.x>
370. Ndungu FM, Bull PC, Ross A, Lowe BS, Kabiru E, Marsh K. Naturally acquired immunoglobulin (Ig)G subclass antibodies to crude asexual *Plasmodium falciparum* lysates: evidence for association with protection for IgG1 and disease for IgG2. *Parasite Immunol*. 2002 Feb;24(2):77–82.
371. Immunoglobulin class switching. *Curr Opin Immunol*. 1996 Apr 1;8(2):199–205.
372. Oropallo MA, Cerutti A. Germinal center reaction: antigen affinity and presentation explain it all. *Trends Immunol*. 2014 Jul;35(7):287–9.

373. DeFranco AL, Rookhuizen DC, Hou B. Contribution of TLR signaling to germinal center antibody responses. *Immunol Rev.* 2012 May;247(1):64–72.
374. Tongren JE, Drakeley CJ, McDonald SLR, Reyburn HG, Manjurano A, Nkya WMM, et al. Target antigen, age, and duration of antigen exposure independently regulate immunoglobulin G subclass switching in malaria. *Infect Immun.* 2006 Jan;74(1):257–64.
375. Evans S, Li L. A comparison of goodness of fit tests for the logistic GEE model. *Stat Med.* 24(8):1245–61.
376. Zou KH, O'Malley AJ, Mauri L. Receiver-Operating Characteristic Analysis for Evaluating Diagnostic Tests and Predictive Models. *Circulation.* 2007 Feb 6;115(5):654–7.
377. The meaning and use of the area under a receiver operating characteristic (ROC) curve. | *Radiology* [Internet]. [cited 2018 Jul 17]. Available from: <https://pubs.rsna.org/doi/abs/10.1148/radiology.143.1.7063747>
378. Vidal M, Aguilar R, Campo JJ, Dobaño C. Development of quantitative suspension array assays for six immunoglobulin isotypes and subclasses to multiple *Plasmodium falciparum* antigens. *J Immunol Methods.* 2018 Apr;455:41–54.
379. Kinyanjui SM, Conway DJ, Lanar DE, Marsh K. IgG antibody responses to *Plasmodium falciparum* merozoite antigens in Kenyan children have a short half-life. *Malar J.* 2007 Jun 28;6(1):82.
380. Mankarious S, Lee M, Fischer S, Pyun KH, Ochs HD, Oxelius VA, et al. The half-lives of IgG subclasses and specific antibodies in patients with primary immunodeficiency who are receiving intravenously administered immunoglobulin. *J Lab Clin Med.* 1988 Nov;112(5):634–40.
381. Morell A, Terry WD, Waldmann TA. Metabolic properties of IgG subclasses in man. *J Clin Invest.* 1970 Apr 1;49(4):673–80.
382. Nutt SL, Hodgkin PD, Tarlinton DM, Corcoran LM. The generation of antibody-secreting plasma cells. *Nat Rev Immunol.* 2015 Mar;15(3):160–71.
383. Auner HW, Beham-Schmid C, Dillon N, Sabbattini P. The life span of short-lived plasma cells is partly determined by a block on activation of apoptotic caspases acting in combination with endoplasmic reticulum stress. *Blood.* 2010 Nov 4;116(18):3445–55.
384. Liu Y-J, Zhang J, Lane PJJ, Chan EY-T, MacLennan ICM. Sites of specific B cell activation in primary and secondary responses to T cell-dependent and T cell-independent antigens. *Eur J Immunol.* 2005 Dec 6;21(12):2951–62.

385. Harms Pritchard Gretchen, Pepper Marion. Memory B cell heterogeneity: Remembrance of things past. *J Leukoc Biol*. 2018 Jan 17;103(2):269–74.
386. Ghani AC, Sutherland CJ, Riley EM, Drakeley CJ, Griffin JT, Gosling RD, et al. Loss of Population Levels of Immunity to Malaria as a Result of Exposure-Reducing Interventions: Consequences for Interpretation of Disease Trends. *PLoS ONE*. 2009 Feb 9;4(2):e4383.
387. Wipasa J, Suphavitai C, Okell LC, Cook J, Corran PH, Thaikla K, et al. Long-Lived Antibody and B Cell Memory Responses to the Human Malaria Parasites, *Plasmodium falciparum* and *Plasmodium vivax*. *PLoS Pathog* [Internet]. 2010 Feb [cited 2013 Jan 23];6(2). Available from: <http://www.ncbi.nlm.nih.gov/pmc/articles/PMC2824751/>
388. Kiessling P, Lledo-Garcia R, Watanabe S, Langdon G, Tran D, Bari M, et al. The FcRn inhibitor rozanolixizumab reduces human serum IgG concentration: A randomized phase 1 study. *Sci Transl Med*. 2017 Nov 1;9(414):eaan1208.
389. Kitaura K, Yamashita H, Ayabe H, Shini T, Matsutani T, Suzuki R. Different Somatic Hypermutation Levels among Antibody Subclasses Disclosed by a New Next-Generation Sequencing-Based Antibody Repertoire Analysis. *Front Immunol* [Internet]. 2017 [cited 2018 Nov 28];8. Available from: <https://www.frontiersin.org/articles/10.3389/fimmu.2017.00389/full>
390. Kim S-H, Yang E-M, Jung H-M, Pham DL, Choi H-N, Ban G-Y, et al. Association of TLR3 gene polymorphism with IgG subclass deficiency and the severity in patients with aspirin-intolerant asthma. *Allergy Asthma Respir Dis*. 2016 Jul 1;4(4):264–70.
391. Damelang T, Rogerson SJ, Kent SJ, Chung AW. Role of IgG3 in Infectious Diseases. *Trends Immunol*. 2019 Mar 1;40(3):197–211.
392. Chong AS, Ansari MJ. Heterogeneity of memory B cells. *Am J Transplant*. 2018 Feb 13;18(4):779–84.
393. Krishnamurty AT, Thouvenel CD, Portugal S, Keitany GJ, Kim KS, Holder A, et al. Somatic Hypermutated *Plasmodium*-Specific IgM(+) Memory B Cells Are Rapid, Plastic, Early Responders upon Malaria Rechallenge. *Immunity*. 2016 16;45(2):402–14.
394. Ahmed Ismail H, Tijani MK, Langer C, Reiling L, White MT, Beeson JG, et al. Subclass responses and their half-lives for antibodies against EBA175 and PfRh2 in naturally acquired immunity against *Plasmodium falciparum* malaria. *Malar J* [Internet]. 2014 Nov 5 [cited 2018 Apr 5];13. Available from: <https://www.ncbi.nlm.nih.gov/pmc/articles/PMC4232678/>

- 395. Amanna IJ, Carlson NE, Slifka MK. Duration of Humoral Immunity to Common Viral and Vaccine Antigens. *N Engl J Med*. 2007 Nov 8;357(19):1903–15.
- 396. Bouchaud O, Cot M, Kony S, Durand R, Schiemann R, Ralaimazava P, et al. Do African Immigrants Living in France Have Long-Term Malarial Immunity? *Am J Trop Med Hyg*. 2005 Jan 1;72(1):21–5.
- 397. Färnert A, Wyss K, Dashti S, Naucner P. Duration of residency in a non-endemic area and risk of severe malaria in African immigrants. *Clin Microbiol Infect*. 2015 May 1;21(5):494–501.
- 398. Wotodjo AN, Doucoure S, Diagne N, Sarr FD, Parola P, Gaudart J, et al. Another challenge in malaria elimination efforts: the increase of malaria among adults after the implementation of long-lasting insecticide-treated nets (LLINs) in Dielmo, Senegal. *Malar J*. 2018 Oct 25;17(1):384.
- 399. Nogaro SI, Hafalla JC, Walther B, Remarque EJ, Tetteh KKA, Conway DJ, et al. The Breadth, but Not the Magnitude, of Circulating Memory B Cell Responses to *P. falciparum* Increases with Age/Exposure in an Area of Low Transmission. *PLoS ONE* [Internet]. 2011 Oct 4 [cited 2014 Dec 17];6(10). Available from: <http://www.ncbi.nlm.nih.gov/pmc/articles/PMC3186790/>
- 400. Pène J, Gauchat J-F, Lécart S, Drouet E, Guglielmi P, Boulay V, et al. Cutting Edge: IL-21 Is a Switch Factor for the Production of IgG1 and IgG3 by Human B Cells. *J Immunol*. 2004 May 1;172(9):5154–7.
- 401. Valentine KM, Davini D, Lawrence TJ, Mullins GN, Manansala M, Al-Kuhlani M, et al. CD8 Follicular T Cells Promote B Cell Antibody Class Switch in Autoimmune Disease. *J Immunol*. 2018 Jul 1;201(1):31–40.